Universitat Politècnica de Catalunya
Electrical Engineering Department

Institut de Recerca en Energia de Catalunya
Catalonia Institute for Energy Research

PhD Thesis

Experimental validation of optimal real-time energy management system for Microgrids

Author: **Mousa Marzband**

Advisors: **Andreas Sumper**
Bogdan Tomoiagă

Barcelona, November 21, 2013

UNIVERSITAT POLITÈCNICA DE CATALUNYA
BARCELONATECH
UPC **Escola de Doctorat**

Acta de qualificació de tesi doctoral

Curs acadèmic:

Nom i cognoms

Programa de doctorat

Unitat estructural responsable del programa

Resolució del Tribunal

Reunit el Tribunal designat a l'efecte, el doctorand / la doctoranda exposa el tema de la seva tesi doctoral titulada

_____

_____ _____.

Acabada la lectura i després de donar resposta a les qüestions formulades pels membres titulars del tribunal, aquest atorga la qualificació:

☐ NO APTE   ☐ APROVAT   ☐ NOTABLE   ☐ EXCEL·LENT

(Nom, cognoms i signatura) President/a	(Nom, cognoms i signatura) Secretari/ària
(Nom, cognoms i signatura) Vocal	(Nom, cognoms i signatura) Vocal

(third Vocal box:) (Nom, cognoms i signatura) Vocal

_____, _____ d'/de _____ de _____

El resultat de l'escrutini dels vots emesos pels membres titulars del tribunal, efectuat per l'Escola de Doctorat, a instància de la Comissió de Doctorat de la UPC, atorga la MENCIÓ CUM LAUDE:

☐ SÍ   ☐ NO

(Nom, cognoms i signatura) Presidenta de la Comissió de Doctorat	(Nom, cognoms i signatura) Secretària de la Comissió de Doctorat

Barcelona, _____ d'/de _____ de _____

To my wife, my
father, mother,
brothers and sis-
ter.

Abstract

Nowadays, power production, reliability, quality, efficiency and penetration of renewable energy sources are amongst the most important topics in the power systems analysis. The need to obtain optimal power management and economical dispatch are expressed at the same time. The interest in extracting an optimum performance minimizing market clearing price (MCP) for the consumers and provide better utilization of renewable energy sources has been increasing in recent years. Due to necessity of providing energy balance while having the fluctuations in the load demand and non-dispatchable nature of renewable sources, implementing an energy management system (EMS) is of great importance in Microgrids (MG). The appearance of new technologies such as energy storage (ES) has caused increase in the effort to present new and modified optimization methods for power management. Precise prediction of renewable energy sources power generation can only be provided with small anticipation. Hence, for increasing the efficiency of the presented optimization algorithm in large-dimension problems, new methods should be proposed, especially for short-term scheduling. Powerful optimization methods are needed to be applied in such a way to achieve maximum efficiency, enhance the economic dispatch as well as provide the best performance for these systems. Thus, real-time energy management within MG is an important factor for the operators to guarantee optimal and safe operation of the system. The proposed EMS should be able to schedule the MG generation with minimum information shares sent by generation units. To achieve this ability, the present thesis proposes an operational architecture for real time operation (RTO) of a MG operating in both islanding

and grid-connected modes. The presented architecture is flexible and could be used for different configurations of MGs in different scenarios. A general formula is also presented to estimate optimum operation strategy, cost optimization plan and the reduction of the consumed electricity combined with applying demand response (DR). The proposed problem is formulated as an optimization problem with nonlinear constraints to minimize the cost related to generation sources and responsive load as well as reducing MCP. Several optimization methods including mixed linear programming, pivot source, imperialist competition, artificial bee colony, particle swarm, ant colony, and gravitational search algorithms are utilized to achieve the specified objectives. The main goal of the thesis is to validate experimentally the design of the real-time energy management system for MGs in both operating modes which is suitable for different size and types of generation resources and storage devices with plug-and-play structure. As a result, this system is capable of adapting itself to changes in the generation and storage assets in real-time, and delivering optimal operation commands to the assets quickly, using a local energy market (LEM) structure based on single side or double side auction. The study is aimed to figure the optimum operation of micro-sources out as well as to decrease the electricity production cost by hourly day-ahead and real time scheduling. Experimental results show the effectiveness of the proposed methods for optimal operation with minimum cost and plug-and-play capability in a MG. Moreover, these algorithms are feasible from computational viewpoints while having many advantages such as reducing the peak consumption, optimal operation and scheduling the generation unit as well as minimizing the electricity generation cost. Furthermore, capabilities such as the system development, reliability and flexibility are also considered in the proposed algorithms. The plug and play capability in real time applications is investigated by using different scenarios. As shown in this thesis, with decrease/increase of present microsources capacity or change of their specifications, it is not necessary to apply major changes for making the proposed algorithms compatible with new conditions. Also, this thesis aims to operate the MG in both operating modes, ensuring uninterruptable power supply services and reducing the global cost of generated power.

Resumen

Actualmente, producción, fiabilidad, calidad de la energía, eficiencia y penetración de las energías renovables son algunos de los temas más importantes en el análisis de sistemas eléctricos de potencia. Por eso, la gestión óptima de potencia y las políticas de despacho económicos son necesarias al mismo tiempo. En los últimos años ha aumentado el interés por la obtención de un gran rendimiento minimizando el precio óptimo del mercado de compensación (MCP) para los consumidores, además de mejorar el uso de las fuentes renovables de energía. Debido a la necesidad del balance de potencias y a la variabilidad de la demanda y del carácter no gestionable de las fuentes renovables, se requiere implementar un sistema de gestin de energía (EMS) dentro de la Microred (MG). La aparición de nuevas tecnologías como el almacenamiento de energía (ES) ha provocado grandes modificaciones en la gestión del sistema eléctrico. Además, la predicción de la generación de las fuentes de energía renovables sólo puede realizarse con precisión a corto plazo. Por lo que, para aumentar la eficiencia del algoritmo de optimización, nuevos métodos deben ser propuestos. Se necesitan métodos de optimización capaces de lograr el máximo rendimiento, aumentar el despacho económico, así como la adquisición de las mejores prestaciones de estos sistemas. Además, la gestión de potencia en tiempo real dentro de MG es necesaria para garantizar un funcionamiento óptimo y seguro del sistema. El EMS debería ser capaz de programar la generación de la MG con la mínima información requerida. Con este fin, esta tesis presenta una arquitectura para operar la MG en tiempo real (RTO) la cual puede encontrarse trabajando tanto en modo isla o conectado a la red. La arquitectura presentada es

flexible y se podría utilizar para diferentes configuraciones de MG también en diferentes escenarios. Una fórmula general se presenta tambin para la estimación de la estrategia de funcionamiento óptimo, plan de optimización de costes y la reducción de la electricidad consumida combinado con respuesta de la demanda (DR). El problema propuesto se formula en combinación como un problema de optimización con restricciones no lineales para reducir al mínimo el coste relacionado con las fuentes de generación y la carga de respuesta. Se formula como un problema de optimización no lineal. Varios métodos de optimizacin como la programación lineal mixta, fuente de pivote, la competencia imperialista, colmena artificial, enjambre de partículas, colonia de hormigas, algoritmos de búsqueda gravitacionales son utilizados para lograr objetivos específicos. El objetivo principal de esta tesis es validar experimentalmente el diseño de un sistema de gestin de energía óptimo en tiempo real para los MGs en ambos modos de funcionamiento adecuado para diferentes tamaños y tipos de recursos de generación y dispositivos de almacenamiento con estructura de plug- and-play. Como resultado, este sistema es capaz de adaptarse a los cambios en la generación y activos de almacenamiento, en tiempo real, y la entrega de órdenes de operación óptimas para los activos de forma rápida, el uso de un mercado local de energía (LEM) estructura basada en una sola cara o de doble cara subasta. El estudio está dirigido a exponer la operación óptima de micro- fuentes a, así como para disminuir el costo de producción de electricidad por día y por hora en tiempo real por delante de programación. Los resultados experimentales muestran la eficacia de estos. Por otra parte, estos algoritmos son factibles desde puntos de vista computacionales. Por otra parte, también se consideran funciones como el desarrollo del sistema, la fiabilidad y la flexibilidad en los algoritmos propuestos. La capacidad de adaptación en aplicaciones de tiempo real se investiga mediante el uso de diferentes escenarios. Como se muestra en esta tesis, con la reducción/ aumento de la capacidad de las micro-fuentes presentados o el cambio de su especificación, los cambios importantes para la toma de los algoritmos propuestos compatibles con las nuevas condiciones no es necesario.

Acknowledgements

First and foremost, I would like to express my sincere gratitude to my supervisors Dr. Andreas Sumper and Dr. Bogdan Tomoiagă for their continuous support throughout my PhD. I particularly thank Dr. José Luis Domínguez-García for his patience, motivation and immense knowledge.

The studies discussed in this thesis would not have been possible without the support of the EERA group at IREC. I would also like to thank the following colleagues, Ramon, Albert, Lázaro, Jordi, Lucía, Cristina, Miguel, Mikel, David, Gerard, Oscar, Joaquim, Ignasi, Antoni, and Manel, for their encouragement and insightful comments. This group has been a source of friendship as well as good advice and collaboration. I am particularly grateful to Ramon who has patiently collaborate with me during my effort and in keeping with my commitment to alone time.

Finally, I would like to thank my family for their continuous support and encouragement during the development of this thesis. Specially, thank to my wife Samane, for her love, affection and patience; since they provide me the strength necessary to do not give up and to be able to finish this work.

Contents

Contents

Contents

List of Tables

List of Figures

List of Figures

XIV

XV

List of Figures

XVI

XVII

List of Figures

XVIII

Nomenclature

ABC	Artificial bee colony
BES	Battery Energy Storage
BIO	Biomass
CAE	Compressed Air Energy Storage
CCU	Central Controller Unit
CEMS	Centralized Energy Management System
COE	Cost of Energy
CTU	Combustion Turbines Unit
DAC	Data Acquisition
DAM	Day-Ahead Market
DER	Distributed Energy Resources
DGN	Diesel Generator
DSA	Double Side Auction
DSP	Digital Signal Processing
DR	Demand Response
ECS	Electrochemical System
EGP	Excess Generated Power
EMS	Energy Management Systems
ES	Energy Storage
ESc (ES+)	ES During Charging Mode
ESd (ES-)	ES During Discharging Mode
EWH	Electric Water Heater
EOS	Energy and Operation Schaduling
ESS	Energy Storage System

List of Figures

STS	Solar Thermal System
TCP	Total Consumed Power
TPP	Total Produced Power
TGP	Total generation power
TRP	Total Required Power
UP	Undelivered Power
WT	Wind Turbine

Variables

π^A	The supply bids by A ($€$/kWh)
	$A \in \{WT, PV, MT, ESd, ESc, UP, DR \ \& \ EWH\}$
λ_t^{MCP}, $\lambda_t'^{MCP}$, $\lambda_t''^{MCP}$	MCP at each time t in $MCEMS$, $EMS - MINLP$ and $EMS - MACO_{-LEM}$, respectively ($€$/kWh)
P_t^B, $P_t'^B$, $P_t''^B$	Available power of B in $MCEMS$, $EMS - MINLP$ and $EMS - MACO_{-LEM}$, respectively (kW)
$\tilde{P}_t^B$, $\tilde{P}_t'^B$, $\tilde{P}_t''^B$	Real power set-points of B in $MCEMS$, $EMS - MINLP$ and $EMS - MACO_{-LEM}$, respectively (kW)
	$B \in \{A, TCP, TPP \& EGP\}$
$P_{i,t}^B$	Available power of B in i^{th} scenario (kW)
$P_{i,t}^n$	Uncontrollable load demand at each time step in i^{th} scenario (kW)
	$i \in \{1, 2, 3, 4\}$, $i = 1$: Normal Operation, $i = 2$: Scenario 1, $i = 3$: Scenario 2, $i = 4$: Scenario 3
SOC_t, SOC_t', SOC_t''	Battery SOC in $MCEMS$, $EMS - MINLP$, $EMS - MACO_{-LEM}$, respectively (%)
$\overline{P}$, $\underline{P}$	Limit of power (kW)
$\overline{E}$, $\underline{E}$	Limit of energy (kWh)
$\overline{SOC}$	Maximum State-of-Charge (SOC) (%)
$\underline{SOC}$	Minimum SOC (%)
$Q_t^{j,b}$	The quantity produced by generation unit j in step b at time t, in (kWh)
Q_t^{TRE}	The total required energy by costumers (kWh)
Q_t^{TGE}	The total generated energy by micro-sources (kWh)
$P_t^{g,i}$	Active power generated by source i at time t (kW)
$P_t^{c,j}$	Active power consumed by Responsible Load Demand (RLD) j (kW)
$\overline{T}^i$, $\underline{T}^i$	Minimum up/down time of unit i, respectively (min)
$\overline{R}^i$, $\underline{R}^i$	Ramp up/down rate of unit i, respectively (kW/min)
t	Time interval
d	Duration of a time interval

List of Figures

n	Total number of sources
m	Total number of consumers
α, β	Coefficients with number values
c_1, c_2	Self-learning coefficients
I	Number of recursions
$\bar{I}$	Maximum recursions
$X_{t,j}^b$	The best position of the j the particle at instant t
$X_{t,j}^i$	The present position of the jth particle at instant t and the ith recursion
$X_{t,Tot}^b$	The best position that all the particles have obtained in the search space
$V_{t,j}^i$	Status the velocity vector of the jth particle at the ith recursion and at instant t
$V_{t,j}^b$	The velocity of the jth particle in the direction of the least optimum point found by each individual particle up to this instant
$V_{t,Tot}^b$	The velocity of the particle in the direction of the least optimum point found by all of the particles up to this instant
r_1, r_2	Random number between 0 and 1
Δt	Energy management time step

XXII

1

Introduction

1.1 Microgrid concept

While smart grid is known as power system for future, smart microgrids (briefly called microgrid) are considered as the driving technology to achieve smart grids′ goals [2,3]. Although the idea of MGs seems to be similar to the various areas of operation in the traditional power system, they are different in which they have to be fully capable of autonomous operation in islanded mode. In addition, MGs could be formed in a small-scale as a commercial building to as large as power system of a town. A typical configuration of a MG is shown in Figure 1.1. Its consists of a group of radial feeders, a point of common coupling, responsive and non-responsive loads and micro-sources [4]

Since high penetration of renewable energy and storage devices are expected to be employed in the MGs, their stable operation through frequency and voltage control (traditionally known as ancillary services in the power system) is an important issue for the future power system. This goal can be obtained by balancing the generation and load demand in real time. For an islanded MG, traditional ancillary services (i.e., spinning and non-spinning reserve) are not available while more variation in generation would exist because of uncertain nature of renewable energy systems (e.g., wind and solar systems). The uncertainly of the operation increases with any failure of the generation systems and unpredictable load variations. Storage devices (such as batteries) are usually available to match generation and load demand instantly, but their capacity is limited because of their costs. In addition, demand response (DR) might be available for balancing service.

MG can significantly improve the efficiency of energy production to main-
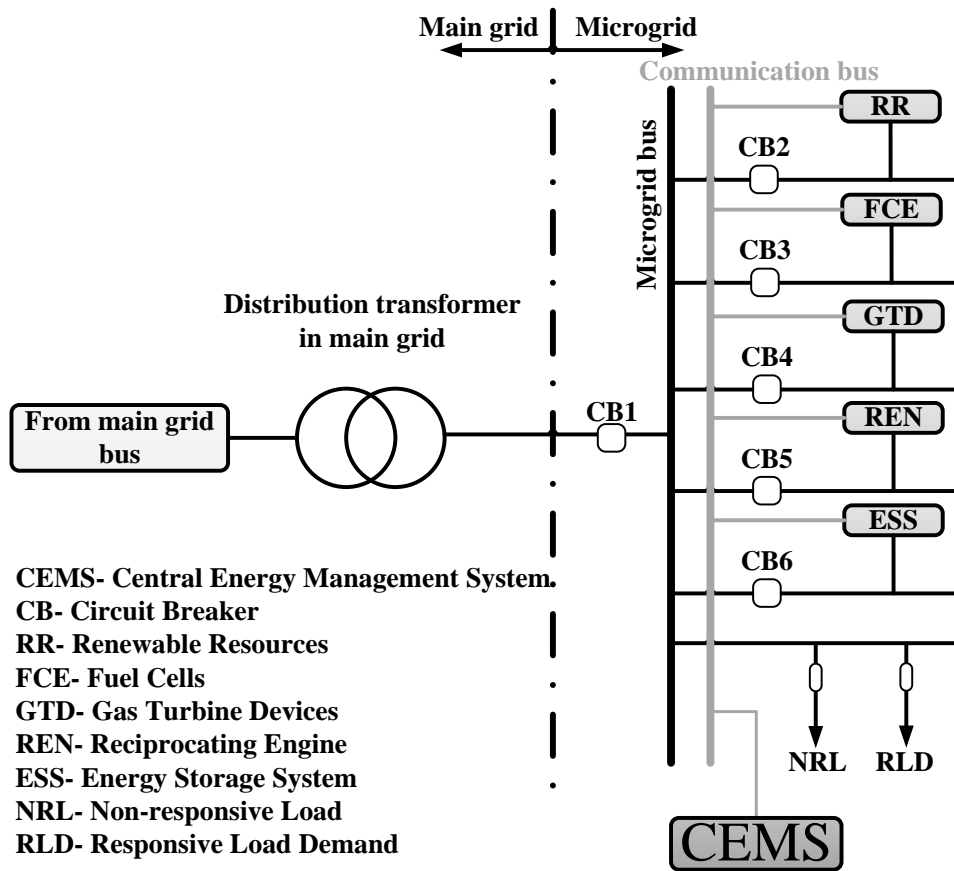
Figure 1.1: A basic MG architecture

tain the balance between power generation and load demand mostly at the distribution level. It is also desired to obtain measurable reduction in environmental emissions and increased power quality through MGs.

If a MG system wants to ensure the feeding of its consumers in line with the increase of reliability, stability of power supply and proper cost and price, presenting new initiatives for the optimization of the performance of these systems and also the exact programming of the microsources should be considered as a critical fact. In concentrated and grid connected MG, the fluctuations of load demand results in frequency problems and reactive power fluctuations, but the feeding of electricity can decrease or increase in accordance with the demand. That is because, these systems obtain part of their energy from technologies that are controllable and dispatchable. How-

ever, isolated MG system often use renewable energy technologies that are considered non-dispatchable and may vary depending on the climatic conditions. So, variations in feeding and conformity of electricity production and its consumption by the customers are considered as a challenging problem in the systems based on DGs [5–11]. An isolated MG, with no choice has much more limitations than a MG connected to a Macrogrid [12, 13].

The isolated MG based on renewable sources has limited amount of energy in access. Moreover, in such systems, there exists fluctuation in most of time intervals which depend on climatic conditions [12]. Hence, intelligent systems shall be developed for feeding the energy needed by the consumers by using non-dispatchable DG units [7, 12]. In the present power systems, the adequate feeding of the demand side sources have significant importance because of the limitations of using renewable sources. In this route, different methods for balancing energy in the MGs has been presented in the literature [7]. Reference [14] suggested to eliminate the problems regarding to energy storage technologies. Surplus electrical power generated by energy distributed sources which is more than the local loads demand can used to help to other sources that are not able to supply the power needed by their local loads. At present, energy storage can be implemented only in small scale and in a short time interval, although, technologies such as lead-acid have had significant growth in the current years [2, 3].

Moreover, demand response mechanism can cause reduction of the fluctuations resulting from random and unwanted requests [15–19].

In recent years, application of substitute energy sources such as wind, biomass, solar, hydro and etc has become more common as the result of continuous increase of the need for more reliability, better power quality, higher flexibility, lower electricity price and less environmental effects. In other words, in recent years, distributed generation sources such as PV, microturbines, fuel cells and energy storing sources have significant role in generating electricity more economically and with lower carbon emission [2, 3, 5, 9, 20]. Meanwhile, the high penetration of DGs in the grid have created new challenges about safe and effective use of these systems in power grids. The challenges can be removed to some extent by applying MGs that are defined as a set of DGs, electrical loads and generation sources connected to each other [12, 21–23]. In this regards, methodologies that are continuously improving are implemented for the management and control of MGs performance to make these grids more optimized and effective. In the other hand, severe need is felt for presenting algorithms for implementing more precise scheduling of energy sources in the MGs by including different objectives such as reducing production cost, increasing the profit of the

generators, reducing environmental pollutions and etc. [24–26]. So far many research works on MG system performance scheduling under various loading conditions by considering different objectives have been developed [8,27–30].

Using DERs and competitive markets that have been created during the recent years have revealed the need for specific technical conditions considering the characteristics of smart grid [2,3,31]. Furthermore, recently, generation of electricity from WT and PV systems plays an important role in designing smart grid systems especially in isolated operating mode. But, the main problems encountered with RES are the problems related to continuity and unpredictability of these sources. The output of some of these sources are affected by climatic conditions. In order to solve this problem, energy storage (ES) systems can be used to support these sources. Although, there is no limitation in the select the type and choosing of the capacity of ES systems, the main problem of these systems is high initial capital investment. Moreover, DR shall also be considered as a very suitable energy source in connection with other energy resources for optimizing production cost [32]. In addition, application these sources in smart grids necessitates the present on of new control methodologies which improve the performance. Thus, an EMS whose function is to continually monitor the energy consumption, improve the utilisation of the system as well as to increase the reliability of the system could be used to optimize the operation.

Application of DER have also increased the number of variables that must be considered in the problems related to economic dispatch. With a very large number of variables it is necessary to find proper tools for solving these complex problems. So, new approaches should be developed in order to improve the efficiency of economic dispatch methods. Using deterministic optimization techniques for solving DER scheduling problems needs very fast computing devices with enough memory.

Artificial intelligence techniques such as heuristic methods inspired by biological process can have competitive advantages compared to common optimization techniques. The problems of applying common deterministic methods for scheduling DER in a realistic environment has motivated using these methods.

Electricity generation by using DG is an adequate paradigm of providing a reliable electricity source. DG can become integrated through controllable platform called MG inside distributed systems [2,3]. In the MGs, if energy generation sources cannot provide sufficient power for feeding the requested load, the system will encounter supply demand mismatch.

1.2 Energy management system

According to the above explanations, a supervisory control and top-level management system is a necessary part of MGs to operate the system with minimum cost within safe margins. Modern energy management and control systems could help to reduce the cost of energy. However, they are applied either in a complex manner or a too simple way to achieve the desired goal. To maximize energy savings, minimize related costs and obtain a fast payback in MG systems, it is vital and most desirable to optimally operate an aggregated number of micro-sources to achieve the lowest possible production cost. In a MG, this can be achieved by applying optimization methods and adjusting the generators output to minimize the production costs. The optimization procedure may interact with public network information. For example, energy for storage devices can be bought when prices are low, and sold when required. It is also desired for the EMS to adapt itself in real-time to any changes in the types and capacity of the generation and storage assets without any manual modification in the EMS. Other objectives of the EMSs are maximizing the benefit of MG operation (equivalently minimizing the cost of operation) [21, 23, 27, 33, 34], minimizing the emission [35], maximizing the lifetime of assets [35], increasing the reliability of the MG [10, 36–53] or a combination of multiple objectives as a multi-objective EMS [21]. The EMSs fall in two different categories: central energy management system (CEMS) and distributed energy management system (DEMS). There are certain advantages and drawbacks for each one as reviewed in [54]. Various configurations for EMS with different algorithms and different MG structures have been presented in the literature [2, 55–73].

Some references have developed optimization methods for EMSs aiming to obtain scheduling operations and optimal operating strategy [2, 57–66]. The objective function (OF) in these references allows autonomous or grid-connected decision-making to determine the hourly optimal dispatch of generators depending on system constraints and market parameters. The economic concepts of EMSs in the MG market and the development of strategies to achieve such benefits are reported in [67–73].

Effective energy management can provide the necessary optimal and sustainable energy supply with maximum ability. Furthermore, given the intermittent nature of renewable energy resources, EMS should be able to find the best solution to supply consumers quickly and continuously, i.e., every minute or few minutes. In general, gradient-based optimal EMSs are too slow to be used for real-time energy management problems. As a result, recent research in this area has been focused on the off-line application

of intelligent methods for energy utilization in the hybrid energy systems, e.g. [74, 75]. Only few other studies have been reported with limited simulation evaluations for real-time management in specific applications [33, 76]. This thesis has focused on real-time implementation of EMS with additional constraints for battery operation and its life time extension. Real time operation have been investigated in the literature [33, 77, 78] but these algorithms have never been tested in experimental MGs.

The increase of distributed generation (DG) penetration into power systems and the introduction of private market in recent years have caused numerous challenges in the design and planning [2, 3, 70–73]. In the future, the consumers can have an isolated MG that includes micro generation systems and their consumption management can be done by EMS according to real time electricity cost.

Among the main constraints related to renewable energy sources are problems related to reliability and dispatchability associated with their performance [79] because the output power of renewable sources changes with weather conditions. As a result, power balance between producers and consumers considering reserve sources for supplying shortage of system power is considered as a key problems in EMS design. Complex constraints and the impossibility of complete accordance of all DG generation sources with the paradigms of power system, has led to the presentation of smart grid concept. The main specifications of a smart grid are as follows:

1. Capability of executing programs such as demand response management for controlling the shiftable loads (shift to times with lower cost and less electricity consumption);

2. Error tolerance, this tolerance must also be considered for confronting the transient errors;

3. Load curtailment ability when the MG cannot feed its load completely or when the electricity prices are high [79];

4. High reliability, power quality, security and system efficiency;

5. Self revival which means that the system can revive itself after the occurrence of error in it;

6. Plug and play capability of all the devices that are added to the system as microsources with any capacity or are put out of the system is provided automatically by EMS.

For obtaining the characteristics mentioned for SGs, it is necessary to consider short-term scheduling (STS) and very short-term scheduling (VSTS). STS can fulfill the characteristics (1-3) mentioned above.

Short term economic dispatch [79–89] is a very important choice in the modern energy management systems and by using it, the system performance cost can be reduced. It is demonstrated that demand response as a very important energy source which it must be paid attention to such as generating sources and ES sources to optimize the system performance. Distributed energy resources (DER)s significantly increase the number of variables that must enter the economic dispatch problem. So, it is necessary to present new methodologies for improving the efficiency of these methods.

For presenting these methodologies, very fast and adequate response must be considered for the optimization problems with a lot of variables [79, 90]. Deterministic optimization techniques need significant calculations and also the execution time of these methods is not compatible with short-term scheduling.

So, it is necessary to use alternative methodologies which have the fast response for multi-variable optimization problems. Intelligent competitive techniques called methaheuristic methods inspired from biological process can provide this desired characteristic.

Applying proper EMS is also crucial in order not to encounter this problem. An EMS makes the optimum use of distributed energy sources possible alongside assurance of their quality and reliability. Although, it is possible that these systems fail in load feeding if the total demand is more than the maximum accessible capacity of the generation sources. Under such a scenario, applying supporting systems such as diesel generators, distributed storages or implementing demand side management (DSM) options can be useful to reduce the supply-demand mismatch [5, 9, 26, 91]. In recent years, the operation and maintenance costs and the levels of emission of pollutants in the generators based on fossil fuel has been increasing significantly. As a result, special attention is considered in using such support systems in addition to DSM and storage systems. The main objectives of DSM program is minimizing mismatch between fed power and load during consumption peak by changing the system load curve. The variation of system load curve can be done through both the distribution system facilities and end-use customers [92–94].

7

1.3 Research motivations and objectives

In this thesis, a general CEMS framework with plug-and-play structure will be proposed to minimize the operation cost of the MG. The plug-and-play capability of the proposed CEMS facilitates automatic modification of the management problem since any change in the generation and storage resources is dealt with in real-time to achieve optimal operation of the MGs. It is also assumed that each generation and storage device sends a signal to the CEMS to establish itself in the management system at the time of attaching to the MG. As a result, the proposed CEMS can be developed as an autopilot product, capable of adapting itself to any MGs.
As mentioned earlier, the objective of the proposed CEMS is to optimally operate any MG with any size and types of generation and storage devices by minimizing the cost of operation. To achieve this goal so in real-time, a comprehensive database of available generation and storage technologies for MG operation (called technology database in this thesis) is considered with appropriate mathematical cost function and operational constraints. Assuming a two-way communication between each asset in the MG and CEMS (which is an inherent feature of smart MG), each device at the beginning of connection and after each change will inform the CEMS about its type and capacity. The proposed CEMS framework also includes optimization unit, LEM unit and real time dispatching, which are explained in Chapters 2 and 3. The LEM is based on SSA and DSA to calculate the price of energy in real-time for the consumers.

In this thesis, by using the profile of non-dispatchable sources and non-responsive loads, the optimum power setpoints for the spinning reserve sources, energy storage and also demand response are sent to them by using the proposed algorithm by the central controller unit (CCU). Moreover, the concept of virtual generation sources has been introduced and are extracted according to the information of load demand and the total power generated in each time interval. Some DR constraints are manipulated and stated by using the modeled information with the situation flags. Optimum scheduling in a combinatorial topology of production sources and DR by minimizing the total system performance cost and the reducing MCP in each time interval using several proposed optimization algorithms are considered as one of the main innovations of this thesis. The cost function presented includes the cost of all generation and storage assets considering the DR cost with respect to the constraints considered for each one of them.

1.4 Thesis contributions

The contributions of this thesis can be briefly clarified as follows:

1. Proposal of a CEMS which is flexible to adapt itself to any type of MG [J7];

2. Develop of a plug-and-play operation of the generation and storage assets in real-time with comprehensive technology database of generation and storage devices, NRL and Responsive Loads (RL) [J1, J7];

3. Applying a real-time optimization for the future generation forecast [J9];

4. Proposal of a fast, flexible and extendable RTO architecture to coordinate DAS and RTS and improve of ES operation considering two extra operation modes for the ES including Over Charging Protection Mode and Over Discharging Protection Mode [J1];

5. Presentation of some novel optimal EMSs in a day-ahead market to minimize the total cost of operation in both islanded and grid connected MG [J2-J10];

6. Experimental implementation of the proposed optimization algorithms over on a real MG Testbed [J1-J10].

1.5 Thesis outline

The organization of this thesis falls into seven chapters:

1. **Chapter 2** defines the generalized formulas and the proposed structure including the optimization and local energy market units that will be used intensively in the rest of the thesis [J5].

2. **Chapter 3** studies several local energy market structures to obtain unit commitment based on cost considering the production cost minimization. The results presented in this chapter have also appeared in [2, 3].

3. **Chapter B** provides a review of heuristic algorithms tends to make an assessment of their advantages and drawbacks relative to others regarding the real time operation support [J6-J10].

9

4. **Chapter 4** allows us to address the mathematical subtleties of the optimization algorithms while being able to satisfy all constrains. Results of this chapter have also contained in [J2-J10].

5. **Chapter 5** presents the simulation and experimental approaches and the results and discussion for MG in both isolated and grid-connected operation mode [J2-J10].

6. **Chapter 6.1** summarizes the previous chapters, draws the achieved conclusion about this research and gives some suggestions for future improvements and work.

<div style="text-align: right; font-size: 3em;">2</div>

The central energy management system (CEMS)

2.1 Introduction

As discussed in the introduction, safe and optimal operation of MGs is a primary concern for the power system developer in the smart grid area. Regardless of the EMSs central or distributed architectures, they have to be able to make optimal decisions in a short time (i.e., real-time as system operation point of view). Cost-effective operation of the MGs is a primary concern for the power system operators. In addition, it is quite important for the EMS to enhance plug-and-play operation particularly in larger MGs with different generation and storage devices. In other words, the EMS should adapt itself in real-time with any changes in the type and capacity of generation and storage assets within MG.

In this study, a comprehensive CEMS is proposed to overcome the problems discussed above where the plug-and-play operation is provided with an embedded technology database (as shown in Figure 2.1). As mentioned before, this database contains cost function and technical constraints of different generation resources, storage devices, and responsible consumers′ loads, commonly utilized in MGs (to the best knowledge of the authors). This database is the core of the plug-and-play idea where each plugged-in device informs the CEMS with its type.

Then, the overall cost function and technical constraints will be updated with the new available technology. The technology database could be updated regularly for the technologies of future and possible improvement in

the cost functions and constraints. The communication link between different devices with the CEMS is a major feature of the future smart grid and has been assumed to exist in this study.

The optimization unit makes optimal decisions (i.e., setpoints to the technology) at each time intervals based on the MG characteristic matrix which defines the overall objective functions and constraints. In order to consider the future behavior of the system in decision making of each interval, the proper optimization structure includes the future forecasted generation and demand (until the end of current day). Therefore, overall operation of the system for current day will be optimized. Large MGs usually perform under multi-ownership market where different generation, storage, and DR resources are owned by different people and/or companies. On the other hand, small MGs (such as the one in this study) commonly have single owner. In this study, single ownership is considered to simplify the market structure and focus on the main issues addressed here, e.g., plug-and-play structure and real-time optimal operation. In the case of multi-ownership MG, the SSA model of this study can be easily replaced by the new one in the LEM unit which will be the authors′ future work.
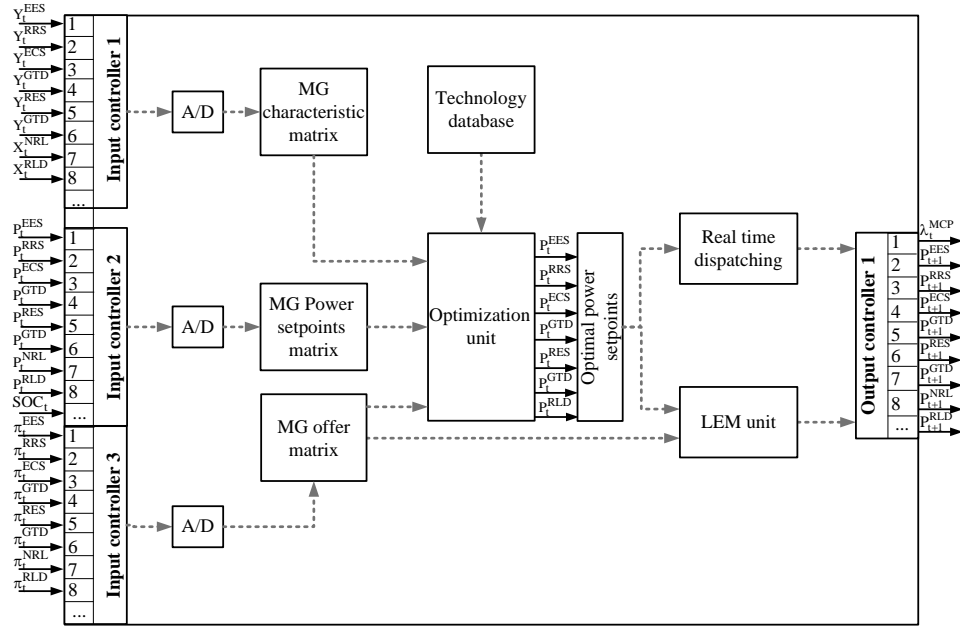
Figure 2.1: Block-diagram representation of the proposed CEMS

In the following subsections, each unit of the proposed CEMS will be

discussed in detail. The term "technology" interchangeably is used instead of either generation, storage, or DR assets throughout this thesis.

2.2 Technology Database

The technology database is formed with seven different classes as shown in Figure 2.2. Each technology will be identified with its class. Seven classes include all generation resources, storage devices, and consumers′ load demand which are commonly utilized in MGs (to the best knowledge of the authors). In each class, similar technologies (only generation and storage) in terms of operational cost and technical constraints are considered. In other words, the same type of cost function and technical constraints can be recognized for all technologies available in the same class. To clarify the proposed classification, consider class 4, where it accommodates conventional rotating generation sources with the same operational constraints including minimum on and off time, and ramp-up and ramp-down limits. Consumers′ loads are also considered in two different categories based on their availability for management: non-responsive load (NRL) and responsive load demand (RLD). The first class of loads (i.e., NRL) includes a part of consumers′ critical loads which always must be satisfied regardless of the MG situation (e.g., the electricity price, on-peak load hours and so on). However, RLD represents consumers′ responsive loads which are available for DR. This class of consumers′ load may participate in the market with their offer price to respond to the utility command to move their power consumption from on-peak hours to off-peak hours or from higher electricity price periods to cheaper hours. HVAC loads, Electric Water Heaters (EWHs), and heat pumps are good examples of this category. Note that the price offer of the members in the same class might be different in the market.

The proposed classification of devices avoids unnecessary large database, gives a better understanding of the plug-and-play structure, enhances the future modification with new technologies, and more importantly enables an automatic real-time modification of the overall objective function and constraints in the optimization algorithm.

The proposed plug-and play structure is formed based on a "MG characteristic matrix". This matrix contains a specific and unique binary variable for each class (Y_t^i, $i = 1, \cdots, 7$) and individual members of each class ($X_t^{i,j}$, $i = 1, \cdots, 7$, j = members in class i), as shown in Figure 2.3. This approach is similar for all generation sources, storage devices, and consumers′ loads
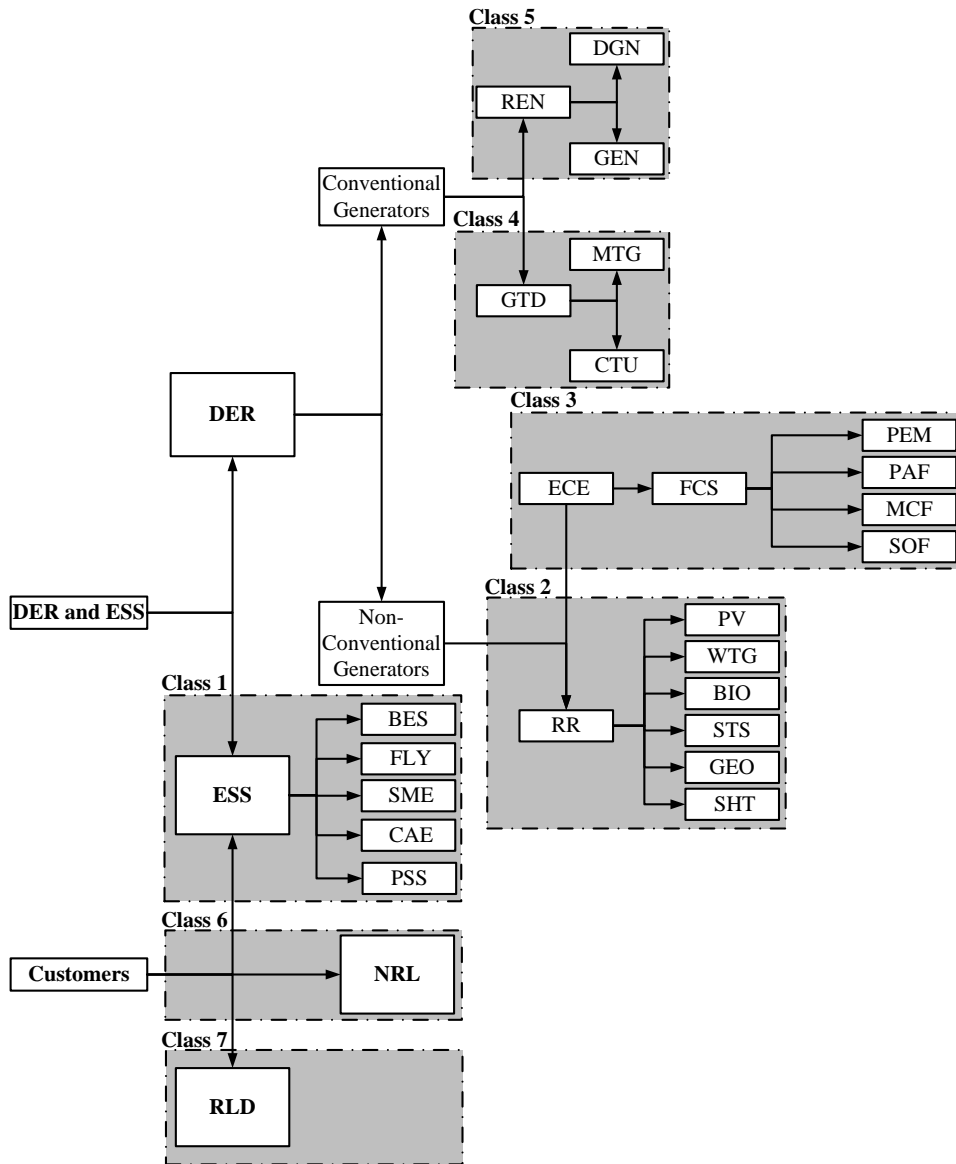
Figure 2.2: Technology database classification of the proposed CEMS

available in the technology database. The MG characteristic matrix is given as:

$$
X_t = [\overbrace{X_t^{PV}, X_t^{WTG}, X_t^{BIO}, X_t^{STS}, X_t^{GEO}, X_t^{SHT},\cdots}^{Y_t^{RES}}
$$

$$
\overbrace{X_t^{BES}, X_t^{FLY}, X_t^{SME}, X_t^{CAE}, X_t^{PSS},\cdots}^{Y_t^{ESS}}
$$

$$
\overbrace{X_t^{SOF}, X_t^{MCF}, X_t^{PAF}, X_t^{PEM},\cdots}^{Y_t^{ECS}}
$$

$$
\overbrace{X_t^{DGN}, X_t^{GEN},\cdots}^{Y_t^{REN}}
$$

$$
\overbrace{X_t^{MTG}, X_t^{CTU},\cdots}^{Y_t^{GTD}}
$$

$$
X_t^{RLD}] \tag{2.1}
$$

where t is the time.

The default value of the binary variable for all devices and classes is zero at the beginning, except for the NRL which always has to be satisfied regardless of the MG situation. As a result, the binary characteristic variable for NRL is always one and is not included in the MG characteristic matrix. For the rest of the variables, once a technology (generation, storage, or DR) plugs into the MG, the associated binary variable for that specific device $(X_t^{i,j})$ and its associated class binary variable (Y_t^i) will switch to one from zero. Therefore, the class binary variable (Y_t^i) will be one if and only if at least one of the class members' binary variable is one. Otherwise, both binary variables (class (Y_t^i) and class member $(X_t^{i,j})$ binary variable) will remain zero at the CCU. In the ESS class, devices can act as a load (charging mode) or generation source (discharging mode), which are distinguished by positive (for charging) and negative (for discharging) sign.

It is simply achieved by "OR" logical operator on the binary variables of each class (e.g., $Y_t^{ECS} = X_t^{SOF} \| X_t^{MCF} \| X_t^{PAF} \| X_t^{PEM}$).

As one may notice from Eq.(2.1), the proposed plug-and play structure with the MG characteristic matrix can be easily expanded to include any new technology in the future.

Based on the characteristic matrix in Eq.(2.1), the scheduled power for each device can be represented by another matrix as
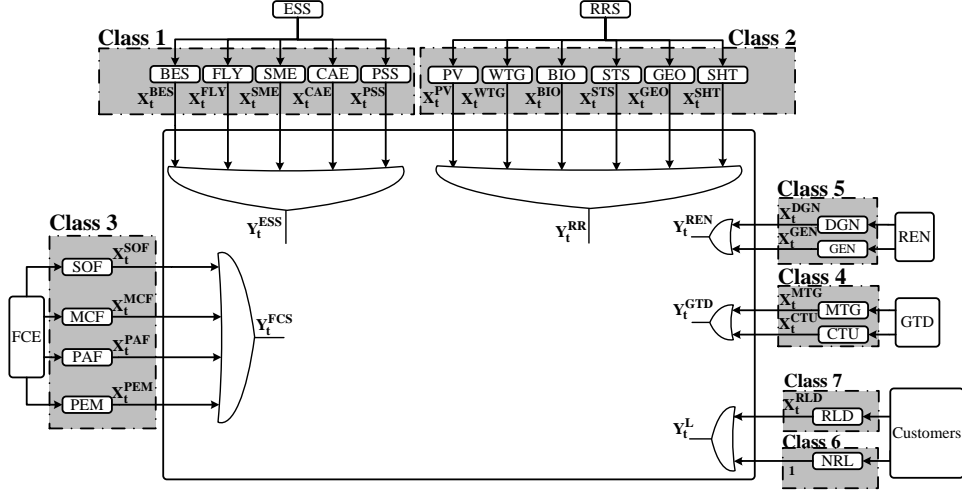
Figure 2.3: Block-diagram representation of MG characteristic matrix

$$P_t = \quad [\overbrace{P_t^{PV}, P_t^{WTG}, P_t^{BIO}, P_t^{STS}, P_t^{GEO}, P_t^{SHT}, \cdots}^{P_t^{RES}}$$
$$\overbrace{P_t^{BES}, P_t^{FLY}, P_t^{SME}, P_t^{CAE}, P_t^{PSS}, \cdots}^{P_t^{ESS}}$$
$$\overbrace{P_t^{SOF}, P_t^{MCF}, P_t^{PAF}, P_t^{PEM}, \cdots}^{P_t^{ECS}} \quad (2.2)$$
$$\overbrace{P_t^{DGN}, P_t^{GEN}, \cdots}^{P_t^{REN}}$$
$$\overbrace{P_t^{MTG}, P_t^{CTU}, \cdots}^{P_t^{GTD}}$$
$$\overbrace{P_t^{NRL}, P_t^{RLD}}^{P_t^{L}}]$$

By applying the communication links between the CEMS and devices, the MG characteristic matrix (i.e., Eq.(2.1)) will be updated once a new technology plugs in to the MG, or one of the existing technology disconnects from the MG, or the capacity of the attached technology changes. Then, the optimal management algorithm will also be updated at the beginning of each interval to generate a new setpoints for the attached technologies.

2.3 Optimization unit

In this section, a general optimization structure is presented to determine the MG′s technologies setpoints with minimum cost of operation at each time interval. The optimization unit includes a general cost-based objective function which will be updated by the MG characteristic matrix. Therefore, the objective function is always up to date with latest changes in the MG. Similar to the technology database which contains all available technologies within the MG, the optimization unit is required to have a database of cost function and technical constraints of all available technologies in the technology database. As mentioned in Section 2.2, all technologies in the same class have similar operational constraints; hence seven set of operational constraints can be recognized in the database of optimization unit. Similar to the technology database, this part can also be updated offline in the future with any new class of technology or modifications in the operational constraints. The proposed optimization unit is developed based on several assumptions for the MG operation as follows:

- voltage levels are considered to be the same at different part of the MG;

- power losses have been ignored in the model;

- reactive power flows are not considered in this study.

In order to develop the overall objective function based on the operation cost of the MG, it is essential to get the offer price from different available technologies.

The offers from different generation and storage assets and DR will be received by the CEMS unit at each time interval. MG offer (bid) matrix is defined to integrate all offers in a matrix structure similar to the MG characteristic matrix as:

$$\pi_t = [\pi_t^{RES}, \pi_t^{ESS-}, \pi_t^{ECS}, \pi_t^{REN}, \pi_t^{GTD}, \pi_t^{ESS+}, \pi_t^{RLD}] \qquad (2.3)$$

where:

$$\pi_t^{RES} = [\pi_t^{PV}, \pi_t^{WT}, \pi_t^{BIO}, \pi_t^{STS}, \pi_t^{GEO}, \pi_t^{SHT}, \cdots] \qquad (2.4)$$

$$\pi_t^{ESS-} = [\pi_t^{BES-}, \pi_t^{FLY-}, \pi_t^{SME-}, \pi_t^{CAE-}, \pi_t^{PSS-}, \cdots] \qquad (2.5)$$

$$\pi_t^{ECS} = [\pi_t^{SOF}, \pi_t^{MCF}, \pi_t^{PAF}, \pi_t^{PEM}, \cdots] \tag{2.6}$$

$$\pi_t^{REN} = [\pi_t^{DGN}, \pi_t^{CEN}, \cdots] \tag{2.7}$$

$$\pi_t^{GTD} = [\pi_t^{MTG}, \pi_t^{CTU}, \cdots] \tag{2.8}$$

$$\pi_t^{ESS+} = [\pi_t^{BES+}, \pi_t^{FLY+}, \pi_t^{SME+}, \pi_t^{CAE+}, \pi_t^{PSS+}, \cdots] \tag{2.9}$$

Each technology participate in this matrix with its own offer price (bid). It can be seen from Eq.(2.3), that the ESS class participates with two different offers: charging offer (π_t^{ESS-}) and discharging offer (π_t^{ESS+}). In this study, the MG offer matrix is considered to be constant throughout a day of operation. Further, the overall objective function of the MG optimization problem can be defined incorporating the MG offer matrix as

$$\mathbf{MIN}[\sum_{\mathbf{t}} \left(\begin{array}{c} \sum_{i=1}^{5}\sum_{j=1}^{n_i} X_t^{i,j} \times P_t^{i,j} \times \pi_t^{i,j} \\ -\sum_{i=6}^{7}\sum_{j=1}^{n_i} X_t^{i,j} \times P_t^{i,j} \times \pi_t^{i,j} \\ +P_t^{UP} \times \pi_t^{UP} \end{array} \right) \times \Delta t] \tag{2.10}$$

where $i = 1, \cdots, 6$ is the number of classes in the technology database, except the NRL class which always has to be satisfied regardless of the electricity price, $j = 1, \cdots, n_i$ is the number of assets in class i which is currently attached to the MG and participates in the market, and Δ is the length of the management time interval (min). As mentioned before, the overall objective function is dynamic since the MG characteristic matrix (X_t) will be updated in real-time with any changes in the MG. According to the MG offer matrix, the ESS class is included with different cost function for charging and discharging. Since it is desired to meet the NRL completely, a penalty cost (π_t^{UP}) is considered in the objective function for undelivered NRL demand (P_t^{UP}).

The Objective function, given in Eq.(2.10), will be minimized at each interval (every 5 minutes in this study) until the end of current day to determine the optimal operation setpoints of the MG. Therefore, the updated

MG characteristic matrix at each time interval will be used as the MG structure for the rest of the day as well. In this day, predictive optimization will be carried out instead of instantaneous optimization. Former one results in optimal solution for the whole day. It is important to remember that variable generation and load demand forecast will be used in the objective function for the time intervals ahead. The forecasted values are assumed to be ready at each time interval; thus, the forecasting algorithm will not be discussed in this thesis.

Despite the fact that each technology might have linear or nonlinear cost function, it participates with a single offer in the MG operational cost function. Therefore, the responsibility of cost calculation for each technology is stayed at the local controller (operator) which generates the offer price at each time interval. The updated offer then will be transmitted to the CEMS through existing communication.

In Eq.(2.10), linear cost function is considered for each class because the optimization unit receives offer from each technology. In other words, each technology owner is responsible to calculate the cost of electricity in that unit, where the cost function might be linear or nonlinear; however the MG operator should decide based on the load demand, available power, and their offers. Although single-ownership MG is considered in this study, Eq.(2.10) is still valid for multi-ownership MG where different technologies participate with different offers. In both cases, the MG operator always desires to run the MG with minimum cost through minimizing Eq.(2.10) at each interval.

In an optimization-based EMS (such as the one proposed in this thesis), the excess power (P_t^{EGP}) will be available in different circumstances based on the minimum cost of operation. Such condition is when the total Reciprocating Engine (REN) generation exceeds NRL.

In an islanded MG, the excess available power can be delivered to one or a combination of the following assets:

1. Charging the ESS devices such as BES when it is in charging mode (i.e. the SOC of the BES is less than 80%)

2. Delivering to the RLD (responsive loads which will be utilized as DR resources)

When ESS is fully-charged and no RLD is remained, the excess power will remain unused. The decision in this regard will be made through the optimization unit by cost function evaluation.

The UP concept is graphically shown in Figure 2.4. Where, any shortage in generation can be calculated with the following equations:

19

$$P_t^{UP} = P_t^{NRL} - \sum_{i=1}^{5}\sum_{j=1}^{n_i} P_t^{i,j} \tag{2.11}$$

where $\displaystyle\sum_{i=1}^{5}\sum_{j=1}^{n_i} P_t^{i,j}$ can be obtained from Eq.(2.2). As it can be realized from Eq.(3.4), the UP only exist when total REN generation and maximum generation from dispatchable units and storage devices cannot meet the NRL. This statement is valid since high penalty cost is considered for the UP in the overall objective function, i.e., Eq.(2.10).
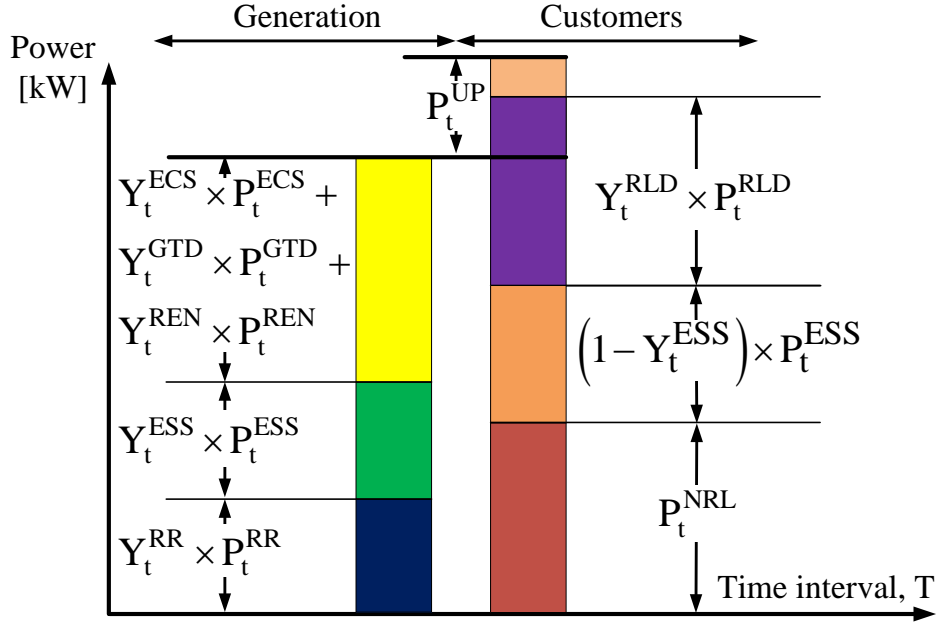
Figure 2.4: UP in both proposed EMS

To generate the MG and individual technologies safe operation, several constraints should be included in the optimization unit. Generation and demand balance is a key operational constraint in a power system, which is given as follow:

$$\sum_{i=1}^{5}\sum_{j=1}^{n_i} X_t^{i,j} \times P_t^{i,j} = P_t^{NRL} - P_t^{UP} \tag{2.12}$$

In Eq.(4.11), available power from generation resources and storage devices in discharging mode are given in the right side of the equation while load demands (NRL and RLD) and storage devices in charging mode are in the other side. P_t^{EGP} might be positive (more load is added to utilize excess available generation) or negative (in power shortage) based the system conditions. Therefore, the excess available generation can be stored in the RLD and/or ESS in the charging mode.

Eqs.(2.13)-(2.16) simply limit the scheduled power of the renewable energy sources (RES) between the minimum and maximum forecasted power or their rated capacity.

 - Generation limit for the micro-sources in the RES class

$$Y_t^{RES} \cdot \times (\underline{P}^{RES} \leq P_t^{RES} \leq \overline{P}^{RES}) \tag{2.13}$$

 - Generation limit for the micro-sources in the REN class

$$Y_t^{REN} \cdot \times (\underline{P}^{REN} \leq P_t^{REN} \leq \overline{P}^{REN}) \tag{2.14}$$

 - Generation limit for the micro-sources in the ECS class

$$Y_t^{ECS} \cdot \times (\underline{P}^{ECS} \leq P_t^{ECS} \leq \overline{P}^{ECS}) \tag{2.15}$$

 - Generation limit for the micro-sources in the GTD class

$$Y_t^{GTD} \cdot \times (\underline{P}^{GTD} \leq P_t^{GTD} \leq \overline{P}^{GTD}) \tag{2.16}$$

The generation upper and lower limits can be updated in real-time similar to the MG characteristic and offer matrices for variable generation technologies based on updated forecasts from each unit. Technologies available in the Gas Turbine devices (GTD) class have extra operational constraints including start-up time and ramp-up and down limit. These technical constraints are expressed in Eqs. (2.17)-(2.20).

 - Maximum and minimum operating times in the GTD class

21

$$[Y_t^{GTD} - \overline{T}^{i,GTD}] \cdot [I_{t-1}^{i,GTD} - I_{t-1}^{i,GTD}] \geq 0 \qquad (2.17)$$

$$[-Y_{t-1}^{GTD} - \underline{T}^{i,GTD}] \cdot [I_t^{i,GTD} - I_{t-1}^{i,GTD}] \geq 0 \qquad (2.18)$$

- Ramp-up and ramp-down limits in the GTD class

$$[P_t^{i,GTD} - P_{t-1}^{i,GTD}] \leq \overline{R}^{i,GTD} \qquad (2.19)$$

$$[P_{t-1}^{i,GTD} - P_t^{i,GTD}] \leq \underline{R}^{i,GTD} \qquad (2.20)$$

where $\overline{T}^{i,GTD}$ and $\underline{T}^{i,GTD}$ are maximum and minimum up and down time of unit i in the GTD class (min), respectively, $\overline{R}^{GTD}$ and $\underline{R}^{GTD}$ are ramp up and down of unit i in the GTD class (kW/min), and $I_t^{i,\overline{GTD}}$ is the operate on status of unit i in the GTD class (i.e., $I_t^{i,GTD} = 1$ when the unit is on, and $I_t^{i,GTD} = 0$ when it is in off state). t is the current time interval (min).

Different constraints are given for safe and efficient operation of the ESS in Eqs.(2.21)-(2.28) [3]. These constraints are explained as follows:

- Energy storage limit

$$E_t^{ESS} \leq \overline{E}^{ESS} \qquad (2.21)$$

- Maximum charging limit

$$((1 - Y_t^{ESS}) \times P_t^{ESS}) \leq \overline{P}^{ESS+} \qquad (2.22)$$

where Y_t^{ESS} is a binary variable which is defined to represent the ESS's mode of operation. The ESS is in charging mode when $Y_t^{ESS} = 0$. Eq.(2.22) shows that when the ESS is in the charging mode (i.e.,$Y_t^{ESS} = 1$), the discharging power cannot exceed the maximum discharging power of the ESS. The same operation characteristic is defined for the discharging mode, which is given in Eq.(2.22).

- Maximum discharging constraint

$$(Y_t^{ESS} \times P_t^{ESS}) \leq \overline{P}^{ESS-} \tag{2.23}$$

- Maximum discharging constraint based on the stored energy

$$(Y_t^{ESS} \times P_t^{ESS} \times \Delta t) \leq (E_{t-1}^{ESS}) \tag{2.24}$$

Eq.(2.24) simply ensures that the discharged energy will not exceed the total available energy in the ESS. Also, total discharging energy and stored energy up to time t cannot exceed the maximum energy stored in the ESS. Both conditions are modeled in Eq.(2.25).

- Maximum charging constraint based on the stored energy

$$(((1 - Y_t^{ESS}) \times P_t^{ESS} \times \Delta t) + E_{t-1}^{ESS}) \leq \overline{E}^{ESS} \tag{2.25}$$

Eq.(2.26) is to ensure the energy balance of the ESS. In other words, the energy stored in the ESS (at time t) should be equal to the total stored energy (up to time $t-1$) and the energy stored in the ESS in charging mode at time t. In this case, the stored energy in the ESS must be added to the available energy of the ESS from the previous interval. Otherwise, the energy at time t must be subtracted from the previous value if the ESS is in the discharging mode.

- Energy balance of the storage device

$$E_t^{ESS} = E_{t-1}^{ESS} + ((1 - Y_t^{ESS}) \times P_{t-1}^{ESS} - Y_t^{ESS} \times P_{t-1}^{ESS}) \times \Delta t \tag{2.26}$$

In order to increase battery lifetime, the SOC of the battery should be continuously monitored, based on Eq.(2.27), to always stay within the pre-defined rated deadband which is given in Eq.(2.28).

- Maximum and minimum energy capacity of the ES

$$SOC_t = \frac{E_t^{ESS}}{E_{Tot}^{ESS}} \qquad (2.27)$$

$$\underline{E}^{ESS} \leq E_t^{ESS} \leq \overline{E}^{ESS} \qquad (2.28)$$

The RLD loads are also considered with Eq.(2.29) where the controllable power should always be less than the pre-defined maximum of the load. This is because it is desired to store excess generation power in the ESS.

$$\sum_t X_t^{RLD} \times P_t^{RLD} = \sum_t P_t^{UP} \qquad (2.29)$$

At each time interval, new operation settings can be decided by the proposed CEMS with respect to the latest changes in the MG. In other words, modified objective function and constraints would be able to generate the optimal setpoints for the MG based on the available generation, storage and demand and their associated prices.

So far in this section, required dynamic objective function and constraints suitable for MG plug-and-play and real-time operation are introduced. However, an optimization technique is required to solve the optimization problem at each interval. To satisfy the real-time MG operation, in this study, the proposed CEMS will be updated every 5 minutes. Therefore, the optimization algorithm should be fast enough to solve the problem with optimal or near optimal solutions in less than 5 minutes (including communication delays between the CEMS and individual devices). In this study, mixed-integer nonlinear programming (MINLP) is utilized in the optimization unit to solve the MG optimization problem [95]. MINLP refers to mathematical programming with continuous and discrete variables and nonlinearities in the objective function and constraints. [95]. The use of MINLP is a natural approach for formulating problems in which it is necessary to simultaneously optimize the system structure (discrete) and parameters (continuous). The general form of a MINLP is as follows [95]:

$$
\begin{aligned}
&minimize \quad f(x,y) \\
&\text{subject to} \\
&\qquad g(x,y) = g'(x,y) \\
&\qquad h(x,y) \leq h'(x,y) \\
&\qquad \text{x} \in \text{X} \\
&\qquad \text{y} \in \text{Y}
\end{aligned}
\qquad (2.30)
$$

where $f(x,y)$ is a linear/nonlinear objective function and $g(x,y)$ is a linear/nonlinear constraint function; x and y are the decision variables where

24

y is required to be integer valued (e.g., the MG characteristic matrix); and X and Y are bounding-box-type restrictions on the variables. More details about MINLP is given in [96]. The General Algebraic Mathematical System (GAMS) package with "CONOPT" solver is used in this study to implement MINLP technique [95].

As mentioned before, the proposed optimization unit attempts to minimize the cost of operation in the MG in real-time. However, it is also desired to guarantee the optimality of the solutions for the whole day of operation, not only for the current interval. The same objective function and constraints with the latest MG characteristic and offer matrices and forecasted RES generation and load demand are considered in the optimization with 5 minutes interval until the end of the day.

This structure is very useful in the optimization of time-dependent system since it considers the possible condition of the MG in the future (e.g., variation of RES class and the SOC of the ESS class). It is assumed that the consumers' demand pattern repeats each day, therefore one day of cycle is considered with optimization horizon until the end of current day. This idea is depicted in Figure 2.5.

Finally, the optimal setpoints will be passed to the LEM unit to calculate the MCP for the consumers. The setpoint also will be sent to the RTD unit to be dispatched to different devices in the MG testbed.

2.4 Local energy market (LEM) unit

In this section, a LEM is presented to calculate the cost of energy (COE) for the consumers. Once the optimization unit calculates the optimal solutions at each time interval, the LEM unit determines the market clearing price (MCP) for the consumers. The calculated MCP in the LEM might be used as the price of electricity in the consumers' monthly bill. It will also be utilized in this study to show the effectiveness of the proposed optimal CEMS in the MCP reduction.

The LEM structure could be formed either as single- or double-sided auction model [2, 3]. A Single Side Auction (SSA) model is a mechanism in which every player only can be buyer or seller, not both simultaneously. In this market structure, the auction goes to the highest bidder. Since the market structure is not a primary concern in this study, the SSA model is used in this study to keep it as simple as possible. The LEM unit can be easily modified to presents any other market structure without changing the overall proposed CEMS.
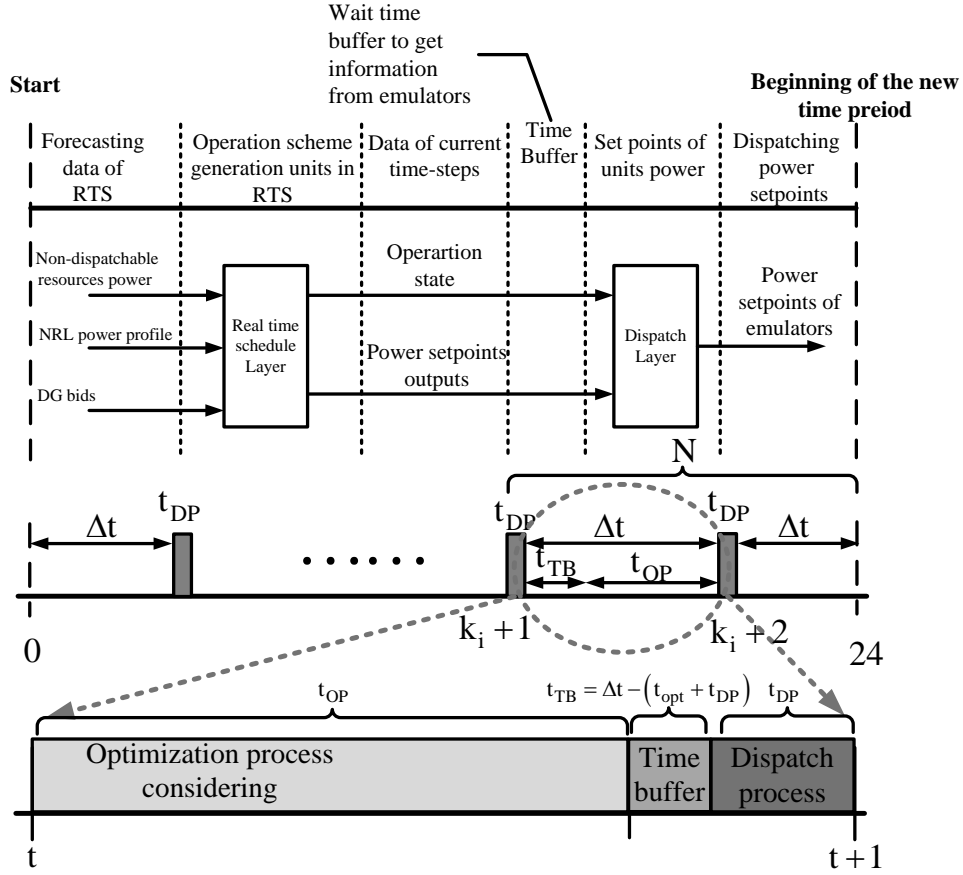
Figure 2.5: Block-diagram representation of the proposed optimization structure

The block-diagram in Figure 2.6 represents the proposed LEM structure. The optimal setpoints generated by optimization unit and the MG offer matrix are the essential inputs to the LEM unit. In the proposed LEM structuer, the load demand offer has been ignored. In this structure, the offer prices from DER and ESS units will be arranged in ascending order with step-wise functions. Eventually, the MCP is the intersection of the offer prices from the producers and the offer prices from a combination of producers who can meet the load demand as a whole. More details about the LEM unit can be found in Chapter 3 [2, 3].
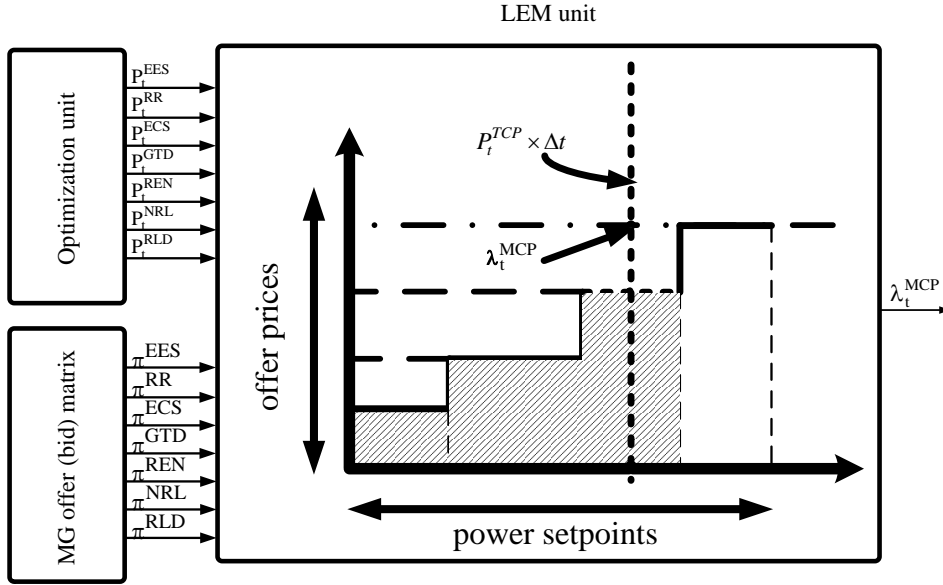
Figure 2.6: The LEM unit block-diagram representation

2.5 The real-time operation (RTO) architecture

In order to evaluate the performance of the proposed CEMS, real-time emulator environment is adapted with real communication links and delays. The block-diagram in Figure 2.7 shows the proposed RTO. Here, the idea is to model each technology and consumers' load using an emulator in the testbed. As it can be observed from Figure 2.7, the RTO structure includes four main units, namely DAQ, CEMS, RTD, and MG testbed. Different units of the proposed RTO are explained in the following subsections.

2.5.1 Data acquisition (DAQ) Unit

This unit is responsible for receiving and storing data from different devices in the MG. These data will be sent to the CEMS in order to find the optimal solution of the MG operation.

2.5.2 CEMS Unit

This unit contains the optimization unit, technology database, and LEM unit which are explained in details in Section 2.1.

Figure 2.7: Block-diagram representation of the proposed RTO

2.5.3 real-time dispatching (RTD) Unit

This unit is responsible for data transmitting from the CEMS unit (optimal operation setpoints) to the MG testbed unit. The data transmission speed and data package lost are two important parameters for data transmission [2,3]. To make sure that the data has been received by each specific device (emulator in this case), confidential signals are designed between the RTD unit and each individual device in the MG testbed.

2.5.4 The Microgrid (MG) Testbed

In this thesis, different generation resources and consumers′ load with battery storage are considered in the MG testbed, as shown in Figure 2.8. PV, WTG, and MTG are considered as the generation resources of the MG. BES is considered in the MG testbed as storage device. The consumers′ load is divided to NRL and RLD. Figure 2.9 shows a picture of the experimental MG testbed in the laboratory setup. The designed structure is modular in which more emulators for extra generation and storage devices can be

Table 2.1: The offers suggested by the micro-sources and the consumers have been presented [€/kWh]

π^{WTG}	π^{PV}	π^{MTG}	π^{ES-}	π^{ES+}	π^{UP}	π^{RLD}
0.083	0.1	0.15	0.145	0.125	1.5	0.105

added to the system without any further modifications in the running software. More information on the experimental setup is given in [2, 3]. Actual WTG, PV, and load demand data are used in this study which are taken from [2, 3]. These data are measured every 5 minutes of a same day. The real-time operation is performed every 5 minutes because of the following reasons:

1. Sending and receiving data from/to the devices (i.e., emulators) takes 1.5-3 seconds. The best performance is achieved with 3 seconds delay. In addition, the optimization unit spends 3 minutes in average to find the optimal solutions

2. The measured data does not show any meaningful variation in 5 minutes interval

In Table 2.1, the constant offer prices used for different devices are reported.

2.6 Proposed timing schedule for distributed energy

The DER scheduling method suggested in this thesis consists of optimizing accessible sources with three different time intervals such as Day ahead, hour ahead and 5 minute ahead. This method is shown in Figure 2.10.

As it is observed in this figure, this method has hourly day-ahead scheduling (HDAS) and five minute real-time scheduling (FMRTS) blocks. Day-ahead scheduling is used as input data for the HDAS method. Based on the figure, the inputs related to HDAS block are respectively energy price offers, the contracts related to DR and the specifications related to DER sources considered in the system. But, the information related to forecast data in each five minute interval for renewable energy sources and loads, the specification of new equipment connected to the system or disconnected from

Figure 2.8: Schematic diagram of the IREC′s MG testbed

the system, the information related to the incident that take place in the system and also the execution time of these incidents have been considered as FMRTS block inputs.

The information that the central control unit (CCU) receives from the HDAS block includes load management and curtailment signal and DR value with minimum cost of operation.

The FMRTS block output has the responsibility of load and DR management and all real-time scheduling. In real-time scheduling the aim of CCU is to find the best and fastest method for responding to the incident occurred in the system and to give DERs and consumers the necessary orders.
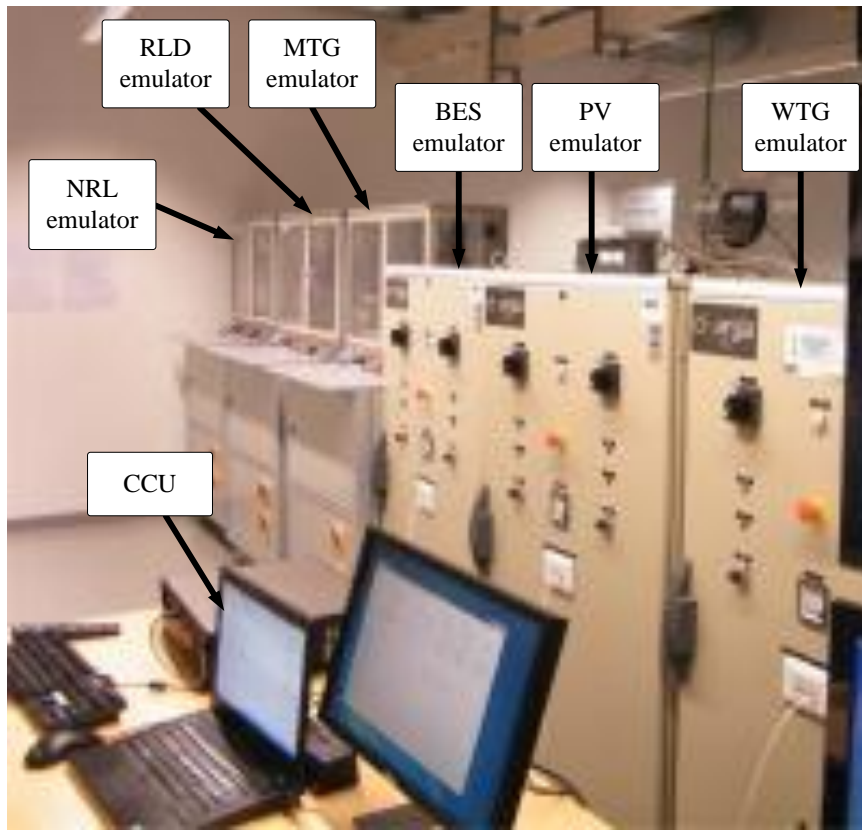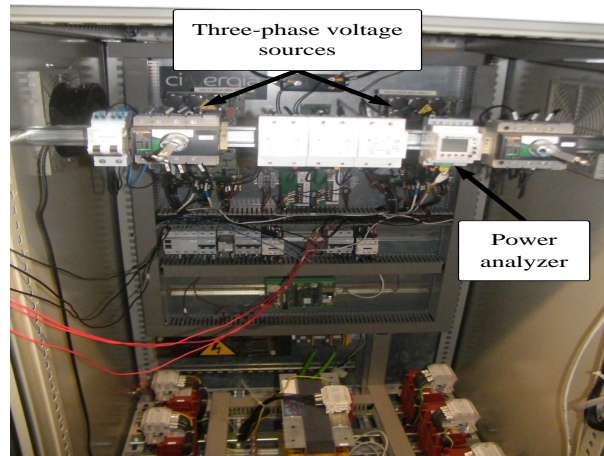
(a) IREC′s MG

(b) Cabinet inside details

Figure 2.9: System configuration of IREC′s MG Testbed

Figure 2.10: Methodology suggested for investigating HDAS and FMRTS in the isolated system

3

Local energy market (LEM) unit

3.1 Introduction

In a day-ahead energy auction, micro-sources submit supply offers and load representatives submit load declarations for each trading interval (hour or half-hour in the present study) of the next day to the system (or market) operator. Supply offers and load declarations can be either "priced", in the form of a set of price-quantity (€/kWh-kWh) pairs, or "non-priced", in the form of quantity (kWh) only offers or bids. The system operator processes the supply offers and the load declarations and computes the price (market clearing price: MCP) that clears the market as well as the trading volume.

In the DA energy market each generating unit submits energy offers for each trading interval of the following day. In deregulated markets, auction is the most common pricing mechanism used to match the active power demand supply.

An auction can be viewed as an assignment problem. The problem is to assign an offer from a seller to a buyer. The objective is to maximize the satisfaction of both the buyer and the seller. Several types of auctions exist, but this thesis will be focused on two of them, namely Single-side (SSA) and Double-side auction (DSA) mechanisms and specifically DSA market will be developed on the proposed system.

Over a period of 24 hours of work in islanded mode, the MG may have an excess of power generation (caused by weather conditions or a decrease of consumption) or a lack of power generation (due to the shutdown of

microsources and sudden increase of consumption, among others).

Two different algorithms for EMS namely $MCEMS_{-LEM}$ and $EMS-MINLP_{-LEM}$ are compared in this thesis. The implementation and development of the LEM unit are presented as follows.

In the conventional EMS, when the sum of power generation by the WT (P_t^{WT}) and the PV (P_t^{PV}) is more than the main load demand (P_t^n), the MG will have power excess. This is shown in Figure 3.1(a) and, stated by

$$P_t^{EGP} = (P_t^{WT} + P_t^{PV}) - P_t^n \qquad (3.1)$$

However, in $EMS - MINLP_{-LEM}$, the excess power is created when the sum of the power generated by the micro-sources is greater than the main load demand as is shown in Figure 3.1(b). This subject can also be stated by

$$P_t'^{EGP} = P_t^{TPP} - P_t^n \qquad (3.2)$$

where

$$P_t^{TPP} = P_t^{WT} + P_t^{PV} + P_t^{MT} + P_t^{ES,d} \qquad (3.3)$$

In both of the presented EMS algorithms, when the MG is unable to feed the main load, the lack of power can be calculated by the following equation (as shown in Figure 3.1(c)).

$$P_t^{UP} = P_t^n - P_t^{TPP} \qquad (3.4)$$

The excess of generated power (EGP) in the isolated MG can be used, if necessary, to feed other MG elements, for example, ES, DR loads and auxiliary EWH. In $MCEMS_{-LEM}$, the EGP is used to charge ES. If the EGP exceeds the power required for charging the ES, its difference is used for feeding the DR, and, if no DR exists, the ES can be used for feeding EWH.

The $EMS - MINLP_{-LEM}$ is treated in a different way. Since within this algorithm, the central control selects the best performance method and schedules generation sources to ensure minimum cost, the EGP can be used simultaneously for feeding one or more consumption sources (including ES, DR and EWH) depending on objective function.

(a) EGP in $MCEMS$

(b) EGP in $EMS - MINLP$

(c) UP in both EMS
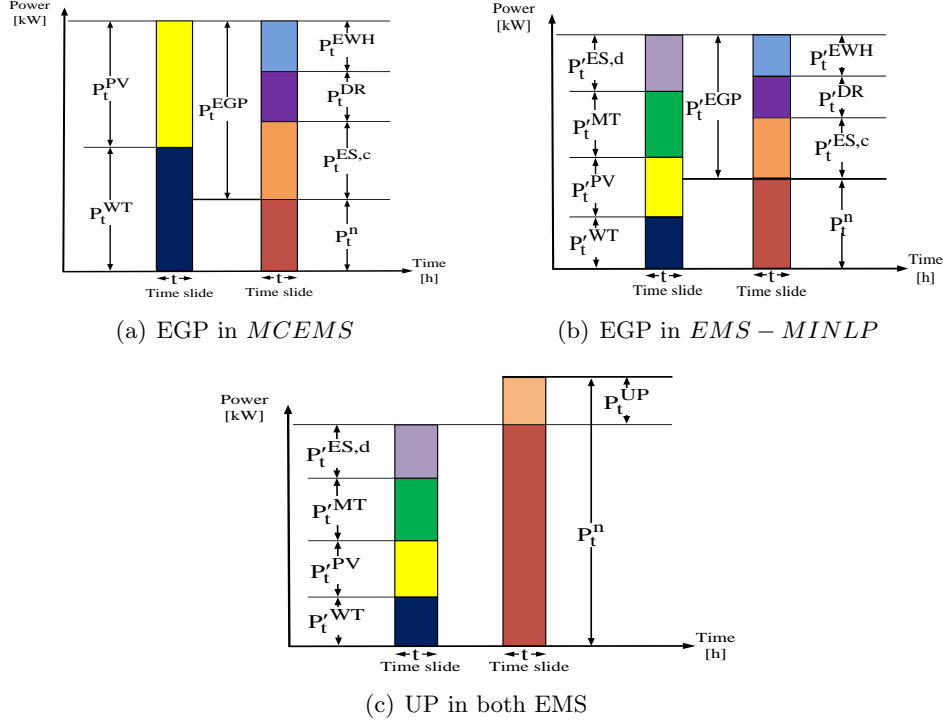
Figure 3.1: EGP and UP in both proposed EMS

3.2 Single side auction (SSA)

SSA ignores demand side bidding and it has been used for pricing where one of the parties offers to sell a resource willing to receive certain amount of money. Bids are sorted in ascending order based on the price. The energy offers of the units are sorted in the form of increasing stepwise functions consisting of up to four price (€/kWh-kWh) -quantity (kWh) pairs as shown in Figure 3.2. Two cases will occur in the calculation of Market Clearing Price (MCP). At the first case, P_t^{TCP} is less than the summation of the produced power by generation units (P_t^{TGP}). In this case, MCP will be the intersection between quantity demand line and the proposed price by generation unit in order to completely meet the demand. The covered demand is shown within shaded area in Figure 3.2. In the other case, the requested demand is bigger than the generated power and the MG is not able to supply the demand completely. MCP will be calculated as the maximum proposed offer by generation units [2,3].
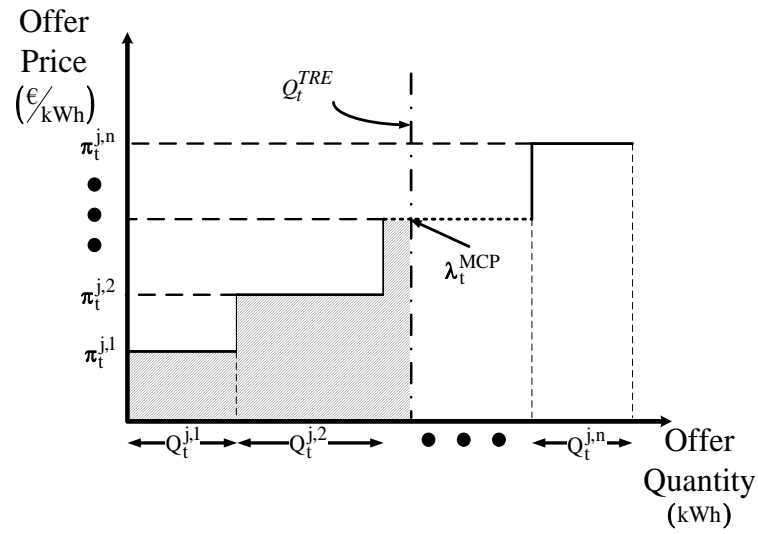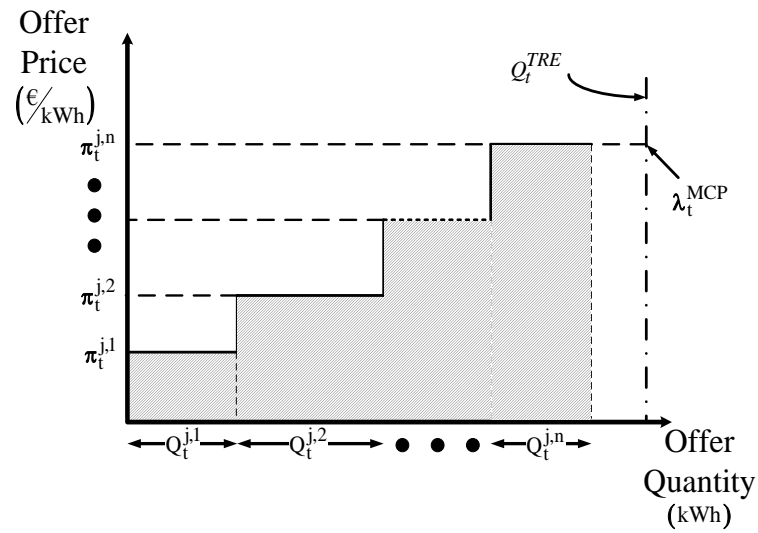
(a) $Q_t^{TRE} \le Q_t^{TGE}$

(b) $Q_t^{TRE} \ge Q_t^{TGE}$

Figure 3.2: Step-wise energy and offer price by micro-source and demand in MG

The presented LEM ignores the demand side bidding, since only SSA market is considered. SSA is a mechanism in which there are only potential

buyers or sellers, but not both at the same time. In this system, auction goes to the highest bidder. Energy offers are sorted in the form of increasing stepwise functions consisting of up to four price ($\text{\euro}$/kWh-kWh)-quantity (kWh) pairs as shown in Figure 3.2. In this study, two possibilities are considered for the MCP calculation. The first possibility is when $Q_t^{TRE} \leq Q_t^{TGE}$. As a result MCP will be the intersection between quantity demand line and the offer (Figure 3.2(a)). The covered demand is shown within the shaded area in Figure 3.2. The second possibility is $Q_t^{TRE} \geq Q_t^{TGE}$ (Figure 3.2(b)). In this case, some customer loads, equal to the unmet power, have to be shed to cope with the current situation. Thus, MCP will be calculated as the maximum proposed offer by generation units. MCP calculation is done by Algorithm 1.

Algorithm 1 LEM UNIT

Require: Wholesales energy prices, the number of generation unit (n) and total generation and consumers energy of the MG.

1: $Stop \leftarrow 0$
2: $i \leftarrow 1$
3: **while** $Stop = 0$ **do**
4:     **if** $Q_t^{TRE} \leq \sum_{k=1}^{i} Q_t^{j,k}$ **then**

$$\lambda_t^{MCP} = \pi_t^{j,k}; \tag{3.5}$$

$$Stop \leftarrow 1$$

5:     **else if** $i \geq n$ **then**

$$\lambda_t^{MCP} = \pi_t^{j,n}; \tag{3.6}$$

$$Stop \leftarrow 1$$

6:     **else**
7:         $i \leftarrow i + 1$
8:     **end if**
9: **end while**
10: **return** λ_t^{MCP}

3.3 Double side auction (DSA)

In the case of double-side auction, sellers and buyers, offer price and quantity as seen in Figure 3.3. Clearing-house collects the information and based on the bids and also the created cases which will be explained in detail in the next section, MCP can be obtained under different conditions.

The flowchart of the proposed DSA algorithm is demonstrated in Figure 3.4 which accounts for some of the following cases:

- Case 1:

  if the maximum offer price by customers $(\pi_t'^{i1})$ is less than the minimum offer price by generation units (π_t^{i1}) $(\pi_t'^{i1} \leq \pi_t^{j1})$, MCP will be equal to the minimum offer price by generation units. Mathematically, it can be formulated as:

$$\lambda_t^{MCP} = \pi_t^{j1} \tag{3.7}$$

$$P_t^{TCP} = 0 \tag{3.8}$$

$$P_t^{TGP} = 0 \tag{3.9}$$

$$P_t^{UP} = C_2/\Delta(t) \tag{3.10}$$

$$P_t^{EGP} = P_t^{TGP} \tag{3.11}$$

  where

$$C_2 = Q_t'^{i1} + Q_t'^{i2} + Q_t'^{i3} \tag{3.12}$$

- Case 2:

  if the offer price by customers is equal zero but its previous offer price is bigger than the previous offer price proposed by generation, the following cases should be investigated:
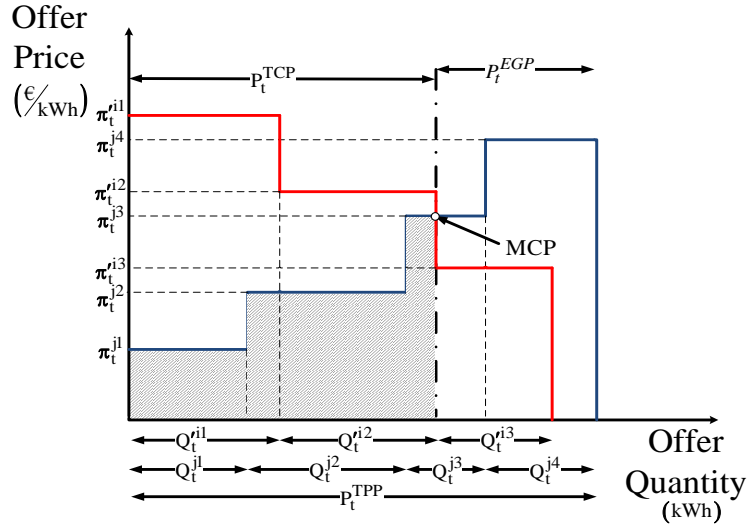
(a) Case 1
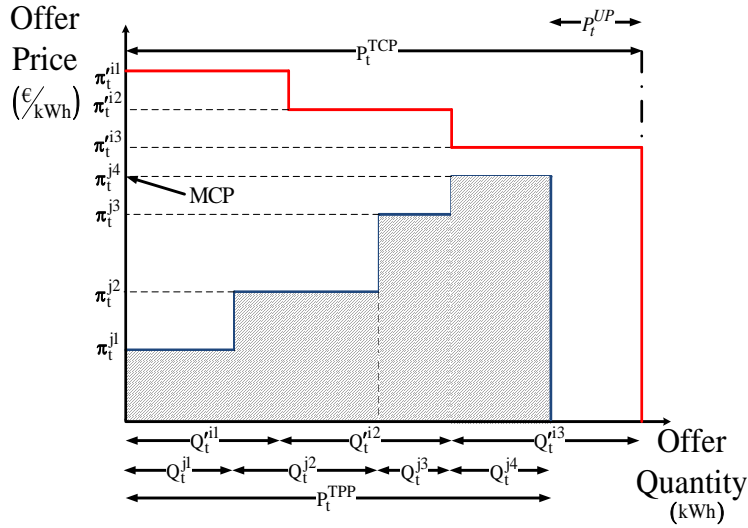
(b) Case 2

Figure 3.3: Step-wise energy and price offer in DSA market

$$\lambda_t^{MCP} = \begin{cases} \pi_t^{j1} & C_2 \leq Q_t^{j1} \\ \pi_t^{j2} & Q_t^{j1} \leq C_2 \leq G_1 \\ \pi_t^{j3} & G_1 \leq C_2 \leq G_2 \\ \pi_t^{j2} & G_2 \leq C_2 \leq G_3 \\ \pi_t^{j4} & C_1 \geq C_3 \end{cases} \qquad (3.13)$$

39
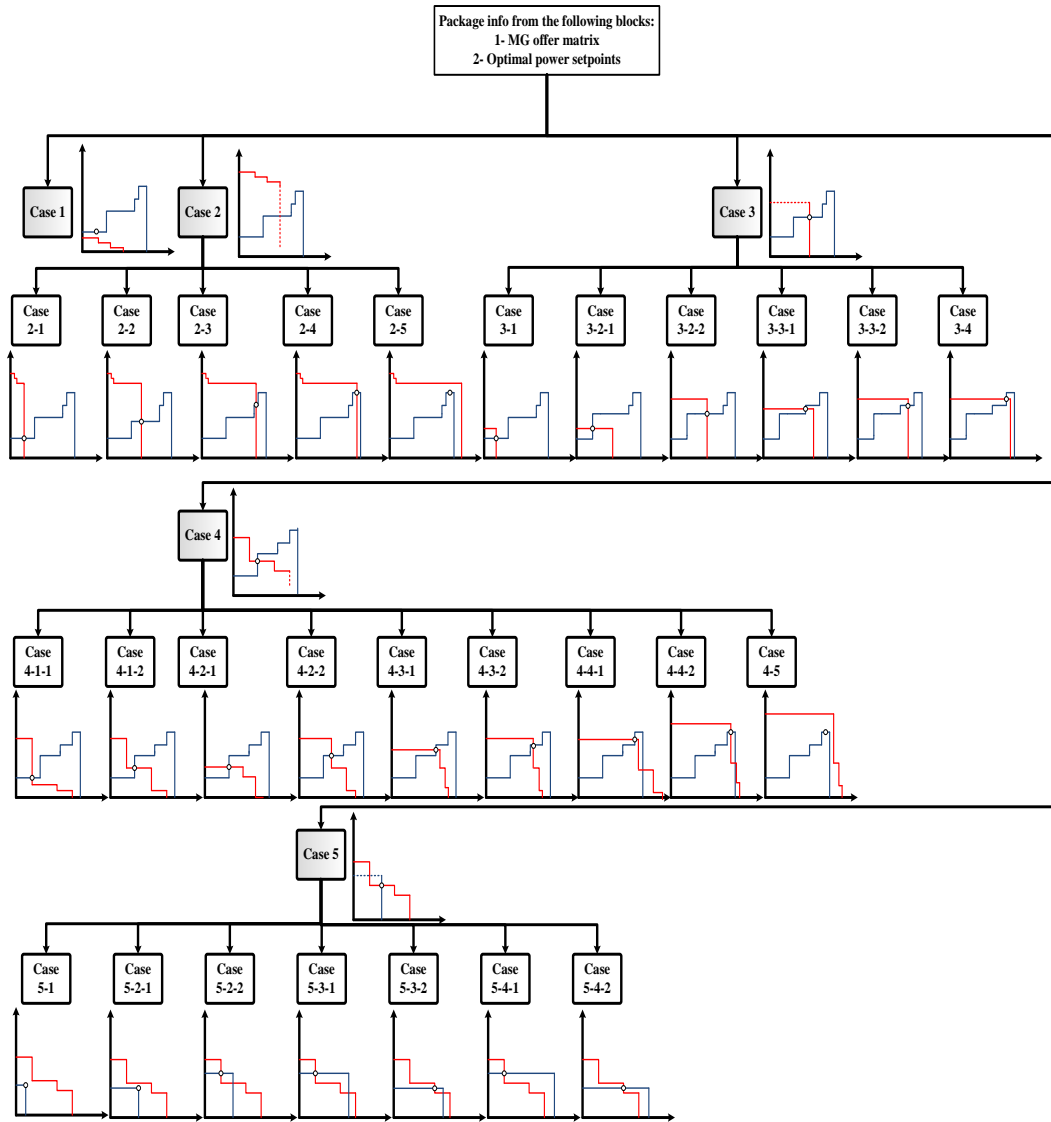
Figure 3.4: Some cases considered in DSA market

$$P_t^{TCP} = \begin{cases} G_3 & C_1 \geq G_3 \\ C_2 & Otherwise \end{cases} \qquad (3.14)$$

$$P_t^{UP} = \begin{cases} C_2 - G_3 & C_1 \geq G_3 \\ 0 & Otherwise \end{cases} \tag{3.15}$$

$$P_t^{EGP} = \begin{cases} 0 & C_1 \geq G_3 \\ G_3 - C_2 & Otherwise \end{cases} \tag{3.16}$$

were

$$G_1 = Q_t^{j1} + Q_t^{j2} \tag{3.17}$$

$$G_2 = G_1 + Q_t^{j3} \tag{3.18}$$

$$G_3 = G_2 + Q_t^{j4} \tag{3.19}$$

- Case 3:

  if the offer price by customers is equal zero but its previous offer price is bigger than the previous offer price proposed by generation, the following cases should be investigated.

$$\lambda_t^{MCP} = \begin{cases} \pi_t^{j1} & Q_t'^{i1} \leq Q_t^{j1} \\ \pi_t'^{i1} & \max(Q_t^{j1}, G_2) \leq Q_t'^{i1} \leq \min(G_1, G_3) \\ \pi_t^{j2} & Q_t^{j1} \leq Q_t'^{i1} \leq G_1 \\ \pi_t'^{i1} & G_1 \leq Q_t'^{i1} \leq G_2 \end{cases} \tag{3.20}$$

$$P_t^{TCP} = \begin{cases} Q_t^{j1} & \pi_t'^{i1} \leq \pi_t'^{j2} \\ Q_t^{j2} & \pi_t'^{i1} \leq \pi_t'^{j3} \\ Q_t'^{i1} & \max(\pi_t^{j1}, \pi_t^{j3}) \leq \pi_t'^{i1} \leq \pi_t'^{j2} \end{cases} \tag{3.21}$$

$$P_t^{UP} = \begin{cases} Q_t'^{i1} - Q_t^{i1} & \pi_t'^{i1} \leq \pi_t^{j2} \\ Q_t'^{i1} - G_1 & \pi_t'^{i1} \leq \pi_t'^{j3} \\ 0 & Otherwise \end{cases} \tag{3.22}$$

$$P_t^{EGP} = G_3 + Q_t'^{i1} \tag{3.23}$$

- Case 4:

  In this case, all of costomers proposed their offers (as shown in Figure 3.4). Under this situation, it is possible to meet a lot of cases which some of these cases can be stated by Algorithm 2.

- Case 5:

  MCP can be calculated by a Pseudo-code in Algorithm 3.

Algorithm 2 CALCULATING OF λ_t^{MCP} IN CASE 4

Require: Generation units and load demand active power profiles, supply
  bids (according to Table 5.2), MG charactristic (according to Table 5.1)
  if $\pi_t'^{i2} \leq \pi_t^{j2}$ **then**
    if $Q_t'^{i1} \leq Q_t^{j1}$ **then**
      if $\pi_t'^{i2} \leq \pi_t^{j2}$ **then**
        if $Q_t'^{i1} \leq Q_t^{j1}$ **then**
          if $\pi_t'^{i2} \leq \pi_t^{j1}$ **then**   ▷ Case 4-1-1

$$
\begin{cases}
\lambda_t^{MCP} = \pi_t^{j1} \\
P_t^{TCP} = Q_t'^{i1} \\
P_t^{UP} = C_2 - P_t^{TCP} \\
P_t^{EGP} = G_3 - P_t^{TCP}
\end{cases}
\tag{3.24}
$$

          else   ▷ Case 4-1-2

$$
\begin{cases}
\lambda_t^{MCP} = \pi_t'^{i2} \\
P_t^{TCP} = Q_t^{j1} \\
P_t^{UP} = C_2 - P_t^{TCP} \\
P_t^{EGP} = G_3 - P_t^{TCP}
\end{cases}
\tag{3.25}
$$

          end if
        else if $Q_t^{j1} \leq Q_t'^{i1} \leq G_1$ **then**
          if $\pi_t'^{i1} \leq \pi_t^{j2}$ **then**   ▷ Case 4-2-1

$$
\begin{cases}
\lambda_t^{MCP} = \pi_t'^{i1} \\
P_t^{TCP} = Q_t^{j1} \\
P_t^{UP} = C_2 - P_t^{TCP} \\
P_t^{EGP} = G_3 - P_t^{TCP}
\end{cases}
\tag{3.26}
$$

          else   ▷ Case 4-2-2

$$
\begin{cases}
\lambda_t^{MCP} = \pi_t^{j2} \\
P_t^{TCP} = Q_t'^{i1} \\
P_t^{UP} = C_2 - P_t^{TCP} \\
P_t^{EGP} = G_3 - P_t^{TCP}
\end{cases}
\tag{3.27}
$$

          end if

43

Algorithm 2 (continued)
___

$\qquad$ **else if** $G_1 \leq Q_t'^{i1} \leq G_2$ **then**

$\qquad\quad$ **if** $\pi_t'^{i1} \leq \pi_t^{j3}$ **then** $\hfill \triangleright$ Case 4-3-1

$$\begin{cases} \lambda_t^{MCP} = \pi_t'^{i1} \\ P_t^{TCP} = G_1 \\ P_t^{UP} = C_2 - P_t^{TCP} \\ P_t^{EGP} = G_3 - P_t^{TCP} \end{cases} \tag{3.28}$$

$\qquad\quad$ **else** $\hfill \triangleright$ Case 4-3-2

$$\begin{cases} \lambda_t^{MCP} = \pi_t^{j3} \\ P_t^{TCP} = Q_t'^{i1} \\ P_t^{UP} = C_2 - P_t^{TCP} \\ P_t^{EGP} = G_3 - P_t^{TCP} \end{cases} \tag{3.29}$$

$\qquad\quad$ **end if**

$\qquad$ **else if** $G_2 \leq Q_t'^{i1} \leq G_3$ **then**

$\qquad\quad$ **if** $\pi_t'^{i1} \leq \pi_t^{j4}$ **then** $\hfill \triangleright$ Case 4-4-1

$$\begin{cases} \lambda_t^{MCP} = \pi_t'^{i1} \\ P_t^{TCP} = G_2 \\ P_t^{UP} = C_2 - P_t^{TCP} \\ P_t^{EGP} = G_3 - P_t^{TCP} \end{cases} \tag{3.30}$$

$\qquad\quad$ **else** $\hfill \triangleright$ Case 4-4-2

$$\begin{cases} \lambda_t^{MCP} = \pi_t^{j3} \\ P_t^{TCP} = Q_t'^{i1} \\ P_t^{UP} = C_2 - P_t^{TCP} \\ P_t^{EGP} = G_3 - P_t^{TCP} \end{cases} \tag{3.31}$$

$\qquad\quad$ **end if**

$\qquad$ **else** $\hfill \triangleright$ Case 4-5

$$\begin{cases} \lambda_t^{MCP} = \pi_t^{j4} \\ P_t^{TCP} = G_3 \\ P_t^{UP} = C_2 - P_t^{TCP} \\ P_t^{EGP} = 0 \end{cases} \tag{3.32}$$

$\qquad\quad$ **end if**
$\qquad\quad$ **end if**
$\qquad$ **end if**
end if
$\qquad$ **return** λ_t^{MCP}

Algorithm 3 CALCULATING OF λ_t^{MCP} IN CASE 5

Require: Generation units and load demand active power profiles, supply bids (according to Table 5.2), MG charactristic (according to Table 5.1)
  if $Q_t^{j1} \leq Q_t'^{i1}$ **then**   ▷ Case 5-1

$$
\begin{cases}
\lambda_t^{MCP} = \pi_t^{j1} \\
P_t^{TCP} = Q_t^{j1} \\
P_t^{UP} = C_2 - P_t^{TCP} \\
P_t^{EGP} = 0
\end{cases}
\tag{3.33}
$$

    else if $Q_t'^{i1} \leq Q_t^{j1} \leq C_1$ **then**
      if $\pi_t^{j1} \leq \pi_t'^{i2}$ **then**   ▷ Case 5-2-1

$$
\begin{cases}
\lambda_t^{MCP} = \pi_t^{j1} \\
P_t^{TCP} = Q_t^{j1} \\
P_t^{UP} = C_2 - P_t^{TCP} \\
P_t^{EGP} = 0
\end{cases}
\tag{3.34}
$$

      else   ▷ Case 5-2-2

$$
\begin{cases}
\lambda_t^{MCP} = \pi_t^{j1} \\
P_t^{TCP} = Q_t'^{i1} \\
P_t^{UP} = C_2 - P_t^{TCP} \\
P_t^{EGP} = Q_t^{j1} - P_t^{TCP}
\end{cases}
\tag{3.35}
$$

      end if
    else if $C_1 \leq Q_t^{j1} \leq C_2$ **then**
      if $\pi_t^{j1} \leq \pi_t'^{i2}$ **then**   ▷ Case 5-3-1

$$
\begin{cases}
\lambda_t^{MCP} = \pi_t^{j1} \\
P_t^{TCP} = Q_t'^{i1} \\
P_t^{UP} = C_2 - P_t^{TCP} \\
P_t^{EGP} = Q_t^{j1} - P_t^{TCP}
\end{cases}
\tag{3.36}
$$

      else if $\pi_t^{i3} \leq \pi_t^{j1} \leq \pi_t'^{i2}$ **then**   ▷ Case 5-3-2

$$
\begin{cases}
\lambda_t^{MCP} = \pi_t^{j1} \\
P_t^{TCP} = C_1 \\
P_t^{UP} = C_2 - P_t^{TCP} \\
P_t^{EGP} = Q_t^{j1} - C_2
\end{cases}
\tag{3.37}
$$

Algorithm 3 (continued)

   else if $Q_t^{i1} \geq C_2$ **then**
       if $\pi_t^{j1} \leq \pi_t'^{i2}$ **then** $\triangleright$ Case 5-4-1

$$\begin{cases} \lambda_t^{MCP} = \pi_t^{j1} \\ P_t^{TCP} = Q_t'^{i1} \\ P_t^{UP} = C_2 - P_t^{TCP} \\ P_t^{EGP} = Q_t^{j1} - P_t^{TCP} \end{cases} \tag{3.38}$$

       else if $\pi_t'^{i3} \leq \pi_t^{j1} \leq \pi_t'^{i2}$ **then** $\triangleright$ Case 5-4-2

$$\begin{cases} \lambda_t^{MCP} = \pi_t^{j1} \\ P_t^{TCP} = C_1 \\ P_t^{UP} = C_2 - P_t^{TCP} \\ P_t^{EGP} = Q_t^{j1} - P_t^{TCP} \end{cases} \tag{3.39}$$

       end if
     end if
   end if
     return λ_t^{MCP}

4

Mathematical implementation of the optimization units

In this thesis, some algorithms for implementing EMS based on LEM by using heuristic technique and no optimization method are presented as shown in Figure 4.1. The advantages of these algorithms in terms of system′s real time performance are investigated in Chapter 5. This algorithm is presented for implementing EMS in both isolated and grid connected MG and has abilities including flexibility, high speed in decision making and adaptability after adding or eliminating micro-sources in the system. This algorithm is made up of two units namely EMS and LEM units as shown in Figure 4.1. How to implement LEM unit has been investigated in Chapter 3. The performance and implementation of each units are explained in detail in the following subsections.

4.1 Modified conventional energy management systems (MCEMS) unit

MCEMS unit is proposed to dispatch power set points in a MG comprises PV, WT, MT and ES systems. The proposed unit is illustrated by a Pseudo-code in Algorithm 5. In this unit, when the sum of the produced power by the PV and WT is more than the load demand, and the battery is not in Fully Charged Mode, the battery bank can be operated in two operation
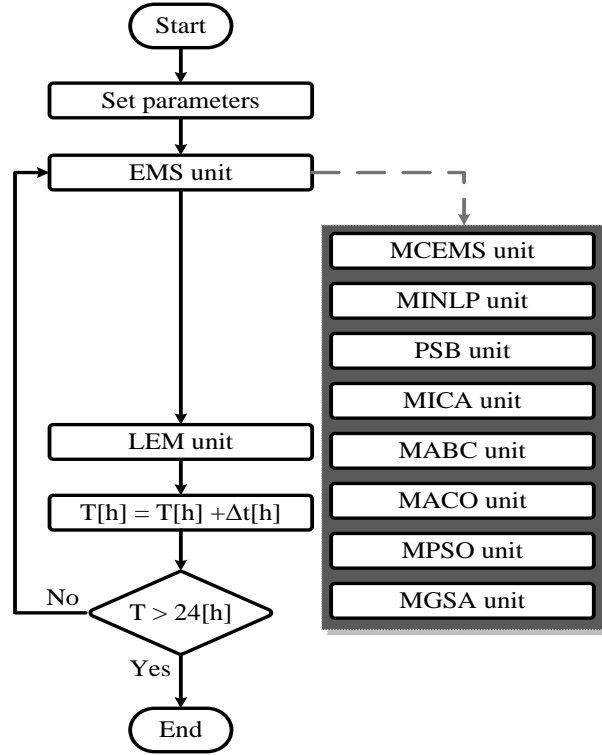
Figure 4.1: The proposed algorithms for EMS

modes (i.e. Charging and Over Charging Protection Modes). Likewise, the discharge process can be used in the case when the power generated by the hybrid system does not meet the load demand completely. In this case, ES can also work in two operation modes namely Discharging and Over Discharging Protection Modes during Discharging Mode.

Each of operation modes have been presented in detail in [97].

The main goal of MCEMS unit is to ensure that the customer demand is met at all times. Summarily, objectives of MCEMS unit are identified as follows:

- To maximize utilization of the available renewable resources;

- To maximize battery life by monitoring and controlling both SOC and charge/discharge process;

- To maximize the average of available stored energy in the battery, improving system reliability;

- To use the excess available WT and PV to supply a useful dump load when the battery is fully charged in order to increase system efficiency.

This algorithm is used for implementing EMS in the isolated and grid connected MG and has abilities including flexibility, high speed in decision making and adaptability after adding or eliminating micro-sources in the system [2]. But in this algorithm, the related setpoints for generation units could not reach the optimal points.

For implementing the MCEMS algorithm the following cases are considered:

- If the sum of power generated by WT and PV is more than the load consumed power, excess power can be used for charging the battery under the following conditions:

  a) Excess power must be less that $\overline{P}_t^{ES,c}$ so ES cannot operates within the limits;

  b) battery SOC after charging must be less than $\overline{SOC}$. This means that the energy stored in ES after its charging must be greater than $\overline{E}^{ES}$ (Eq. (2.21));

- If the conditions stated in the first item do not met, the total or a part of the mentioned power can be used for feeding EWH;

- If sum of power generated by WT and PV is less than the load consumed power, the power shortage for supplying the total load can be supplied by ES discharging under these conditions:

  a) The amount of power shortage shall not be more than $\overline{P}_t^{ES,d}$;

  b) Battery SOC after discharge must be more than $\underline{SOC}$. This means that the energy stored in ES after its discharge shall not be less than $\underline{E}^{ES}$ (Eq. (2.21))

- If the conditions stated in item 3 do not hold, in that case the total or a part of the shortage can be supplied by MT considering the following conditions:

  a) If the difference between lack of power and $\overline{P}_t^{ES,d}$ is more than $\underline{P}_t^{MT}$, the battery is discharged to the amount that is possible and then the rest of the power required will be supplied by MT.

  b) If the difference between power and $P_t^{ES,d}$ is less than $\underline{P}_t^{MT}$, in that case battery discharge will be neglected and MT enters service with its minimum power. In these conditions, part of the

power generated by MT is spent on the complete feeding of the consumed load and its other part is also used for charging the battery. In all of the cases mentioned, SOC must be smaller than $\overline{SOC}$ after charging and greater than $\underline{SOC}$ after discharging. Under these conditions the life of ES system and as a result the reliability of microgrid system will increase.

4.2 Mixed integer non-linear programming (MINLP) unit

Linear programming (LP) has a diverse range of real-life applications in economic analysis, planning, operations research, computer science and engineering due to its simplicity [98]. It is well-known that the number of iterations in the LP is just a small multiple of the problem dimension [99], which consequently hold it as a promising candidate in this study.

Where some nonlinear equations in the model are non-linear, hence nonlinear programming is also used to solve the problem. Mixed integer linear programming (MINLP) refers to mathematical programming with continuous and discrete variables and nonlinearities in the objective function and constraints [95]. The use of MINLP is a natural approach of formulating problems where it is necessary to simultaneously optimize the system structure (discrete) and parameters (continuous). The general form of a MINLP is as [95]:

$$
\begin{aligned}
minimize \quad & f(x,y) \\
subject\ to \quad & \\
& g(x,y) = g'(x,y) \\
& h(x,y) \leq h'(x,y) \\
& x \in X \\
& y \in Y
\end{aligned}
\tag{4.1}
$$

where $f(x,y)$ is a linear/nonlinear objective function and $g(x,y)$ is a linear/nonlinear constraint function; x,y are the decision variables, where y is required to be integer valued (e.g., the MG characteristic matrix); and X and Y are bounding-box-type restrictions on the variables. More detail about MINLP is given in [96]. The General Algebraic Mathematical System (GAMS) package with "CONOPT" solver is used in this study to implement MINLP technique [95].

4.3 Pivot source based (PSB) unit

PSB unit make the necessary decisions for each productive resources present in the MG system in each time interval to operate, to schedule optimally by e.g. minimizing production costs in such systems. This unit is illustrated in Figure 4.2. In fact, this unit puts a series of decisions such as the determination of power setpoints related to each power resources. These cases must be considered with attention to reducing COE as well as finding the lowest MCP in each time interval.

The cost function considered is based on minimizing the production cost by taking into account all the constraints on each micro-source.

$$MIN\left[\sum_{t=1}^{24}\left(\sum_{i=1}^{n}P_t^{g,i}\times\pi^{g,i}-\sum_{j=1}^{m}P_t^{c,j}\times\pi^{c,j}+P_t^{UP}\times\pi^{UP}\right)\right]\times\Delta t \qquad (4.2)$$

Where $P_t^{g,i}\times\pi^{g,i}$ and $P_t^{c,j}\times\pi^{c,j}$ are cost of energy produced by generation units and consumed by costumers, respectively. Also, $P_t^{UP}\times\pi^{UP}$ represent the penalty cost due to unmet power.

Moreover, some constraints are defined according with system limitation and requirement. These constraints are:

- High and low limitations for renewable resources

$$\underline{P}^{g,i}\leq P_t^{g,i}\leq\overline{P}^{g,i} \qquad (4.3)$$

- Constraints related to minimum down and up time in non-renewable resources

$$\left[X_{t-1}^i-\overline{T}^i\right]\cdot\left[I_{t-1}^i-I_t^i\right]\geq0,\forall i,t \qquad (4.4)$$

$$\left[-X_{t-1}^i-\underline{T}^i\right]\cdot\left[I_t^i-I_{t-1}^i\right]\geq0,\forall i,t \qquad (4.5)$$

- Constraints related to the ramp rate in non-renewable resources

$$P_t^{g,i}-P_{t-1}^{g,i}\leq\overline{R}^i \qquad (4.6)$$

$$P_{t-1}^{g,i}-P_t^{g,i}\leq\underline{R}^i \qquad (4.7)$$

Figure 4.2: EMS-PSB algorithm

- Maximum power during changing and discharging in the ES system

$$P_t^{ES,d} \leq \overline{P}^{ES,d} \qquad (4.8)$$

$$P_t^{ES,c} \leq \overline{P}^{ES,c} \qquad (4.9)$$

- Maximum and minimum stored energy in the ES system

$$\underline{E}^{ES} \leq E_t^{ES} \leq \overline{E}^{ES} \tag{4.10}$$

- Power balance

$$\sum_{i=1}^{n} P_t^{g,i} + P_t^{ES,d} = \sum_{j=1}^{m} P_t^{c,j} + P_t^{ES,c} \tag{4.11}$$

- Power limitation for responsive load demand (RLD)

$$P_t^{c,j} \leq \overline{P}^{c,j} \tag{4.12}$$

EMS establishes a string of decisions containing the set points for devices, step by step, for each time interval and the energy management problem can be seen as one of planning. In this case we have to know, if at each time interval the optimal solution will be chosen, at the end of the entire process (e.g. one day), the EMS will obtain or not the global optimal solution. Unfortunately, the Bellman′s principle of optimality ("an optimal policy has the property that whatever the initial state and initial decision are, the remaining decisions must constitute an optimal policy with regard to the state resulting from the first decision." [100]) is not satisfied in this case because of the ES device:

1. there are time intervals where the microgrid needs to use the ES device in charging mode, but it cannot because the ES is fully charged or cannot be used in charging mode an entire time interval;

2. there are time intervals where the microgrid needs to use the ES device in discharging mode, but it cannot because the ES is fully discharged or cannot be maintained in discharging mode the entire time interval.

It is obvious that, for each time interval, the steady state of each device from the microgrid is influenced by the SOC of the ES, which was established in the previous time interval. Consequently, an effective and fast heuristic algorithm based on a pivot source is proposed, which is focused on the principle: avoid wastage of the existing renewable potential at each time interval (sunlight, wind, water, etc.). Having the ordered list of sources, the crossing point with the vertical line, indicating the total required power by consumers (loads), represents the "pivot source" (Figure 4.3); concomitantly,

all offers located on the left side of this line are selected as power sources for the microgrid. This decision is valid up to the next time interval, when the presented procedure is once again put into operation. This approach has two important advantages:

1. this algorithm does not working with a set of potential solutions as genetic algorithms or swarm intelligence approaches do. Due to this fact, the proposed algorithm satisfies an important aim, i.e. to be as simple as possible in order to be a fast one.

2. the optimization algorithms based on genetic paradigm or swarm intelligence have different behavior at each run; for the same set of input data, at each run, the output data is slightly different because of the stochastic behavior of these approaches. The proposed algorithm, due to its structure, for the same set of input data, always provides the same output data at each run and the algorithm is complex enough in order to obtain a good quality solution.
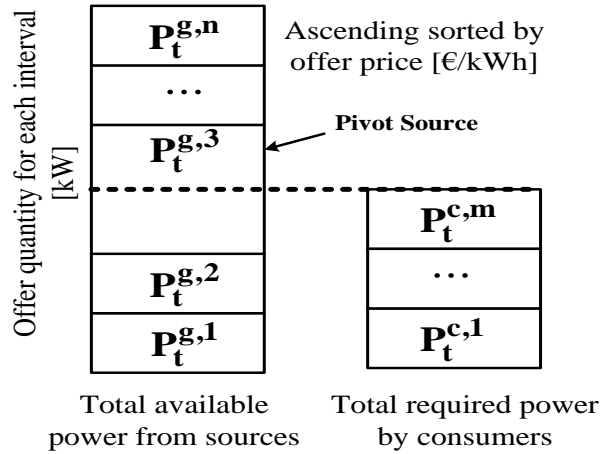
Figure 4.3: Finding the pivot source at a time interval

4.4 Multi-dimension imperialist competition algorithm (MICA) unit

Imperialist competition algorithm that is based on population and political and social evolution of human societies; is introduced by Atashpaz and

Lucas in the year 2007 [101]. This algorithm has several advantages such as simplicity, accuracy and saving time. On the other hand, because of high convergence speed and the ability of finding general optimum solution compared to other innovative optimum methods, it can be reached economic results with high reliability [102]. In this algorithm, first an array of problem variables is created that must be optimized. Each one of the components of this array is called a country.

The implementation steps of the MICA algorithm is as follows:

Step 1: shaping the initial empire;

Step 2: modeling the absorption policy (the movement of the colonies toward the imperialist);

Step 3: the process of revolution (the sudden change in the political and social properties of a country);

Step 4: the displacement of the imperialist and the colony position;

Step 5: determining the total power of an empire;

Step 6: the process of imperialistic competition;

Step 7: the collapse of weak empires;

Step 8: convergence;

Each one of these steps and the related mathematical relations have been explained in the following subsections.

4.4.1 Formation of the initial empire

At first, an array of the problem variables that must be optimized, is created. Each unit of this array is called as a country. The countries are in fact the possible solutions in the search space. In a problem with the dimensions N_{var}, a country has the dimension $1 \times N_{var}$ that is defined as

$$country = [P_t^1, P_t^2, \cdots, P_t^{N_{var}}] \tag{4.13}$$

where, $P_t^i : i = 1, 2, \cdots, N_{var}$ are variables that must become optimum [103, 104]. These variables can also have decimal values. The constituent parts of a country can be considered social-political properties of that country, such as culture, language, and economic structure. In fact, in solving the optimization problem, the algorithm is after finding the best country (a country with the best social-political properties). Finding this country is in fact finding the best parameters of the problem that generates the least value of the objective function.

Figure 4.4 shows a country by using some of the social and political properties [105].
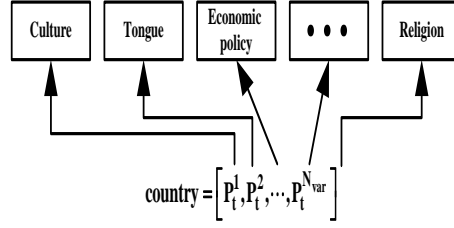
Figure 4.4: The social-political properties forming a country

The expense of a country is calculated by replacing the variable of the desired country in the objective function as the following relation.

$$\mathbb{C}_t^{country,i} = OF(country_t^i) = OF(P_t^1, P_t^1, \cdots, P_t^{N_{var}}) \tag{4.14}$$

At the beginning $N_{country}$ initial countries according to the defined constraints for the desired problem is generated randomly with uniform distribution (or other adequate distribution function) [105]. As a result, a matrix that constitutes different countries is defined as follows [106, 107].

$$country = \begin{bmatrix} country_t^1 \\ country_t^2 \\ country_t^3 \\ \cdots \\ country_t^{N_{country}} \end{bmatrix} \tag{4.15}$$

The generated population based on the expense (calculated by using Eq.(2.10) is divided into two groups of imperialist and colony. By the number of N_{imp} from the best members of the initial population (countries having the least value of objective function) is chosen as imperialist. Number of N_{col} from the remaining members also from the colonies that each of them are assigned to an empire. In this thesis, 10% of the countries have been considered as imperialist states and the rest will be the colonies of those imperialist states. For assigning initial colonies among the imperialists, to each imperialist a number of colonies proportional to its power is assigned as follows. For reaching this goal, by having the expense of all the imperialist, the expense of their normalization can be determined according to [105]

$$\mathbb{C}_t'^{Imp,n} = \underbrace{max}_{i} \left\{ \mathbb{C}_t^{Imp,i} \right\} - \mathbb{C}_t^{Imp,n} \tag{4.16}$$

where, $\mathbb{C}_t^{Imp,n}$ is the expense of the nth imperialist, $\underbrace{max}_{i} \left\{ \mathbb{C}_t^{Imp,i} \right\}$ is the maximum expense among the imperialist and $\mathbb{C}_t'^{Imp,n}$ is the normalized expense of these imperialists at time t. The imperialist that has more expense (is considered a weaker imperialist), will have less normalizing expense. By having the normalizing expense, the relative power of normalizing each imperialist is calculated in the form of the following relationship and based on it, the colonies are divided among the imperialists [105].

$$\mu_t^{Imp,n} = \left| \frac{\mathbb{C}_t^{Imp,n}}{\sum\limits_{i=1}^{N_{imp}} \mathbb{C}_t^{Imp,i}} \right| \tag{4.17}$$

Noting that the normalization power of an imperialist is in fact the ratio of the colonies that are managed by that imperialist; so, the initial value of an imperialist can be calculated as follows.

$$N_{I,col} = round \left\{ \mu_t^{Imp,n} \cdot N_{col} \right\} \tag{4.18}$$

In this relation, $N_{I,col}$ is the initial number of the colonies of an empire and also N_{col} is the total number of the colonies present in the population of the initial countries. Number of $N_{I,col}$ from the initial colonies are selected randomly for each empire and is assigned to the nth imperialist. Figure 4.5 shows how the initial empires are formed. As it is observed in this figure, the strongest imperialist will have more number of colonies and the weaker imperialist will have less colonies [105].

4.4.2 Modeling the absorption policy

After creating the initial empires, the imperialists increase their colonies through the absorption policy for increasing their power. The imperialists by following up the absorption policy, force their colonies to be driven towards them in line with different political-social aspects including culture, language and religion.

By implementing this policy, the colony approaches the imperialist in line with the mentioned aspects. The schematic of this process is shown in Figure 4.6. The distance between the imperialist and the colony is d and the direction of movement, is a vector from colony to the imperialist as it is observed in this figure. In the absorption policy, the colony is displaced
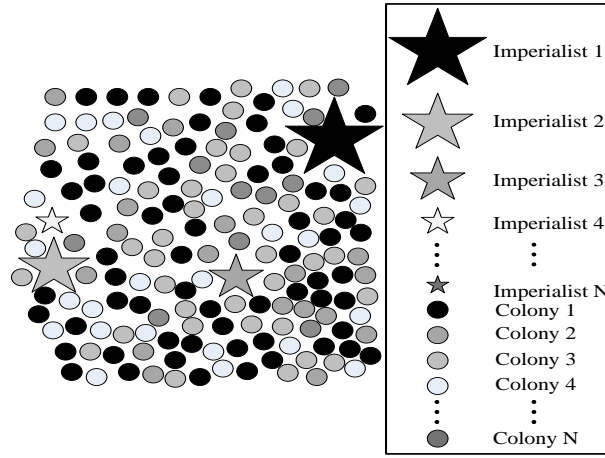
Figure 4.5: How the initial empires are formed

toward the imperialist by the amount x. x is a random variable with uniform distribution (and or any other suitable distribution) that can be calculated by using [105]

$$x \sim U(0, \beta \times d) \tag{4.19}$$

In this relation, β is the absorption coefficient and is considered bigger than one. If β is close to one will cause the reduction of search ability by the algorithm. Whereas if β is considered greater than one ($\beta \geq 1$), it means that it is possible that the colonies at sometimes have better position relative to their imperialist [103, 105].

The direction of movement is not necessarily a vector of the colony to the imperialist and always there will be deviations in the result of the work. For modeling this fact and for the increase of the ability of searching more regions around the imperialist, the direction of the movement of the colony toward the imperialist deviate with a little angle as is shown in Figure 4.7. The angle θ is determined randomly and with uniform distribution (and or any other adequate distribution) as

$$\theta \sim U(-\gamma, \gamma) \tag{4.20}$$

Here, θ is a parameter that regulates deviation from the main rout. The increase of this parameter causes the increase of search around this imperialist. Otherwise, its decrease causes the colonies to move as much as possible close to the vector connecting the colony to the imperialist [105].
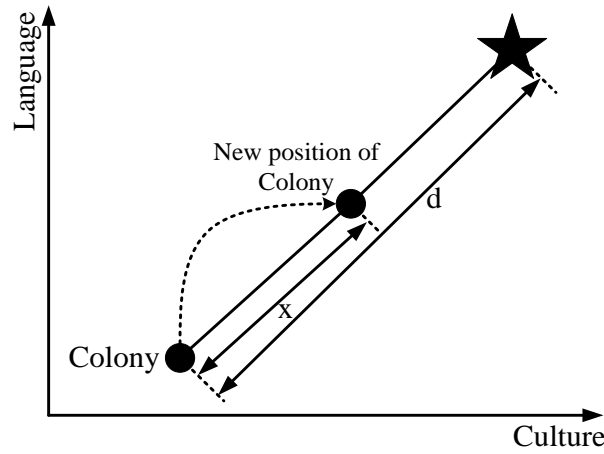
Figure 4.6: Schematic of the movement of the colonies toward the imperialist
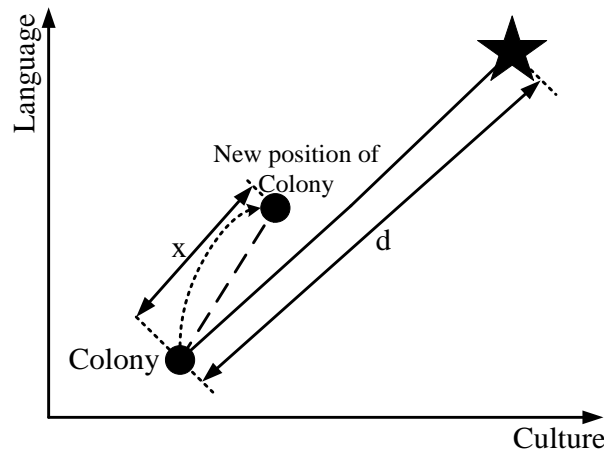
Figure 4.7: Real movement of the colonies toward the imperialist

4.4.3 The revolution process

In the real world, revolution causes the social and political properties of a country to change suddenly as is shown in Figure 4.8. Revolution in ICA, is modeled with the random change of some of the colonies of the empire and is similar mutation process in the Genetic algorithm (GA). As a result of the revolution process, exploration in the algorithm increases and prevents early convergence to the local optimum point. By using a coefficient by the name of revolution rate, increases the chance of reaching better responses

and causes the creation of diverse responses. The revolution rate in the algorithm shows a percent of colonies in each empire that their position changes randomly. Considering the revolution rate with high value, reduce the exploitation power in the algorithm as well as to reduce the convergence rate [105, 107].
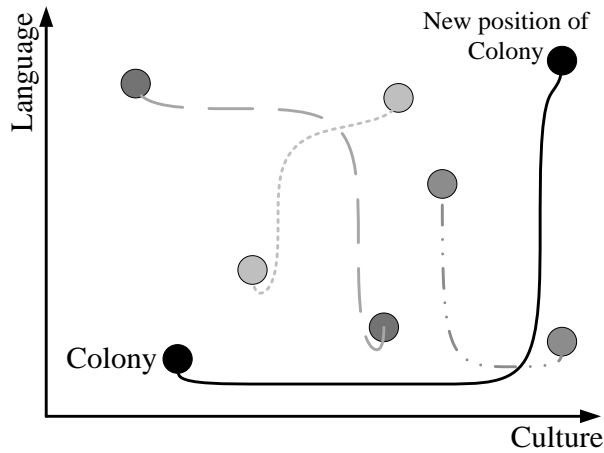
Figure 4.8: Revolution process in the ICA algorithm

4.4.4 The displacement of the imperialist and the colony position

During the absorption policy and the revolution process, a colony may reach a position better than the imperialist (to points with less cost).

In this case, the imperialist and the colony, change their position with each other. Hence, the colony changes to a new imperialist, while the old imperialist changes to a colony in the same empire. The algorithm with the imperialist in the new position continues its performance and the new imperialist starts implementing absorption policy over its colonies. The change of place of imperialist and colony, has been shown in Figure 4.9. In this figure, the best colony of the empire (that has less expense than the imperialist itself) has been shown with a solid (darker) color. As depicted in this figure, all the empire has been shown after the change of position of the empire with the imperialist [104, 105].

4.4.5 The total power of an empire

Expense (proportional to power) is defined as an empire as the sum of the expense of the imperialist country plus a percent of the total expense of its
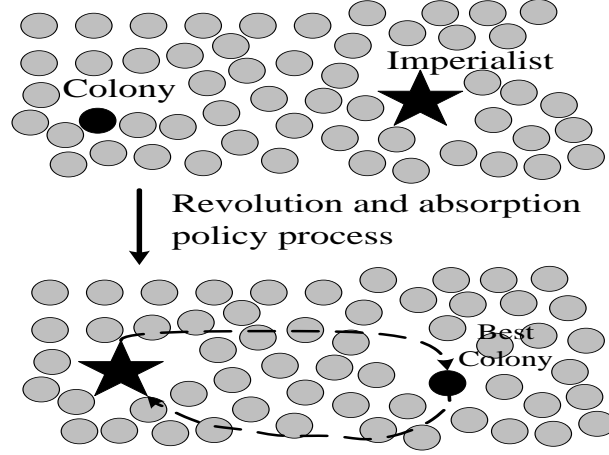
Figure 4.9: The change of place of imperialist and colony after the implementation of the revolution process

colonies. In other words, the total expense of an empire can be calculated as follows.

$$\mathbb{C}_{t,Tot}^{Imp,n} = \mathbb{C}_t^{Imp,n} + \xi \times mean\left\{\mathbb{C}_t^{Col,n}\right\} \tag{4.21}$$

Where, $\mathbb{C}_{t,Tot}^{Imp,n}$ is the total expense of the nth empire, $\mathbb{C}_t^{Imp,n}$ the expense of the nth imperialist, $\mathbb{C}_t^{Col,n}$ expense of the colonies belonging to the nth empire at the moment t. Also, ξ is a positive number at the interval [0, 1]. If ξ is considered as a small value, the total expense of an empire is approximately equal to the related imperialist. But, increasing ξ causes the increase of the effect of the amount of the expense of the colonies of an empire in all of its expense. For reaching the desired response in most of the cases $\xi = 0.1$ [105].

4.4.6 Imperialistic competition process

Imperialistic competition has special importance in the ICA algorithm. During this process, all the empire try to acquire the colonies of other empires. Any empire that cannot increase its power and loses its competition power, gradually will be eliminated in the imperialistic competitions. It means that by the passing of time, weak empires, lose their colonies and stronger empires, own these colonies and increase their power. During this process, the algorithm chooses one or several of the colonies present in the weakest

empire and for owning these colonies, creates a competition among all the empires. In this competition, each of the empires based on their total power (Eq.(4.23)) have a special probability for owning the mentioned colonies. The mentioned colonies will not necessary owned by the strongest empire, but the stronger colonies, have more probability of ownership. Figure 4.10 shows the schematic of the imperialistic competition process [105].
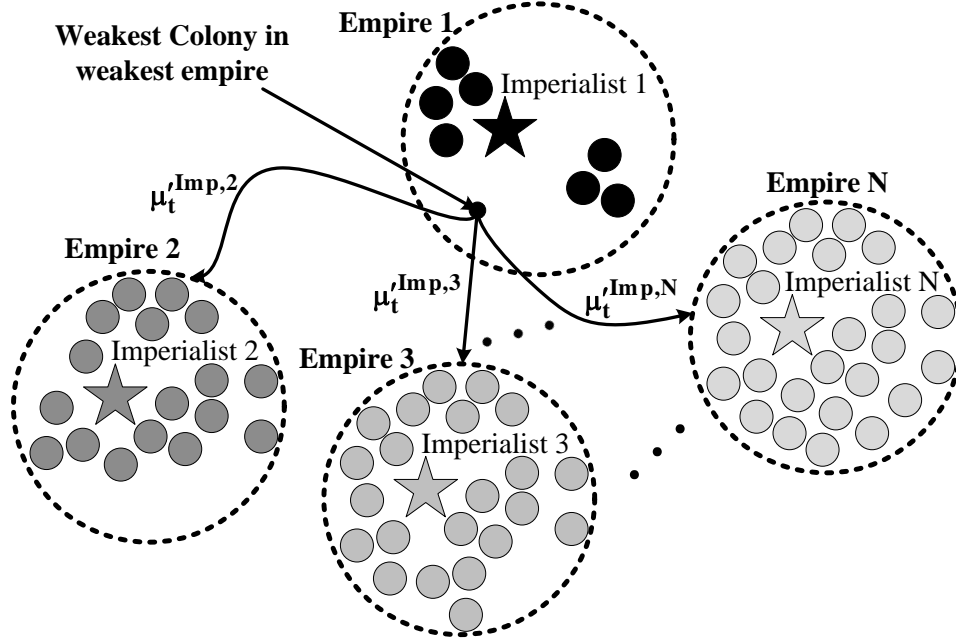
Figure 4.10: The schematic of imperialistic completion process

As it is observed from Figure 4.10, empire I which has less colonies, is considered the weakest empire. As a result one of its colonies is under imperialistic competition and the empire II to N compete with each other for owning this colony. For modeling the competition between the empires for owning these colonies, first the weakest colony from the weakest empire is chosen. Then, the probability of owning each empire will be calculated by considering the expense of all the empire as follows [105, 108].

$$\mathbb{C}_{t,Tot}^{\prime Imp,n} = \underbrace{max}_{i} \left\{ \mathbb{C}_{t,Tot}^{Imp,i} \right\} - \mathbb{C}_{t,Tot}^{Imp,n} \qquad (4.22)$$

In this relation, $\mathbb{C}_{t,Tot}^{Imp,n}$ is the total expense of the nth empire and $\mathbb{C}_{t,Tot}^{\prime Imp,n}$ is also the total normalized expense of that empire at instant t. Each empire

that has a smaller $\mathbb{C}_{t,Tot}^{Imp,n}$ will have bigger $\mathbb{C}_{t,Tot}'^{Imp,n}$. In other word, $\mathbb{C}_{t,Tot}^{Imp,n}$ is equivalent to the total expense of an empire and $\mathbb{C}_{t,Tot}'^{Imp,n}$ is equivalent to its total power. The empire with the least expense has the most power. By having the total normalized cost, the possibility of owning the colony under competition, by each empire is calculated as follows.

$$\mu_t'^{Imp,n} = \left| \frac{\mathbb{C}_{t,Tot}'^{Imp,n}}{\sum\limits_{i=1}^{N_{imp}} \mathbb{C}_{t,Tot}'^{Imp,i}} \right| \tag{4.23}$$

After calculating the probability of owning each empire, a mechanism is needed so that puts the colony under competition with the probability proportional to the power of the empires at the disposal of one of them [105]. The mechanism used can take place by using methods such as roulette wheel, ranking, random sampling, tornometry selection [105]. In this thesis, roulette wheel method has been used. By owning the colony by one of the empires, the operations of this step of this algorithm will also end.

4.4.7 The process of collapse of weak empires

During the execution of the algorithm, weak empires collapse gradually and their colonies fall in the hand of stronger empires. Different conditions can be considered for the collapse of an empire as a result its elimination. In the suggested algorithm, a time empire is considered eliminated that has lost its colonies. Figure 4.11 shows the process of the collapse of an empire. In this figure, empire number 4 because of the loss of all its colonies, doesn′t have power for competition anymore and must be eliminated [105]. As it is observed from this figure, the imperialist related to the empire collapse with a probability (by using relation (4.23)) is transferred as a colony to the other empires.

4.4.8 Convergence

After some time, all the empires collapse and only one empire remains and the rest of the countries stay under the control of this unit empire. In the real world, all the colonies are managed by one united empire and the positions and the costs of the colonies, is equal to the positions and cost of the imperialist country. Under these conditions, no difference exists among

63
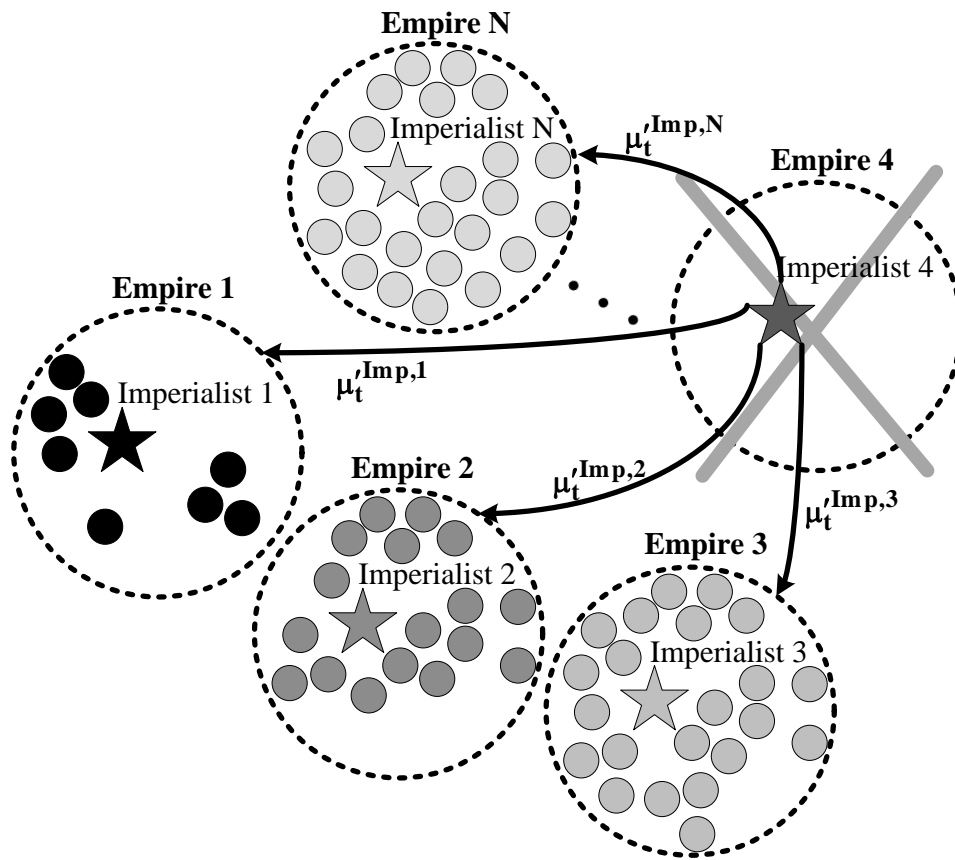
Figure 4.11: The collapse of the weak Empire

the colonies and also among the colonies and the imperialist country. In other words, all the countries are considered meanwhile both colony and imperialist. The last empire shows the best solution for this problem. The implemented algorithm continues its function until the fulfillment of a convergence condition. Different criteria for stopping the search are considered:

1. When only one empire exists, the imperialistic competition ends;

2. When the number of iterations reaches a predefined value by the name of maximum decade, the algorithm will be stopped;

3. If in several consecutive iterations an improvement in the best solution is not observed, the algorithm will be stopped.

$MICA$ **unit flowchart**

The flowchart of the $MICA$ unit is shown in Figure 4.12.

The problem is solved in a 24 h period that the measured data are in half hour intervals. So, the COUNTRY matrix that has the dimension 48×7 shall be created. The matrix elements are $country_t^1$ to $country_t^{48}$ that each one of these vectors have dimensions equal to 1×7. The variables of the problem can be divided into two groups of dependent and independent. The independent variables are variables that are related to non-dispatchable sources (PV and WT in this study) and the variation of the values of other variables has no effect over them and is only dependent on the accessible power in each time interval. While, the dependent variables are variables that their values are sensitive to the variations of independent variables. The output power of the dspatchable sources (MT in this study), the generated and consumed power of ES sources in the charging and discharging mode and the power of responsive load demand (RLD) (EWH as controllable load and DR as shiftable load) are considered one of the dependent variables. The aim is finding the optimum value of all the independent and dependent variables while fulfilling all the presented constraints for them that finally leads to finding the least amount of electricity generation cost by using the cost function (Eq. 2.10). So, according to the presented explanations, country is defined as $country = [P_t^1, P_t^2, \cdots, P_t^7]$ vector that each of its elements are considered $P_t^1 = P_t^{WT}, P_t^2 = P_t^{PV}, P_t^3 = P_t^{MT}, P_t^4 = P_t^{ES,c}, P_t^5 = P_t^{ES,d}, P_t^6 = P_t^{EWH}$ and $P_t^7 = P_t^{DR}$. First the initial populations for the independent variables (P_t^{WT} and P_t^{PV}) shall be created randomly by considering the maximum generated power by these sources. Then, by noting these independent variables and also the constraints discussed for solving the problem, values will be created randomly for the dependent variables. Then, all the eight steps discussed in the Section 4.4 shall be executed according to the Pseudo-code presented in algorithm 8 by the suggested algorithm.

4.5 Multi-dimension artificial bee colony (MABC) unit

Similar to the algorithms based on heuristic methods, the ABC algorithm is also an iterative process that starts with an initial population that includes acceptable responses (the responses that fulfill the constraints considered for the problem). The implementation steps of the ABC algorithm is as follows:
Step 1: initial value giving to the food sources;
Step 2: the initial value giving of the working bees;
Step 3: calculating the probable value of the selections;

Step 4: evaluating the onlooker;
Step 5: evaluating the pioneer bees.

In the following sections each one of these steps has been explained in detail.

4.5.1 Initial value giving to the food sources

Each food source shows a possible response of the problem. Each source has special properties such as the amount of nectar, quality of nectar, proximity and remoteness from the beehive that these properties determine the merit and the amount of its profitability. So, the initial population of the responses are made up of N_P number of random D-dimensional vectors with real values. Each response is shown as $X_t^{i,d} = x_t^{i,1}, x_t^{i,2}, \cdots, x_t^{i,D}$ which shows the ith food source in the created population. Then, each food source is generated as

$$X_t^{i,j} = \underline{x}^j + \rho \times (\overline{x}^j - \underline{x}^j) \tag{4.24}$$

where $X_t^{i,j}$ means the jth parameter from the ith response at time t, $i \in 1, 2, \cdots, N_P$ and $j \in 1, 2, \cdots, D$ are respectively the upper and lower of the $\overline{x}^j$ and $\underline{x}^j$ component. These food sources have been allocated randomly to N_P employed bees and their profitability value is evaluated. ρ is also a random number in the [0, 1] interval.

4.5.2 Initial value giving to the employed bees

In this step, each employed bee by using food source x_t^i generator a new food source $x_t'^i$ in the neighborhood of its position by using response search equation. Response search equation can be calculated from

$$x_t'^{i,j} = x_t^{i,j} + \rho' \times (x_t^{i,j} - x_t^{k,j}) \tag{4.25}$$

In this relation, the values of $k \in 1, 2, \cdots, N_P$ and j are selected randomly and k is considered opposite to i. A random number for ρ is considered in [-1, 1]. After determining $x_t'^i$ must be compared with x_t^i. If its fitness is better than x_t^i as a result the value of $x_t'^i$ replaces the value of x_t^i and will be considered as a new member of the population. Otherwise, the value of x_t^i will remain.

4.5.3 Calculating the possible value of the choices

After finishing the searching process by employed bees, in the hive dance salon the information related to the amount of nectar and the position of the discovered sources is shared with onlooker. Then, the onlooker after evaluating the information related to nectar, selects the position of the food source with the probability that is proportional to the amount of nectar present in the source. This selection is probability dependent on the amount of fitness of the responses. The selection process based on fitness can take place by using methods such as roulette wheel, ranking, random sampling tornometry selection [1, 109, 110]. In this thesis roulette wheel method has been used. Roulette wheel selection in each iteration proportional to the fitness value can be calculated from the following relation:

$$P_t^i = \frac{fit_t^i}{\sum_{j=1}^{N_P} fit_t^j} \tag{4.26}$$

fit_t^i in this relation is the fitness value related to the ith response at time t. It is clear that the higher fit_t^i means higher probability for selecting the ith source.

4.5.4 Evaluating the onlooker

A spectator bee after getting the information related to the nectar from all the employed bees, evaluates these information. Then, selects the X_t^i source by noting its possible value (that is P_t^i) after the spectator bee chooses its food source, by using Eq.(4.24), the new source calculates $x_t'^i$. If the modified source, has nectar equal to or more than the source x_t^i, replaces the new source with the x_t^i source and include it as a new member of the population.

4.5.5 Evaluating the pioneer bees

If the food source x_t^i cannot improve during the predetermined iterations, this source is considered as released source. Then, the bee will transform to a pioneer bee proportional to this source. The pioneer bee randomly generates the food source by:

$$x_t^{i,j} = \underline{x}^j + \rho'' \times (\overline{x}^j - \underline{x}^j) \tag{4.27}$$

where ρ'' is a random number in the [0, 1] interval.

$MABC$ **unit flowchart**

The flowchart of MABC unit is shown as diagram in Figure 4.13. Each response for the optimization problem has D variables that in this thesis $D = 7$ is considered and includes parameters such as wind turbine, solar turbine, microturbine, charging and discharging power ES, EWH and DR. The aim is finding the values of these variables that finally results in finding the least value of the cost of generating electricity by using cost function (relation (1)). Therefore, X_t^i is defined as $X_t^i = x_t^{i,1}, x_t^{i,2}, \cdots, x_t^{i,7}$ vector that each one of its components are as

$x_t^{i,1} = P_t^{i,WT}$, $x_t^{i,2} = P_t^{i,PV}$, $x_t^{i,3} = P_t^{i,MT}$, $x_t^{i,4} = P_t^{i,ES+}$, $x_t^{i,5} = P_t^{i,ES-}$, $x_t^{i,6} = P_t^{i,EWH}$, and $x_t^{i,7} = P_t^{i,DR}$

Noting this point is essential that all the members of the population must fulfill all the problem constraints completely. These variables are divided into two types of dependent and independent variables. The output powers MT, ES, EWH and DR are considered as dependent variables and the output powers WT and PV are considered as independent variables. Its reason is that the generation sources WT and PV are as Non-dispatchable generation sources and depending on the climatic conditions their output power is variable and is independent of the load power and or other generation sources. Although, the output power MT and ES can vary depending on the power that is generated by the renewable sources (WT and PV) and amount of the consumed load. As a result, first independent variable ($P_t^{i,WT}$ and $P_t^{i,PV}$) must be randomly created considering the maximum production power by sources.

Then, by noting these independent variables and also the constraints discussed for solving the problem, values will be created randomly for the dependent variables. Furthermore, when the response or the released sources is present, the pioneer bee this way (first independent and then dependent) finds its new source. The $MABC$ unit is implementable by the Pseudo-code in the form of Algorithm 9.

4.6 Multi-layer ant colony optimization (MACO) unit

The ants optimization algorithm uses the performance of the ants in improving its movement pass stepwise. Eventually, they can help with each other′s to find the shortest pass from the nest to a food source. This method is such that each of the ants first randomly chooses a path for reaching food and returning home. Along the path they leave a substance from them-

selves called pheromone that in the next passes helps them in finding the pass. The concentration of this substance increases/decreases with the increment/decrement of the ants passing. The shorter the pass, the time spent for one time going and returning becomes less and as a result in a certain time interval the number of goings and returning increase.

The ants instinctively choose a path which the concentration of pheromone is more, because they know it's probably a shorter path. The more ants pass through this route, the concentration of this substance increase and as a result encourage more ants to use this route [111–114].

Finally all the ants will use a route which is the shortest one. This algorithm can be used efficiently in different optimization problems. In the optimization process of the system cost function by the ants algorithm, the powers generated by the microsources $P_t^{MT}, P_t^{WT}, P_t^{PV}, P_t^{ES,d}$ and the power consumed by the consumers P_t^{MT}, P_t^{EWH} and P_t^{DR} are dependent on each other based on demand side management considering physical relations and constraints presented in Section 2.3. The previous and next energy stored in the battery during charging and discharging mode is very important. So, there is no possibility for random selection of the value for each of these powers separately at every iteration.

The process of executing MACO optimization algorithm is shown in Figure 4.14, in which the number of layers are equal to the number of design variables and the number of nodes in each particular layer is equal to the number of allowable values corresponding to each variable. As it is observed in this figure, the problem of cost function optimization with 48 layers (variables) and ten allowable values according to technical constraints for each layer is considered. The layers are the same times in which information is processed in them and allowable values are values that each include values corresponding to the powers $P_t^{MT}, P_t^{WT}, P_t^{PV}, P_t^{ES,c}, P_t^{ES,d}, P_t^{EWH}$ and P_t^{DR}.

In this respect, we consider governing rules between mentioned powers and the value of stored energy in the battery at the before and after time interval during the definition of allowable values. Each allowable value is defined by a set including these powers, and by considering physical relations and constraints presented in Section 2.3. By selecting the suitable cost function and using the algorithm of Figure 4.14 allowable values in each layer will be obtained with the minimum COE. In this problem the number of layers is considered equal to 48 which is in the number of calculation iterations. Also, 10 allowable values and 1000 ants have been considered for each layer. These ants randomly choose the allowable values and in each time interval this process will be repeated from 00:00 to 23:30. The probability of selecting

each of the allowable values in the first iteration is considered equal by placing the same pheromone over them. After all, the ants reach the time 23:30, cost function is calculated for each ant and the least cost function is selected. The pheromone of the route with the least expense is increased. As a result, this attempt will raise the possibility of choosing this route by the ants in the next iteration. For this reason, the pheromone of other routes is decreased. In this way, again the ants randomly start choosing the allowable values and routes while this time the chance of selecting virtual values that are in the optimum path is higher. By repeating this process, the algorithm converges and finally a path will be obtained that all the ants will pass it in which this route provides the minimum cost function.

In addition to this, for implementing the MACO unit also the x variable is defined with t layers and i allowable values for each layer according to

$$\begin{bmatrix} MPMT_t^{MT} & MPWT_t^{WT} & MPPV_t^{PV} & MPESd_t^{ES,d} & MPESc_t^{ES,c} & MPEWH_t^{EWH} & MPDR_t^{DR} & MPUP_t^{UP} \\ \downarrow & \downarrow & \downarrow & \downarrow & \downarrow & \downarrow & \downarrow & \downarrow \\ P_1^{MT,1} & P_1^{WT,1} & P_1^{PV,1} & P_1^{ES,d,1} & P_1^{ES,c,1} & P_1^{EWH,1} & P_1^{DR,1} & P_1^{UP,1} \\ \vdots & \ddots & \ddots & \ddots & \ddots & \ddots & \ddots & \vdots \\ P_t^{MT,i} & P_t^{WT,i} & P_t^{PV,i} & P_t^{ES,d,i} & P_t^{ES,c,i} & P_t^{EWH,i} & P_t^{DR,i} & P_t^{UP,i} \end{bmatrix}$$
$$(4.28)$$

In this study, t and i are respectively equal to 48 and 11.

4.7 Multi period particle swarm optimization (MPSO) unit

Movement towards the function optimum point is done in $EMS - MPSO$ according to the information of the best obtained point from each one of the factors present in the initial population also the best found point by the neighboring points. By noting figure 4.15, the bases of the PSO algorithm operation will be explained in detail as follows.

First, in the considered search space a number of points are chosen as initial population. The points are placed in different groups based on Euclidean distance. For example, particle in the recursion i include three searching factors as it is observed in Figure 4.15. The value of the function is calculated according to the parameters present in the search space and it is specified in each recursion that which point, has made the value of the object function minimum or maximum. In this order, the best point is specified in the each iteration. On the other hand, by having the previous information of each particle, it can be specified the best point that has been discovered by it up to now so the information of the optimum point of each iteration and each

parameter be specified. Initial value giving for the optimum points that all of the particles have also obtained the optimum point related to this particle until this instant is given before the start of the algorithm. By having this information, each particle is moved along the direction of the vector below by [115]

$$X^i_{(t+1),j} = X^i_{t,j} + V^i_{(t+1),j};\qquad(4.29)$$

$$\begin{aligned}V^i_{(t+1),j} &= w \times V^i_{t,j}+\\ &+ r_1 \times c_1 \times (X^b_{t,j} - X^i_{t,j})\\ &+ r_2 \times c_2 \times (X^b_{t,Tot} - X^i_{t,j})\end{aligned}\qquad(4.30)$$

$$w \in \{\underline{w}, \overline{w}\};\qquad(4.31)$$

In other words, the particles with the two factors of positions and velocity can move in a multi-dimensional space in each iteration. In fact members of a group communicate with the other members of the group that are in a better position and they adjust their position and velocity according to them.

In this relation the expression is related to inertia, show the social effect of each particle over each other. Inertial coefficient can be constant [14] and or its value can reduce during optimization process [15]. In [3] a coefficient by the name of constriction factor that its value has been considered constant and has increased the efficiency of the method for solving the problem has been considered. By adding the constriction factor to relation 25 the following relation is obtained by

$$\begin{aligned}V^i_{(t+1),j} &= x \times [V^i_{t,j}+\\ &+ r_1 \times c_1 \times (X^b_{t,j} - X^i_{t,j})\\ &+ r_2 \times c_2 \times (X^b_{t,Tot} - X^i_{t,j})]\end{aligned}\qquad(4.32)$$

[9] has suggested fully informed PSO in which a particle has been noticed by other particles in its neighbors. Each particle can by using different topologies such as Fully Connected Topology, Star Topology, Ring Topology, Four Clusters, Pyramid, Square and etc have been shown in the Figure 4.16.

Noting the stated topics, each particle needs the following information in each time interval and each iteration to create necessary changes in its velocity and position:

- Present velocity of the particle.

- Distant from the best point that up to now a particle has been able to find it.

- Distance from the best place in the entire search points that all of the members have found it.

Under these conditions, PSO algorithm will be able at consecutive iterations, to find the global optimum point (during 24 hour performance of the system under study) of the considered function optimum and will be able to obtain the optimum data for different variables. For the better understanding of the algorithm implemented by PSO, the nature of particle movement in the search space has also been shown in Figure 4.17. As it is observed in the figure, the jth particle at instant t and at the iteration i has the position $X_{t,j}^i$. the particle at this instant starts moving with the velocity $V_{t,j}^i$ in its previous movement direction. Then the particle tries also to move in the direction of the best position that has found up to the present instant in the search space. Finally, the particle also tries to move towards the best search position that all of the particles have found in the search space up to this instance. Totally, after performing this iteration, the particle will reach its new position that is $X_{(t+1),j}^i$ with the velocity $V_{(t+1),j}^i$.

$EMS - MPSO$ **unit**

The main purposes of implementing this unit are the same as the cases mentioned for the $EMS - MINLP$ unit. Flowchart for implementing the $EMS - MPSO$ unit is shown in Figure 4.18. The stages of implementing this algorithm are as follows:

1. Determination of initial value for N particles including random value for the position of the particles, velocity and the number of iterations

2. Evaluating cost function related to the particles

   The position of each particles must be compared with the best position that particle has obtained up to the instant in the search space. If the new position is one particle better that $X_{t,j}^b$ in that case it must be replaced with the value of the new position.

3. Position of each particle must be also compared with the best position that all of the particles have obtained up to the present instant. If the new position of a particle be better that $X_{t,Tot}^b$, in that case the value of $X_{t,Tot}^b$ will be updated

4. According to the Eqs. (4.29) and (4.32) for updating position and new velocity for the particle, these variables will be updated

5. If the number of iterations has reached the determined value, algorithm will be finished; otherwise, the program will be executed again from stage 2.

In each certain time interval a number of particles have been considered in the number of variables then optimization is done for the defined cost function. For each variable from among particles considered, we obtain the best particle position as the optimum point of that variable. This act is repeated this way for the other variables. Finally the value of each optimum particle for different variables in the object function are taken into consideration and after summing up of the values of the function in all of the time intervals, the final value of the system production cost will be calculated during its daily performance. In the suggested algorithm by considering the stated advantages in the other references, finally the values of self learning coefficients $c_1 = c_2 = 2$, $\overline{w} = 0.9$ and $\underline{w} = 0.2$ have been included.

4.8 Multi-dimension gravitational search algorithm (MGSA) unit

4.8.1 A Review of Newton′s gravitational laws

Gravitation is in fact the tendency of masses in attracting each other and becoming accelerated towards each other. According to Newton′s law the value of the gravitational force between two bodies is proportional to the product of the masses of the two bodies divided by the square of the distance between them.

$$F = G\frac{M_1 \cdot M_2}{R^2} \tag{4.33}$$

where F is the attraction force, G is the gravitational constant, R is the distance between the two bodies and M_1 and M_2 are the masses of body 1 and body 2 respectively. According to Newtons′ second law, when a force E is exerted on a body with mass M, it is accelerated in the direction of that force according to:

$$a = \frac{F}{M} \tag{4.34}$$

The bigger body and the smaller its distance with other masses, the effect of its gravitational force will be more (Eq. 4.33). In addition, the heavier mass have less acceleration in changing its position (Eq. 4.34).The gravity constant depending on the life of the world changes can be calculated as

$$G_t = G_{t0} \times (\frac{t_0}{t})^\beta \tag{4.35}$$

where G_t is the gravity constant at time t, G_{t0} is the gravity constant at the time of formation of masses and β is a number smaller than one.

4.8.2 Mathematical implementation of the MGSA

In this algorithm, the search of optimum points is done based on the gravitational mass and Newtons$'$ laws governing the dynamics of the masses. In this method, N masses are considered and each of the masses is placed in the D dimensional space. The position of each mass is an answer of the problem. The gravitational force, the acceleration of motion and the new position of the masses are calculated according to inertia between masses and the gravitational forces of other masses. Then, the evaluation of the masses is done based on the objective function. The heavier masses have higher fitness values; they depict good optimal solution to the problem and they move slowly than lighter ones representing worse solutions.

This process continues until the convergence of the results and fulfillment of stopping condition. Consider a system with N masses. The position of the mass i in the D dimensional space is defined as

$$^D X^i = (^1 X^1, \cdots, ^d X^i, \cdots, ^D X^i) \tag{4.36}$$

$$\begin{cases} ^D X^i = (^1 X^1, \cdots, ^d X^i, \cdots, ^D X^N) \\ \qquad\qquad\qquad\qquad\qquad i = (1, 2, \cdots, N) \end{cases} \tag{4.37}$$

where $^d X^i$ is the position of mass i in the dimension d. The force exerted on mass i from mass j in the direction of dimension d at the time t (iteration t) is defined as

$$^d F_t^{j,i} = G_t \frac{M_i \times M_j}{R_t^{j,i} + \varepsilon} (^d X_t^j - ^d X_t^i) \tag{4.38}$$

where M_i and M_j are masses of body i and j, $R_t^{j,i}$ is distance between i and j at t^{th} repetition and ε is an extremely small constant. $R_t^{j,i}$ can be achieved

$$R_t^{j,i} = \sqrt[2]{\sum_{d=1}^{D} (^dX_t^j - ^d X_t^i)^2} \tag{4.39}$$

The resultant of the forces applied on mass i in the dimension d is calculated by

$$^dF_t^i = \sum_{j=1, j \neq i}^{N} \rho \times ^d F_t^{j,i} \tag{4.40}$$

where ρ is a random number between zero and one. The resulting response becomes farther than the optimum response because of using the random places which makes larger masses to decrease. As a result, relation (4.40) is modified as

$$^dF_t^i = \sum_{j=1, j \neq i}^{N} 1 \times ^d F_t^{j,i} \tag{4.41}$$

The force exerted on mass i creates acceleration in the direction of dimension d as

$$^d a_t^i = \frac{^dF_t^i}{M_i} \tag{4.42}$$

Velocity and relocation mass i in the direction of dimension d can be calculated as

$$^dV_{t+1}^i = \rho \times ^d V_t^i + ^d a_t^i \tag{4.43}$$

$$^dX_{t+1}^i = ^d X_t^i + ^d V_{t+1}^i \tag{4.44}$$

In the velocity relation, using random function (i.e. ρ) causes the increase of the exploration of the algorithm. In these relations, the time duration parameter of the motion is considered 1 second. In the modified algorithm, the control parameter T is considered as the time duration of the mass i from the present position to the next position. Moreover, it is indicated that the value of 2 seconds leads to a better answer. So, the relations of velocity and displacement are modified as

$$^dV_{t+1}^i = \rho \times ^d V_t^i + ^d a_t^i \times T \tag{4.45}$$

$$^{d}X_{t+1}^{i} =^{d} X_{t}^{i} +^{d} V_{t+1}^{i} \times T \tag{4.46}$$

The gravitational constant G according to a function of time is obtained by

$$G_t = G_0 \times \exp(-\alpha \frac{t}{\bar{I}}) \tag{4.47}$$

where G_0 is the initial value giving to the gravitational constant (equal to 100), α is the controlling parameter (equal to 5), t is the current iteration and $\bar{I}$ is the total number of iterations. After each iteration and movement, the bodies must be evaluated based on the objective function in their new positions. In this order, the masses with better position (smaller objective function) have heavier mass and members with more position have lighter mass. For calculating the masses is used as

$$M_t^i = \frac{fit_t^i - \overline{fit}_t}{\underline{fit}_t - \underline{fit}_t}) \tag{4.48}$$

where fit_t^i is the value of the objective function of mass i in the tth iteration, $\underline{fit}_t$ and $\overline{fit}_t$ are respectively the worst and the best value of the objective function in the tth iteration. These parameters can be computed as

$$\overline{fit}_t = max(fit_t^i) \tag{4.49}$$

$$\underline{fit}_t = min(fit_t^i) \tag{4.50}$$

The adequate solution for establishing equilibrium between exploration and exploitation is to reduce the number of masses when certain time passes. After several iterations only the best masses are chosen for calculating the gravity force exerted on other masses. Although this process requires high accuracy, the highest accuracy should be provided in using this policy. For example, at the beginning of the process, all the masses participate in the gravity force all the masses participate in the gravity force in local optimum points. But, this number reduces in next iterations. In order to reach this goal, the percentage of members at the end of time is defined as a control parameter ξ (for example 10% of the masses) also the parameter Ψ_t the best of the masses at each iteration. Ψ_t can be estimated as

$$\Psi_t = round([\xi + 1 - \frac{t}{\bar{I}} \times (100 - \xi)] \times N) \tag{4.51}$$

On this basis the resultant of the forces exerted on mass i in the dimension d is calculated according to the following relation

$$^dF_t^i = \sum_{j \in \Psi_t, j \neq i}^{N} 1 \times^d F_t^{j,i} \qquad (4.52)$$

To propose an algorithm for MG application, it is supposed that masses have still not reached stability and the specific orbit at the begining. This feature is similar to the formation of planets of a solar system. Each one of the masses are effected by each other. At the end of the process, they can be stable at a point and at a moving orbit. The biggest masses having stable stage at a point are the answer of the problem.

Noting the consideration of a one day period (24 half hour period) the total space has the dimensions 48×D. D is the number of independent parameters. The problem which space and the number of variables must be determined at first moment. The value of ES charge and discharge can be determined by noting the previous and current value of SOC. So, the variables $P_t^{ES,c}$ and $P_t^{ES,d}$ are dependent on the variable SOC. It can only use SOC for determining the situation of ES in the position definition of a mass. There is a variable that shows the value of lack of power (i.e. P_t^{UP}) at any time. In other words, $P_t^n > (P_t^{WT} + P_t^{PV} + P_t^{MT} + P_t^{ES,d} + P_t^{DR})$ shall be established considering P_t^{EWH} is equal to zero. If $P_t^n < (P_t^{WT} + P_t^{PV} + P_t^{MT} + P_t^{ES,d} + P_t^{DR})$ be established as a result the extra power can be supplied for P_t^{EWH} and P_t^{UP} will be zero. Independent variables in the matrices $\overline{XM}_j$ for mass j is defined as

$$\overline{XM}_j = (\vec{P}_j^{WT}, \vec{P}_j^{PV}, \vec{P}_j^{MT}, \vec{E}_j^{ES}, \vec{P}_j^{DR}) \qquad (4.53)$$

The variables $\vec{P}_j^{WT}, \vec{P}_j^{PV}, \vec{P}_j^{MT}, \vec{E}_j^{ES}$ and $\vec{P}_j^{DR}$ are the vector of the powers of Wind Turbine (WT), Photovoltaic (PV), Micro-turbine (MT), the condition of the charge of the ES and Demand Response (DR) power respectively, by noting the MGSA method are placed in a space with the dimension $nT \times 5 \times N$. Where, nT represent the number of the periods, 5 the number of independent variables and N is the number of masses. The rest of the variables are extractable based on the values determined for the mentioned variables. In fact, the position of the masses are determined by the matrices $\overline{XM}_j$ and the forces between the masses affect this variables directly. By knowing $\vec{E}_j^{ES}$ at different times of a period, the parameters $\vec{P}_j^{ES,c}$ and $\vec{P}_j^{ES,d}$ can be derived from Eq. (2.26). Now by having the generated and consumed powers, the parameters $\vec{P}_j^{EWH}$ and $\vec{P}_j^{UP}$ can be obtained by

noting the power balance Eq. (4.11). For this purpose two matrix variables namely EM and YM are defined as

$$\overline{EM}_j = (\vec{P}_j^{ES,c}, \vec{P}_j^{ES,d}, \vec{X}_j^{ES}) \tag{4.54}$$

$$\overline{YM}_j = (\vec{P}_j^{UP}, \vec{P}_j^{EWH}) \tag{4.55}$$

In this order the variables $\overline{EM}_j$ and $\overline{YM}_j$ are calculated indirectly. It should be noted that all the independent and dependent variables take part in the calculation of objective function Eq. (2.10). As a result, in calculating the mass agent take part but the effect of gravitational forces is directly applied over $\overline{XM}_j$. $\overline{EM}_j$ and $\overline{YM}_j$ which are estimated subsequently.

The universe can be divided into several space with shorter time periods (solar system). Figure 4.19 shows a part of this space. In this order, the total response can be achieved from the combination of optimum responses obtained in similar spaces. The number of N masses are considered in each space. Optimum point can be determined by noting the cost function Eq. (2.10) and the technical constraints considered Eq. (4.11)-(2.29). The initial SOC in each space is equal to the last condition of the ES in the previous space.

The flowchart of implementing this algorithm is shown in Figure 4.20. The stages of the process are briefly listed as

1. Identification of the search space (Eqs. (4.36) and (4.37));

2. The random initial value giving to the masses;

3. Evaluating the masses by calculating the values of the objective function (Eq. (2.10));

4. Updating the values of M_t^i, $\overline{fit}_t$, $\underline{fit}_t$ and G_t for all the masses (N masses) (Eq. (4.47)-(4.50));

5. Calculating the force resultant in different directions (Eqs. (4.34)-(4.40) and (4.47));

6. Calculation of acceleration and velocity (Eq. (4.42) and (4.45));

7. Updating the position of the masses (Eq. (4.46));

8. Iteration of the stages 3 to 7 until the stopping conditions ($\overline{I}$ are fulfilled);

9. End

4.9 Mathematical modeling of the system in grid connected mode

The defined cost function in this thesis is a function according to total performance cost and MG energy includes the cost resulting from renewable resources, dispatchable units, storage units, the cost resulting from purchasing power from the grid minus the income obtained from RLD loads, charging of ES sources and the amount of income gained from selling power to the national grid. In the objective function, the penalty cost due to the mismatch power of the consumers is also considered. Objective function can also be formulated by

$$
\mathbf{Min}[\sum_{\mathbf{t=1}}^{\mathbf{NT}} \begin{pmatrix} \sum_{i=1}^{N_{NDU}} P_t^{NDU,i} \times \pi^{NDU,i} \\ +\sum_{j=1}^{N_{DGU}} P_t^{DGU,j} \times \pi^{DGU,j} \\ +\sum_{k=1}^{N_{ES}} P_t^{ES-,k} \times \pi^{ES-,k} \\ +P_t^{GRID-} \times \pi^{GRID-} \\ +P_t^{UP} \times \pi^{UP} \\ -\sum_{l=1}^{N_{RLD}} P_t^{RLD,l} \times \pi^{RLD,l} \\ -\sum_{m=1}^{N_{ES}} P_t^{ES+,m} \times \pi^{ES+,m} \\ -P_t^{GRID+} \times \pi^{GRID+} \end{pmatrix} \times \Delta t] \tag{4.56}
$$

subject to

- Power balance

$$
\sum_{i=1}^{N_{NDU}} P_t^{NDU,i} + X^{DGU} \times \sum_{j=1}^{N_{DGU}} P_t^{DGU,j} + P_t^{UP} \times \pi^{UP} \\ +(1 - X^{GRID}) \times P_t^{GRID-} = P_t^{NRL} + X^{GRID} \times P_t^{GRID+} \\ + \sum_{l=1}^{N_{RLD}} P_t^{RLD,l} + (1 - X^{ES}) \times \sum_{m=1}^{N_{ES}} P_t^{ES+,m} \tag{4.57}
$$

- Real power generation capacity

$$
0 \leq P_t^{NDU} \leq \overline{P}^{NDU} \tag{4.58}
$$

$$
X^{DGU} \times (\underline{P}^{DGU} \leq P_t^{DGU} \leq \overline{P}^{DGU}) \tag{4.59}
$$

State variable $X \in X_t^{ES}, X_t^{GRID}, X_t^{DGU}$

$$
X_t^{GRID} = \begin{cases} 1 & \textit{Selling to the national grid} \\ 0 & \textit{Buying to the national grid} \end{cases} \tag{4.60}
$$

$$X_t^{DGU} = \begin{cases} 1 & Service\ in \\ 0 & Service\ out \end{cases} \tag{4.61}$$

- Constraints related to the dispatchable generation units (Eqs.(2.21)-(2.28) [3]

- Constraints related to RLD

$$\sum_{t=1}^{NT} \sum_{l=1}^{N_{RLD}} P_t^{RLD,l} \leq 20\% \times \sum_{t=1}^{NT} P_t^{NRL} \tag{4.62}$$

- Interchange power between Microgrid and main Grid

$$P_t^{GRID+} \leq X_t^{GRID} \times \overline{P}^{GRID} \tag{4.63}$$

$$P_t^{GRID-} \leq (1 - X_t^{GRID}) \times \overline{P}^{GRID} \tag{4.64}$$

$$\overline{P}^{GRID} \leq 50\% \times \begin{pmatrix} \sum_{i=1}^{N_{NDU}} P_t^{NDU,i} \\ +X_t^{DGU} \times \sum_{j=1}^{N_{DGU}} P_t^{DGU,j} \\ +X_t^{ES} \times \sum_{k=1}^{N_{ES}} P_t^{ES-,k} \end{pmatrix} \tag{4.65}$$
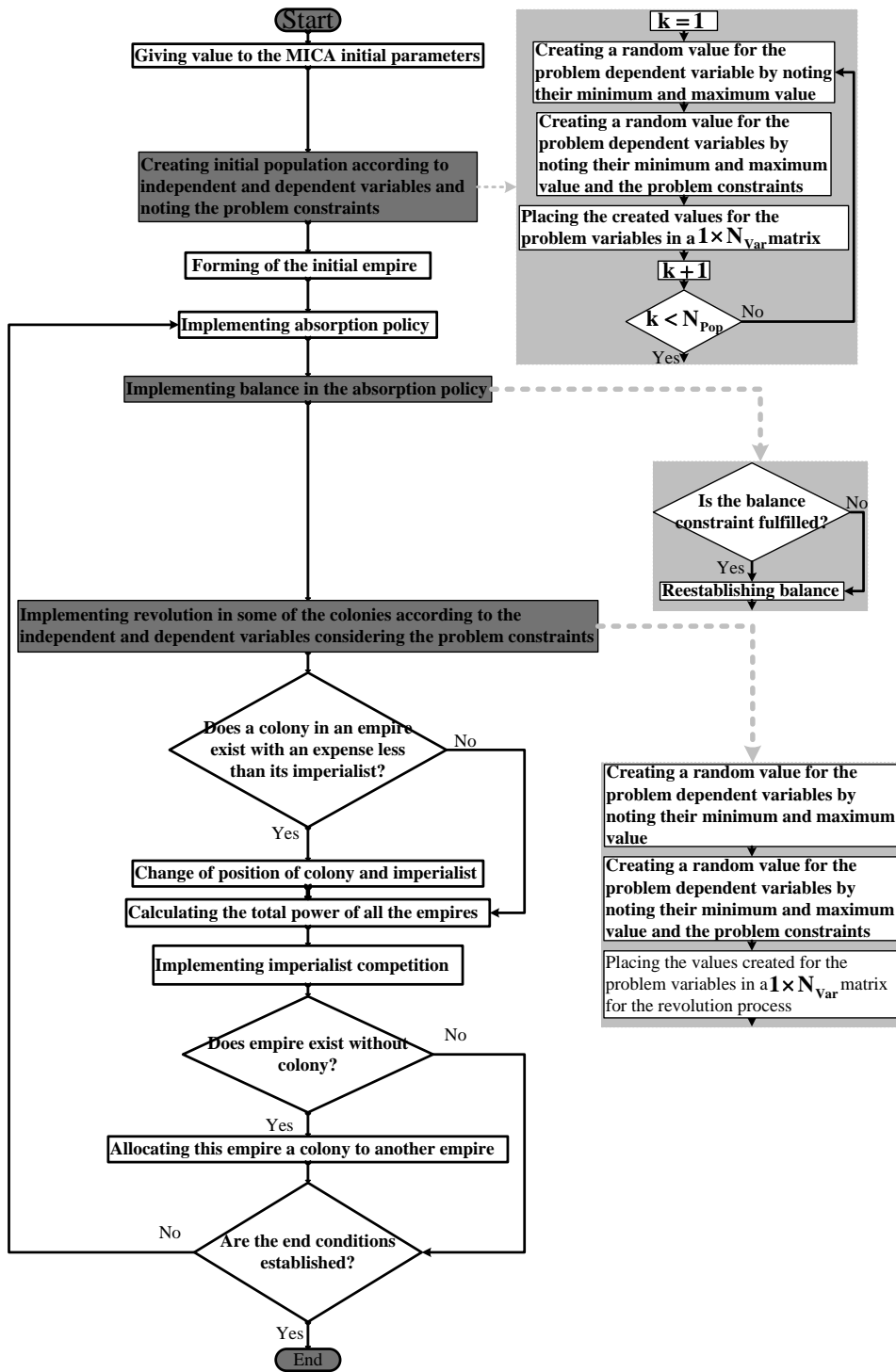
Figure 4.12: The graphic illustration of the process undertaken in the $MICA$ unit

Figure 4.13: The graphical representation of the process undergone in the *MABC* unit
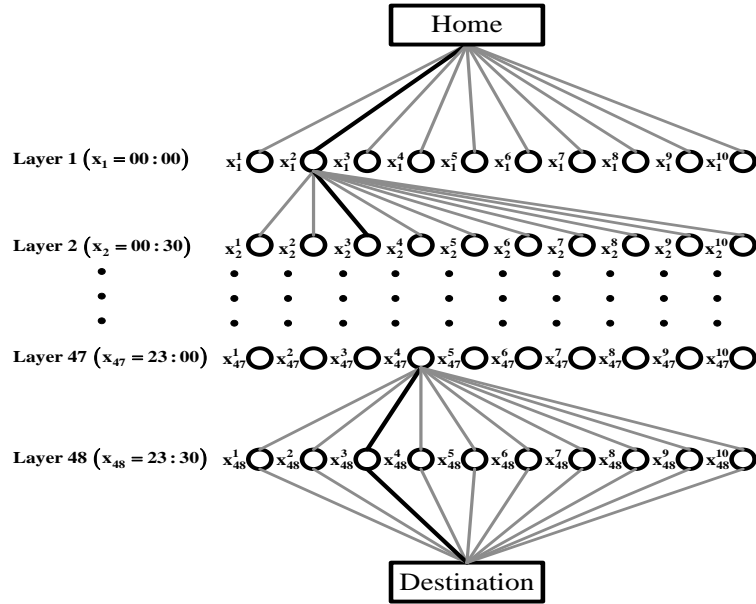
Figure 4.14: Graphical representation of the ACO process in the form of a multi-layered network
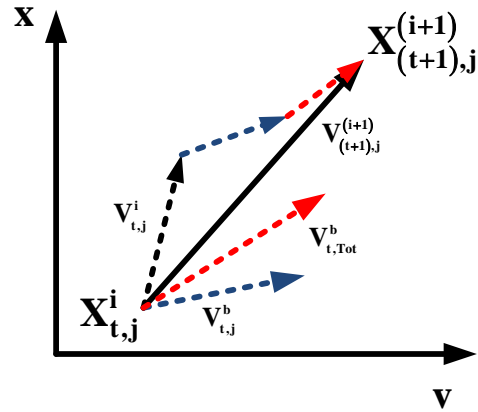
Figure 4.15: The shape of the vectors in the PSO algorithm

(a) Fully Connected topology

(b) Ring topology

(c) Star topology
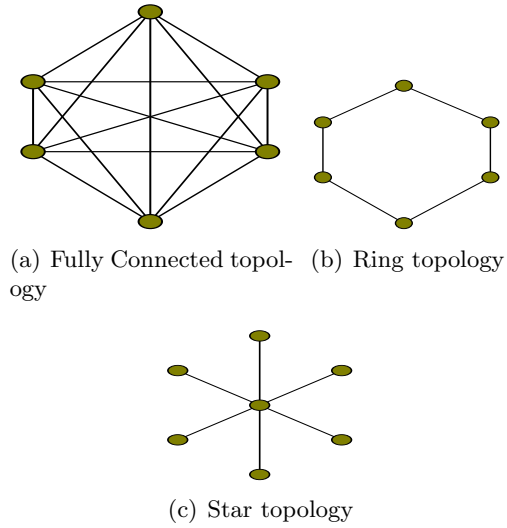
Figure 4.16: Different topologies used for arranging particles in the search space
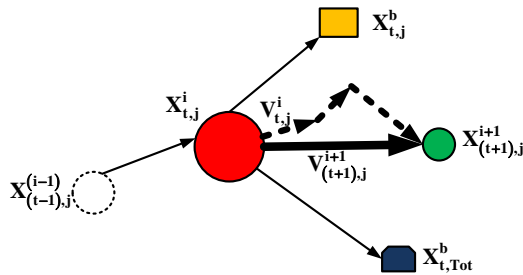
Figure 4.17: The method of particle movement in the PSO algorithm search space
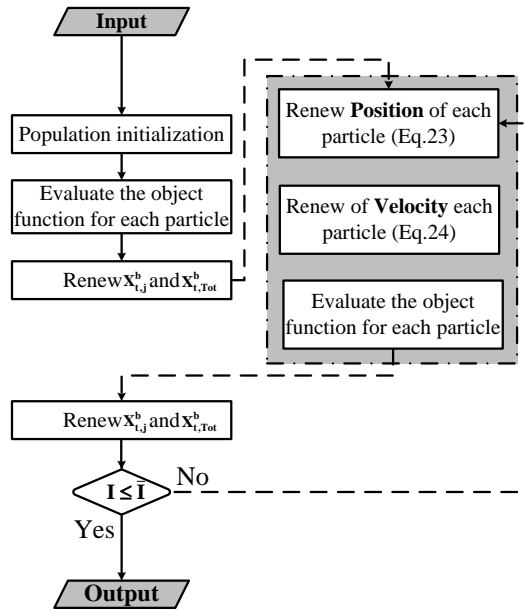
Figure 4.18: $EMS - MPSO$ unit
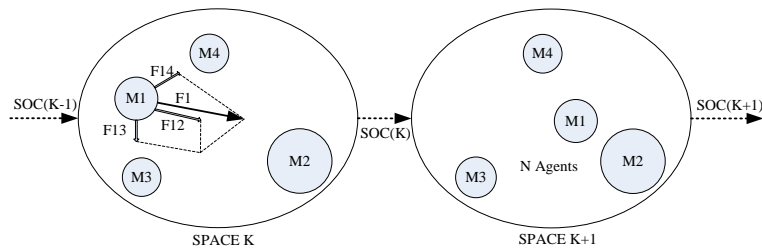
Figure 4.19: The method of placement of the masses in the search space and the resultant of the forces applied between them
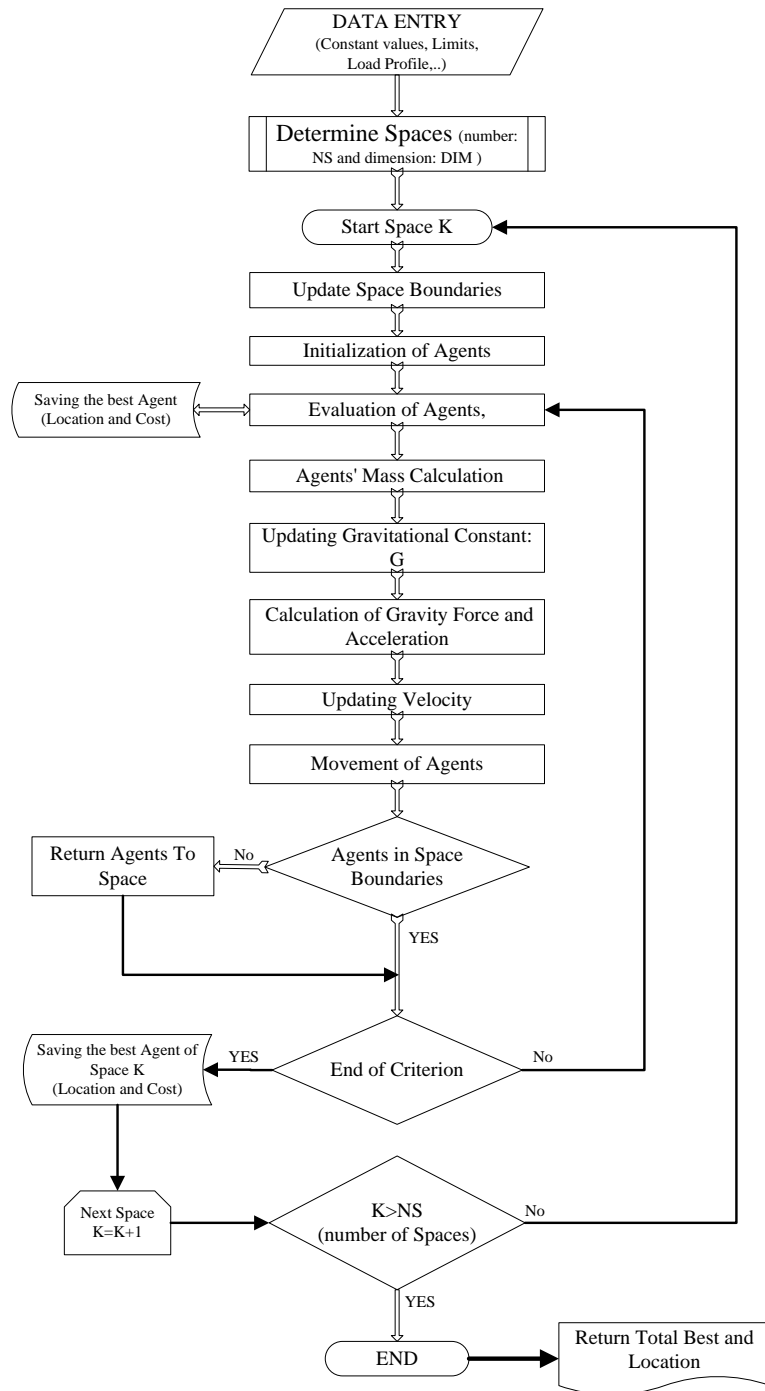
Figure 4.20: Graphical illustration of the process undertaken in the *MGSA* unit

5

Results and discussion

In this chapter, the achieved results due to the proposed algorithms have been compared with each other. In this direction, advantages and the existence limitations for each of them have been investigated as well. On the other hand, the obtained results from each of the proposed algorithms in both operating mode (isolated and grid connected) have been compared to together with accuracy discussion. The proposed real time optimization has been presented at the first. Then, a MCEMS algorithm has been presented as a basic algorithm. After that, to study the performance of other proposed algorithms including MINLP, PSB, MICA, MABC, MACO, MPSO, and MGSA, the obtained results have been compared with MCEMS algorithm. In the grid connected mode, the implemented EMS based on MACO, MPSO, MICA and MABC have been investigated their capabilities in production cost minimization. Furthermore, their capabilities in reduction of MCP have been compared with MINLP algorithm.

Moreover, this section presents the results of experimental evaluations over both islanded and grid connected IREC′s MG carried out to verify the EMS operation under different scenarios.

The scenarios bellow have been considered for testing the performance and efficiency of the suggested algorithm:

- Scenario ♯1

    In this scenario, the system is in normal operation mode and the optimum power and the proper timing of each one of the present microsources in the system will be obtained by the suggested algorithm

- Scenario ♯2

Sudden load increase has occurred during the periods 17:00-17:30 and 18:00:18:30.

- Scenario ♯3
  The system plug and play ability can be investigated by this scenario. WTG has shutdown during 19:30 to 21:00 periods. Also, PV has shutdown during 19:30-20:00 periods.

5.1 Islanded mode

5.1.1 The Proposed Real time Optimization

In Figure 5.1 the SOC is shown in scenario 1 and 2. As it is observed, in the first scenario from 00:20 o′clock the BES system starts charging and at 00:35 reaches the value $\overline{SOC}$. In this instant, BES system is suddenly discharged at about 58%. After that about 10 minutes the BES system starts charging and again during the periods 00:55 to 01:35. Hence, the value of $SOC_{1,t}$ is more than the value of $SOC_{2,t}$ at similar time that shows the system discharge during this period at scenario 2. During the first 6 hours of the system operation (from midnight to early in the morning) at about 46% of the times the value of $SOC_{1,t}$ is more than $SOC_{2,t}$ that shows that during this time period in the system scenario is used more and at about 36% of the times is also opposite of this case. At 18% of the times also the values of SOC in both of the two conditions are not changed.

During the second 6 hours of system operation (from noon to sunset) this trend is become the opposite. In this time interval about 42% of the times the value of $SOC_{1,t}$ is become greater than $SOC_{2,t}$ and at 53% of the times the opposite is true. Finally, at 5% of the times also BES system in this time interval is not changed under the two conditions. From 13:55 to 16:30 the SOC profile in both of the scenarios are similar to each other and significant changes is not observed. At the third 6 hours of the system operation (from sunset to the night) at 18:15, $SOC_{2,t}$ reaches the value $\underline{SOC}$ this is while the value of $SOC_{1,t}$ at similar time is about 77%. The significant point is that, during the time interval 19:30-21:00 despite the occurrence of scenario 2 however SOC is equal to $\overline{SOC}$ in both of the scenarios 1 and 2. This means that the algorithm in this time interval is not used the BES system.

As it is observed from Figure 5.2, although at 17:00 and 18:00 scenario 2 is occurred however the system in the time intervals 16:40 and 18:05 to 18:15 is encountered UP. At 16:40 that the value of the required power for NRL is equal to $28.15kW$, BES system is operated in the discharging mode and
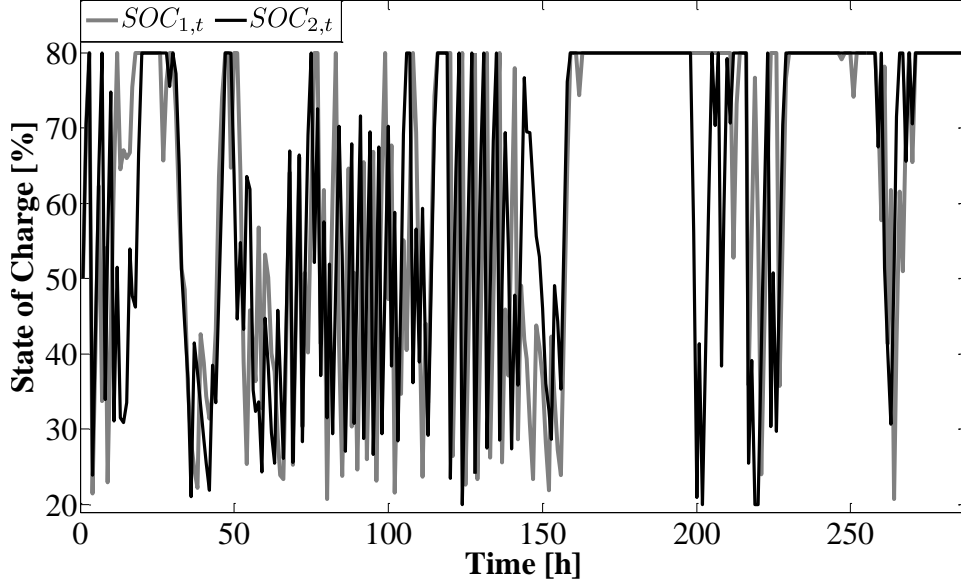
Figure 5.1: The situation of SOC at scenarios 1 and 2

after supplying part of the required power the value of its SOC reaches $\underline{SOC}$. Exactly at this moment MTG also enters service with the power $9.6kW$ and although it can give more power for feeding load to the system however the algorithm is decided that some UP be generated and MTG enters service with less power. At 17:55 although the value of NRL power is equal to $24.18kW$ under these conditions MTG enters service with the power $\overline{P}^{MTG}$ and also BES system with the power $\overline{P}^{BES+}$ supplies another part of the consumed load, so at this moment despite high load demand, the system has no UP. At 18:05 MTG system is entered service with the power $\overline{P}^{MTG}$ and BES system also supplies part of the power by discharging but because the value of $SOC_{2,t}$ at this moment reaches the value $\underline{SOC}$, so some UP is generated. Also at 18:10, MTG continue its work with the power $\overline{P}^{MTG}$ but BES by noting its SOC situation, cannot take part in supplying power. In this moment under these conditions more UP will be generated relative to the previous case.

The comparison of SOC under different scenarios are shown in Figure 5.5. As it is observed, during one working day of MG system performance, about 40% of the times the value of $SOC_{1,t}$ is more than $SOC_{3,t}$. Also, at about 29% of the times the opposite of this fact is true. Also at 33% of the times their value are equal. From 17:00 that scenario 3 occurs, until 17:30 the

89
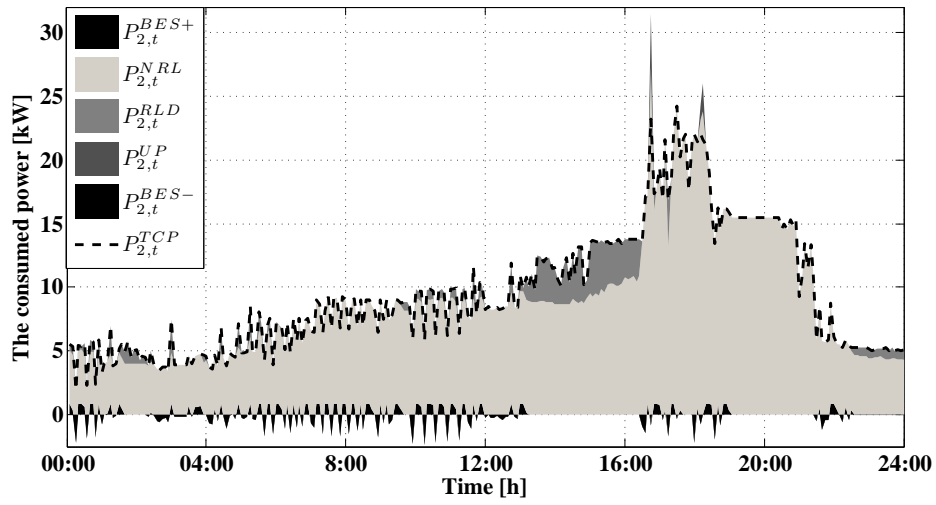
Figure 5.2: TCP and the rest of the consumers related to scenario 2
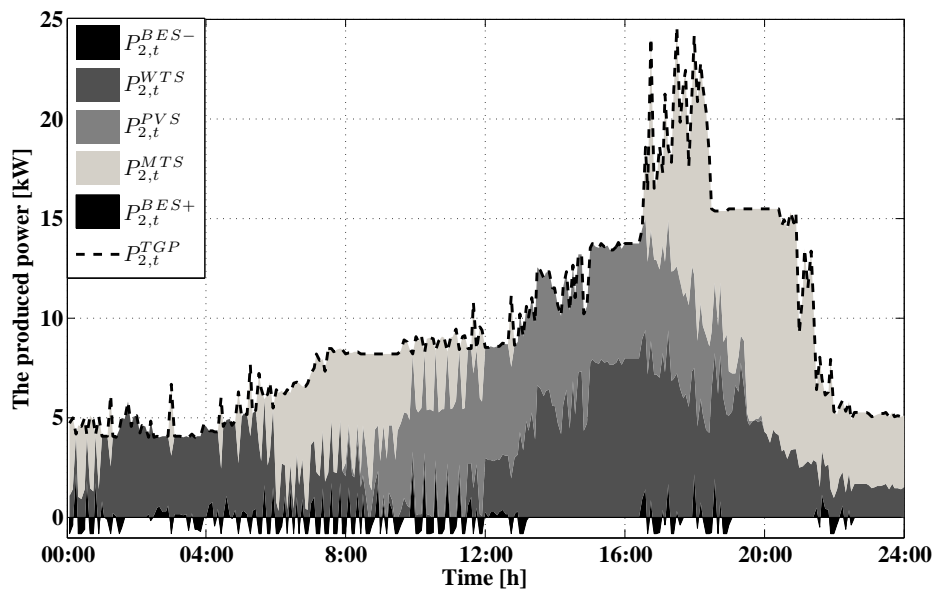
Figure 5.3: TGP and the power of the rest of the generators related to scenario 2

values of SOC in scenarios 1 and 3 are equal to $\overline{SOC}$. At 17:30 BES system at scenario 3 starts discharging and the value of SOC reaches about 35% this is while its value at scenario 1 stays at the same previous amount. The significant point is that BES system at scenario 3 starts to operate in charging mode at 17:40. But exactly at this hour at scenario 1, it starts discharging but finally the values of SOC at both scenarios are almost equal to each other (about 53%). Opposite of this state takes place at 17:45. That is BES at scenarios 3 and 1 starts to operate discharging and at scenario 1 starts charging.

Although the value of $SOC_{1,t}$ at 18:00 reaches $\overline{SOC}$ however the value of $SOC_{3,t}$ at this instant is equal to 26%. At this instant one more time also load demand has increased significantly, despite this, at scenario 3 the battery starts charging and at 18:25 its value reaches $\overline{SOC}$. It means that in this scenario the algorithm has used MTG with maximum capacity and has presented to use some UP. From 19:35 to 21:00 although the value of $SOC_{1,t}$ is equal to $\overline{SOC}$ but the value of $SOC_{3,t}$ has reached $\underline{SOC}$ during this time interval. That is during this time interval the algorithm at both scenario has preferred to use MTG for feeding the consumers.
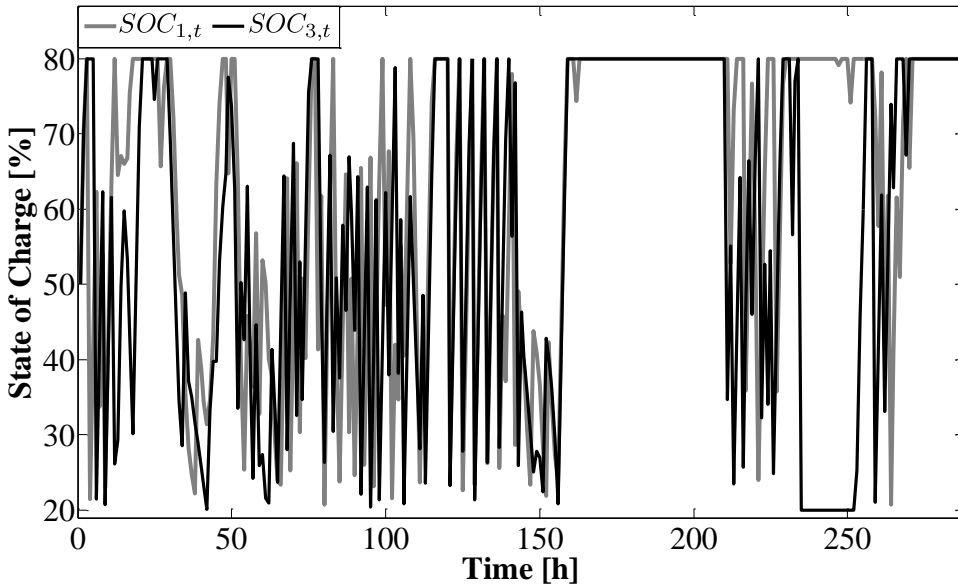
Figure 5.4: The situation of SOC at scenarios 1 and 3

The value of TCP and TGP power during 24 hour MG system performance under scenario 3 is shown in Figures. 5.5 and 5.6. At 19:25 the power required

by NRL is equal to $15.5kW$ that part of it is supplied by MTG, and other part also will be fed by BES system with $2.4kW$ discharging power. But at this instant BES system is discharged completely and the value of $SOC_{3,t}$ during the occurrence of this scenario (from 19:25-20:50) is equal to $\underline{SOC}$. Also at this instant the value of UP by noting that BES can also have role in supplying power, is a less value relative to other hours. During this period, MTG is also in service with the power $\overline{P}^{MTG}$ however the system has encountered UP. From 20:25 to 20:50 periods by noting that the value of the power required by NRL is reducing, as a result of it the value of UP is also reducing.
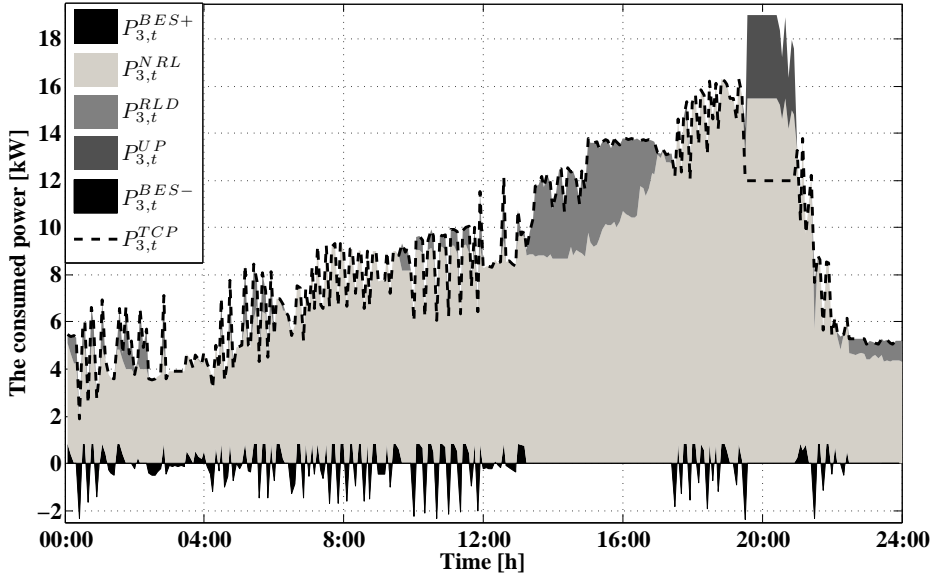
Figure 5.5: TCP and the rest of the consumers related to scenario 3

5.1.2 MCEMS

Application to test grid

The stand-alone MG system is shown in Figure 5.7. The full details about this system has been presented in $[97, 116, 117]$. IREC's MG has been configured as PV, WT, MT, ES, EWH and load demand emulators. Emulators run for the system with real life data summarized in Table 5.1. Due to cabinet limited power (maximum 5 kVA) firstly all of the calculated data using
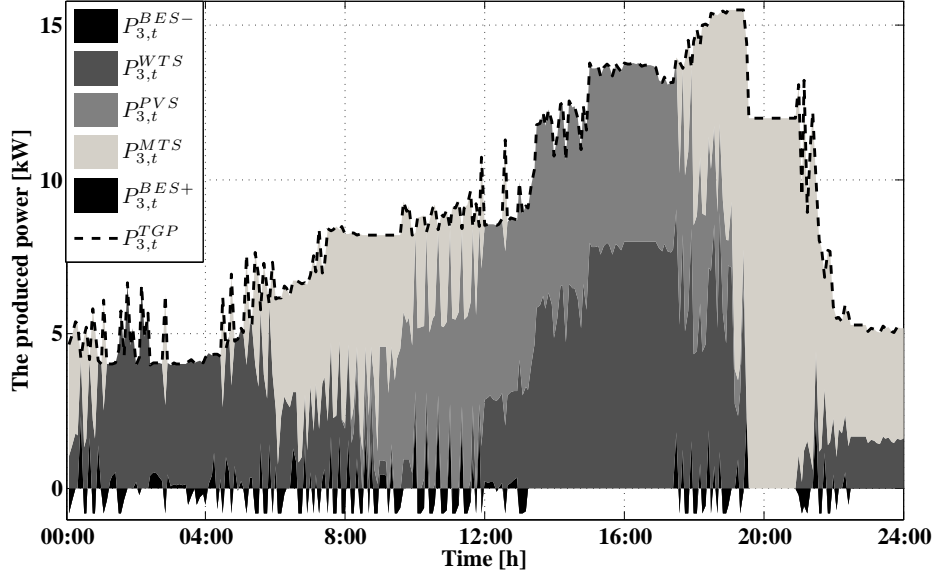
Figure 5.6: TGP and the power of the rest of the generators related to scenario 3

MCEMS algorithm have been scaled down to the maximum power then for more visibility, the real data have been extracted.

Lithium-ion batteries were emulated as energy storage in this study [118]. The battery model emulated in this simulation is SYNERION 24M, with the parameters presented in the Table 5.1. Wind data used was obtained from online records from the weather station at Museu de Badalona, Badalona (Spain) [119]; affiliated with the Generalitat de Catalunya Weather Network. The hourly average wind speed data recorded at a height of 6 meters was chosen for the 24-hour simulation study [119]. The output power of the WT corresponding to the wind speed profile presented in [120] and also real data of WT emulator are shown in Figure 5.8(a).

The solar data, such as the global and direct normal irradiance were obtained from the online records of the Manresa, Barcelona (Spain) [121]. PV output and real data of the related emulator are also shown in Figure 5.8(b).

Load demand profile was also obtained from [122]. The demand profile and real data of the related emulator are shown in Figure 5.9.

Simulation and experimental studies are carried out for a typical day.

The supply bids by generation units are also shown in Table (5.1).

93

Table 5.1: The proposed MG specifications

Parameter	Symbol	Value
ES system		
Voltage (V)	V_t^{ES}	24
Nominal capacity (Ah) at $+25°C$	N^{ES}	84
Fully Charged voltage (V)	$\overline{V}^{ES}$	26
Cut-Off discharge voltage (V)	$\underline{V}^{ES}$	21
The maximum of continuous charge current (A)	$\overline{I}^{ES,c}$	34
The maximum of continuous discharge current (A)	$\overline{I}^{ES,d}$	160
The maximum battery power during charging mode (kW)	$\overline{P}^{ES,c}$	0.816
The maximum battery power during discharging mode (kW)	$\overline{P}^{ES,d}$	3.84
The maximum delivered power by converter (kW)	$\overline{P}^{ES}$	4
Initial SOC at T (%)	SOC_I	50
The maximum SOC (%)	$\overline{SOC}$	80
The minimum SOC (%)	$\underline{SOC}$	20
The initial stored energy in the battery (kWh)	E_I^{ES}	1
The maximum stored energy in the battery (kWh)	$\overline{E}^{ES}$	1.6
The minimum stored energy in ES (kWh)	$\underline{E}^{ES}$	0.403
The maximum capacity of the battery (kWh)	E_{Tot}^{ES}	2
The charge efficiency factor (%)	η_c	96
PV system		
Maximum instantaneous power (kW)	$\overline{P}^{PV}$	6
Minimum instantaneous power (kW)	$\underline{P}^{PV}$	0
WT system		
Maximum instantaneous power (kW)	$\overline{P}^{WT}$	8
Minimum instantaneous power (kW)	$\underline{P}^{WT}$	0.45
MT system		
Maximum instantaneous power (kW)	$\overline{P}^{MT}$	12
Minimum instantaneous power (kW)	$\underline{P}^{MT}$	3.6
Start-up time of the MT (min)	T_{ON}^{MT}	10
Shut-down Time of the MT (min)	T_{OFF}^{MT}	10
Ramp down limit (kW)	R_l	6
Ramp up limit (kW)	R_u	6
EWH system		
Maximum EWH power (kW)	$\overline{P}^{EWH}$	6
Minimum EWH power (kW)	$\underline{P}^{EWH}$	0

WT | PV | ES | MT | EWH | Load

8 kW | 6 kW | $\overline{P}^{ES,c} = 0.816\,\text{kW}$ | 12 kW | 5 kW | 15.5 kW

$\overline{P}^{ES,d} = 3.84\,\text{kW}$
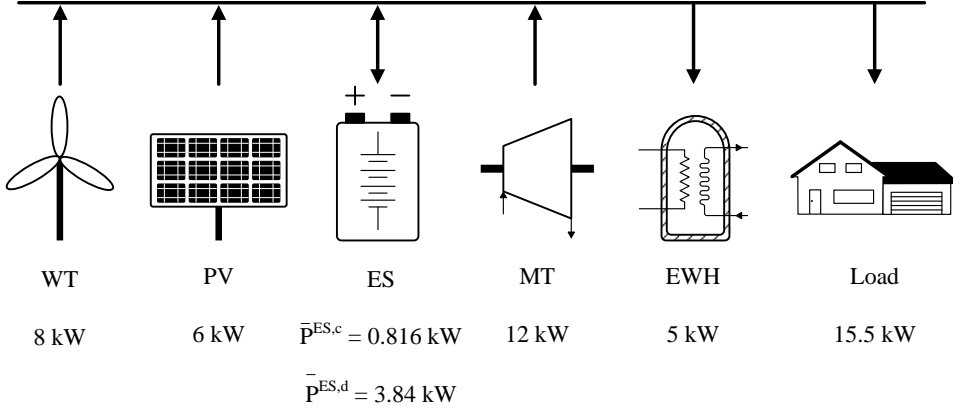
Figure 5.7: Configuration of the proposed system

Table 5.2: The supply bids by generation units into a supply curve [€/kWh]

π^{WT}	π^{PV}	π^{MT}	$\pi^{ES,d}$
0.083	0.112	0.152	0.112

Results and discussion

Figure 5.10 shows SOC of the battery for six operation mode including Charging Mode, Discharging Mode, Over Charging Protection Mode, Over Discharging Protection Mode, Fully Charged Mode and Fully Discharged Mode. Meanwhile, the initial SOC is assumed to be SOC_I in order to show charge/discharge pattern clearly.

The battery power profile is shown in Figure 5.11. This figure also shows the comparison of the calculated set points due in simulation and the real values obtained from emulators by CCU. The small difference between the two waveforms is due to the fact that the experimental waveform is gotten directly from DSP. As seen in this figure, in the time intervals 01:30, 02:00, 04:00, 05:00 and 13:30-17:00, MG system can raise the battery charging.

The battery maximum charging and discharging power are limited to $\overline{P}^{ES,c}$ and $\overline{P}^{ES,d}$ to keep the battery in the healthy condition to achieve its maximum possible life time [97]. As a result, the ES cannot provide the necessary discharge power during 18:00-18:30; therefore MT is employed to meet the load demand as shown in Figure 5.12. The MT produces power
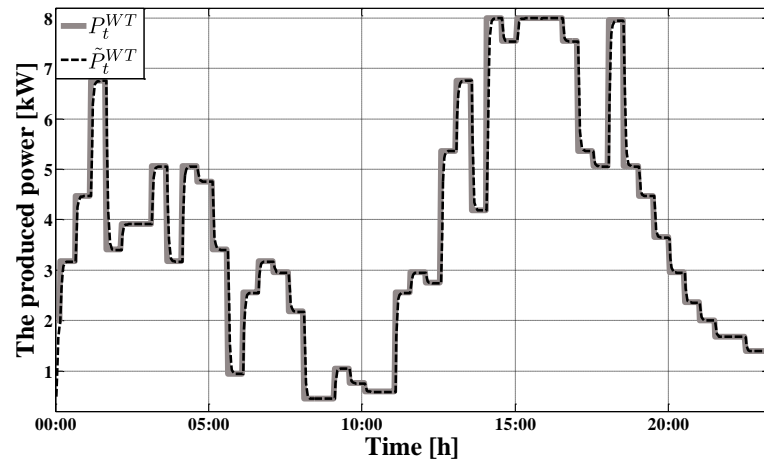
(a) WT
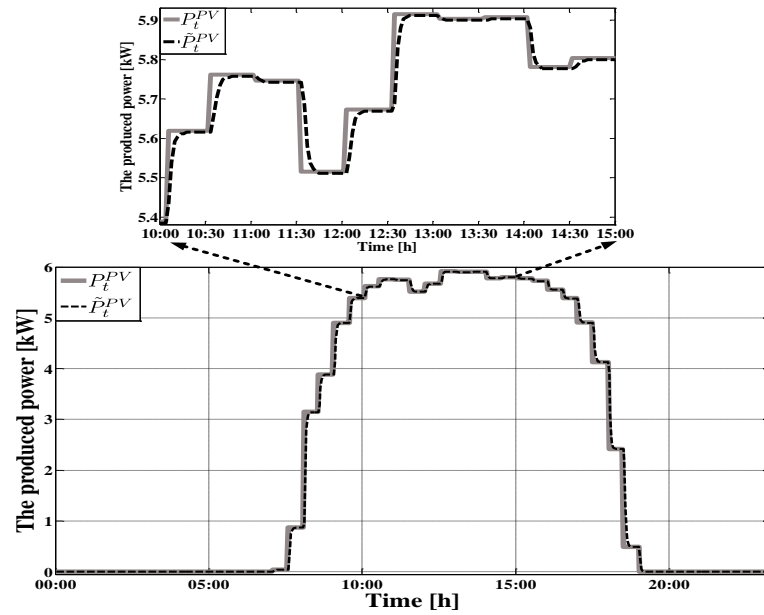
(b) PV

Figure 5.8: Comparison of renewable resources set point profiles (solid curve) and measured value (dotted curve) during twenty-four hours system work

when the available wind power, PV and battery are not sufficient to meet the demand. In $MCEMS$, when the SOC is equal or less than $\underline{SOC}$, the MT
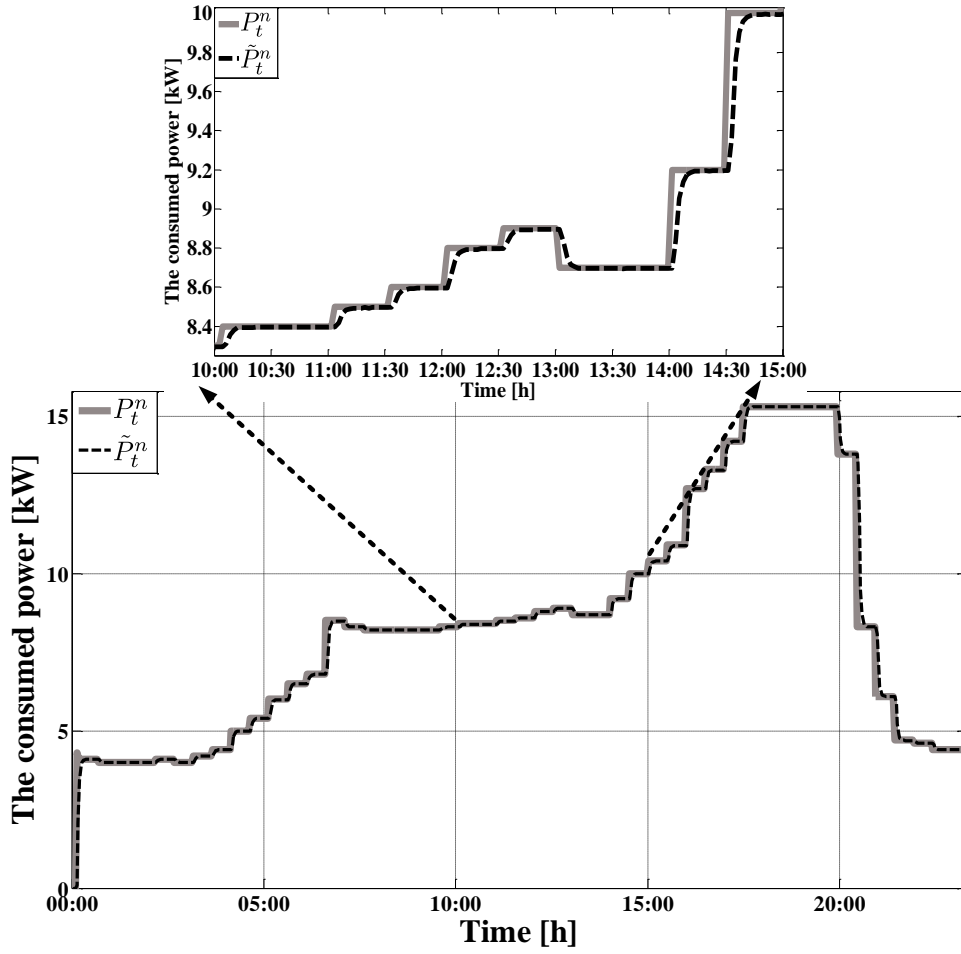
Figure 5.9: Comparison of hourly load demand set point profile (solid curve) and measured value (dotted curve) during twenty-four hour service

will be turned on and the remainder of the required power will be supplied by the MT. If the shortage power is less than $\underline{P}^{MT}$ and ES is in Fully Discharged Mode, MT will be turned on with the minimum of its rated power. Afterwards, the shortage power will be supplied by MT completely and the rest of the power generated by MT can be used to charge ES. This case can be seen in Figure 5.12 during 10:00-11:30, 12:00, 13:00 and 22:30.

If the produced power by WT and PV are higher than the demand while ES is in Fully Charged Mode, the excess power will be used to supply a useful dump load (e.g., an EWH) as shown in Figure 5.13. Another case is
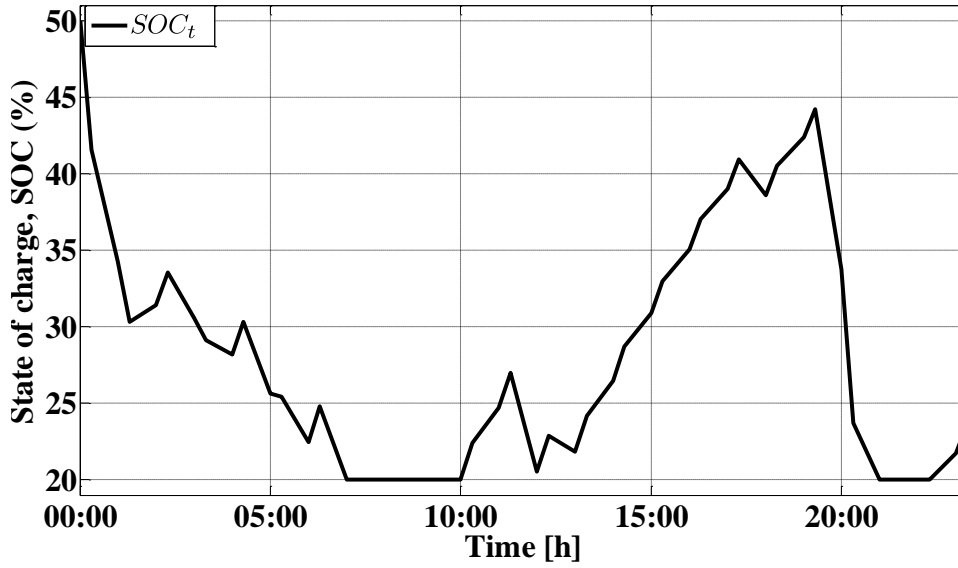
Figure 5.10: SOC of battery during 1-day-storage battery bank in the charge and discharge modes

when surplus power is larger than $\overline{P}^{ES,c}$ as a result this power can be used to supply EWH. This condition can happen during 04:00, 06:00, 10:00-11:30, 12:00 and 13:00-17:30 periods.

TRP is measured from common point between load demand, EWH and ES emulators and it has been drawn as shown in Figure 5.14(a) to compare the obtained results from simulation and experimental setup. As seen in this figure, emulator follows these set points. Likewise, TGP is measured from a common point between WT, PV, MT and ES and its experimental and simulation values are compared as shown in Figure 5.14(b).

As seen in these figures, RTO can be used to perform tasks precising a very fast time response (e.g., electric security and stability) and tasks implying a high information exchange with the units (e.g., execution of $MCEMS$ algorithm). However, the time delay between experimental and simulation results has demonstrated to be in good agreement to develop the similar structures in the industrial applications.

The total load and generation profile (simulation output) used to validate the algorithm are shown in Figure 5.15. All shown and used powers are active powers. As seen in this figure, the explained stand-alone hybrid system can meet all the power demands by the load during normal operation.

The market price of WT is usually significantly lower than the market
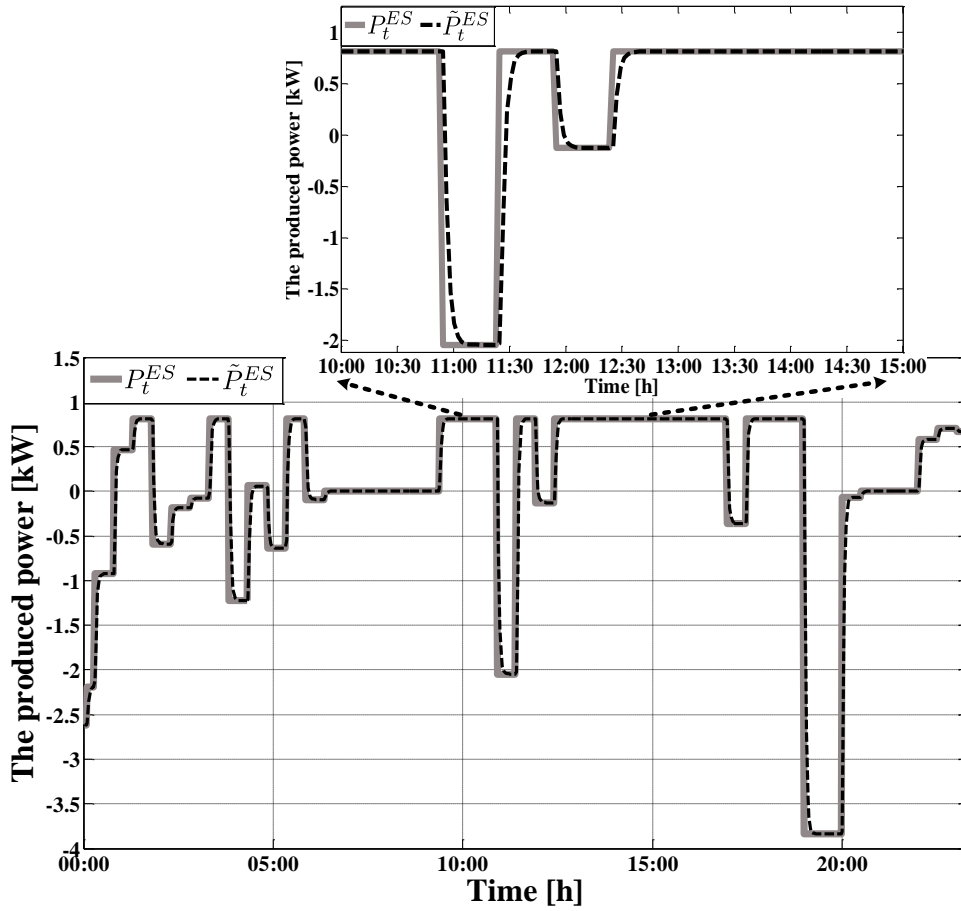
Figure 5.11: Case study battery power (simulation output (solid curve) and measured value (dotted curve))

price of the other micro-sources; as a result the WT is the preferred dispatch power in this MG and the full available power is assumed to be always generated. Figure 5.16 depicts the calculated results of the local market algorithm applied to the MG using the proposed algorithm in Chapter 3. As seen in the figure, MCP can be obtained at each iteration.

The amount of participation of micro-sources changes during the day. The participation of the proposed prices by WT and ES in the market is equal to 50% from midnight to the morning. However, from morning to noon, when PV starts to generate power, its offer can be accepted during 10:00-11:30 and its participation in the LEM is around 34%. The proposed price by MT
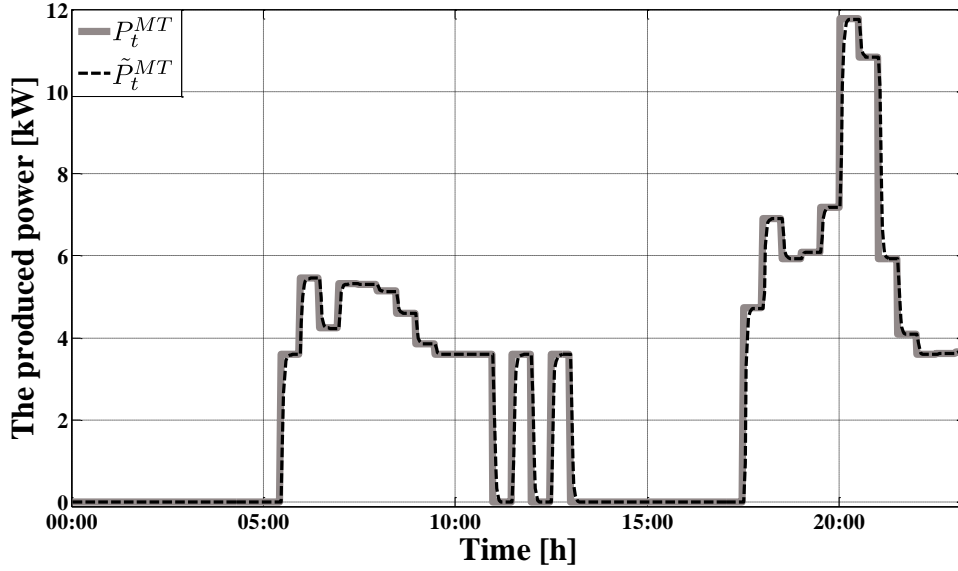
Figure 5.12: Comparsion of hourly MT produced power set point profile (solid curve) and measured value (dotted curve) during twenty-four hour service

will be accepted during 06:00-10:00 and its offer will be accepted around 67% during this period. From noon until evening, the offer of WT and PV will be accepted and their participations in the market are 42% and 58%, respectively. The proposed offer by these devices plays no significant role in the market clearing during 18:00-23:30 periods but the offers of ES and MT have been accepted during this period. The offers of the MT unit show the biggest role in the LEM around evening. The offered prices of MT unit have been accepted around 92% in the evening while the offers of ES have just been accepted around 8% during this period.

In order to show the capability of the proposed approach, simulation has been repeated for the same system when MT always on and generates at least the minimum of its rated power. As seen in the Figure 5.16, although λ_t^{MCP} sometimes is bigger than $\lambda_t'^{MCP}$ (i.e. during 00:00-01:30, 02:30, 04:30, 05:30, 11:30 and 19:30-20:30), the total cost of generation units has been significantly reduced (around 8.5%) during a day.
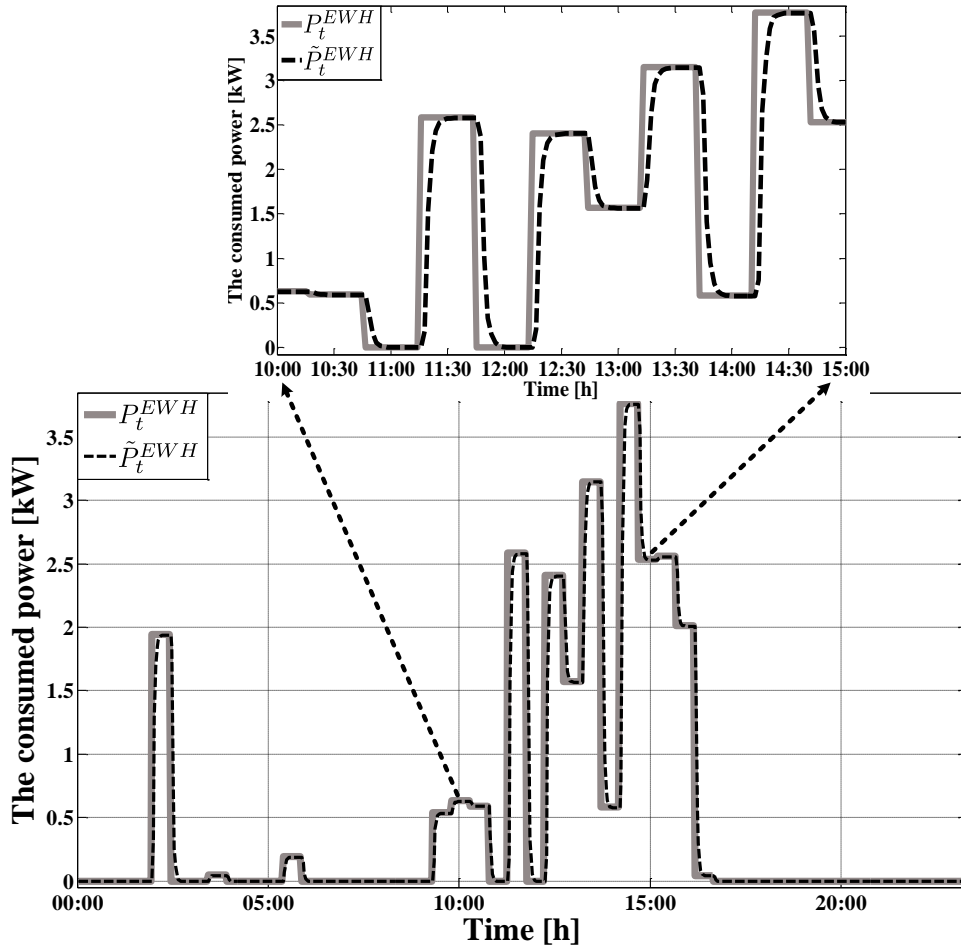
Figure 5.13: The hourly EWH consumed power during twenty-four hour service (measured value (dotted curve) and simulation output (solid curve) calculated by the EMS

Conclusion

In this has presented a MCEMS algorithm for stand-alone and grid connected MGs incorporating different renewable energy resources and storage units based on two market indicators: single ownership and LEM. The LEM proposed has been designed to obtain the best purchasing price in a DAM, as well as to increase the utilization of the existing DER. Simulation results on a four generation unit test system for the presented algorithm have demonstrated that it is capable to locate a global solution of the related
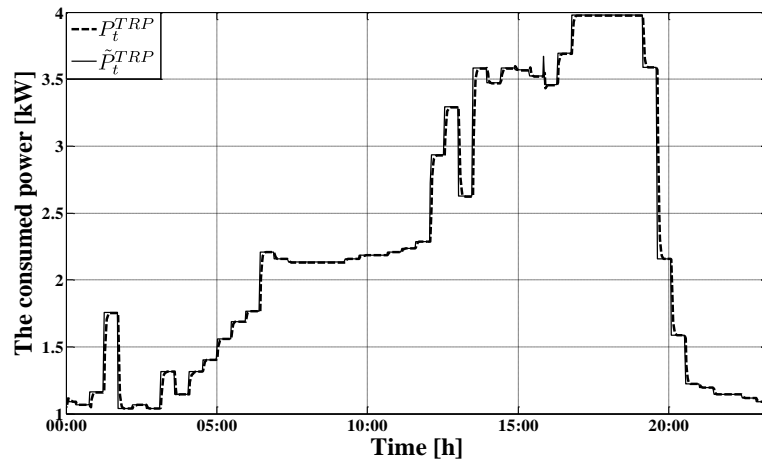
(a) TRP
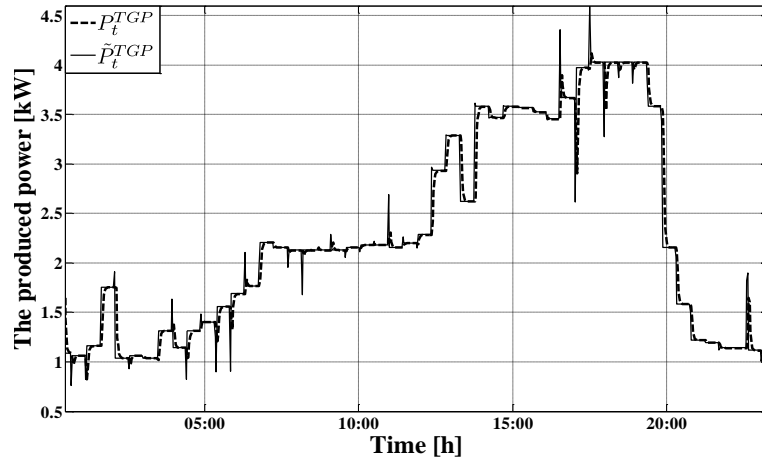
(b) TGP

Figure 5.14: Hourly total load consumption and power production during the day (set point values (solid curve) and experimental measurement (dotted curve))

MCP problem. This algorithm has been developed and verified by experimental setup. Real life experimental data obtained from IREC has been used to test the performance and accuracy of the proposed algorithm. It is applied to IREC's MG to demonstrate some real time algorithm into a MG. The studies scenarios have demonstrated fast response of emulators in sending set-points through CCU, flexibility of control modes and the ability
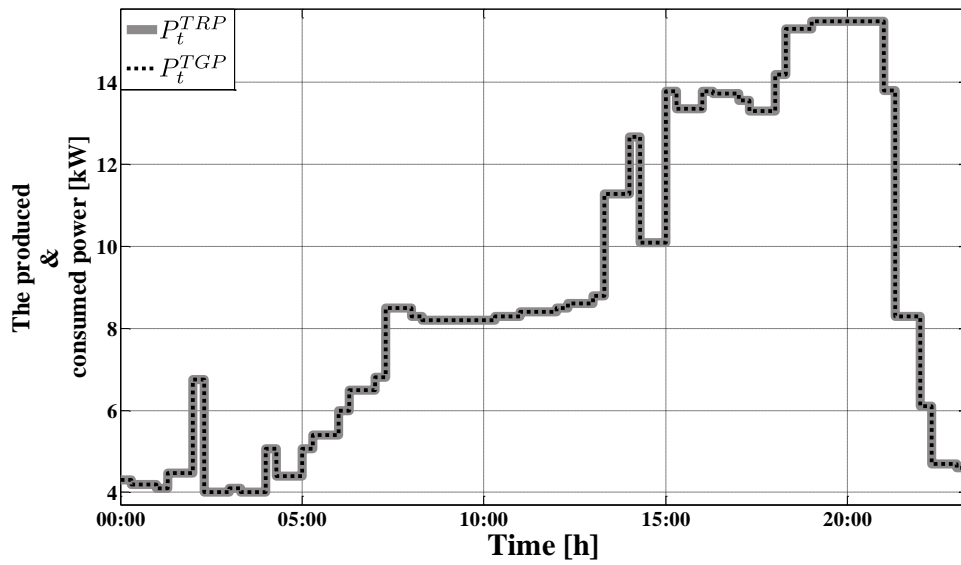
Figure 5.15: Hourly total load consumption and power production during the day
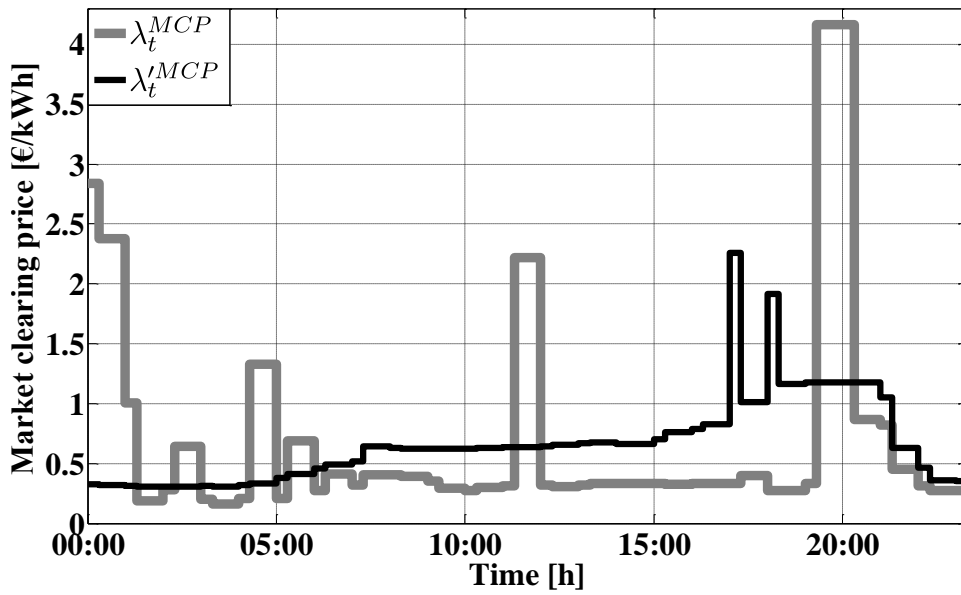
Figure 5.16: MCP during twenty-four service of system

of island and grid connected operation in a suitable manner. The results obtained in laboratory have demonstrated to be in good agreement with simulation results. Moreover, the use of the proposed LEM have led to a reduction of the total cost of power generation (8.5% approximately). Simulations and experimental evaluations have been carried out using real data to test the performance and accuracy of the MG testbed. This algorithm aims to operate the MG in both operating modes, ensuring uninterruptable power supply services and reducing the global cost of generated power. Results demonstrate the effectiveness of the proposed algorithm and show a reduction in the generated power cost by almost 8.5%. The proposed algorithm, in addition to online monitoring, control and optimization of the overall power system performance, could be used to optimize energy consumption, most especially during critical periods. In $MCEMS$, LEM was used to obtain the best buying price in a day-ahead energy market, as well as to maximize the utilization of the existing DER considering different scenarios. To compensate for the UP due to unpredictable events in MG during islanded operation mode, DR concept was employed. The performance and accuracy of the proposed algorithm, when tested with real life experimental data obtained from IREC, was really impressive. The electricity generation cost was significantly reduced by around 10% using DR management.

5.1.3 MINLP

Application to test grid

Simulation and experimental evaluations are performed for a stand-alone WT-PV-MT-ES system shown in Figure 5.17. The IREC Testbed is presented in Figure 2.9. In short, the Testbed is built from power emulators able to generate or consume any desired power profile. Detailed explanation concerning the structure and configuration setting is found in [2, 116, 117]. As, it is observed from Figure 5.17, this system has a central controller to which data will be sent. This data includes the offer of each producer, the value of predicted power related to renewable sources and main load, the value of stored energy in the battery in the previous time and the general properties of each micro-source. Then, through the presented algorithms, this controller can make the required decisions for energy exchange within the MG considering micro-sources and load consumption.

The output power of the WT is shown in Figure 5.18. As shown in this figure, the WT is faced with a shutdown during 19:30 until 21:00 periods and the PV system is also faced with a shutdown during 19:30 period as shown in
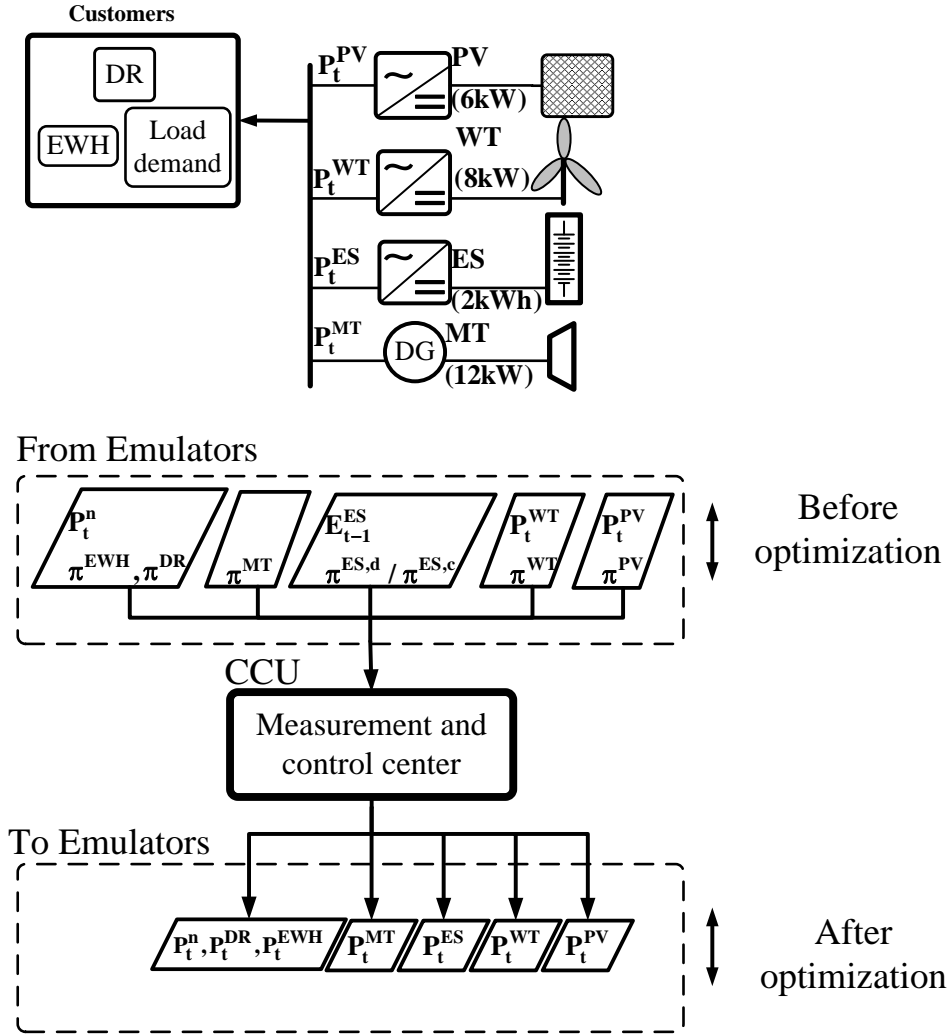
Figure 5.17: Configuration of the proposed test system

Figure 5.19. As seen in this figure, all of the available power by PV has been used in $MCEMS$ algorithm during 16:30-17:00 and 19:30-20:00 periods as well as 3.015 and 0.5 kW were not used in $EMS - MINLP$, respectively.

The total aggregate hourly average load demand is shown in Figure 5.20. As shown in this figure, the load demand has some fluctuations from 17:00 until 18:00 hours.

The offers suggested by different generation units have been presented in [2].
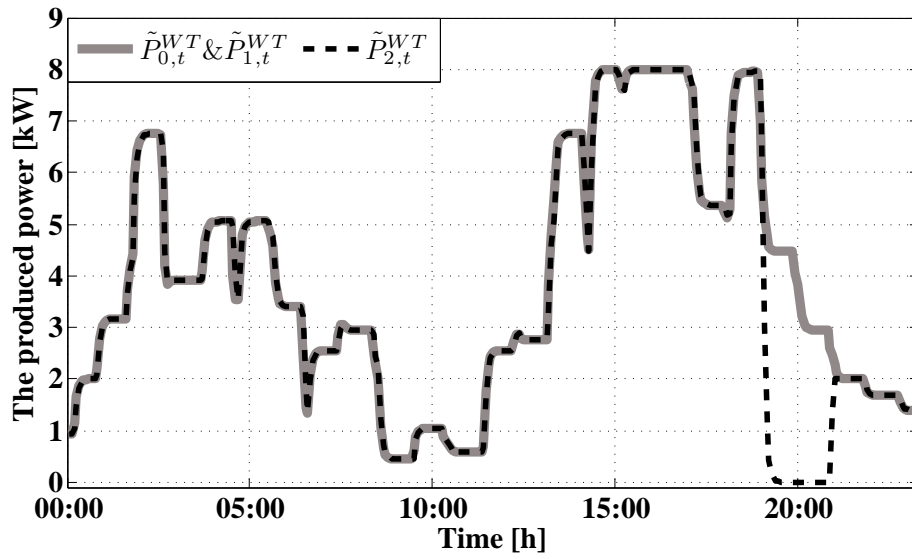
Figure 5.18: WT profile in experimental evaluation
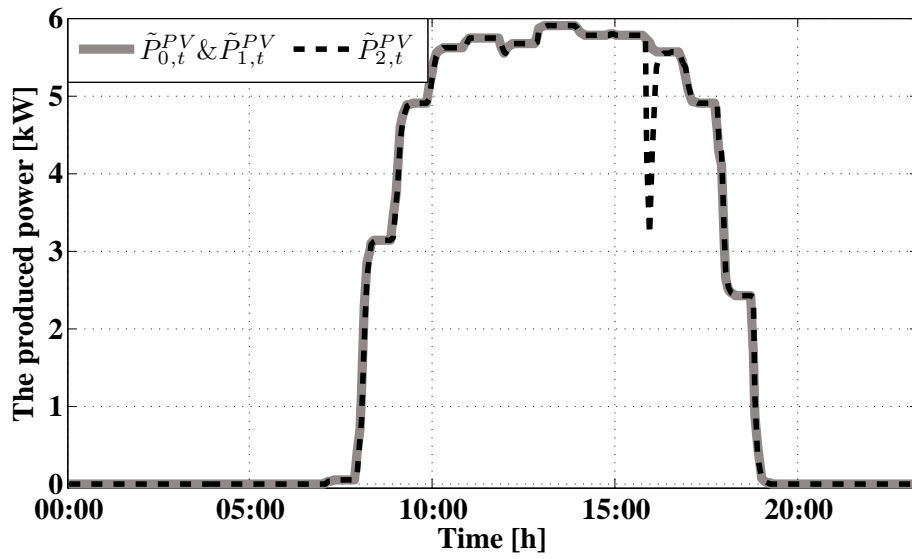
Figure 5.19: PV profile in experimental evaluation
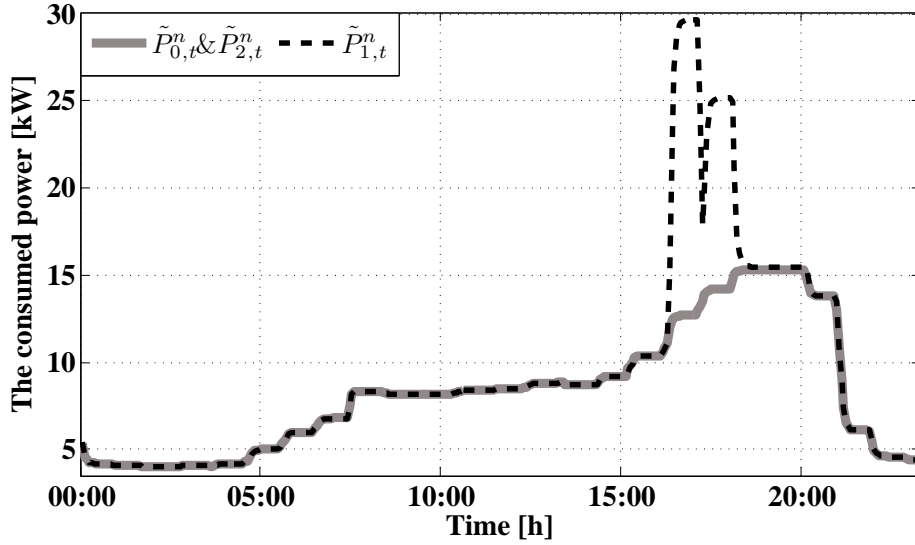
Figure 5.20: Hourly demand profile during twenty-four hours system work in experimental evaluation

Results and discussions

To show the performance of the proposed algorithms, a case study is presented. The studied MG comprises renewable energy sources (WT and PV), and a power and heat combining unit (MT in this study). These are connected to an energy storage system (a battery in this study), as shown in Figure 5.17. The outputs of the algorithms are explained in the following four subsections including execution time of the algorithms, the outputs of the EMS unit, the outputs of DR unit and finally the outputs related to LEM unit.

Execution time of the presented algorithms

In a real-time central EMS, decisions have to be made in a fraction of a second, considering several issues such as the data communication delays, the time required for data transmission from individual micro-sources, ESs, and load entities. This time depends on the application and varies between couple of seconds (in primary frequency control applications such as governor droop control) to couple of minutes (in secondary frequency control application such as automatic generation control) [2]. Therefore, the two

107

proposed EMS algorithms should be able to fulfill this requirement in a short period. The proposed $EMS - MINLP$ algorithm is 27 times faster than the $MCEMS$ algorithm, which makes it a better option for real-time applications in larger systems.

By noting that both of the suggested algorithms for implementing a real time EMS in IREC′s MG Testbed is presented, the execution time of these algorithms has a significant importance. Because central controller must be able to send and receive its necessary data from the micro-sources. It must be able to make proper decisions for optimizing the performance and decreasing the cost in the system. After measuring the execution time of the algorithms in a similar central controller system, $EMS - MINLP$ has obtained the necessary outputs about 27 times faster than $MCEMS$ algorithm. This subject can be because of many rings that have been written for implementing the investigated model in the C program nest to that presented mathematical model in the GAMS software environment nested loops have not been used. The very high speed of $EMS - MINLP$ algorithm can make this algorithm for using in real time applications of energy management in systems having several micro-sources with energy storage equipment, very useful and with high efficiency.

EMS unit (in $MCEMS$ and $EMS - MINLP$ algorithms) outputs

From Figure 5.21, it can be seen that the charging period of the battery in $EMS - MINLP$ is lower than $MCEMS$; however, the stored energy in the battery in $EMS - MINLP$ is larger.

Figure 5.22 shows the MT output power profile for both algorithms. In $MCEMS$ when there is a shortage in the generated power (by WT, PV and ES), the MT supplies the required power. Moreover, in that case the MT is put in service, if SOC is less or equal to $\underline{SOC}$.

As it is observed in this figure, although MT cost is higher than other micro-sources, it has been used more in $EMS - MINLP$. This means that even with the inclusion of MT, the cost is minimum. As it can be seen from Figure 5.22, during some periods the output power of the MT is equal in both algorithms.

As explained before, in the $MCEMS$ algorithm, EGP by the PV and WT micro-sources can also be used for feeding an auxiliary load (such as EWH in this study) after charging the battery. But in $EMS - MINLP$, it can also be used for feeding other consuming sources. As seen in Figure 5.23, extra power exists in $MCEMS$, and it has been used to supply EWH.
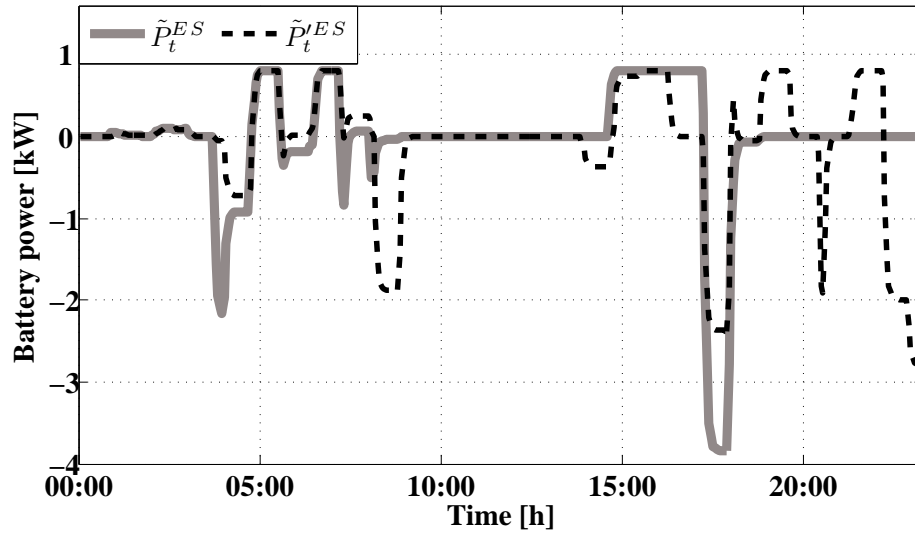
Figure 5.21: ES profile in experimental evaluation
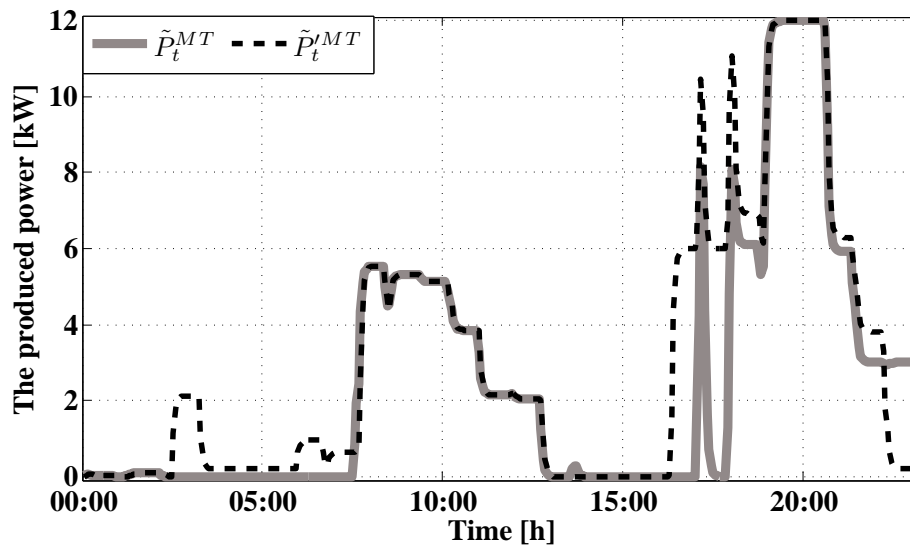
Figure 5.22: MT profile in experimental evaluation
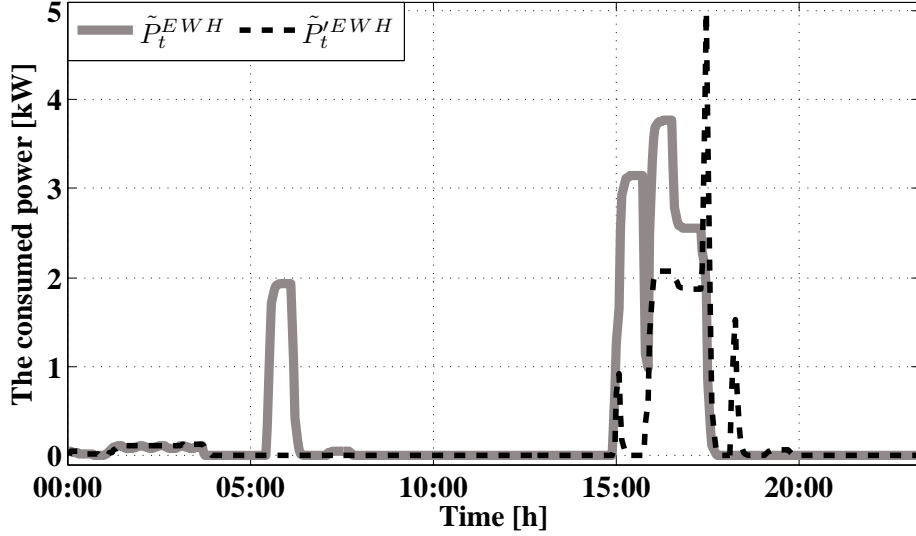
Figure 5.23: EWH profile in experimental evaluation

DR unit output

As it is shown in Figure 5.24, in the $MCEMS$ algorithm, an amount of UP has been observed during the day. By noting the relatively high cost coefficient for the UP considered in the cost function (Eq (2.10)), the $EMS-MINLP$ will try to find the best power supply composition to minimize the cost. From this figure, it can be seen that in the $MCEMS$ case, there are more time intervals with UP than in the $EMS-MINLP$, where it happens only during consumption peaks.

It is worth remarking that although at 17:00, the UP reached in $EMS-MINLP$ is larger than for the $MCEMS$ (arround 83%), its value in average is lower in $EMS-MINLP$ case since it is lower in other period of time (arround 68%). In Figure 5.24, it can be seen that DR profile is different for both algorithms due to the optimization process included.

The consumed power of the DR, UP, EWH, EGP and ES in charging and discharging modes are represented as bar diagrams in Figures 5.25(a) and 5.25(b).

As it can be seen from Figure 5.25, battery charging and discharging pattern is significantly different for the two proposed EMS algorithms. This can also be observed in the EWH, DR, and UP curves. It is noticed that no power has been stored in the ES between 15:30 and 16:30 periods in
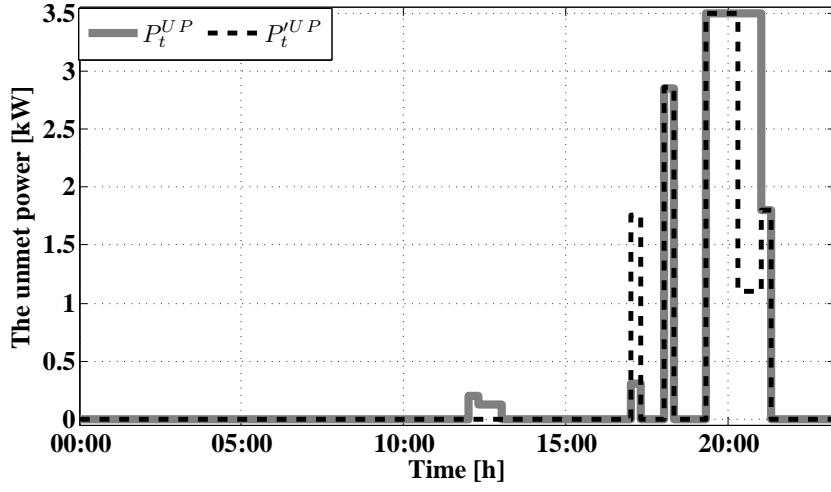
(a) UP profile
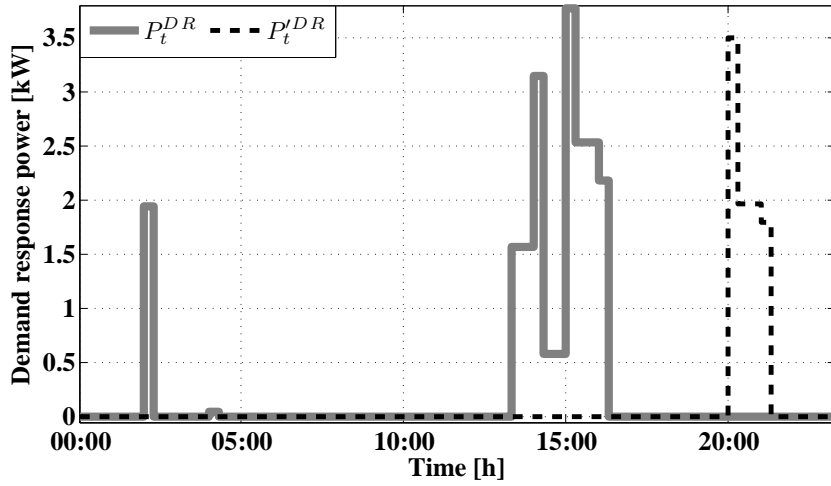
(b) DR profile

Figure 5.24: The hourly UP and DR for both $MCEMS$ and $EMS -$ $MINLP$ during twenty-four hours system work

$EMS - MINLP$, where this amount of excess power has been used in the EWH and DR. The reason is that the SOC of the battery in this case is equal to $\overline{SOC}$ and ES is in fully charged mode. Although the ES is

charged by the excess available power during 17:30 to 18:00 periods in the $MCEMS$ algorithm, it has been discharged at the same time in the case of $EMS - MINLP$ algorithm (as illustrated in Figures 5.25(a) and 5.25(b)).

The EGP generated during the system daily performance in $EMS - MINLP$ is more than $MCEMS$. The total EGP power during one day in $EMS - MINLP$ is 33.3% more than $MCEMS$.

The UP in $EMS - MINLP$ (except at 17:00 periods) is lower than $MCEMS$ and the total UP in $MCEMS$ is about 8% more than $EMS - MINLP$ during the system daily performance.

Although the UP penalty (π^{UP}) is high in this simulation, there is still a small amount of UP at 17:00 period. This is because the battery is fully discharged (the MT is working with its maximum rated power at the same time as seen in Figure 5.22). It is noticeable that the amount of UP in the case of $MCEMS$ is slightly more than the UP in the case of $EMS - MINLP$ for the same time. Since the SOC of the battery at 20:30 period in $EMS - MINLP$ is $\overline{SOC}$, the ES can be discharged to partially meet the load demand. In this case, UP is less than its value in $MCEMS$.

As it is observed from Figures 5.25(a) and 5.25(b), in $EMS - MINLP$, excess power for charging ES during 03:30, 05:00, 18:30-19:30 and 21:30-23:00 has been generated. As a result TCP during these periods is larger than $MCEMS$.

Noting that during the time interval 15:30, 16:00 and 16:30 periods, the ES is in full charging mode, the EGP will be used for feeding the EWH. As it is shown in Figures 5.25(a) and 5.25(b), the EGP in $EMS - MINLP$ is less than the EGP in $MCEMS$ at 15:00 period. During some periods like 21:30-23:00 periods this case has become reverse and during these time intervals, depending on the condition of the ES, the EGP in $EMS - MINLP$ can be used for feeding the ES in charging mode, the EWH and or the DR.

As it can be observed from Figure 5.25, after implementing the DR unit, the EGP in $MCEMS$ has been used during the periods 02:00-02:30 and 13:30-16:00 periods only for supplying DR; but in 16:00 period, part of this power has been used for supplying EWH. At 16:30 period all of this power has been consumed for feeding EWH. This effect is not seen in $EMS - MINLP$. As it is observed in Figure 5.25(b), in addition to these times, EGP has also been produced at 17:30 period. This happens because, the ES has been charged with the power $\overline{P}^{ES,c}$ and excess power can be used for feeding DR and EWH. Also, as it is observed in this figure that between 02:00 and 14:00 all of EGP has been used for feeding DR, while all of this power at 14:30 and 16:30 has been used for feeding EWH. During the rest of the time,

the distribution of this power between consuming sources is managed by the proposed algorithm through its cost function. The algorithm computes the amount of power delivered by each generation/demand point.
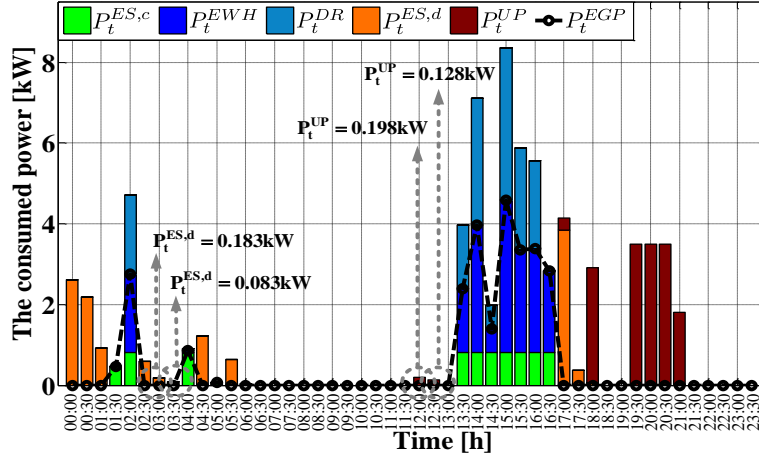
(a) *MCEMS*
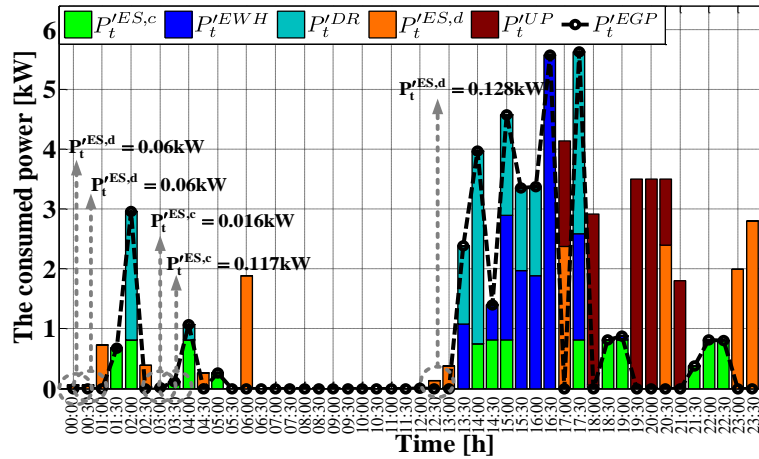
(b) *EMS − MINLP*

Figure 5.25: ES during charging and discharging mode, EWH, UP and EGP in two algorithms

The TCPs calculated by the algorithms are shown in Figure 5.26. As it is observed in this figure, TCP in both algorithms have different values during the time intervals 01:30-02:30, 03:00-04:30, 05:00, 12:00, 15:00 and 16:30-23:00 periods. The MCP in *EMS − MINLP* has always been obtained

113

below the value 0.9 €/kWh but during the period 17:00, 18:00 and 19:30-21:30 periods its value is higher. It means that $EMS - MINLP$ is able to cover all required consumption cheaper than $MCEMS$ case. The TCP in $EMS - MINLP$ during 01:30-02:30, 03:00-04:30, 05:00, 12:00, 16:30, 17:30, 18:30-19:30 and 21:30-23 periods (specially at 17:30 that its value is equal to $P_t'^{TCP} = 5.6kW$) has become more than $MCEMS$. In other words, during these periods, more consumers with less cost in $EMS - MINLP$ will be fed compared to the other algorithm.
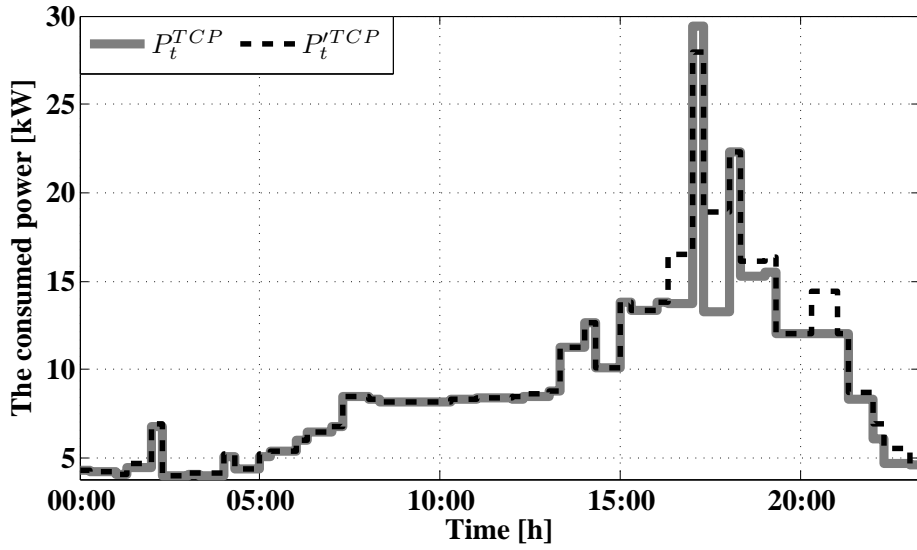
Figure 5.26: TCP due to $MCEMS$ and $EMS - MINLP$ during twenty-four hours system work

In order to prove the right performance of the two proposed algorithms ($MCEMS$ and $EMS - MINLP$), the profile of the total consumed and generated power is shown in Figure 5.27. All the powers shown are active power. As is shown in this figure MG isolated system has covered completely the consumer requested power in both of the EMS algorithms.

Maximum generated power in $MCEMS$ is more than the maximum generated power by the produces in $EMS - MINLP$. As it is observed from this figure, maximum power generated in both of the algorithms has been generated at 17:00. At this time (λ_t^{MCP}) in $MCEMS$ is 52% more than in $EMS - MINLP$. As a result, COE will increase in a growing manner. The other point which can be observed in this figure is that, TPP in

$EMS - MINLP$ during the 01:30, 02:00, 03:00-04:00, 05:00, 12:00-13:00, 16:30, 17:30, 18:30-19:30, 20:30 and 21:30-23:00 has been obtained more than its value the periods 15:00, 17:00 and 18:00 its value in $EMS - MINLP$ is less than $MCEMS$ as a result less consumers can be fed under these conditions. TCP in both of the algorithms during the periods 00:00, 00:30, 01:00, 02:30, 04:30, 05:30-12:00, 13:00-15:00, 15:30-16:30, 19:30-20:30, 21:00 and 23:00-00:00 are equivalent.
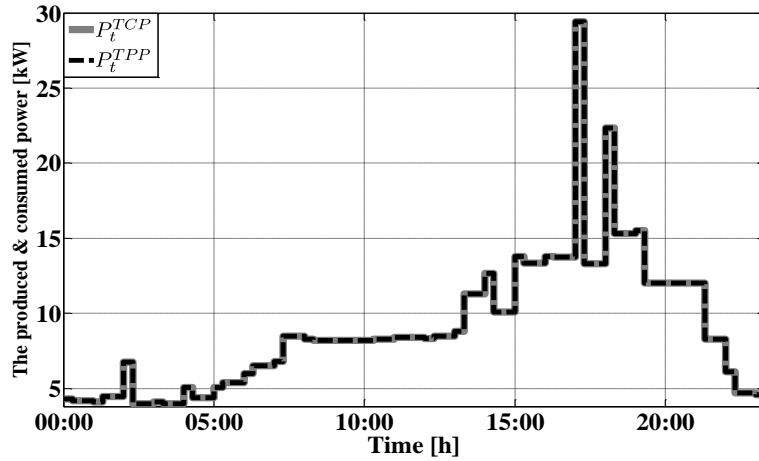
(a) $MCEMS$
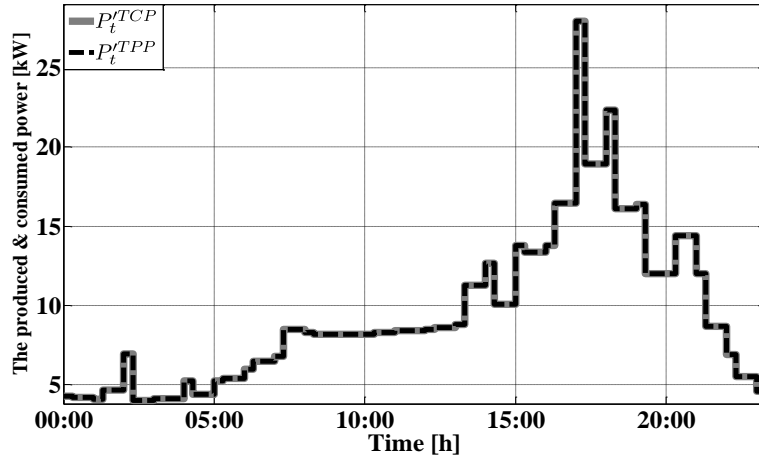
(b) $EMS - MINLP$

Figure 5.27: TCP and TPP during a day

115

LEM unit output

Because the price offer by renewable resources is significantly lower than other resources in MG, it is preferred to use always these resources. Figure 5.28 shows the obtained results from the LEM outputs. In the $EMS - MINLP$, MCP is respectively about 34% (morning) and 9% (afternoon) more than $MCEMS$. At sunset, in $EMS - MINLP$ the amount of its participation has decreased up to 25% relative to $MCEMS$. Despite this, COE is generally decreased.
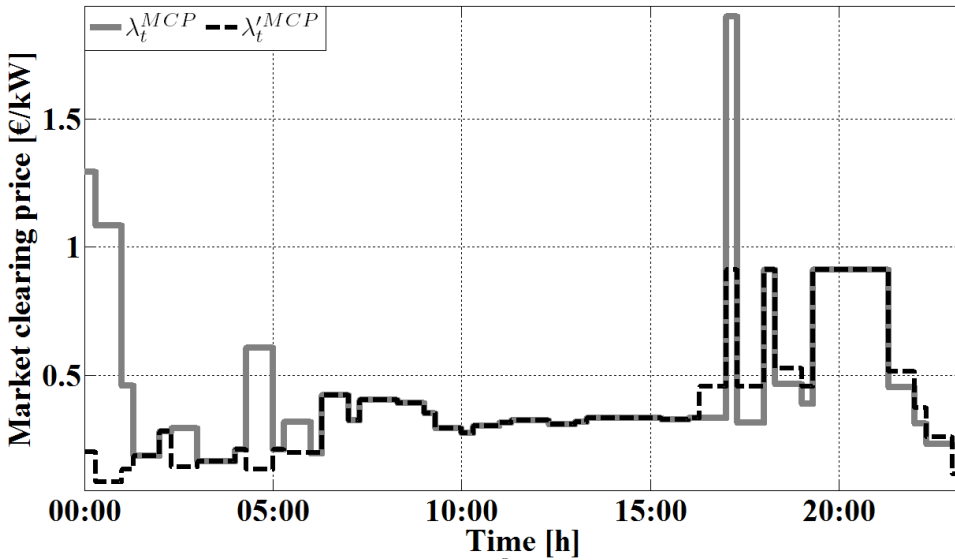
Figure 5.28: MCP during twenty-four work of system for both $MCEMS$ and $EMS - MINLP$

The suggested offer by PV has only been participated from morning to night in the LEM. In the $EMS - MINLP$, the amount of its participation in the market is also about 9% less than the $MCEMS$ during the morning and afternoon. In contrast to the PV, the ES has a defining role in the market after midnight and at the sunset. The amount of its participation in $MCEMS$ after midnight and afternoon is respectively about 41% and 9% more than $EMS - MINLP$ but during sunset has decreased to 9%. As it is observed in Figure 5.28, MCP in $EMS - MINLP$ has always been obtained below the value 0.9 €/kWh but its value during the period 17:00, 18:00 and 19:30-21:30 is more than in the $MCEMS$ case at the same time. As a result, consumers must pay more money per kWh. But in $MCEMS$, MCP during

the periods 00:00-01:00 and 17:00 is more than 1 €/kWh. During these periods, ES offer is accepted and ES is operated in the discharging mode. It is seen in Figure 5.28 that minimum MCP in $MCEMS$ is about 0.162 €/kWh but its value in $EMS - MINLP$ is about 0.111 €/kWh. Also, its maximum value has been obtained equal to 1.901 €/kWh and 0.912 €/kWh at $MCEMS$ and $EMS-MINLP$, respectively. In $MCEMS$, the suggested offer by the MT after midnight and at sunset has played no role in LEM but in $EMS - MINLP$, this micro-source can participate about 9% and 25% during the mentioned periods. The suggested offer by MT plays a significant role in decision making for the MCP in the two suggested algorithms during sunset relative to other micro-sources.

According to the analysis carried out in this section, LEM unit in the proposed algorithm compared to $MCEMS$ is significantly reduced in COE for the consumers about 15% during the daily operation.

Conclusion

The proposed LEM in MINLP algorithm has been introduced to allow the owner of the generation units to establish their own strategy for participating in MG generation with minimum information shared between micro-sources. Indeed, fulfilling the customer's requirements with minimum COE is the main theme of this algorithm. Likewise, DR has been used to avoid the penalty cost due to UP as well as to improve demand side management. Experimental test results using a four-unit test system for both of the presented algorithms demonstrate that $MCEMS$ and $EMS - MINLP$ can allow a global solution of the related MCP problem. The results demonstrated the effectiveness of the proposed EMSs, with a reduction in the cost of about 15% in $EMS - MINLP$ compared to the $MCEMS$.

5.1.4 PSB

The value of ES power has been shown in Figure 5.29. As it is observed from the figure, ES in the EMS-MILP algorithm has only worked three times in the charging mode also three times in the discharging mode and in other cases is in the IDEAL mode. In the EMS-PSB algorithm from sunset to midnight ES system has not worked in any operational mode and during this period it is in the IDEAL mode. Also, in the non-optimum LEM system ES has been discharged in the time interval 19:30 to 20:30 with the power $\overline{P}^{ES,d}$ this is while in the algorithm EMS-MILP the maximum battery discharging power is equal to $3.2kW$ that at 23:30 this power is injected to

the network. In the EMS-PSB algorithm the conditions are different.

In this algorithm, maximum discharging power is at 01:00 A.M that is equal to $0.92kW$. ES system in the non-optimum LEM algorithm works in the time periods 02:00, 04:00, 06:00, 10:00-11:30, 12:00, 13:00-17:00 and 18:00-19:30 with the power in the charging mode. In the EMS-MILP algorithm, only at 02:00 o'clock, ES system works in the charging mode with this power. But, in the EMS-PSB algorithm, these conditions at 04:30 and 15:00 have occurred for ES system. EMS-PSB algorithm has been tested practically over the IREC's MG system and the measured power from the ES emulator is shown in Figure 5.29.
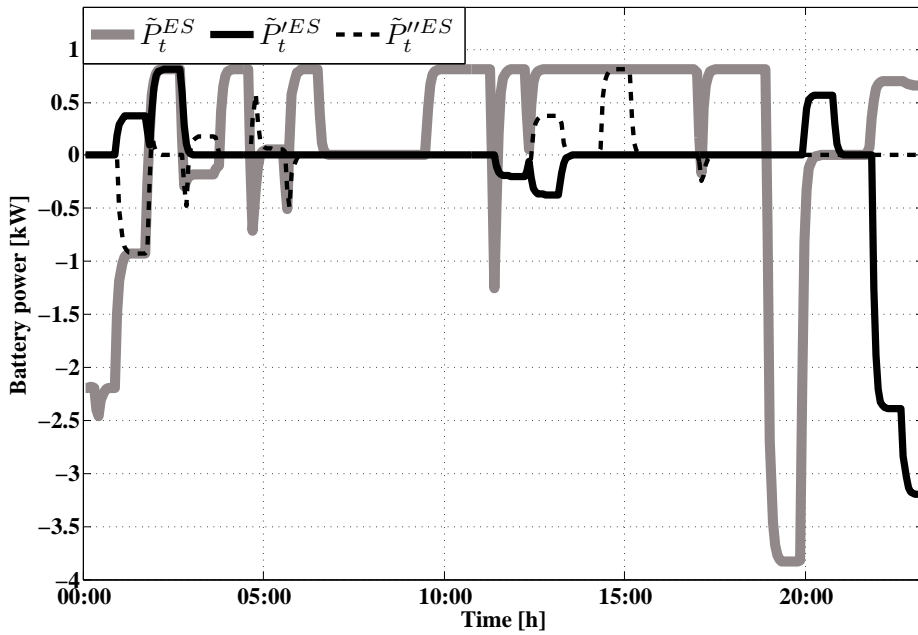
Figure 5.29: The value of charging and discharging power during the system daily performance (Solid light-gray line indicates non-optimum LEM algorithm. Also, solid and dash black lines represent output of EMS-MILP and EMS-PSB algorithms, respectively)

This section presents the results of some experimental evaluation over the islanded IREC's MG carried out to verify the EMS operation using the presented algorithms.

MT power profile is shown in Figure 5.30. In the non-optimum LEM algorithm, MT only operates at 06:00 with the minimum operating power,

i.e. $\underline{P}^{MT}$. This observation implies that the proposed non-optimum LEM algorithm prefers to draw required amount of power from the ES since it participates in the market with lower offer price compared to the price offered by the MT unit. The conditions are different in the other algorithms. In EMS-MILP algorithm despite MT offer is higher than ES offer however in this algorithm MT during the first six hour of system operation (from midnight to morning) is always in source with the power $\underline{P}^{MT}$. In this algorithm, at 01:00 o′clock and 02:00 o′clock in addition to supplying the power required by the load, some part of the power is also used for charging the ES. Maximum generated power by MT for each of the three algorithms is about $11.8kW$ that at 20:30 this power has been generated. In the EMS-MILP algorithm during the time period 07:30 to 08:30 the generated power by MT is approximately 2 times of its value in the other algorithms. Noting that this EGP has not been for feeding ES, we conclude that this power has been used for feeding RLD as it is observed in Figure 5.32. Although the battery charging price offer is larger than the RLD offer price, this result shows that the EMS-MILP algorithm decides to dump the excess available power in the RLD which results in minimum cost of operation. In the fourth period of system operation (from sunset to midnight) in each of the three algorithms MT is in service. In the non-optimum LEM algorithm, only in 4% of daily performance MT has generated power more than $10kW$. But, in EMS-PSB and EMS-MILP algorithms despite the high offer of MT, this participation are respectively equal to 6.5% and 8.33% during the system daily performance. As it is observed, participation of MT in supplying the required power in the EMS-MILP is more than the other algorithms.

In the non-optimum LEM algorithm, MT system has been operating 52% during a working day whereas in the EMS-MILP and EMS-PSB this value is respectively 79% and 60.5%.

This fact indicates that despite the MT offer is high, the optimization algorithms have decided to use MT for compensating the lack of power also changing the battery if possible. The generated power by the MT emulator has been shown in Figure 5.30 in the IREC′s MG system by using all of them.

RLD power profile is shown in Figure 5.31. As it is observed from the figure, maximum consumed power by RLD during system daily performance in the algorithms non-optimum LEM and EMS-PSB is respectively equal to $3.77kW$ and $3.97kW$ and this power has been consumed in the non-optimum LEM algorithm at 15:00 and in the algorithm EMS-PSB at 14:00. The value of maximum consumed power in the EMS-MILP algorithm is also equal to $5kW$ that has been consumed by RLD during the time periods 02:00, 07:30-
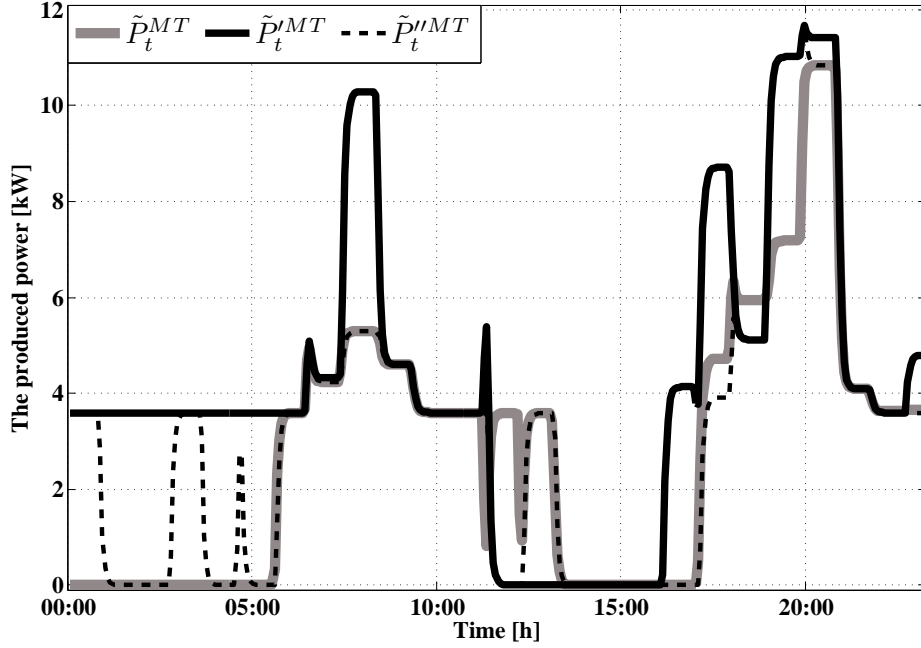
Figure 5.30: The power generated by MT during the system daily performance

08:30, 17:00 and 23:30.

As it is observed from the figure, after 17:30 to 23:30 period, no power has been considered for feeding RLD in the non-optimum LEM algorithm and it has been tried that excess power for feeding ES be used. In the non-optimum LEM algorithm, the excess power has been used for feeding RLD at 23.33% system daily performance while in the algorithms EMS-MILP and EMS-PSB this value is respectively equal to 33% and 23% system daily performance.

Bar graphs related to $P_t^{ES,c}$, $P_t^{ES,d}$, P_t^{RLD}, P_t^{UP} and P_t^{EGP} have been shown in Figure 5.32 for each of the three algorithms. As it is observed, in the non-optimum LEM algorithm, ES system has operated in the charging mode and the battery has been charged with $\overline{P}^{ES,c}$ power at 79% of the times.

As it is observed from the Figure 5.32(a), in the time interval 02:00, 04:00, 06:00, 10:00-11:30, 12:00 and 13:00-17:30 EGP for feeding RLD has been used. Meanwhile, the value of power P_t^{UP} is equal to zero in all of the time
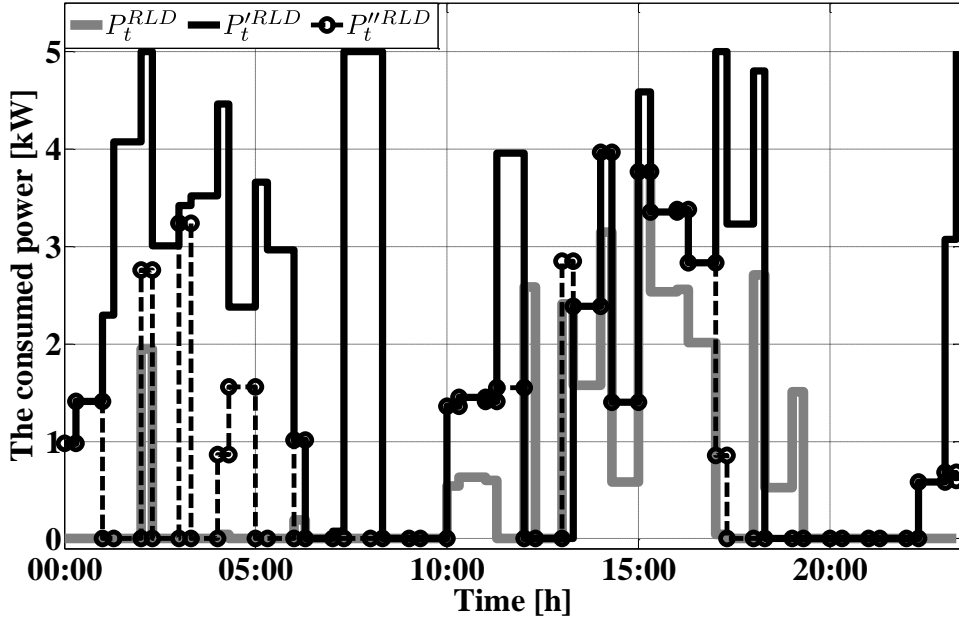
Figure 5.31: The power consumed by RLD during system daily performance

intervals that indicate that the values of power P_t^{TCP} and P_t^{TPP} are equal to each other in all of the time intervals.

As it is observed from Figure 5.32(b), ES system in the EMS-MILP algorithm only operates at hours 01:00, 02:00 and 21:00 in the charging mode. Also, this system at hours 12:00, 13:00 and 00:00-23:00 has operated in the discharging mode. As it is observed from this figure, in the time intervals 00:00-06:30, 07:00-08:30, 10:00-12:00, 13:30-18:30 and 00:00-22:30 all $P_t'^{EGP}$ and or a part of it has been used for feeding RLD. About 69% of system performance in the EMS-MILP algorithm has been generated that in 91% of the times is used completely for feeding RLD. It can be seen that the algorithm utilizes the ES during 00:00-23:00 time interval to feed the RLD, which means that the cost of operation will be minimized if the RLD is electrified by the energy stored in the ES.

As it is observed from Figure 5.32(c), ES system has operated in the time intervals 01:30, 03:00, 04:30, 05:00, 13:00 and 15:00 in the charging mode in the EMS-PSB algorithm. Also, in the time intervals 01:00, 02:30, 05:30, 12:00-13:00 and 17:30, ES system has operated in the discharging mode. Meanwhile, as it is observed from this figure, in the time intervals 00:00-01:00, 02:00, 03:00, 04:30, 06:00, 10:00-12:00, 13:00-17:30 and 00:00-22:30

power has been generated that in 76% of the cases has been used only for feeding RLD. The significant point is that at 03:00 o′clock and 13:00 o′clock although SOC is low and there is more possibility of charging the battery, the algorithm has used most of EGP for feeding the RLD. Also, in this algorithm, P_t^{UP} is equal to zero in all of the time intervals.

In Figure 5.33, TCP power profile has been shown. During the system one day performance, the power consumed by the consumers (NRL, ES during charging performance and RLD) in the EMS-MILP algorithm is about 46% more than its value in the non-optimum LEM algorithm. However, in the EMS-PSB algorithm, the value of power in about 31% of the cases is more than the power of P_t^{TCP} in the non-optimum LEM algorithm.

In about 48% of the cases, the total power consumed by the consumers in EMS-MILP algorithm is more than EMS-PSB algorithm (i.e. $P_t'^{TCP} \geq P_t''^{TCP}$). Maximum and minimum values of $P_t'^{TCP}$ are $16.3kW$ and $4kW$, respectively. The former is at 19:00 o′clock and the latter is at 02:30. Maximum and minimum value of P_t^{TCP} is respectively equal to $19kW$ and $5.3kW$ and its maximum value at 18:00 and its minimum value is also at 00:00 and 22:30 has been used for feeding all the consumers. Finally, the maximum and minimum value for the parameters $P_t''^{TCP}$ is respectively equal to $15.5kW$ and $4kW$ which have been obtained in the time interval 19:00-21:00 (maximum value of $P_t''^{TCP}$) and at the hours 02:30 and 03:30 (minimum value of $P_t''^{TCP}$). As it is observed from this figure, the value of $P_t'^{TCP}$ is more than P_t^{TCP} and $P_t''^{TCP}$ at similar time. The reason is that the EMS-MILP algorithm has specified that if it generates excess power for feeding will become minimized. The difference between $P_t'^{TCP}$ and $P_t''^{TCP}$ in the time interval 07:30-08:30 reaches its maximum value that is $5kW$. As it is observed the Figure 5.34, although in the mentioned time interval the value of $\lambda_t'^{MCP}$ is about two times $\lambda_t''^{MCP}$, however EMS-MILP algorithm has preferred to feed more consumers in this time interval. In this period, EMS-MILP algorithm put MT with more power into service so it feeds RLD. At 13:00 the value of $P_t''^{TCP}$ is more than $P_t'^{TCP}$. As it is observed from Figure 5.34, the values of $\lambda_t'^{MCP}$ and $\lambda_t''^{MCP}$ at this hour are exactly equal to each other, but in the EMS-MILP algorithm ES system operates in the discharging mode. However, in the EMS-PSB this fact is the opposite. Also, in the EMS-PSB algorithm MT system enters service with the power $\underline{P}^{MT}$ and the generated power by it has been used for feeding ES and used more for feeding RLD.

In Figure 5.34, the value of MCP has been shown in each of the suggested algorithms. In the time intervals 00:00-02:00, 03:00, 04:00-05:00, 07:30-08:30, 11:30, 18:00, 19:30-20:30 and 23:30 the value of $\lambda_t'^{MCP}$ in the EMS-MILP algorithm is more than λ_t^{MCP} in the non-optimum LEM algorithm. Maximum

122
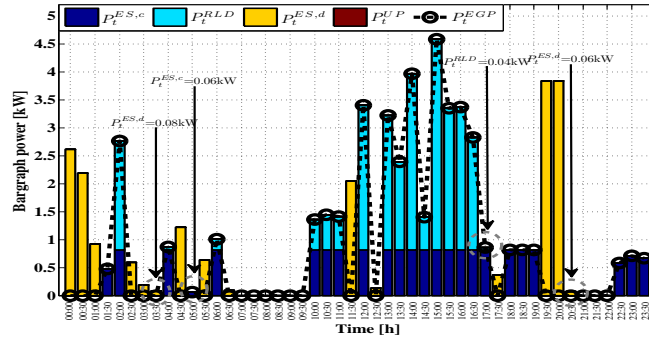
(a) non-optimum LEM
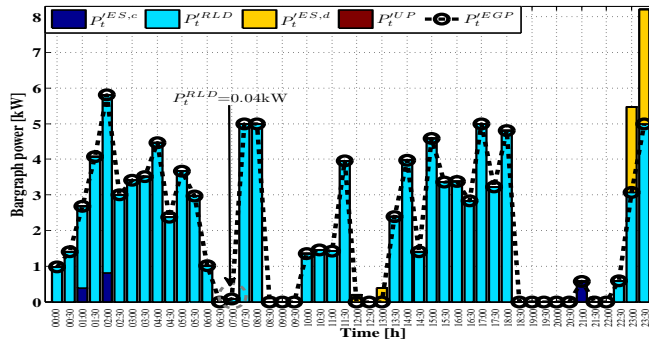
(b) EMS-MILP
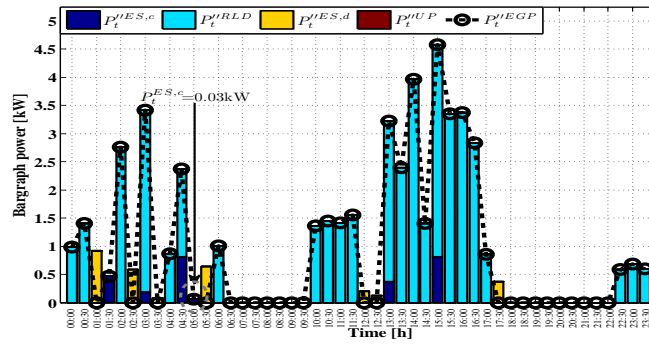
(c) EMS-PSB

Figure 5.32: Bar graph related to charging power and discharging ES, RLD, UP and EGP for each of the algorithms under investigation

123
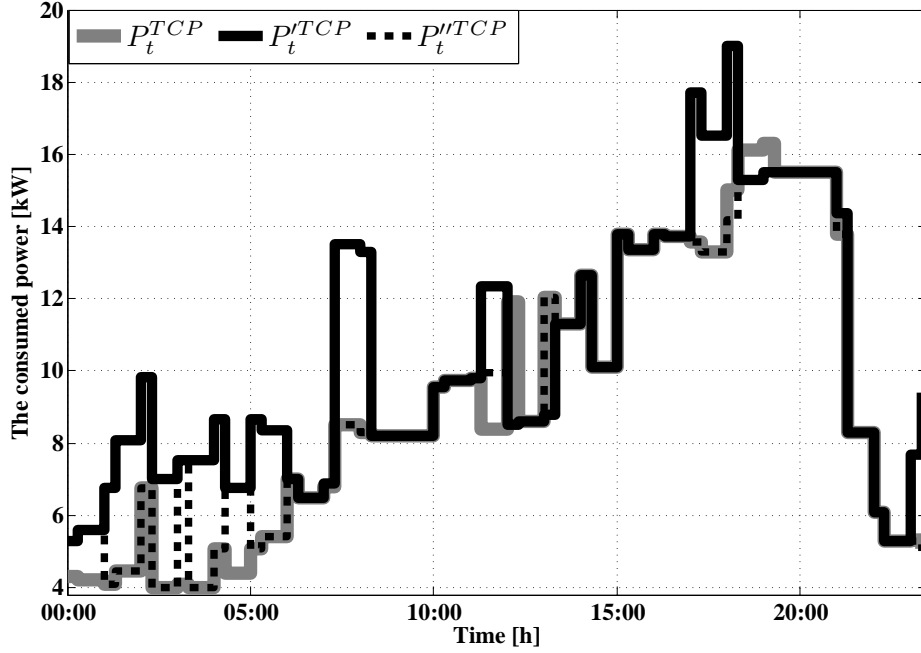
Figure 5.33: TCP power profile in each of the three suggested algorithms

value of difference is equal to 0.3€/kWh at 19:30. In this hour, the ES system in the non-optimum LEM algorithm has been discharged with the power $\overline{P}^{ES,d}$. But because MT in the EMS-MILP algorithm is in service with more power (about 40% more), $\lambda_t'^{MCP}$ has become larger. The value of $\lambda_t''^{MCP}$ in the EMS-PSB algorithm in the time intervals 00:00-01:00, 03:00, 04:30 and 19:30-20:30 is more than the value of λ_t^{MCP} at similar times. Also, in this case like the previous case, the largest difference between λ_t^{MCP} and $\lambda_t''^{MCP}$ exists at 19:30 that the related analysis is similar to the previous case. In the time intervals 01:00-03:00, 03:30-04:00, 05:00-06:00, 07:00-08:30, 11:30, 17:00, 18:00, 21:00 and 23:30, the value of $\lambda_t'^{MCP}$ is larger than $\lambda_t''^{MCP}$ in similar hours. In the time intervals 07:30-08:30 and 18:00 this difference has reached about 0.42€/kWh. By analyzing the obtained data, it has been observed that in these time intervals. EMS-MILP algorithm has been tried so that MT produces power with a higher capacity and EGP has been used for feeding RLD. As it is observed from the figure, about 71% of the cases the value of $\lambda_t'^{MCP}$ is less than λ_t^{MCP} in similar time.

But by using the EMS-PSB algorithm in 87.5% of the cases the value of

124

$\lambda_t''^{MCP}$ has become less than the value of λ_t^{MCP} in similar time. The value of $\lambda_t''^{MCP}$ has been obtained less than the value of $\lambda_t'^{MCP}$ during the system daily performance in 50% of the cases. This fact is specially very important in the time intervals 01:00-03:00, 03:30-04:30, 05:00-06:00, 07:00-08:30, 11:30, 17:00, 18:00, 21:00 and 23:30 that the value of $P_t'^{TCP}$ has become more than $P_t''^{TCP}$. This fact indicates that in these time intervals despite the higher value of MCP, the EMS-MILP algorithm has specified that if it feeds more consumers under these conditions also the general COE will become minimized. With the analyses done, it is observed that although sometimes the value of $\lambda_t''^{MCP}$ is larger than $\lambda_t'^{MCP}$, but in EMS-PSB algorithm, the value of COE has decreased about 3% more related to EMS-MILP algorithm. Also, the results demonstrate about 23% reduction in the cost of operation in the EMS-PSB algorithm, in comparison with non-optimum LEM.
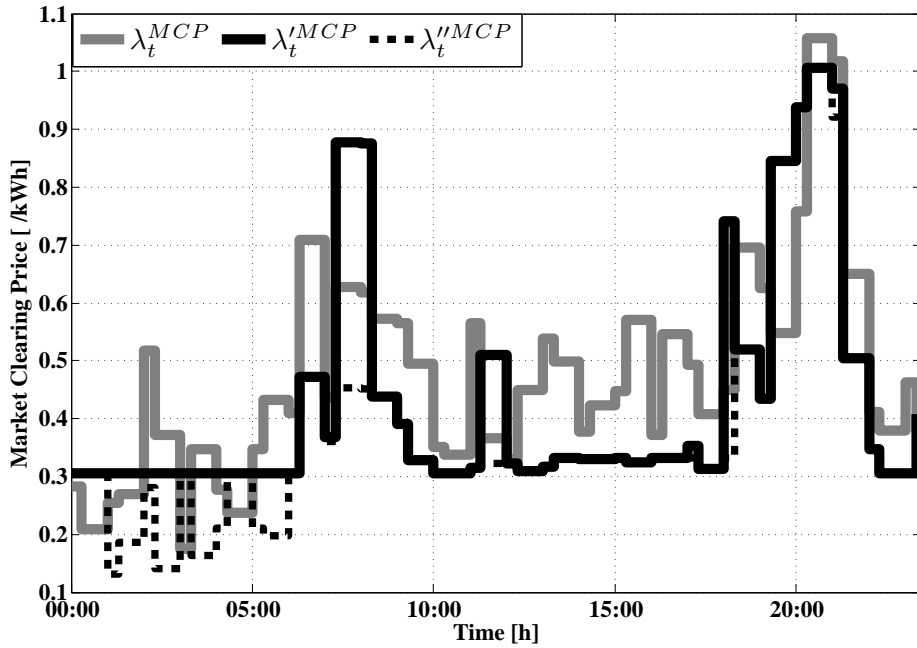
Figure 5.34: The value of MCP during the system daily performance for each of the three algorithms

Conclusion

A pivot source based heuristic algorithm and an algorithm based on MILP method for implementing EMS optimum system have been presented and tested experimentally. In the proposed algorithms, at the first step, CBUC is implemented by using mathematical formulation related to each one of the micro-sources present in MG. Then, LEM unit based on PBUC by using single sided auction structure has been suggested by considering single ownership and sharing minimum information between production unit. For investigating the performance and the capability of $EMS - PSB$ algorithm in a real MG has been tested. $EMS - PSB$ algorithm has been tested on IREC's MG experimentally obtaining results that demonstrate that it has more profit noting CBUC and PBUC planning respect to non-optimum LEM algorithm. Furthermore, among the proposed algorithms in this study, $EMS - PSB$ and EMS-MILP algorithms have shown high successfully for finding optimal solution to improve the optimal operation and scheduling as well as in reducing production cost. Moreover, these algorithms have also comparable analyzing and computing speed but $EMS - PSB$ has better capability to be implemented experimentally noting no need for complex optimization solver. Eventually, it is shown that by using the proposed optimization algorithms, customers have been supplied completely. Also, a significant reduction in cost (about 20% and 23% in $EMS - MILP$ and $EMS - PSB$, respectively) has been achieved in DAM structure comparing to non-optimum LEM algorithm. The results show that the proposed heuristic algorithm is superior to other algorithms since it finds the optimal solution with a high success rate and within a reasonable execution time. Additionally, the proposed algorithm is feasible from a computational viewpoint as well as to reduce operating costs within MG.

5.1.5 MICA

In Figures. 5.35 and 5.36 the situation of SOC and the ES power profile are shown in both of the $MCEMS$ and $EMS - MICA$ algorithms. In the first 6 hours of system operation (from midnight to the morning) after several charging and discharging operation at the end of this time interval, the value of SOC in the $EMS - MICA$ is not changed so much relative to its initial value. This is while, in the $MCEMS$ algorithm at the end of this time interval is reached about its initial value. In this time interval in the $MCEMS$ algorithm only 14% of the excess generated power is used for feeding DR and the rest is spent for feeding ES. While, participation of DR

126

in the $EMS - MICA$ algorithm is reached 29%. Despite the higherness of the offer of charge ES relative to feeding DR, by noting low MCP in this time interval, the optimization algorithm is done proper selection for supplying the feeding of its loads. In the second 6 hours of the system operation (from morning to noon), only in 17% of the times the value of SOC in the $EMS - MICA$ algorithm is less than SOC_I. while in the $MCEMS$ algorithm only 42% of the times its value is reached more than $\underline{SOC}$. As a result, the system reliability in supporting the total load in this time interval in the $MCEMS$ algorithm is reduced significantly. The participation share of DR and ES in the optimization algorithm are equal to each other but most of the generated EGP power is spent charging ES in this time interval. In this time interval, when excess power is present in the $MCEMS$ algorithm first ES operate with the power $\overline{P}^{ES,c}$ in the charging mode. Then, the rest of this generated power is spent for feeding DR. During the third 6 hours of system operation (from noon to sunset), the value of SOC in the $EMS - MICA$ algorithm at 42% of the times has become equal to $\overline{SOC}$ that shows the proper performance of the suggested algorithm in managing the stored energy in ES. In this time interval in the optimization algorithm by noting that the value of SOC most of the times is reached its maximum value. Therefore, part of the excess power is spent on feeding EWH. Although, ES in the $MCEMS$ algorithm is always operated with the power $\overline{P}^{ES,c}$ in the charging mode however the maximum value of SOC is reached more than 39%. The significant point is that by noting the occurrence of the scenarios 2 and 3 the value of SOC at the end of this time interval in both of the algorithms is reached $\underline{SOC}$. At the last 6 hours of the system operation (from sunset to midnight) the $EMS - MICA$ algorithm spends most of the EGP power on feeding ES such that the value of SOC at the end of this time interval is reached about 70%. This is while, despite the performance of ES in the charging mode in the $MCEMS$ algorithm, however the value of SOC at the end of this maximum time interval is reached about 24%. This fact will show support of load demand by ES in the optimization algorithm for the next day.

MT power profile is shown in Figure 5.37. As it is observed, during the first 6 hours of system performance, $MCEMS$ algorithm is only 8.33% times of MT is in service. This is while despite the highness of the offer of MT relative to other production sources, in the optimization algorithm is in service 25% of the times. The EGP power generated at this time is spent on feeding ES and DR. in the second 6 hours of system operation, in the optimization algorithm 17% of the times MT is out of service while in the
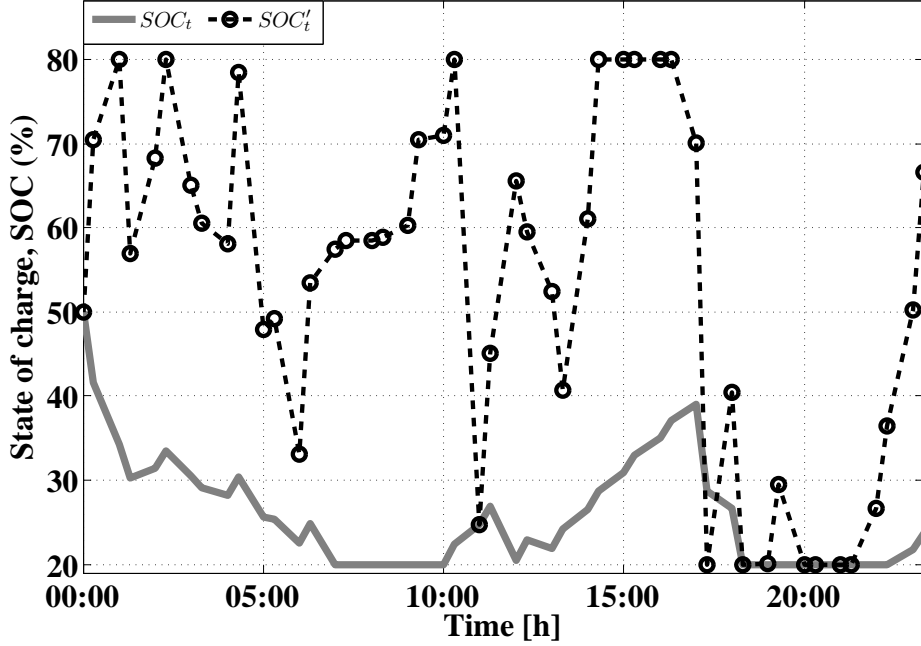
Figure 5.35: SOC during one day system operation

$MCEMS$ algorithm its value is about 8.3%. Although, MT in this time interval is mainly in service, but most of the power generated by it is spent on feeding the power needed by NRL and a small part of it is spent on feeding ES and DR. Also, in this time interval similar to the first 6 hours of system operation, EWH just as before is not entered service in both of the algorithms. At 10:00 and 11:00 different performance for using EGP is observed in both of the algorithms. Scenario 2 is occurred at the third 6 hours of system operation. MT in both algorithms is entered service for the complete supply for load demand with the power $\overline{P}^{MT}$. At the time intervals of the occurrence of this scenario, the average value of $\lambda_t'^{MCP}$ is about 29% less than the average value λ_t^{MCP}. So, power generation by MT with maximum capacity not only causes the increase of the total production cost also significant reduction in the consumed electricity price exists in these time intervals. At the last 6 hours of system operation, MT profile in both of the algorithms has similar model. Noting the occurrence of scenario 3 in this time interval and as a result out of serviceness of non-dispatchable power, with no choice MT must enter service with its maximum power (i.e.
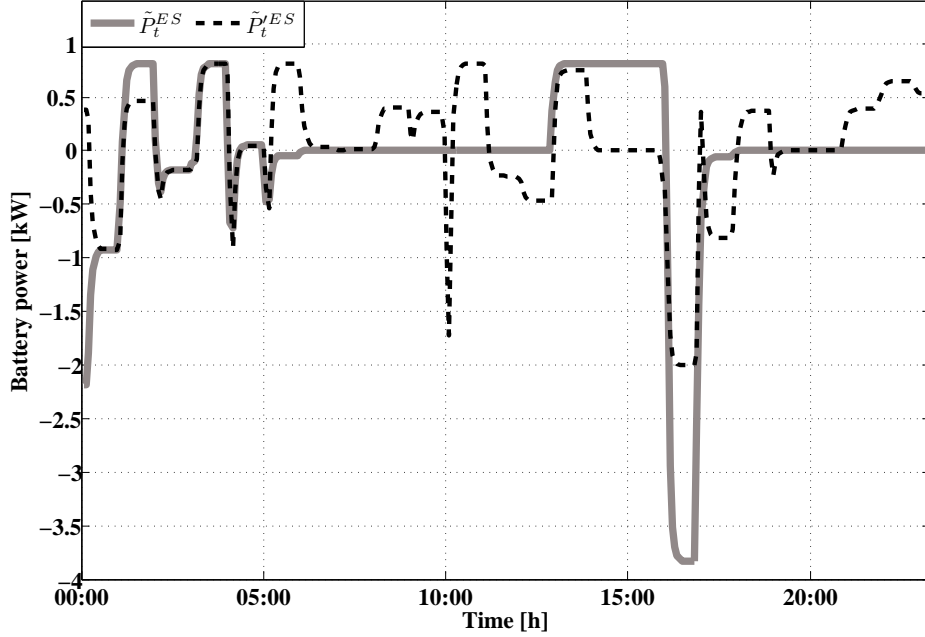
Figure 5.36: ES power profile during system daily operation

$\overline{P}^{MT}$). Noting the high offer of MT relative to other existing sources, so investigating MCP has special importance. As it is observed from Table 5.3, the average value of $\lambda_t'^{MCP}$ is about 25% less than the average value of λ_t^{MCP} in this time interval. This means that despite the presence of MT, the consumers are fed with less electricity price.

The total power consumed by the consumers is shown in Figure 5.38. At time intervals that the values of P_t^{TCP} and $P_t'^{TCP}$ are equal to each other, the average value of $\lambda_t'^{MCP}$ is about 35% less than the average value of λ_t^{MCP}. As a result, the feeding of the consumers equal to the lower electricity price has taken place by the $EMS - MICA$ algorithm. In the intervals that the value of $P_t'^{TCP}$ is greater than P_t^{TCP}, the average value of $\lambda_t'^{MCP}$ is about 36% less than the average value of λ_t^{MCP}. Also at some times the value of MCP is more than its average value in the total time interval. Under these conditions it's better that the suggested algorithm be after the reduction of it's consumers by using DR. As it is observed from the figure, noting the mentioned reasoning sometimes the value of $P_t'^{TCP}$ has become less than P_t^{TCP}. In 58% of the times the value of $P_t'^{TCP}$ at the second 6 hours of system operation. At these times, the average value of

129
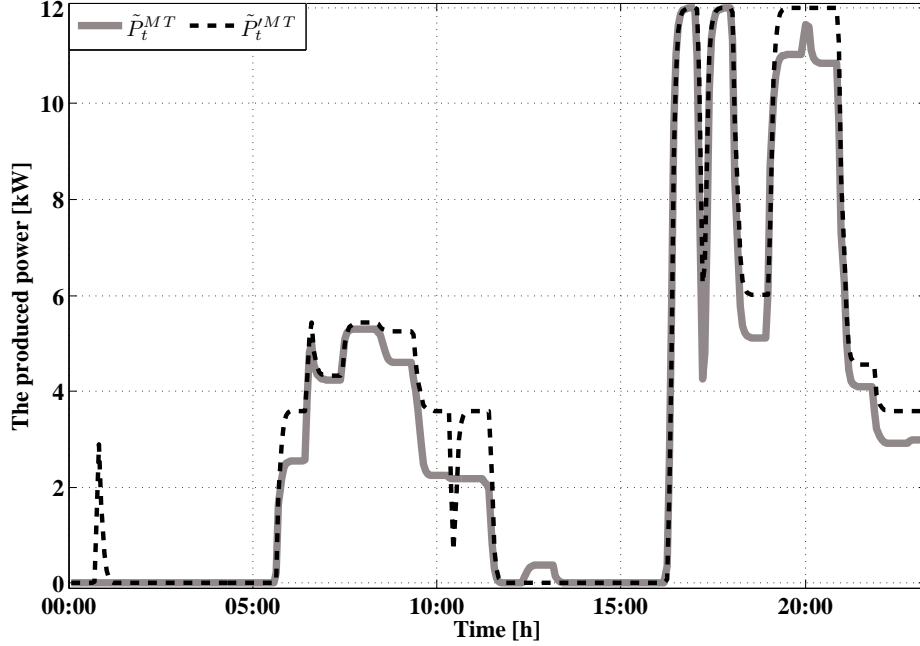
Figure 5.37: MT power profile during the MG daily performance

$\lambda_t'^{MCP}$ is about 32% less than the average value of λ_t^{MCP}. The difference of the generated power is mainly spent on charging ES. At 12:00, P_t^{TCP} has become about 29% more than $P_t'^{TCP}$ its reason has been the feeding of DR at this time interval. The excess power generated is supplied by MT. Because λ_t^{MCP} is about 46% more than its average value during the second 6 hours of system operation, so choosing this time interval for feeding DR by the $MCEMS$ is inadequate. DR and EWH sources in each algorithm is fed during the time interval of the third 6 hours of system operation. In this time interval because of the lowness of $\lambda_t'^{MCP}$ so the $EMS - MICA$ algorithm is spent most of the EGP on feeding DR. At the time of occurrence of scenario 2 (at 17:00), the value of UP in the optimization algorithm is much more than its value in the $MCEMS$ algorithm. Its reason is that ES is discharged with the power $\overline{P}^{ES,d}$ and the value of SOC is reached $\underline{SOC}$. Also, MT is entered in service with the power $\overline{P}^{MT}$. Despite this, the algorithm is not able to fulfill all of the NRL demand. At the end, all the TCP in both of the algorithms have become equal. This is while, the value of $\lambda_t'^{MCP}$ is about 26% less than the value of λ_t^{MCP} at this hour (17:00). As

a result, in addition to supplying equivalent TCP in both of the algorithm with a much lesser MCP, the value of penalty cost resulting from UP is also reduced significantly by the $EMS - MICA$ algorithm. In the third 6 hours of system operation (the time of occurrence of scenario 2), the value of UP in both of the algorithm is about 3% more than its value in the optimization algorithm. Its reason is that, as shown in Figure 5.37, at 17:30 MT enters service with the power $\underline{P}^{MT}$ in the $EMS - MICA$ algorithm, and while providing a part of the power needed by NRL, first, ES charge with the power $\overline{P}^{ES,c}$ and then the rest of the power generated for feeding EWH is used. The mentionable point is that, despite the higherness of DR offer relative to EWH however the optimization algorithm is spent EGP power on feeding EWH. Charging ES is caused the increase of SOC at this time and at the time of occurrence of scenario 2 (18:00 o′clock) part of the power needed is supplied by the discharge of ES in this time interval, at 33% of the times the value of $\overline{P}'^{TCP}$ is greater than the value of $\overline{P}^{TCP}$ by noting that the average value of $\lambda_t'^{MCP}$ is much less than the value of λ_t^{MCP}, so this fact also states more load feeding with less price.
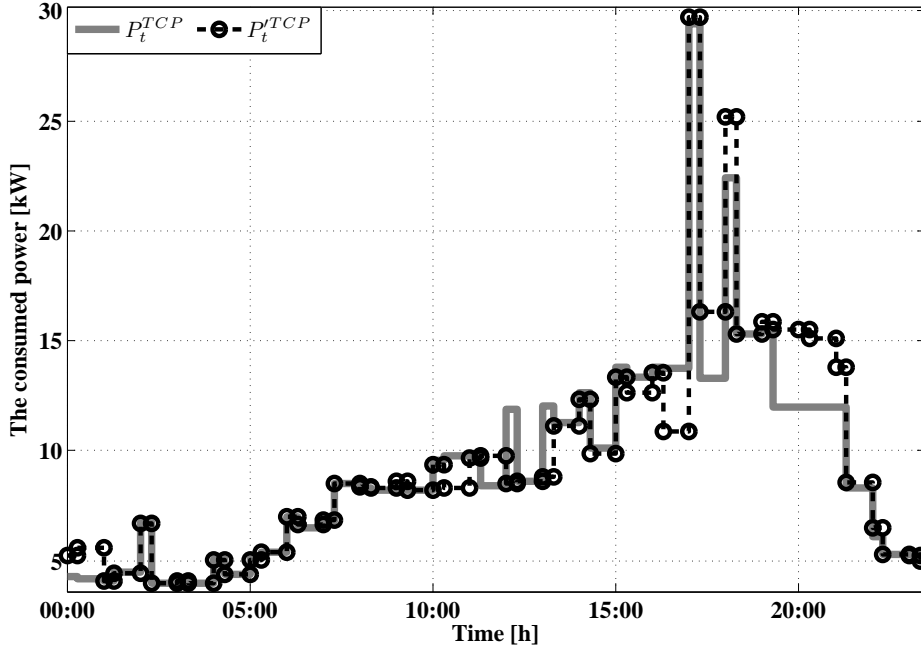
Figure 5.38: The total power consumed by the consumers during the system daily performance

Bar graph of ES power during the charging and discharging modes, EWH, DR and EGP is shown in Figure 5.39. By reviewing the performance flow of ES in both of the two algorithms during a working day of the system it is observed that ES in the $EMS - MICA$ algorithm in both the discharging and charging mode is worked more than the $MCEMS$ algorithm during a working day. Noting that ES is discharged with less power in the optimization algorithm; so the SOC profile in this algorithm is much more adequate than the $MCEMS$ algorithm. Also, in the $MCEMS$ algorithm in the second 6 hours and the fourth six hours of system operation (other than 11:30) ES is not used for supplying load demand and ES is operated in the charging mode. Noting the highness of the average value λ_t^{MCP} in this two time intervals, so charging ES in these conditions causes the increase of the finished price for generating electricity. Charging ES in the $EMS - MICA$ algorithm at the second six hours of system operation that the $\lambda_t'^{MCP}$ average value is adequate, is more than other time intervals. So, supplying the feeding of ES that is one of the consumers, is done with less expense. In the $MCEMS$ algorithm, 50% of DR load is fed in the third 6 hours of system operation that the value of MCP in this time interval is adequate relative to the other time intervals. This is while that in the optimization algorithm 33.33% of the value of DR is fed in the first 6 hours of system operation that the average value of MCP is minimum. It means that, the amount of the load that has been cut during the hours of occurrence of the implemented scenario (the higher average amount of $\lambda_t'^{MCP}$) is fed at other hours in which the amount of MCP is about 58% less. The other point is also that, about 34% of the value of the fed power for EWH is reduced in the optimization algorithm that shows the optimum use of the power generated in this algorithm. Furthermore, about 3.3% of the value of the power consumed by DR during system daily performance has become more in the optimization algorithm.

The MCP curve for both of the algorithms is shown in Figure 5.40. The average value of MCP is also presented for different time intervals in Table 5.3. The average value of MCP during the system daily performance in the optimization algorithm is about 37% less than its value in the MCEMS algorithm. The minimum value of MCP is in the optimization algorithm at the first 6 hours of system operation. So, the best choice of feeding DR loads is in this time interval. Noting that PV in this time interval is out of service as a result significant EGP is not generated in this time interval that at first is used for improving SOC. In this time interval ES is mainly charged with the power $\overline{P}^{ES,c}$ except the time when its SOC is reached the value $\overline{SOC}$
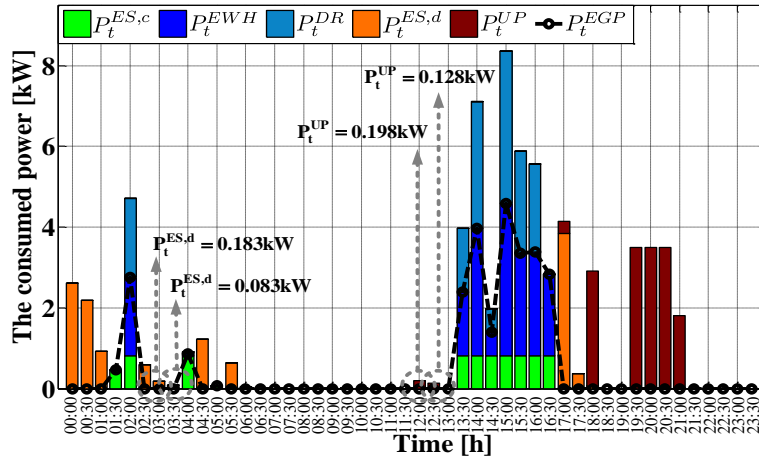
(a) *MCEMS*
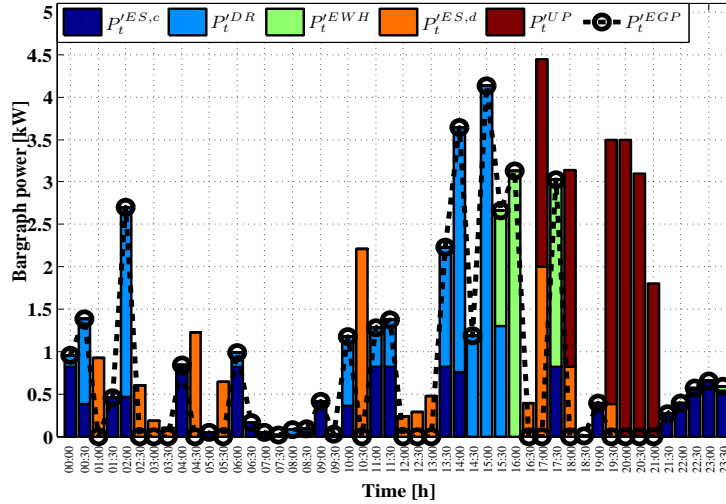
(b) *EMS − MICA*

Figure 5.39: ES during charging and discharging mode, EWH, UP and EGP in both algorithms

that with no choice the rest of the excess power generated is spent feeding DR. As it is observed from this figure, during the period of occurrence of scenarios 2 and 3, there is significant difference in the value of MCP in each algorithm. Despite of this, the values of TCP in both of the algorithm are equal to each other that shows the same load feeding in both algorithms

133

but with lower price in the optimization algorithm. The maximum value of λ_t^{MCP} is equal to 1.33€/kWh that is about 26% more than the maximum value of MCP in the optimization algorithm. This fact is taken place at 18:00 that is the time of the occurrence of scenario 2. The minimum value of λ_t^{MCP} is also equal to 0.2€/kWh that is about 35% greater than the minimum value of MCP in the optimization algorithm. With the analyses done the value of the total cost of electricity in the optimization algorithm is reduced 31% related to the MCEMS algorithm.
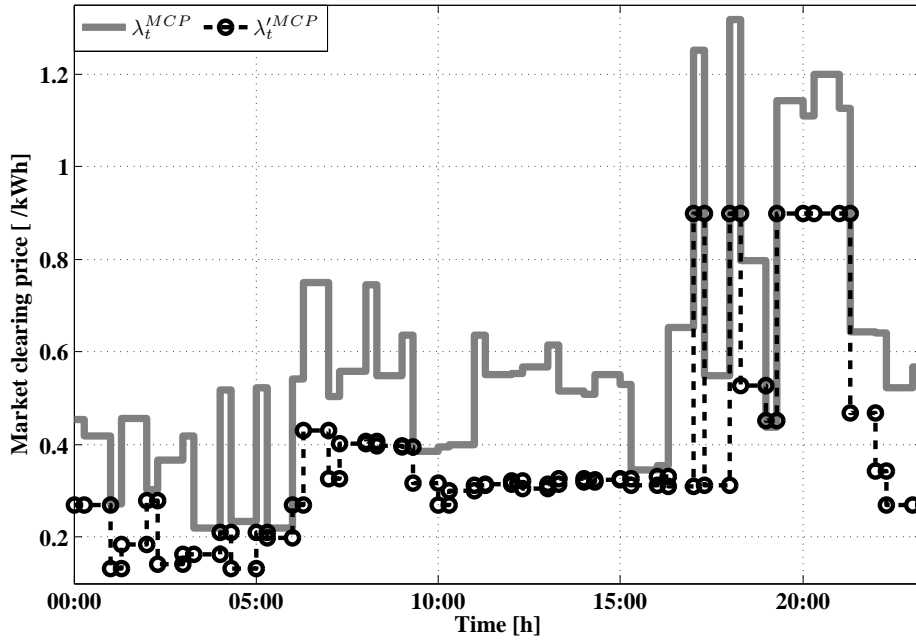
Figure 5.40: MCP during system daily performance

Conclusion

An optimization algorithm based on MICA algorithm for the optimum performance of different RESs by considering the minimum cost of electricity generation is proposed and validated over a typical MG. $EMS - MICA$ algorithm has been implemented based on the local search mechanism by creating initial population including the discussed constraints. The results

Table 5.3: The average value of MCP during each 6 hours period of system performance

	MCP [€/kWh]	
	λ_t^{MCP}	$\lambda_t'^{MCP}$
first 6 hours of system operation (from night to morning)	0.44	0.20
second 6 hours of system operation (from morning to noon)	0.56	0.32
third 6 hours of system operation (from noon to sunset)	0.49	0.32
fourth 6 hours of system operation (from sunset to night)	0.62	0.42

obtained experimentally over IREC′s MG have been compared with the results achieved from the $MCEMS$ algorithm. Several tests and scenarios have been implemented for evaluating the efficiency of the proposed algorithm. The simulation and experimental results show that not only the proposed algorithm has better efficiency relative to the algorithm without optimization but also shows supervising dynamic stability and convergence between the countries. Also, the proposed algorithm obtains a set of optimum solution that fulfill the Pareto conditions that gives the operators different choices for selecting a suitable power dispatch plan according to economic considerations and the technical constraints discussed. Furthermore, the results show that the proposed optimization algorithm can provide optimistic, certain and very definite solutions at an acceptable simulation time for the problems related to EMS. Additionally, 31% reduction in electricity generation cost in the optimization algorithm relative to the $MCEMS$ algorithm states the ability of the effective use of the proposed algorithm in the systems based on isolated MGs. The obtained results demonstrate the efficiency of the proposed algorithm for fulfilling load demand, reduction of the total generation cost (about 31%) and reduction of MCP compared to the $MCEMS$ algorithm.

5.1.6 MABC

SOC profile and the ES power during the 24 hour system operation are shown in Figures. 5.41 and 5.42 respectively. As it is observed from Figure 5.41, during the first 6 hour of system operation (from midnight to the morning), SOC in the $MCEMS$ algorithm almost always is decreasing and at the end of this operation interval is approached the value $\underline{SOC}$. However, in the $EMS - MABC$ algorithm some of the generated power for charging the ES is supplied by MT. As a result, SOC in this algorithm is reached about 70% at the end of this time interval. This value of SOC causes the increase of the ability of supplying load during the rest of the system daily operation. During the second 6 hours of system operation (from morning to noon) also the $MCEMS$ algorithm has just as before is used ES for supplying the shortage of its required power. While in the optimization algorithm, ES system is operated in the charging mode just as before, and after 09:30 A.M. the value of its SOC is reached about $\overline{SOC}$ and until the end of this time interval is stayed at this value. Because in the third 6 hours of system operation (from noon to the sunset) scenarios 2 and 3 are occurred, hence in both of the algorithms despite MT has come to service, however MG is not be able to completely supply the load demand with no choice is used the energy stored in ES completely. SOC at the end of this time interval is reached the value $\underline{SOC}$ in both of the algorithms. At the end hours of the fourth 6 hours of system operation (from sunset to the night) ES in the $MCEMS$ algorithm starts charging and is reached a value little more than $\underline{SOC}$. But, in the $EMS - MABC$ algorithm by the proper selection of MT, ES system operates in the charging mode and is brought its SOC value at the end of this time interval to about 80% that is a significant value. This fact shows that, despite the higher MT offer relative to ES, the optimization algorithm is recognized that if it uses MT for compensating the required shortage of power and meanwhile uses the rest of the generated power for charging ES, the total cost of energy under these conditions will also become minimum. In addition to cost reduction, ES is stored in itself more energy for supplying load in the next day.

MT power profile is shown in Figure 5.43. As it is observed from the figure, during the first 6 hours of system operation, MT in the $MCEMS$ algorithm is out of service, while in the optimization algorithm in some intervals for supplying the feed part of the load and ES charge is entered service. At the second and fourth 6 hours of system operation in both of the algorithms, the MT curve has almost followed a similar profile. The significant point is that, at third 6 hours of system operation in the $MCEMS$, MT enters service
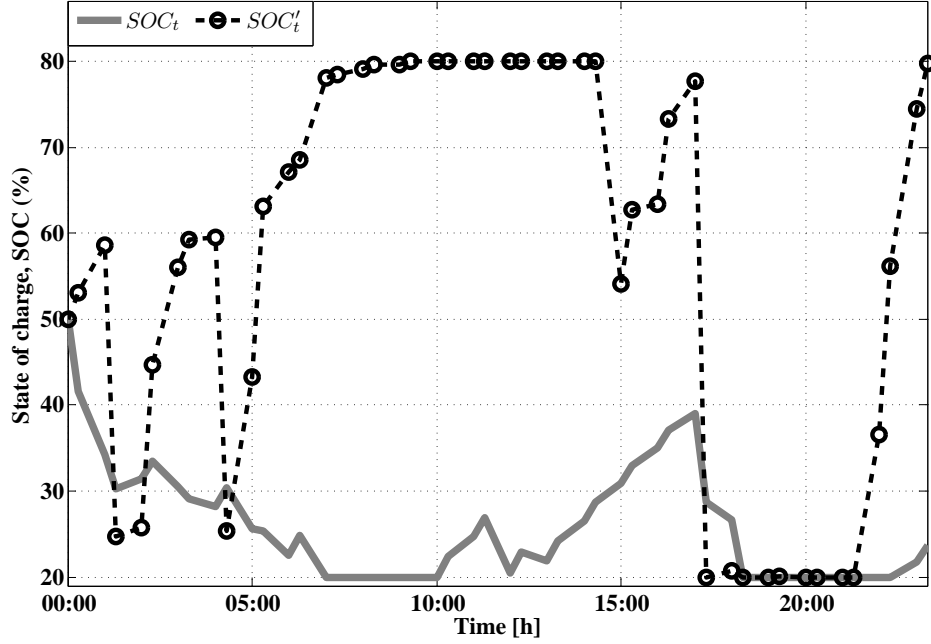
Figure 5.41: SOC of battery during system operation

with the power $\underline{P}^{MT}$ and in addition to supplying the required power by the load is also used part of the generated power for charging ES as a result has to some amount improved SOC. This is while that MT in the $EMS-MABC$ algorithm is out of service. In this time interval the algorithm is preferred to compensate its required power throng ES as is shown in Figure 5.45(b) (in the time interval 14:30-15:00).

The value of the total consumed power by responsive loads (EWH and DR in this study), non-responsive loads and ES in the charging mode) are shown in Figure 5.44. As seen in this figure, P_t^{TCP} is sometimes greater than $P_t'^{TCP}$ at the same time. As it is observed in Figure 5.46, in this time interval the average value of MCP is equal to 0.51 /kWh that is about 40% less than its value in the $EMS-MABC$ algorithm. This fact states that although more amount of consumer is fed in the $MCEMS$ algorithm, however the consumers must pay more MCP for supplying their power. In 40% of the times the value of TCP in the $EMS-MABC$ algorithm is greater than its value in the $MCEMS$ algorithm. Under these conditions, on the average the value of $\lambda_t'^{MCP}$ is about 32% less than the value of λ_t^{MCP}. This fact
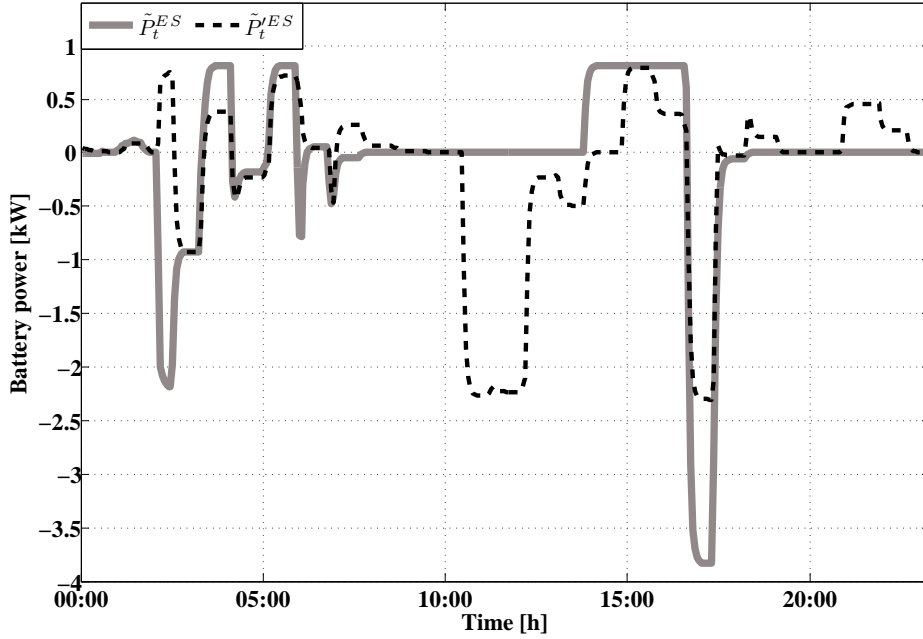
Figure 5.42: charging/discharging power of the battery emulator during system operation

shows significant reduction of the cost paid by the consumers. The total amount of the consumed power by the consumers in the $EMS - MABC$ algorithm is about 2% more than its value in the $MCEMS$ algorithm. In the other hand, noting that the total amount of the generated power must be equal to the total consumed power. Therefore, the optimization algorithm in addition to significant reduction in the total generation cost and the price of the consumed electricity, also is generated more power for feeding the consumers with less cost.

The bar graph related to charging/ discharging power of ES, responsive loads, UP and EGP are shown in Figure 5.45. As it is observed from the figures, MG in both algorithms during the third 6 hours of system operation by noting the occurrence of scenarios 2 and 3 is not able to supply the power required by all its consumers. In the time intervals 17:00-17:30 and 18:00-18:30 the value of UP in the $MCEMS$ algorithm is more than the optimization algorithm because the value of SOC in the $EMS - MABC$ algorithm is reached $\underline{SOC}$ and ES has no more ability to discharge. The significant point is that in this time interval, the about 30% more than its
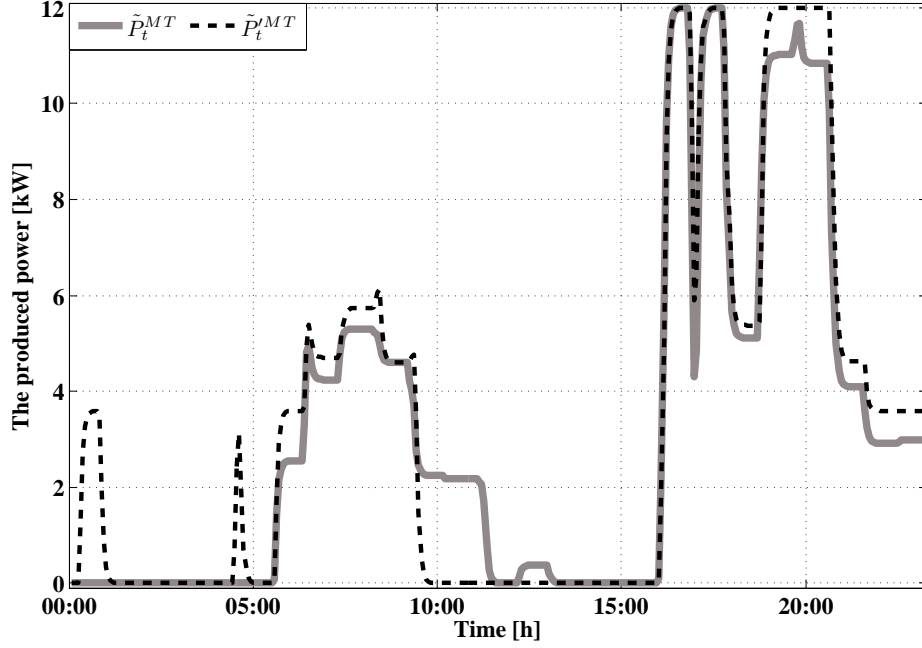
Figure 5.43: The generated power by MT emulator during system operation

value in the optimization algorithm. Therefore, the generator has to pay more penalties for supplying the total power needed by the consumers. As it is observed from Figure 5.45(a), most of the power required by the DR consumer is supplied in the time intervals 02:00, 04:30, 06:00 and 13:00-16:00. In these time intervals, the average value of $\lambda_t'^{MCP}$ is about 0.3 €/kWh but when UP exists the average value of MCP is about 0.9 €/kWh that is become 3 times. Therefore, the $EMS - MABC$ algorithm by cutting a number of consumers (when the value of MCP is high) and feeding them at the other hours of the day with smaller MCP, is significantly reduced the consumed electricity cost by the consumers. EWH is mainly fed in the time interval 15:00-17:00 in both of the algorithms. The average value of λ_t^{MCP} is about 37% greater than the average value of $\lambda_t'^{MCP}$ in this time interval. As it is observed from Figure 5.45(a), ES in the $MCEMS$ algorithm is mainly charged with the power $\overline{P}^{ES+}$. In the time intervals that ES operates in the charging mode, the average value of λ_t^{MCP} is about 0.49 €/kWh. This is while the average value of $\lambda_t'^{MCP}$ for charging the battery is about 0.32 €/kWh that is about 34% less than the value of MCP in the $MCEMS$

139
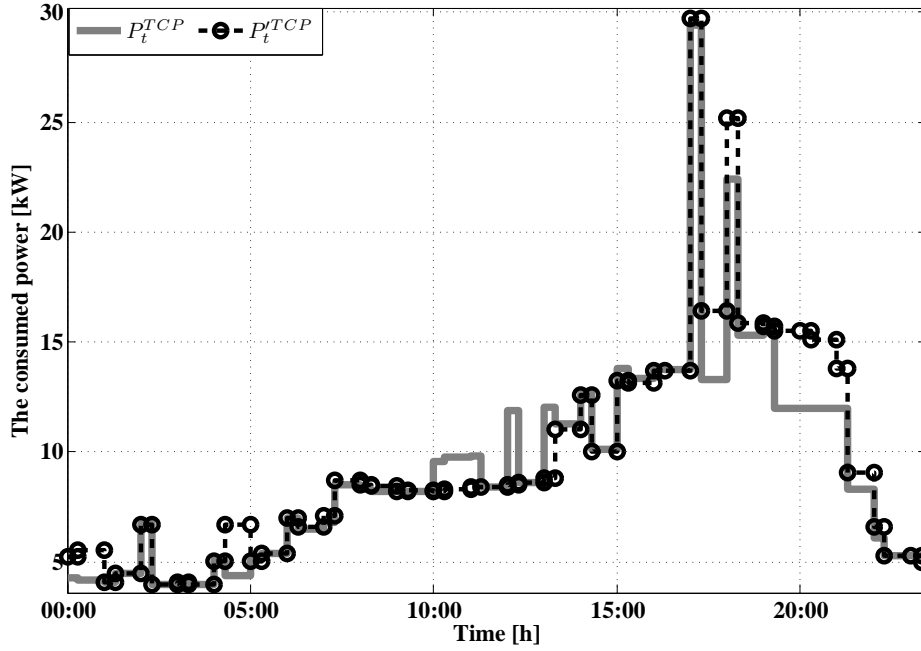
Figure 5.44: TCP profile during 24 hours system operation

algorithm. The average value of MCP for discharging ES for the algorithm $MCEMS$ and $EMS - MABC$ is respectively about 0.39 €/kWh and 0.41 €/kWh. This fact shows that more income from discharging the batter is dedicated to the owner of MG.

The value of MCP during one day system performance is shown in Figure 5.46. The average value of λ_t^{MCP} and $\lambda_t'^{MCP}$ during the day is respectively equal to 0.52 €/kWh and 0.32 €/kWh that shows the 39% reduction of the value of MCP in the $EMS - MABC$ algorithm. The maximum value of λ_t^{MCP} is equal to 1.33 €/kWh and is in the time interval of the occurrence of scenario 2. While, the maximum value of $\lambda_t'^{MCP}$ is equal to 0.90 €/kWh that is obtained in the time interval of the occurrence of scenarios 2 and 3. The minimum value of λ_t^{MCP} and $\lambda_t'^{MCP}$ are also respectively equal to 0.2 €/kWh and 0.13 €/kWh that is obtained for both of the algorithms at the first 6 hours of system operation. The average value of MCP during 24 hours of system operation is mentioned in Table. 5.4 for both algorithms. As it is observed from the table, the value of MCP in both of the algorithms at the first 6 hours of system operation is minimum so the proper act is that
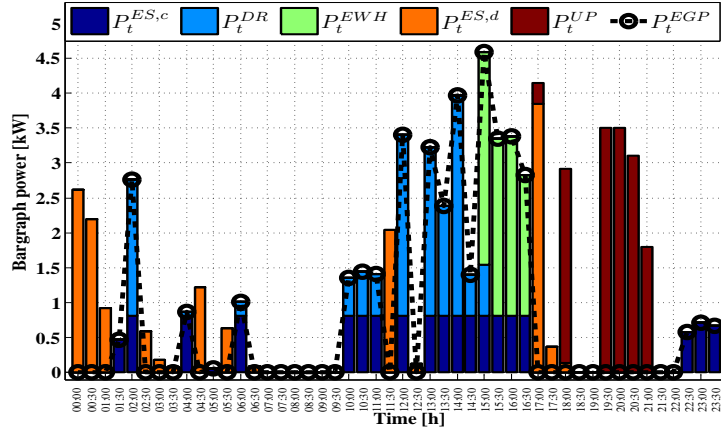
(a) *MCEMS*
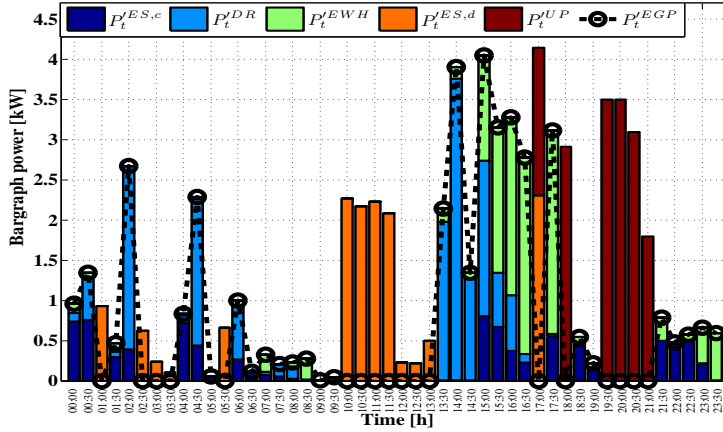
(b) *EMS − MABC*

Figure 5.45: Bargraph related to the responsive loads power, discharging battery and UP during the system 24 hours performance

more number of RLD and ES loads are fed in this time interval.

As it is observed from Figure 5.45, the value of the fed RLD and ES loads in the *EMS − MABC* algorithm is about 46% more than the *MCEMS* algorithm. As a result, these consumers are fed with less price. At the second 6 hours of system operation because MT in both of the algorithms is entered service and noting that its offer is higher than other generation sources, so MCP is increased. So, it is logical that by noting the increase of electricity

141

price, less value of RLD and ES is fed by the $EMS - MABC$ algorithm. With the analyses performed it is specified that about 85% less amount of power is used for feeding RLD and ES that shows the very adequate performance of the proposed algorithm in the demand side management. During the third 6 hours of system operation because PV is entered service and MT is gone out of service and the PV offer is less than MT, so it is natural that the value of MCP reduces significantly. Also, in this time interval about 6% more of the RLD and ES loads in the $MCEMS$ algorithm are fed relative to the proposed algorithm. At the last 6 hours of system operation, the average value of MCP is maximum in both of the algorithms so it is befitting that loads with less offers are fed in this time interval. As it is observed from Figure 5.45, in the $MCEMS$ algorithm in this time interval only ES is fed that is presented the highest offer among consumers. This is while that, in the $EMS - MABC$ algorithm in addition to ES, EWH is also fed. The EWH is proposed the least offer so the consumer pays much less cost for feeding its load.
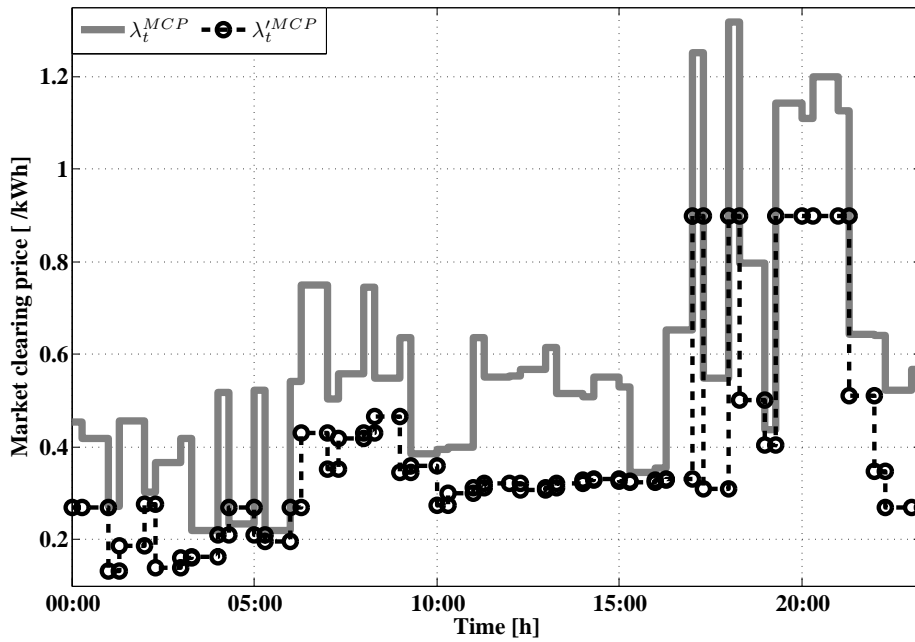
Figure 5.46: MCP for each interval during the system daily performance

Table 5.4: Average value of MCP during each 6 hour period of system operation

00:00:06:00	00:06:12:00	12:00:18:00	18:00:24:00	
0.62	0.49	0.56	0.41	λ_t^{MCP}
0.50	0.33	0.35	0.21	$\lambda_t'^{MCP}$

Conclusion

Modeling the consumers′ information for presenting the specifications of RLD in a DR program and for estimating the quality of their participation in a LEM with the aim of reducing MCP by using the $EMS - MABC$ is proposed. Also, new concept for the virtual generation sources derived from demand sources for estimating the optimum programming of generation sources and DR have been simultaneously introduced in the isolated MG. A cost function of the virtual generation sources by using the information of the consumers taking part in the system under study has been presented. The constraints related to DR by using the flag of its situation, the information of other consumers and EGP has been stated. These cases have been stated for modeling the limiting conditions for the consumers participating in a DR program. Combined optimum programming including generation sources and DR for minimizing the total cost of MG performance has been done by using the information of the consumers. This combined programming has been evaluated over an MG Testbed and the participation of the necessary information also demand sources marginal cost function by using measured real data has been estimated. The practical and simulation results show the reduction of the system operation cost (about 30%) and the significant reduction of the value of MCP in each time interval with adequate and real time control of DR in the suggested algorithm.

5.1.7 MACO

SOC profile is shown in Figure 5.47(a) for each of the two presented algorithms. The initial value of SOC is considered 50% for all the suggested algorithms. At the moment in the algorithm $EMS - MACO$ the battery starts charging while in the algorithm $MCEMS$ exactly at this moment the battery has operated in the discharging mode. As it is observed, almost in both of the algorithms the ES system has operated in the similar operating mode (charging and discharging) during the first 6 hour of system operation

(from 12 at night to 6 in the morning). As it is observed in this figure, in the $MCEMS$ algorithm the battery after 6 hours system performance (from midnight to morning) reaches the value of 22.48%. While in the algorithm $EMS - MACO$ this value is approximately equal to 34%. It means that the value of SOC in the $MCEMS$ algorithm after 6 hours system operation is reached 45% of its initial value this is while in the other algorithm its value has decreased about 32%. Although at the end of second 6 hours work of the microgrid system (from morning to noon) the value of SOC in each of the two algorithms is approximately equal. But this point shall be noticed that its value in $EMS - MACO$ in 58% of the times has reached more than 55%. This fact shows that the microgrid system in $EMS - MACO$ in encountering unwanted incidents such as Scenarios 2 and 3 can better supply the power requested by the consumers by using ES. As a result the reliability of the system under these conditions during this time period will increase. Maximum value of SOC in the $MCEMS$ algorithm is equal to 27%. This is while in this algorithm 75% of this period (from morning to noon) the value of SOC is equal to $\underline{SOC}$. In the third 6 hour of the microgrid system operation (from noon to evening) in each of the two algorithms ES starts charging; therefore, its value at the end of this period for two algorithms are respectively equal to 27% and 41%. In the fourth period of the system operation (from sunset to 12 at night), in each of the two algorithms, most of the times MT is used for feeding the load. As it is observed from the figure, the value of SOC in the $MCEMS$ algorithm has become equal to 23.76% that for the start of system operation in the next day is not a suitable value. But at the end of the day in the $EMS - MACO$ algorithm its value has become 68.9%. Altogether, although the battery performance in the $MCEMS$ algorithm is very well but at the end of the day in the $EMS - MACO$ algorithm the battery will have a better charge value for the next day as a result in addition to the reduction of production cost, altogether reliability in the system has increased significantly.

In Figure 5.47(b) battery power profile is shown during system performance. Battery power profile for each of the three algorithms suggested is different most of the times. Although in some of the times in an algorithm the battery is charged however, exactly at the same time in other algorithms the battery may operate in the discharging mode. During the periods 01:30, 02:00, 04:00, 05:00, 06:00, 14:00 and 22:30-23:30 in each of the three algorithms the battery has operated in the charging mode but the values of charging mode for each of these algorithms are different. During the periods 01:30, 02:30-04:00, 04:30, 05:30, 17:00 and 18:00 in each of the three algorithms the battery has operated in the discharging mode. As it is

observed from this figure, in the MCEMS algorithm at 17:00 the battery is discharged with maximum power while maximum discharging power in both of the other algorithms is almost equal to 2.4kW. With this difference that, in the $EMS - MINLP$ algorithm the battery at 19:30 is discharged with this amount of power but in the $EMS - MACO$ algorithm this incident has taken place at 17:00 that is exactly the time in the MCEMS algorithm when also ES is discharged with maximum power. Although in some of the times in an algorithm the battery is charged however, exactly at the same time in other algorithms it is possible that the battery operates in the discharging mode or idle mode. For example, although in the $EMS - MINLP$ and $EMS - MACO$ algorithms in the time intervals 00:00-01:00 and 17:30 the battery has operated in the charging mode, but in the MCEMS algorithm has operated in the discharging mode. In the MCEMS algorithm during 24 hour system performance in 41.7% of the times battery has operated in the charging mode. While, in the algorithms $EMS - MINLP$ and $EMS - MACO$ is respectively equal to 37.5% and 48%. So the battery in $EMS - MACO$ has the highest amount of charging in addition to this also at the end of the day the value of SOC in it is more than the other algorithms. Its reason is that the battery in this algorithm is charged with a higher power relative to other algorithms (in 33.3% of the cases with $\overline{P}^{ES,c}$). By looking at the battery performance in the discharging mode it will be observed for each of the three algorithms that in MCEMS in 29% of the times during 24 hours system performance, the battery is discharged. This value for the algorithms $EMS - MINLP$ and $EMS - MACO$ is respectively estimated to be equal to 25% and 35.4%. Although the discharging period in the battery in the $EMS - MACO$ algorithm is more than other algorithms, but because the battery discharging power in this algorithm is most of the times less than other algorithms and also the amount of power that is used for charging ES is also more, so at the end of the day the amount of energy stored in ES in this algorithm is more. ES in the algorithms MCEMS, $EMS - MINLP$ and $EMS - MACO$ has respectively operated in the idle state at 29%, 37.5% and 16.67% respectively. This shows the fact that in the algorithm $EMS - MACO$ it is tried that despite the higher offer price of MT relative to ES by considering the minimization of cost function (relation (2.10)) MT is used for feeding the loads. As a result of this action, the battery has more charge and finally the system reliability and stability will increase.

As explained previously, in the $MCEMS$ algorithm when the sum of power generated by PV and WT is less than the power required by the load and the battery is also in the full discharge mode, in that case MT will be

145
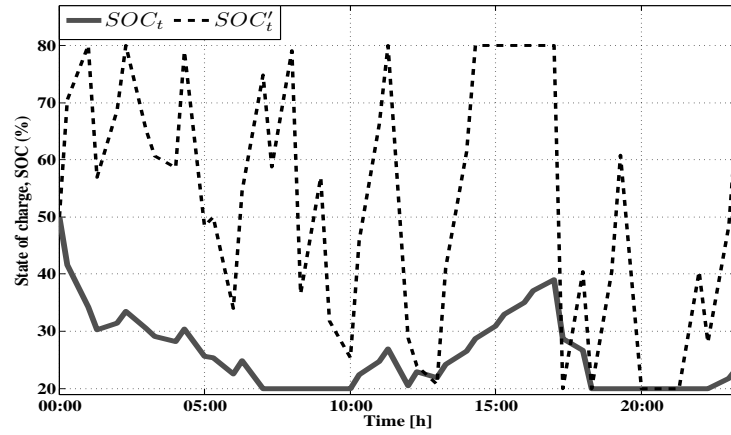
(a) SOC during system daily performance
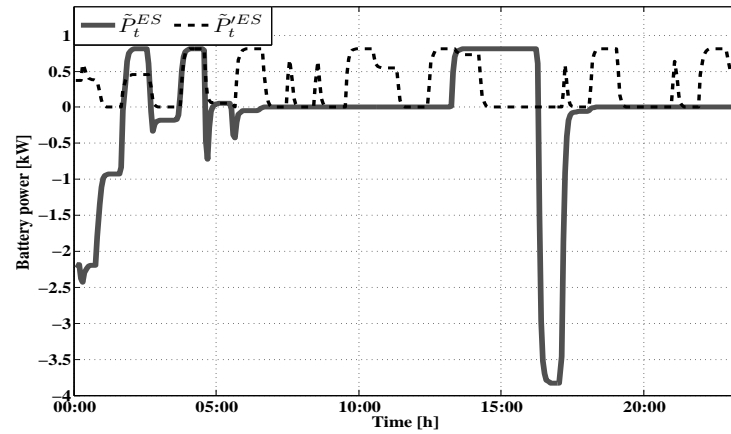
(b) Set points profile (solid curve) and measured value from ES emulator (dotted curve)

Figure 5.47: ES profile during the system daily operation

used. In Figure 5.48 MT power profile is shown. From midnight to morning, except at 06:00 o′clock, in the other cases $MCEMS$ has not used MT. this is while in the $EMS - MACO$ in the time intervals 00:00-01:00 and 06:00, MT is in service with the power $\underline{P}^{MT}$. Maximum power generated by MT for each of the two algorithms is $\overline{P}^{MT}$ this power for all of the suggested algorithm is generated in the time periods 17:00, 18:00, 19:30-21:30. In this time interval the Scenarios 2 and 3 have taken place and microgrid, enters

MT into service for the complete feeding of the loads with maximum power.
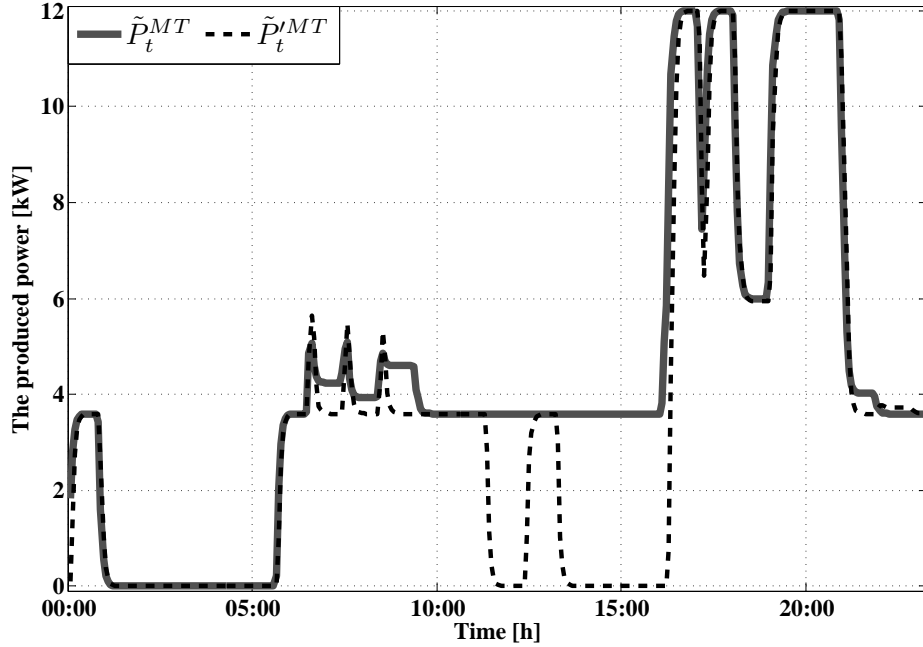
Figure 5.48: MT profile during system daily performance

As was previously explained, in $MCEMS$ if the sum of power generated by PV and WT is more than the load power, the differential of this power is first used for charging the battery. And if the power differential is more than $\overline{P}^{ES,c}$ and or battery SOC is equal to $\overline{SOC}$, in that case this excess power will be used for feeding EWH. But in the other algorithms in which optimization methods have been used, if the sum of the total powers generated by load, in that case this excess power depending on how by allocating it for feeding each of the consumers (ES, EWH and DR) the cost function will become minimum can be used for feeding ES, EWH and DR and or simultaneously each three of them. During the first 6 hours, second 6 hours and fourth six hours of system operation, no power for feeding EWH is used in the $MCEMS$ algorithm. In this algorithm, only during the time periods 15:00-17:00 some excess power is used for feeding EWH as seen in Figure 5.49. In optimization algorithms the conditions are different. From midnight to morning, in the $EMS - MINLP$ algorithm during the hours 00:00, 00:30 and 06:00 MT is put to service with the power $\underline{P}^{MT}$, part of the power generated is used for

147

charging the battery and the other part also feeds EWH. At 00:00 although the battery is not in the full charging mode and can charge more, however the great part of excess power is used for feeding EWH. This means that although the EWH feeding offer is lower relative to the battery charge offer, under these conditions also the algorithm has decided instead of charging the battery with the power $\overline{P}^{ES,c}$ to use less power and use most of the power for feeding EWH. Maximum fed power for EWH in the algorithms $MCEMS$, $EMS - MINLP$ and $EMS - MACO$ is respectively equal to $3kW$, $7kW$ and $3.4kW$ during the 24 hour system performance. This much power is used for feeding EWH in the algorithms $MCEMS$ and $EMS - MINLP$ at 15:00 and in the algorithm $EMS - MACO$ at 16:00.
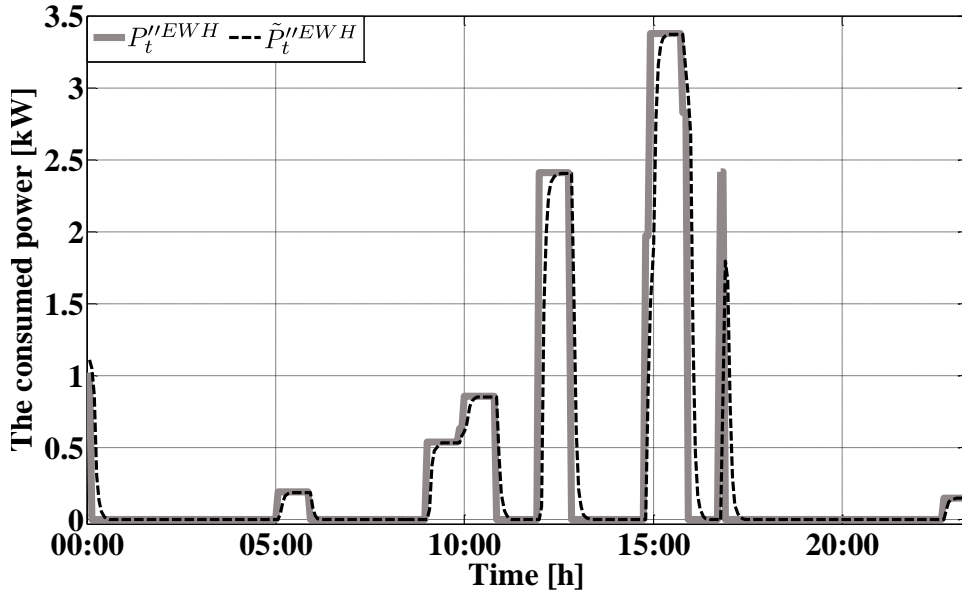
Figure 5.49: EWH profile during the system daily performance

Investigation of the amount of excess power generated in each of the three algorithms is one of the very important cases because by noting it can make the necessary decision making for the better use of the power generated. The amount of allocating this power for feeding different loads also must be evaluated so that the total system performance for load side management is investigated. As shown Figure 5.50, in the time intervals 01:00, 02:30-04:00, 04:30, 05:30, 07:00, 08:00, 09:00-10:00, 17:00, 18:00, 19:30-21:30 and 22:00 no excess power in any of the algorithms is generated. Maximum EGP in the algorithms $MCEMS$, $EMS - MINLP$ at 15:00 and for the algorithm

$EMS-MINLP$ at 16:30. In the algorithms $MCEMS$ and $EMS-MACO$ the excess power generated at 15:00 is as a result of excess power generated by PV and WT and in addition to that these microsources have been able to feed the total main load in the $MCEMS$ algorithm part of their main power is for feeding EWH. But in the $EMS-MACO$ algorithm the total excess power at this moment is used for feeding EWH. In the $EMS-MINLP$ algorithm at 16:30 ES is charged with the power and also other part is used for feeding EWH. As it is observed from the figure, most of the excess power at the third 6 hours (from noon to sunset) is generated in all the algorithms. From the analysis done we can conclude that, in the algorithms $MCEMS$ and $EMS-MACO$, EWH with less capacity relative to the $EMS-MINLP$ algorithm is required.
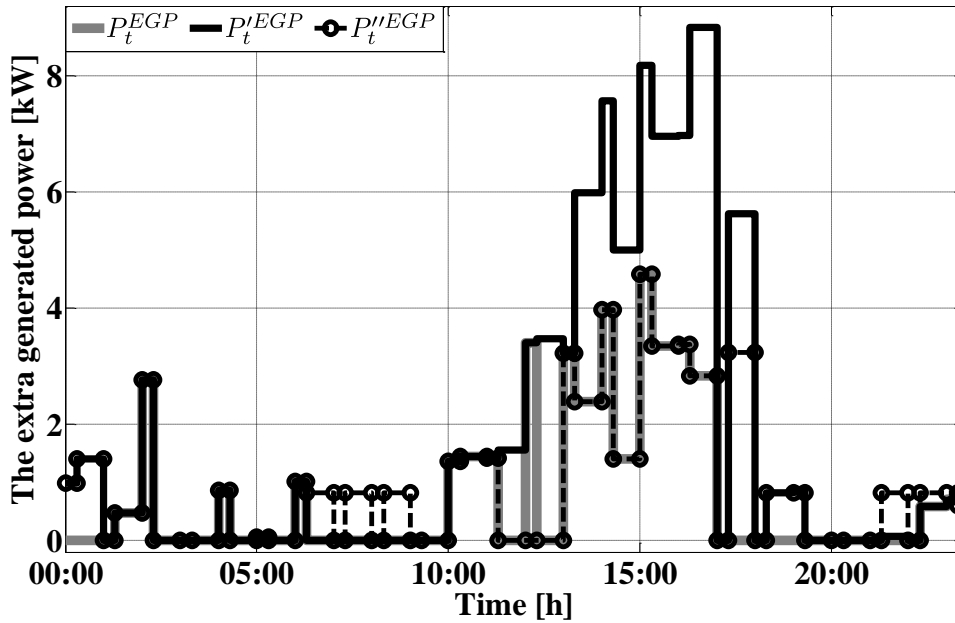
Figure 5.50: Excess power generated during 24 hour system performance

Power profile related to TCP is shown in Figure 5.51. The values of TCP in both of the algorithms in the time intervals 01:00-06:30, 07:00, 08:00, 09:00-12:00, 12:30-17:00, 20:00, 21:00 and 22:00 are equal to each other. At the times 12:00, 17:00, 20:30 and 22:30, the value of P_t^{TCP} has become greater than $P_t'^{TCP}$. At 12:00 because the value of $P_t^{ES,d}$ is less than $P_t'^{ES,d}$ and at 23:30 the value of $P_t^{ES,c}$ is more than $P_t'^{ES,c}$. At 17:00 because of the occurrence of Scenario 2, for supplying the power requested ES system

operates in the discharging mode but at this hour the value of $P_t^{\prime ES,d}$ is less than $P_t^{ES,d}$ and as a result the P_t^{UP} in the $MCEMS$ is obtained less than $P_t^{\prime UP}$. At 20:30 that Scenario 3 has occurred, MT system enter service with the capacity $\overline{P}^{MT}$ but because in both of the algorithms the value of SOC is equal to $\underline{SOC}$, so we have UP in both of the algorithms but $P_t^{\prime UP}$ at this hour is obtained more than P_t^{UP}.
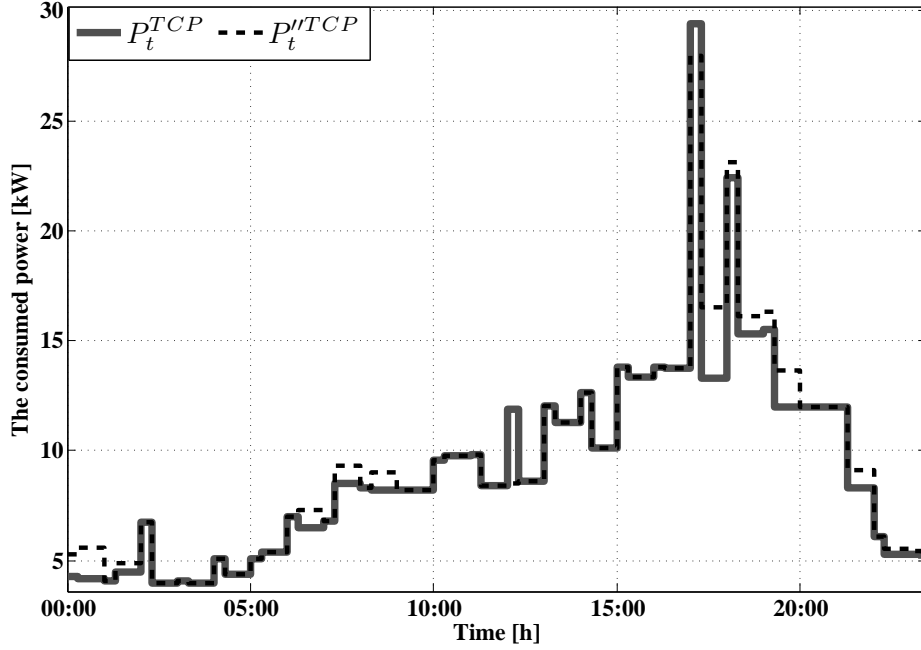
Figure 5.51: TCP profile during system daily operation

UP and DR profile during system daily performance is shown in Figure 5.52. As it is observed from the figure, in each of the three suggested algorithms UP is because of the occurrence of Scenarios 2 and 3. In the $MCEMS$ algorithm the power that is used is in the time intervals 02:00, 04:00, 06:00, 10:00-11:30, 12:00 and 13:00-15:30. In $EMS - MINLP$ the DR load is fed in the time intervals 13:30-14:30 and 15:00-17:00. But in $EMS - MACO$ this time is fed in the time intervals 02:00, 04:00 and 13:30-16:00. Following it will be shown that in these time intervals how much are the values of $\lambda_t^{\prime MCP}$ and $\lambda_t^{\prime MCP}$ and whether the optimization algorithms in choosing the DR feeding hour by considering the minimum production cost has performed correctly or not. As it is observed from the figure, UP in each

of the three algorithms exist at a certain time but the value of this power is different in each of the algorithms.
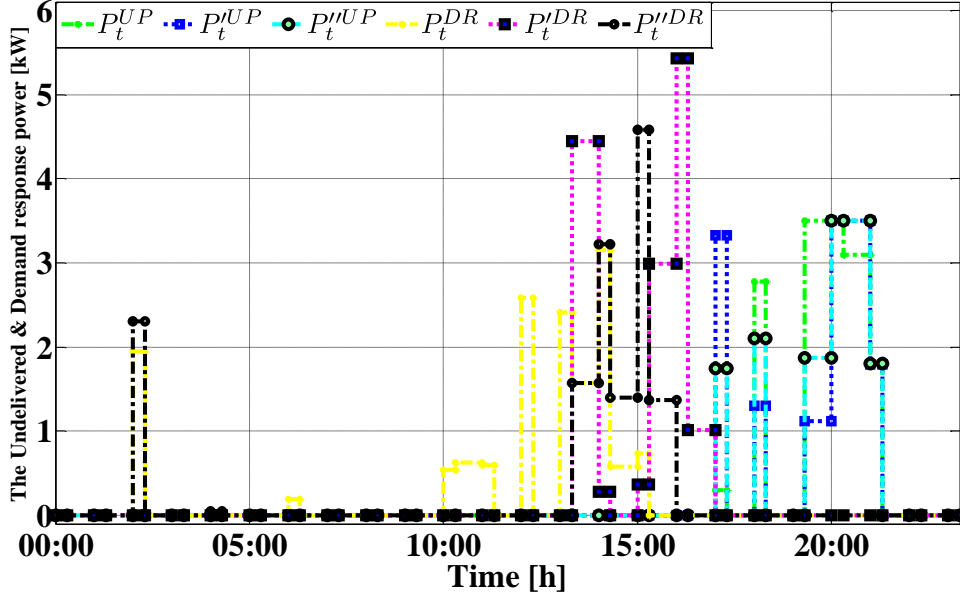
Figure 5.52: UP and DR profile during system daily performance

In summary, the bar graph related to the ES powers during charging and discharging, EWH, UP and EGP have been shown in Figure 5.53 for each of the algorithms. As it is observed form Figure 5.53(a), in most of the times ES is charged with $\overline{P}^{ES,c}$. The other point is that the power DR is consumed before 15:00. In this time interval the value of consumer peak is low and must be investigated afterwards that whether during this time the value of λ_t^{MCP} is high as a result it is observed that under these conditions the value of P_t^{MCP} has reduced and the feeding of some consumers is transferred to other hours in which the value of λ_t^{MCP} is lower. As it is observed from Figure 5.53(b), in the $EMS - MACO$ algorithm also hours in which DR is fed, the value $\lambda_t'^{MCP}$ has a low or average value.

In Figure 5.54 the value of MCP is shown in each time interval. As it is observed from the figure, in all the time intervals except 19:00 the value of λ_t^{MCP} is greater than $\lambda_t'^{MCP}$. Maximum difference between λ_t^{MCP} and $\lambda_t'^{MCP}$ is equal to 0.44€/kWh that occurs at 08:00 o′clock. In this hour, the values of P_t^{TCP} is equal to $P_t'^{TCP}$. This fact shows that at this hour the amount of money that must be spent on TCP in the optimization algorithms is much less than the value of $\lambda_t'^{MCP}$ but in the intervals 07:00, 08:00, 16:30,

151
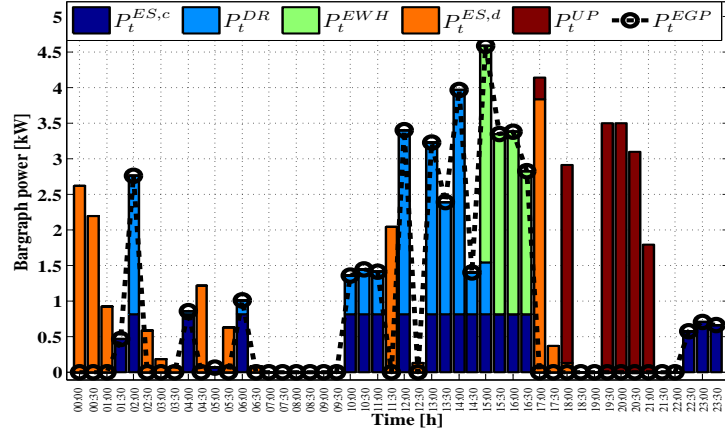
(a) *MCEMS*
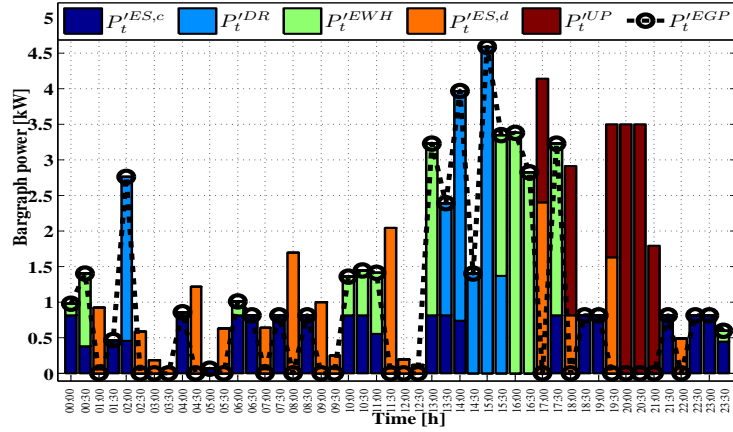
(b) *EMS − MACO*

Figure 5.53: Bar graph related to the ES power during charging and discharging, EWH, DR and EGP

17:30, 19:00 and 22:00 its value is more. At the rest of the hours also their values are equal. Maximum value of λ_t^{MCP} is equal to 1.32€/kWh that is at 18:00 that at this hour Scenario 2 has occurred. Maximum value for $\lambda_t'^{MCP}$ is obtained at hours that Scenarios 2 and 3 have occurred. Also, the minimum value of λ_t^{MCP} is obtained at the hours 03:30 and 05:30. The minimum value for $\lambda_t'^{MCP}$ is equal to 0.3€/kWh that is obtained at 01:00 and 04:30. In both of these hours, ES has operated in the discharging mode

and has compensated shortage of power.
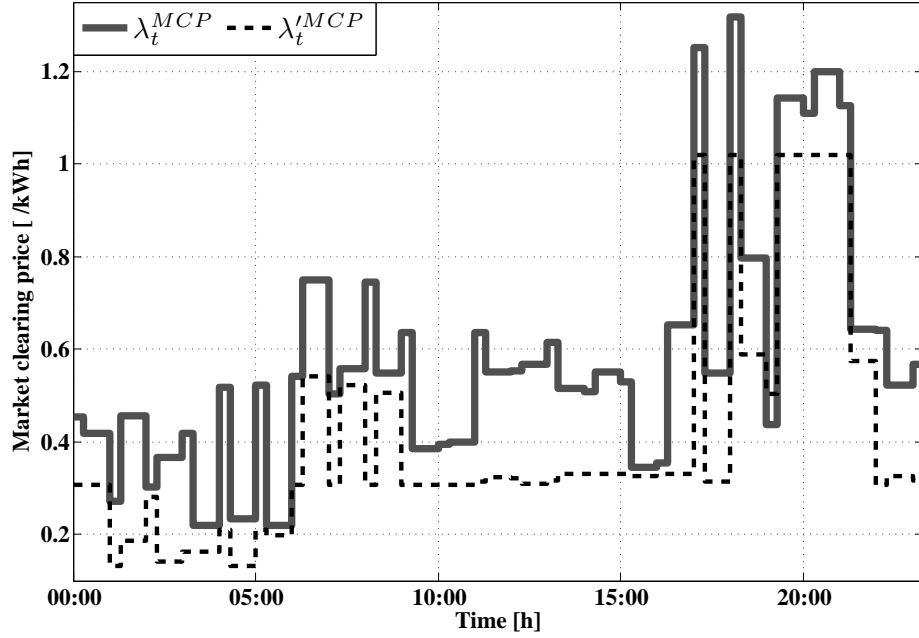
Figure 5.54: The value of MCP during system daily performance

Figure 5.55 shows real time scheduling output for an islanded MG by using $EMS - MACO$ algorithm for one working day with 5 minute intervals. The results show that real time scheduling is done according to the suggested algorithm and MG system stability under different conditions is ensured. Also the plug and play ability in this system by considering 4 mentioned scenarios has acted correctly. Three different positions can be noted in this figure clearly. First, the position A shows a situation in which the WT and PV systems because of reasons such as fault created in the network, annual overhaul program at etc are taken out of service and the power generated by them has become zero (Senario 2). Under these conditions, the feeding of a part of required power is supplied by ES and MT systems. As it is observed from the figure, some of the power required by the load has also not been supplied namely load shedding has taken place in the isolated MG system. As was explained, in this case the load not fed as DR will be fed at another time when there is excess production in the system. Point B is a typical situation at real time performance. As it is observed, severe load fluctuation will be compensated by the systems MT and ES and also a part

of the required power is supplied by these systems. At point C also Senario 4 has occurred. In this capacity scenario the production of WT system has reduced. In this point that EGP by the PV and WT systems existed at normal operation state, and this excess power is used for feeding ES, DR and or EWH system, following this scenario the amount of power consumed by EWH as observed in the figure has reduced.
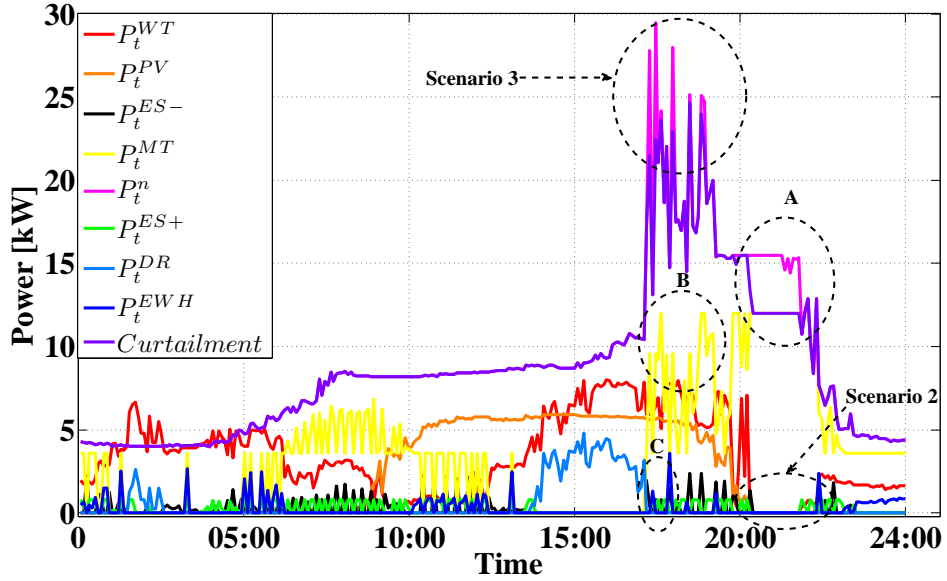
Figure 5.55: Real time scheduling of DERs for an islanded MG

Conclusion

Energy sources short term methodology in a smart grid has also been suggested in this study. In this methodology DAS, HDAS and FMRTS approaches have been investigated precisely. Short term scheduling has been used in reprogramming of MG based on WT and PV forecast data to find effective solutions of used sources scheduling in MG. Real time scheduling to investigate the plug and play capability and the system response ability to counteract the incidents occurred in the system for load and generation sides has been examined. In this study, the ACO optimization technique is deployed to achieve the optimal solutions within an appropriate interval. Feasibility of the method from the technical point of view has been evaluated by using measured real data and testbed in the IREC. Then, the results obtained from $EMS - MACO$ have been compared with those ones from

the $MCEMS$. The mathematical models developed allow real-time analysis of DGs' behavior as well as put the compatibility of constructed plants at disposal for optimization solutions. The case study has been implemented practically in the IREC's MG by using emulators for simulating the behavior of renewable energy sources and responsive/nonresponsive consumers. Eventually, it has been shown that the proposed optimization approach can optimally improve the performance of production sources, moreover, reduce generation and consumption electricity cost. Analysis of obtained results of both algorithms demonstrates that the system performance is improved also the energy cost is reduced about 20% by applying $EMS-MACO$ algorithm.

5.1.8 MPSO

As it is observed from the Figure 5.56(a), the value of power generated WT in the $EMS-MPSO$ algorithm during the time periods 06:30, 07:30, 09:00, 11:00 and 12:00-12:30 is less than the power forecasted at these times. At these points the required consumed power for the load is approximately equal to the sum of powers generated by WT and PV and also MT at the previous half hour is in service, so the algorithm because of the problems that exist for starting up MT or again putting MT out of service, prefers to use MT in these time intervals. Also at these points the algorithm reaches local optimum response. Maximum power difference generated between the forecasted data and also optimum data obtained by the algorithm is equal to $3.18kW$ that this case exists at 07:30. But in the $EMS-MINLP$ algorithm exactly the optimum data have followed the profile related to forecast data.

Also in the time intervals 08:00, 12:00, 14:30 and 19:00 the value of the obtained optimum power for PV is less relative to the value of forecast data as seen in Figure 5.56(b). Maximum value of difference between these two data has been observed at 12:00 o'clock. In the $EMS-MINLP$ algorithm has exactly followed profile optimum data related to the forecast data.

In Figure 5.57 battery charging and discharging profile during 24 hour system profile has been shown. At the end of the first 6 hour operation of the system (from 12 at night to the morning) battery SOC in both of the algorithms are equal and are about 54.41%. During the second period of system operation (from morning to noon) the value of SOC in the $EMS-MPSO$ algorithm has been obtained about 10% more than its value in the $EMS-MINLP$. But in the third period of the system operation (from noon to sunset) the battery during the $EMS-MPSO$ algorithm has mostly worked in the discharging mode so at the end of this period its value has reached $\underline{SOC}$ while in the similar period in the other algorithm its value is
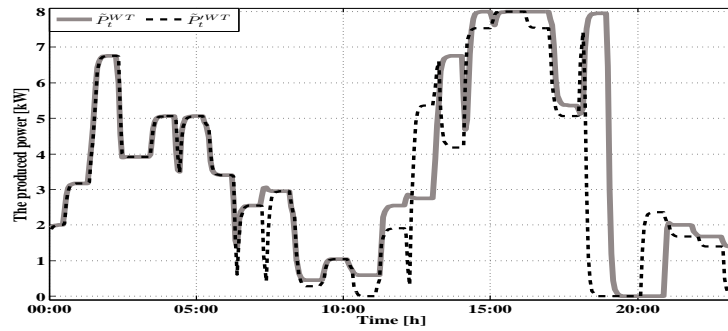
(a) The obtained results from WT emulator
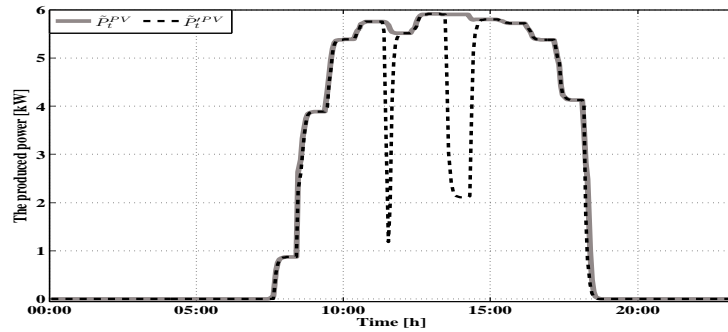
(b) The obtained results from PV emulator
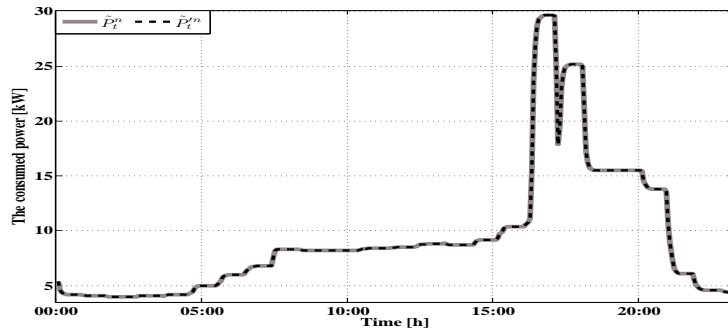
(c) The obtained results from Load emulator

Figure 5.56: The measured data from renewable resources and load demand

about 40% which its value is obtained 2 times its value in the $EMS-MPSO$.

In the fourth period of the system operation (from sunset to midnight) in both of the algorithms the battery has worked mostly in the charging

156

mode so at the end of the day the values of SOC in the $EMS - MPSO$ and $EMS - MPSO$ algorithms are respectively 68.87% and 51.79%. As it is observed, the battery in the $EMS - MPSO$ algorithm has more charge for the next working day so the reliability of the system has also increased.
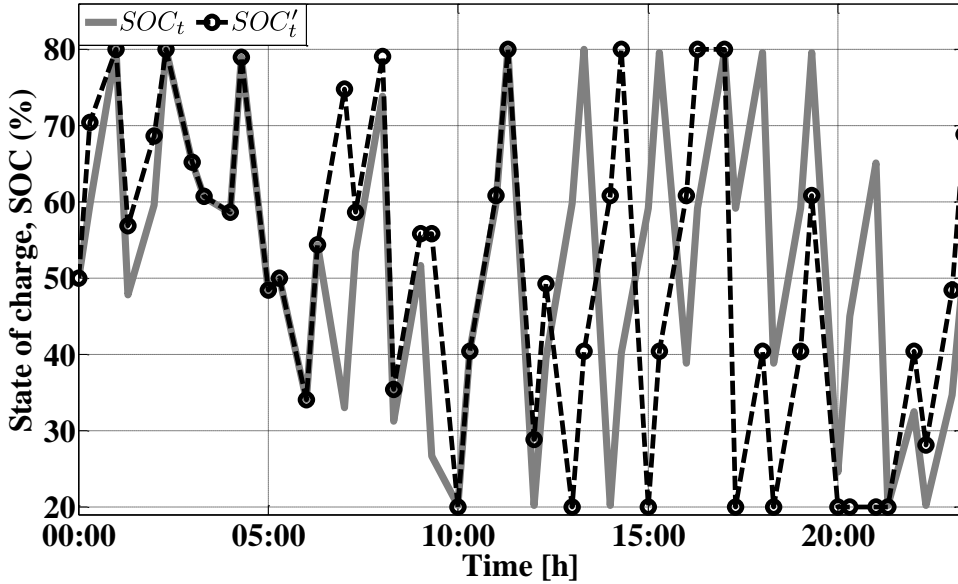
Figure 5.57: Battery SOC during 24 hour system operation

The battery charging and discharging profile during the system daily performance has been shown in Figure 5.58. The interesting point is that in the $EMS - MPSO$ algorithm relative to the $EMS - MINLP$ algorithm at 00:00, 2.125 times the excess power generated for charging the battery has been used this is while in the $EMS - MINLP$ algorithm at 00:30 exactly with this ratio the battery has been charged more than the similar hour in the $EMS - MPSO$ algorithm. The reason for this fact is that in both algorithms the power generated by PV and WT are equal and also in both of the algorithms MT has entered service with the power $\underline{P}^{MT}$. The significant point is that most of the excess power generated (about $600W$) at 00:00 algorithm $EMS - MINLP$ will be spent for feeding DR and the less value of this power will also be used for charging the battery. At similar hour in the $EMS - MPSO$ algorithm most of the excess power generated will be spent for charging the battery and part of it will also be used for feeding EWH. At 00:30 also no power has been used for feeding EWH in the $EMS - MINLP$ algorithm on the contrary most of the excess power

generated has been spent charging the battery and other part of this power has also been used for feeding DR.

But in the $EMS - MPSO$ algorithm most of the excess power has been spent feeding EHW and part of it has also been used for charging the battery. The excess power generated in both of the algorithms at mentioned hours are exactly equal to each other and only allocation of this power for feeding different consumers is different. In the $EMS - MPSO$ algorithm during the time interval 15:00 to 16:30 the excess power generated is more than other times in this algorithm this power has charged the battery with the power $\overline{P}^{ES,c}$ and its definitional will also be used for feeding DR. At 16:00 also part of this power has been used for feeding EWH. In the $EMS - MINLP$ algorithm at 13:30 part of the EGP is generated through discharging ES and the algorithm has indicated that if battery discharging is used for feeding EWH in this case also the cost function will become minimum. At this hour the value of SOC is equal to $\overline{SOC}$ and the battery has been discharged to the value about $\underline{SOC}$. But at 14:00 most of the EGP is spent on feeding the battery so that its SOC value increases. During 24 hour system performance in the $EMS - MINLP$ algorithm at 33.33% battery is charged with the power while in the other algorithm in 39.5% of the total of the day has been charged with the power $\overline{P}^{ES,c}$.

In both of the algorithms in no time ES has been discharged with the power $\overline{P}^{ES,d}$. The maximum power that ES has generated in the discharging mode is equal to $2.4kW$ in both of the algorithms that this power in the $EMS - MINLP$ algorithm has been generated at 11:30 and has been used for feeding DR. in the other algorithm this power has been generated at 14:30 and has been used only for feeding the main load.

In Figure 5.59 MT power profile has been shown. In the first hour of system operation (from midnight to morning) in both of the algorithms MT with $\underline{P}^{MT}$ at similar hours has entered service. During the second 6 hours of system operation (from morning to noon) at time periods 08:00-11:30 are exactly operating with one time power but at the hours 06:30, 07:30 and 12:00 the power generated by MT in the $EMS - MPSO$ is more than the other algorithm. Maximum difference between power generated in both of the algorithms is at 12:00 noon which is about $5.7kW$. At 07:00 and 11:30 the power generated by MT in the $EMS - MINLP$ algorithm is more than the other algorithm. In both of the algorithms MT has been operating 6 times with the power that in both algorithms this power has been generated in the time periods 17:00, 18:00 and 19:30-21:30.

Also MT in the algorithm $EMS - MINLP$ in 48% of its daily performance
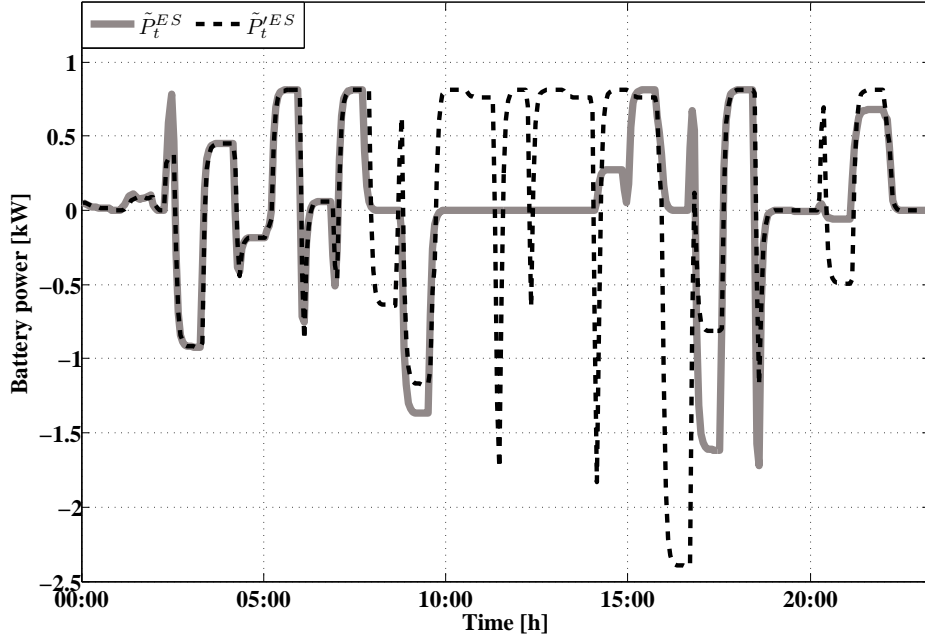
Figure 5.58: The battery power profiles during 24 hour system operation

is in service with $\underline{P}^{MT}$ that 33.33% of the times have been used for charging the battery. This is while in the other algorithm this value is equal to 97% that 16.6% of the times it has been used for charging the battery.

In Figure 5.60 bar graph related to the ES powers during charging and discharging, EWH, DR, UP and EGP during one day system performance has been shown. As it is observed from the Figure 5.60(a), during the time intervals 01:30, 04:00, 06:00, 07:00, 07:30, 08:30, 18:30-19:30, 20:00-21:00, 21:30 and 00:00-22:00 all of power EGP has been used for feeding ES in the charging mode in the $EMS - MINLP$ algorithm. Also in this algorithm at 01:00 o'clock the EGP has been used only for feeding DR. During the time periods 00:00, 00:30 and 10:00-11:30 part of the EGP has been used for feeding ES and other part has been used for feeding DR. This power has only been used for feeding EWH and DR consumers at 13:30 and 15:30 and ES at these times operates in the discharging mode. This means that part of the EGP is supplied by ES and the algorithm has preferred to use ES for feeding EWH and DR. in the periods 12:00, 15:00 and 16:30, EGP will be used for feeding all the consumers (including ES, EWH and DR).

In this algorithm mentioning several points is very important. The first
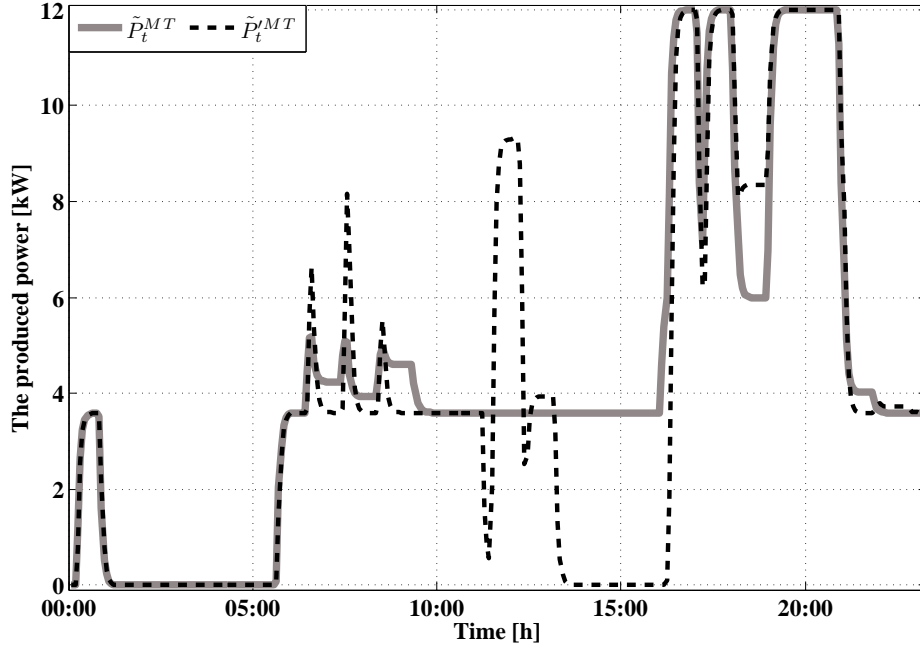
Figure 5.59: Generated power profile by MT during 24 hour system operation

point is that at the hours 01:00, 11:30, 13:30 and 15:30 discharging ES for feeding the consumers has been used. Sometimes discharging power ES has been used only for feeding DR (at 01:00 and 11:30) and sometimes also this power has been used together for feeding DR and EWH (at 13:30 and 15:30). The second point is that at 17:00, 18:00 and 19:30 although ES operates at discharging mode and ES can generate more power but the algorithm has generated UP power. Despite the possibility of generating more power but in none of these intervals ES has not been discharged with the power $\overline{P}^{ES,d}$. The third point is that during the time period 20:00-21:00 despite the existence of UP however the algorithm has preferred from Figure 5.60(a), UP has been generated in the system at the time intervals 17:00, 18:00 and 19:30-21:00. The reason is that exactly at these time intervals scenarios 2 and 3 are applied to the system. Figure 5.60(b) also shows mentioned power profiles in the $EMS - MPSO$ algorithm. During the time periods 01:30, 05:00, 06:30, 07:30, 08:30, 12:00, 13:00, 18:30-19:30, 21:30 and 22:30-23:30 all the EGP has been used for charging ES. Also at 16:30 this power has only be used for feeding EWH. In the time intervals 02:00, 13:30-14:30, 15:00-

16:00 part of the EGP has been used for charging ES and the rest of it also has been used for feeding DR. At 16:00 EGP has been used for feeding all the consumers (including ES, DR and EWH). Several points regarding this figure can be investigated. The first point is that at the hours 17:00, 18:00 and 19:30 although UP power exists but by noting that the value of SOC after ES discharge reaches $\underline{SOC}$ with some power, as a result cannot fulfill shortage of power completely. Also the UP in this algorithm is as a result of implementing scenarios 2 and 3 in the system only at 18:00 that ES cannot discharge more and after discharge its SOC reaches $\underline{SOC}$, the value of UP in this algorithm is more that $EMS-MINLP$ algorithm. Maximum UP in the $EMS-MINLP$ algorithm is equal to $4.3kW$ and in the $EMS-MPSO$ is equal to $3.5kW$. As a result in the $EMS-MINLP$ algorithm more DR power for feeding can be used.

Conclusion

MPSO based on the variation of speed limit during the operation related to finding optimum point in the search space has been suggested. Advantages, accuracy and correctness of performance also the practical ability to implement this method by using IREC's MG for solving problems related to the smart grid has been shown. Likewise, the performance of MPSO has been compared with another alternative method $EMS-MINLP$. $EMS-MPSO$ algorithm has shown a completely competitive time (about 2 times faster than the deterministic method for the case study under investigation). In addition, $EMS-MPSO$ can reduce cost which is enough low that is diversity comparable with the results obtained from the deterministic method. This method has been identified suitable for the problems with big dimensions and very complex and even when the number of production resources is relatively low. Power systems that increasingly by using DERs especially renewable energy resources increase the dimensions of the short term scheduling problems of the resources, are growing. As a result, using the suggested methodology at one time is felt suitable more than before for reaching an acceptable operations cost. The suggested method can answer the different scenarios that can occur in these systems inside an acceptable time frame for the short term scheduling of the resources. In this method, more effective use of renewable production resources and other DERs for the players involved in smart grid has been provided. The good results obtained by the suggested method proves that this method has been found suitable for handling the realistic problems that have a lot of variables as well as to need a very fast decision at a very short time. Its use for addressing
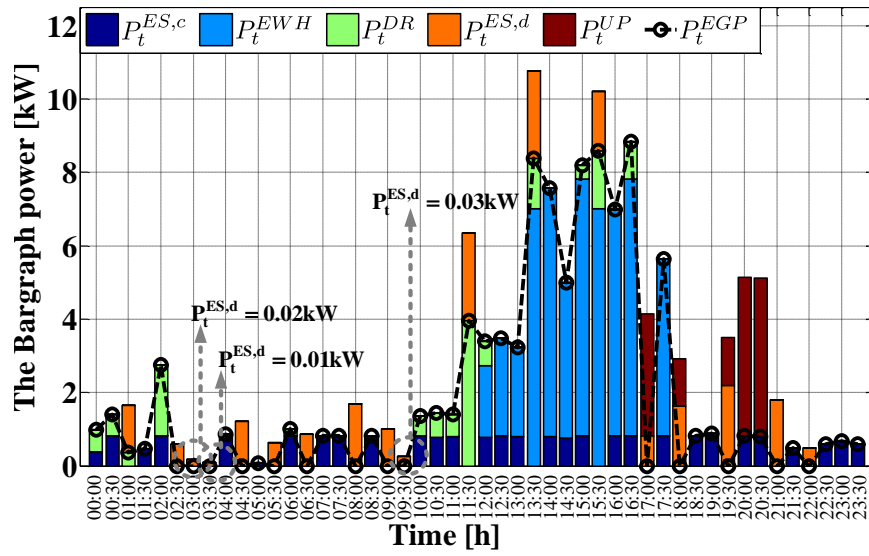
(a) *EMS − MINLP*
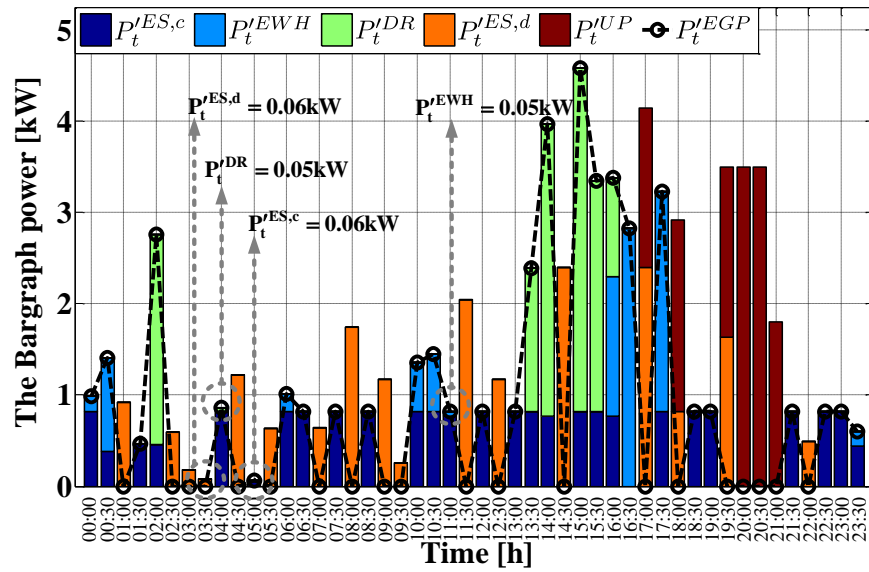
(b) *EMS − MPSO*

Figure 5.60: Bar graph related to power ES during the performance of charging and discharging mode, DR, UP and EGP

the short term DER scheduling has been proved in this thesis. In addition, the use of the suggested method for solving other complex problems with similar specifications such as production scheduling, transfer and rescheduling is also suggested. The obtained experiment results have demonstrated the ability of this algorithm for solving problems with large dimensions that need decision making in short time periods. Furthermore, the cost operation in $EMS - MPSO$ has been reduced (15% approximately) with respect to $EMS - MINLP$ algorithm.

5.1.9 MGSA

State of charge (SOC) is shown in Figure 5.61 for the algorithms $MCEMS$ and $EMS - MGSA$. At the first 6 hours of the system operation (from the night to the morning), ES in $EMS - MGSA$ is always operated in charging mode. Nevertheless, in $MCEMS$, ES is mostly operated in discharging mode. This fact indicates that despite the MT offer is high, the optimization algorithms have decided to use MT for compensating the lack of power. This fact is shown in Figure 5.62(b). The algorithm during this period, in addition to supplying the load required power, produces the excess generated power (EGP) as shown in Figure 5.63(b), for feeding ES, EWH and DR. At the end of the second and third 6 hours of the system operation (from morning to the sunset), ES system in both of the algorithms is almost completely discharged and SOC is approached almost to $\underline{SOC}$. The key point is that at the fourth period of system operation (from sunset to the night), ES in the $EMS - MGSA$ is started to operate in charging mode after a short period of discharging. As a result, the value of SOC in this algorithm reaches about 27% at the end of daily operation. While, its value has reached close to $\underline{SOC}$ in the algorithm $MCEMS$. Hence, ES definitely will show a better capability in the $EMS - MGSA$ to support the system at the beginning of the next day.

ES and MT power profile during the MG daily operation are shown in Figures.5.62(a) and 5.62(b), respectively. In the $MCEMS$, ES is operated about 42% period in charging mode, 29% in discharging mode and 29% in the idle mode during 24h of system operation. However, in the $EMS - MGSA$ algorithm, it is respectively operated 39.55 in the charging mode, 27% in the discharging mode and 33.5% in the idle mode. This shows that despite the higher offer of MT relative to ES, the $EMS - MGSA$ algorithm uses MT in more time intervals. Noting that the minimum power generated by MT is equal to $\underline{P}^{MT}$ so after the deduction of the power required by the load, one of the options of using EGP is the charging of the battery. Despite

163
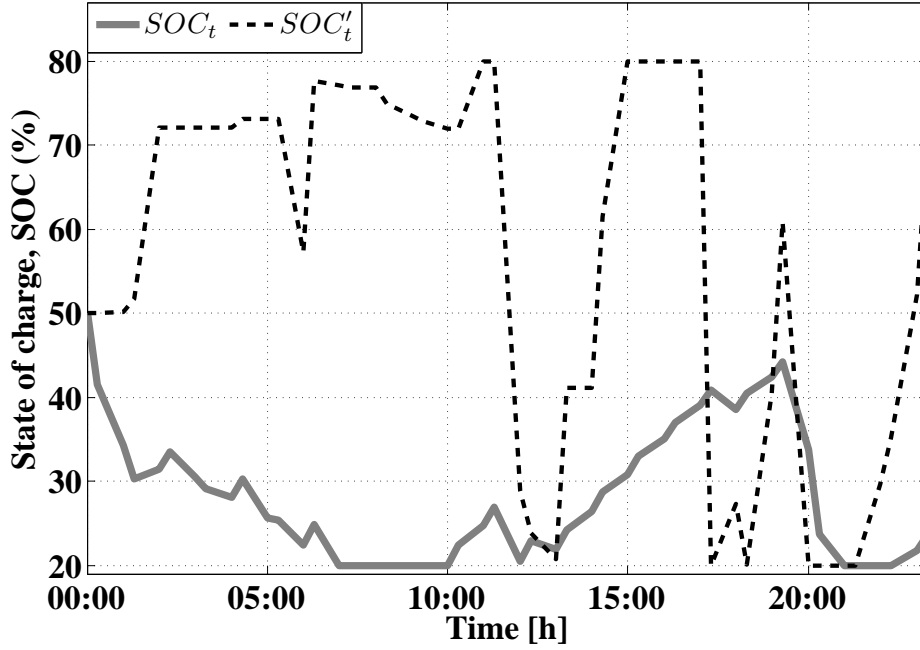
Figure 5.61: SOC during system operation

this fact, as it is observed from Figure 5.63(b), the optimization algorithm is decided to use EGP for feeding the loads including DR and EWH. In the $EMS-MGSA$ algorithm, the selection of generation unit is included by considering the minimization of the objective function. MT in the $MCEMS$ algorithm is off at 46% of the times while in the $EMS-MGSA$ algorithm is reached 14% during MG daily operation. As it is also observed, during the first 6 hours of system operation, MT except at 06:00 o'clock in the rest of the times is off in the $MCEMS$ algorithm. As it is observed from Figure 5.62(b), although in the $EMS-MGSA$ algorithm, MT is used more than ES for supplying the consumers, however $\lambda_t'^{MCP}$ in most of the time intervals is obtained less than λ_t^{MCP}. In addition to the reduction of electricity price in each time interval, it will have the reduction of total generation cost.

The power consumed by DR, EWH, ES during charging and discharging, UP and EGP are shown as a bar graph in Figures.5.63(a) and 5.63(b). ES is operating in charging mode around 42% of the times. ES in the $MCEMS$ algorithm is generated $\overline{P}_{ES,c}$ during 31% of the time operation. Although, this percentage in the $EMS-MGSA$ algorithm reaches 8.33% of
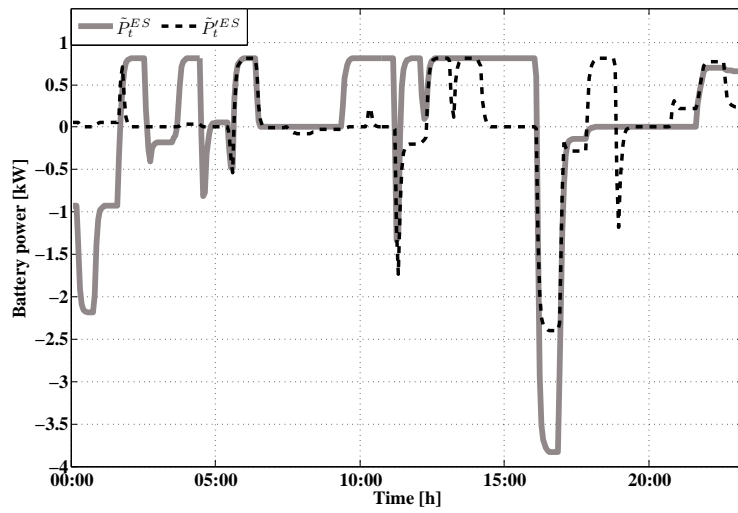
(a) ES
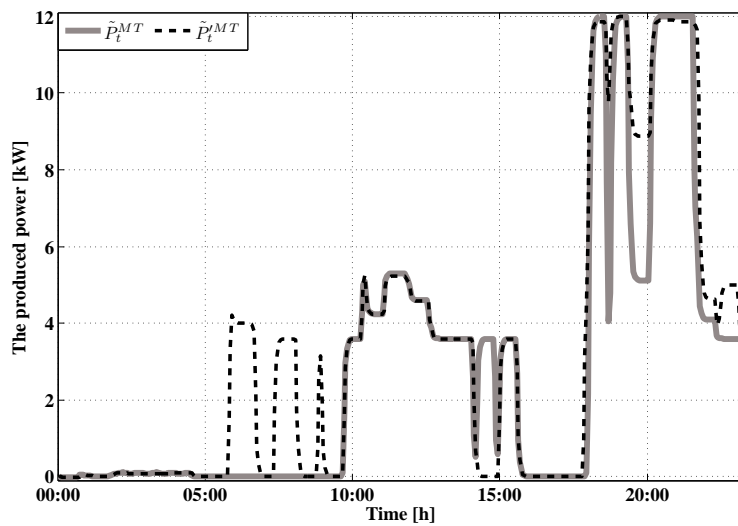
(b) MT

Figure 5.62: ES and MT power during system operation

the times. On the other hand, as it is observed from Figure 5.61, SOC in the $EMS-MGSA$ algorithm is much better than the $MCEMS$ algorithm. This fact shows that the algorithm based on optimization with proper evaluation

165

during system daily operation makes the best decision for using the EGP by the microsources. As can be seen in Figures 5.63(a) and 5.63(b), ES in the $MCEMS$ algorithm is operated in the discharging mode in more time intervals and with a higher discharging power. As seen from these figures, ES in the $MCEMS$ algorithm has operated in the discharging mode at the first 6 hours of system operation. While in the $EMS - MGSA$ algorithm system puts MT into service and uses the EGP mainly for feeding DR. When scenario 2 occurs (during the period 17:00), ES at both of the algorithms is discharged with the power $\overline{P}^{ES,d}$. MT is entered service with the power $\overline{P}^{MT}$ at the same time. From Figure 5.63(a), it is evident that most of DR is fed in the time interval 10:00 A.M to 15:00 P.M. As seen from Figure 5.63(b), all the DR in $EMS-MGSA$ is fed during 00:00-04:30 periods. In this time period, $\lambda_t'^{MCP}$ is variable between 0.16 €/kWh to 0.4 €/kWh. Hence, significant reduction in the cost to supply DR is done by the optimization algorithm. In the time intervals that the scenarios are occurred (time interval 17:00-21:00) and the consumed load is decreased (the system is encountered UP), average of λ_t^{MCP} is equal to 1.2 €/kWh. While in this time interval, the average value of $\lambda_t'^{MCP}$ is equal to 1 €/kWh. It means that the penalty cost is substantially reduced in the optimization algorithm. So, by feeding DR in the first 6 hours of system operation, the optimization algorithm presents the best choice for its feeding with the least possible expense. EWH in the $MCEMS$ algorithm is only fed in the time interval 15:00-16:30. In this time interval, the average of λ_t^{MCP} is equal to 0.51 €/kWh. But in the optimization algorithm, more excess power is generated by noting that MT is in service more.

MCP is shown in Figure 5.64 at each time interval. Its average value is also mentioned in each 6 hours period in Table 5.5. At the first 6 hours of system operation, the average value of MCP in the $EMS-MGSA$ algorithm is much less than the $MCEMS$ algorithm. This means that feeding RLD loads (that is DR and EWH) at this time interval is the best option. As a result, by this way, less expenses will be paid for feeding them by consumers. At the second 6 hours of the system operation, despite the rising of λ_t^{MCP}, the EGP power is used for feeding ES and DR in the $MCEMS$ algorithm. But as it is observed from Figure 5.63(a), most of the EGP power is used for feeding EWH which presents much less offer relative to ES and DR. In the third 6 hours of system operation, the average value of MCP is reduced in both of the algorithms. Considering $MCEMS$ algorithm, in half of this period, EGP power is used only for feeding DR and ES. When feeding DR is completed, the rest of the time is used to feed ES and EWH, respectively.
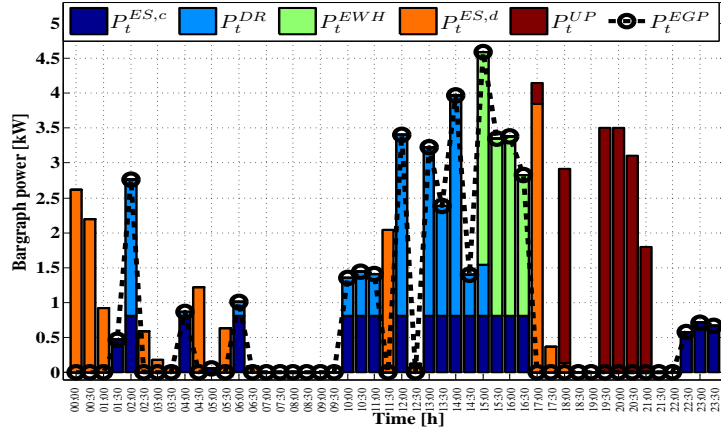
(a) *MCEMS*
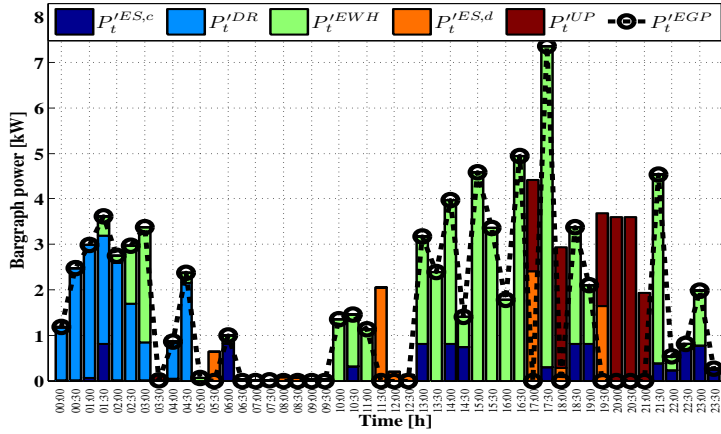
(b) *EMS − MGSA*

Figure 5.63: The baragraph related to the responsible loads power, ES discharging and UP during system performance

However, EGP in the $EMS − MGSA$ algorithm is used for feeding EWH most of the times. At the last 6 hours of system operation, EGP power in the $MCEMS$ algorithm is used only for charging ES. Dispite the ES charge offer is higher than the DR and EWH offers and the average value of λ_t^{MCP} is more than its average value in other periods, an adequate chosen is not intended for the consumers. However, EGP in the optimization algorithm is mostly allocated for feeding EWH that has the least offer among the

Table 5.5: The average value of MCP in each 6 hour period of system performance

00:00:06:00	00:06:12:00	12:00:18:00	18:00:24:00	
0.62	0.49	0.56	0.41	λ_t^{MCP}
0.60	0.33	0.34	0.31	$\lambda_t'^{MCP}$

consumers.

Both experimental and simulation results show that $EMS - MGSA$ algorithm is capable to operate much better in optimal scheduling, optimal operation, economic dispatch and demand side management in the best possible way. The total generation cost and MCP are reduced in the proposed algorithm by efficient management of generation, storage and load assets.
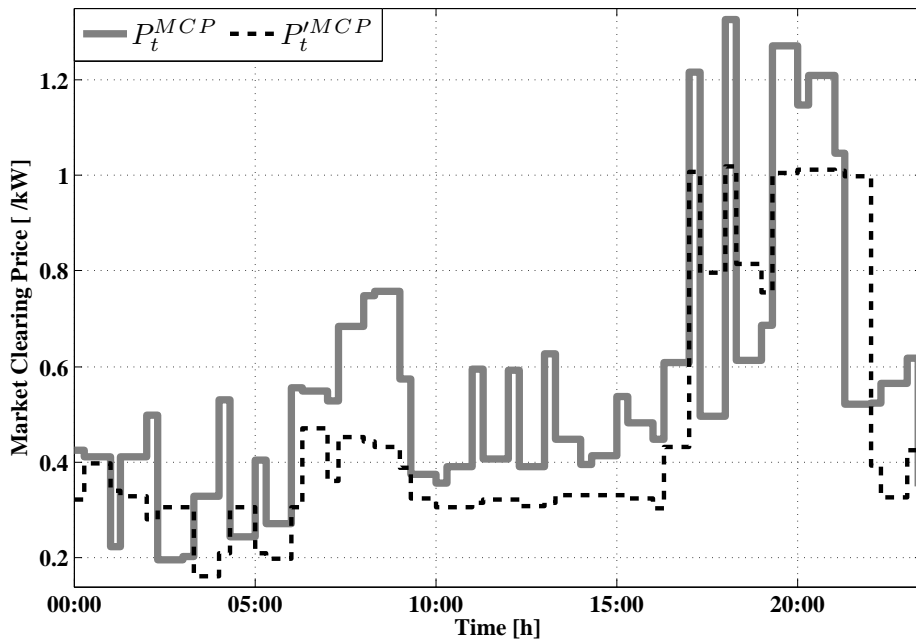
Figure 5.64: MCP for each interval during the system daily operation

Conclusion

The obtained results demonstrate the effectiveness of the proposed algorithm in solving the optimal problems within isolated and grid connected MG. The optimal power setpoints for microsources has been achieved based on previous information and real life experimental data by noting the fulfillment of all technical constraints. The optimization method in accordance with GSA approach has been introduced to minimize the production cost as well as to increase the system efficiency. A strategy for smart grid has been developed to shift the load and the accordance of power generation by renewable and nonrenewable sources. This solution has been implemented experimentally over the IRECs' MG system. Its efficiency and performance has been verified by using different scenarios. The proposed EMS has been expected to adapt itself in real-time to any changes both in the types and capacity of the generation as well as storage assets quickly, without any particular modification. The priority index for consumers to participate in LEM has been considered based on the offer by them and minimizing objective function. The obtained results have shown the improvement of the overall system operation in comparison with $MCEMS$. The experimental and simulation results showed that the increase in the percentage of the load shifting not only could yield more flexibility to the system but also cause using EGP to be promoted. Moreover, it has been observed that the system efficiency in finding the best way would lead to maximize the usage of the power generated by renewable sources. In addition, consumers have participated in DR with high priority index could be supplied with less cost. It is clear that $EMS - MGSA$ has operated much more successfully in reducing overall peak demand, the optimum operation of the present micro-sources and decreasing the total generation cost relative to the $MCEMS$ algorithm. The proposed algorithm proves the efficiency of GSA method for managing and exchanging power in smart grids. Eventually, using the proposed algorithm will enable utility companies to have an energy management tool with the optimization ability of using non-dispatchable and ES assets to supply industrial/commercial and household loads.

5.2 Grid connected mode

5.2.1 The comparison between $EOS - MINLP$, $EOS - MACO$ and $EOS - MGSA$ algorithms

The single line structure of the IREC′s MG is shown in Figure 5.65. The power profile related to renewable devices (PV and WT in this study) and also the power consumed by non-responsive load demand is also derived from [1] and is shown in Figures 5.66(a) to 5.66(c). The price offer related to renewable, non renewable generators, non-responsive load demand, purchasing/ selling electricity tariff from/ to the national grid and penalty resulting from unmet power are mentioned in Table 5.6.
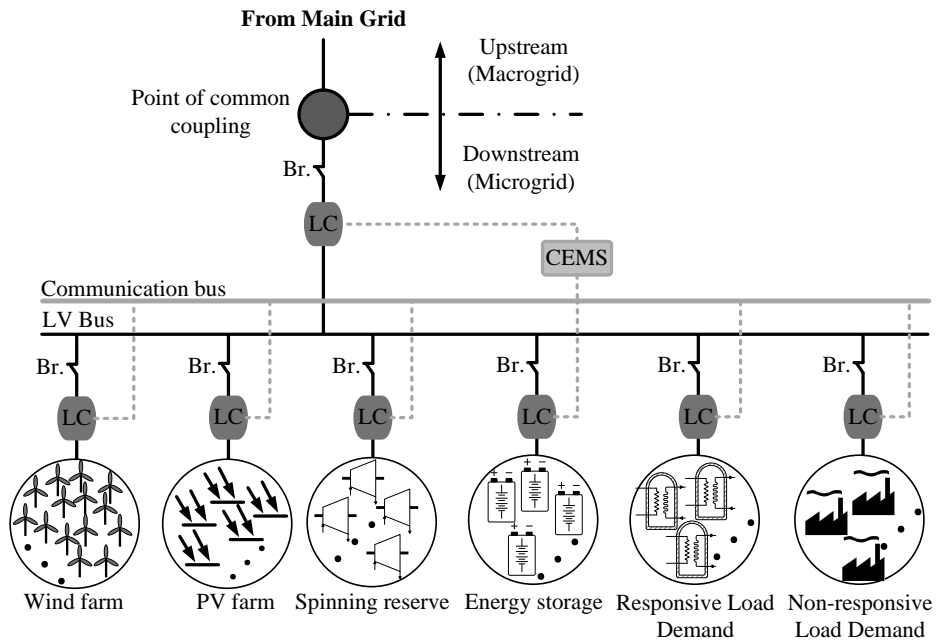
Figure 5.65: Single line diagram of the system under study

Results

In this section the simulation and experimental results resulting from the implementation of the three algorithms are presented. The 24 hour period of the system operation is divided into 4 periods called period 1, period 2, period 3 and period 4 that each period is a six hours period.
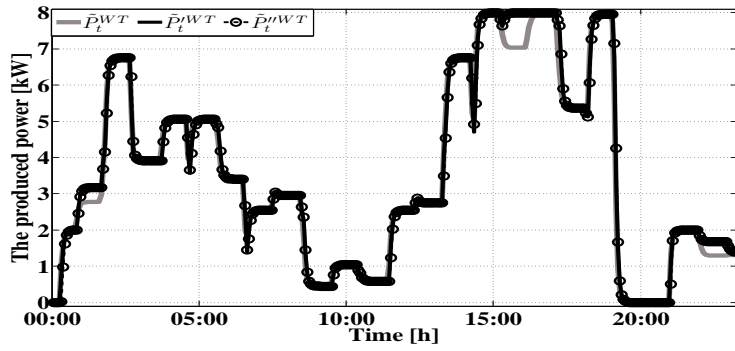
(a) WT emulator
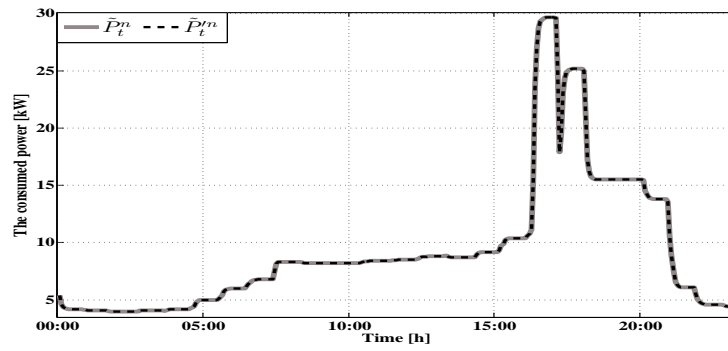
(b) NRL emulator
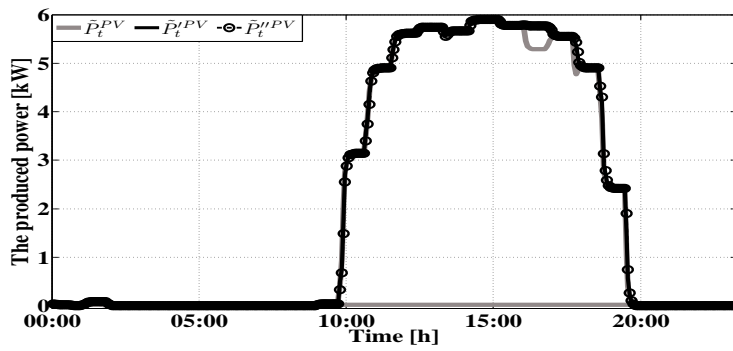
(c) PV emulator

Figure 5.66: The power generated and consumed by each of the WT, PV and NRL emulators in each time interval

Table 5.6: The price offers presented by generation units, consumers and purchasing/ selling electricity from/ to the national grid tariff [€/kWh]

π^{WT}	π^{PV}	π^{MT}	π^{ES-}	π^{ES+}	π^{UP}	π^{RLD}	π^{GRID+}	π^{GRID-}
0.083	0.1	0.17	0.155	0.125	1.5	0.118	0.115	0.140

SOC and ES are shown respectively in Figure 5.67 and 5.68. In the $EOS-MINLP$ and $EOS-MACO$ algorithms the value of SOC at the end of period 1 is reached its maximum value. However, in the $EOS-MGSA$ algorithm its value is about 73%. In the $EOS-MINLP$ algorithm mainly the value of ES charge is supplied through the generated power MT because MT during the period 1 is always in service with the power $\underline{P}^{MT}$. ES in the $EOS-MINLP$ algorithm during the period 00:00-04:30 is operated in the ideal mode. A major part of the power generated by MT (about 74%) is also used during this time interval for feeding RLD and the rest is spent to feed the grid. MT in the $EOS-MACO$ algorithm is put completely out of service during period 1. SOC in the $EOS-MACO$ algorithm is stayed in the value $\overline{SOC}$ until 17:00. At this moment, after the occurrence of scenario 2, ES starts discharging until the power required by the load is supplied. Because before the occurrence of scenario 2, the value of SOC_t'' is reached about $\underline{SOC}$, so is purchased more power for feeding its required load. Using ES in the three algorithms during the time period of the occurrence of scenario 3 (19:30-21:00) is completely different. Noting that SOC in the $EOS-MGSA$ algorithm during this time period is equal to $\underline{SOC}$, so the power supply required by this algorithm is supplied by the national grid. In this algorithm a main part of the power is supplied by MT then the rest of the required power is supplied by the main grid. In the $EOS-MACO$ algorithm this trend is exactly the opposite. That is a major part of the requested power is supplied by the main grid, then the rest is supplied by MT and ES. Furthermore, in the $EOS-MINLP$ algorithm by noting that SOC is equal is equal to $\overline{SOC}$ so part of the load power is supplied by ES and also MT enters in service with the generation capacity $\underline{P}^{MT}$ and only a negligible part of the required power is purchased from the grid. At the end of period 4, the value of SOC_t is a little more than SOC_I while in the heuristic algorithms is almost equal to $\overline{SOC}$. So, in the $EOS-MINLP$ algorithm the reliability of the system for supplying it by ES for the next day in the isolated mode is much less than the other algorithms.

MT power profile is shown in Figure 5.69. Using MT in the $EOS-MACO$
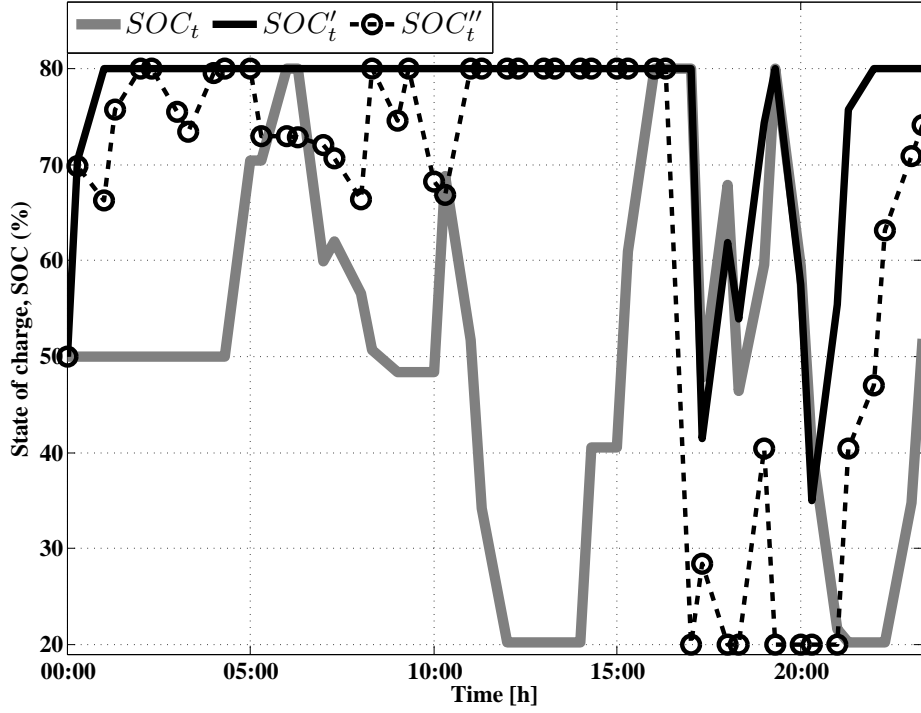
Figure 5.67: SOC during system daily operation

algorithm is only 12.5% during system daily operation and the algorithm in about 77% of the times is preferred to purchase from the grid its required power. This is while in the $EOS - MGSA$ algorithm the participation of MT and the main grid in supplying load demand is respectively about 48% and 65%. This algorithm is preferred to use these resources in a ratio close to each other. The percent of participation of these resources in the $EOS - MINLP$ algorithm is also respectively 75% and 46%. The percent of participation of MT in this algorithm is increased significantly the reason is that in this ES algorithm it has less participation in supplying the power required by the load. MT in the $EOS - MACO$ algorithm during the occurrence of scenario 2 and 3 is operated mainly with the power $\underline{P}^{MT}$ and is purchased most of its required power from the grid. in other algorithms much less power is purchased from the grid and MT is come to service with more capacity.

TCP profile is shown in Figure 5.70. At 36% of the times the value of $P_t'^{TCP}$ is less than the value of $P_t''^{TCP}$ and about 23% of the times is also
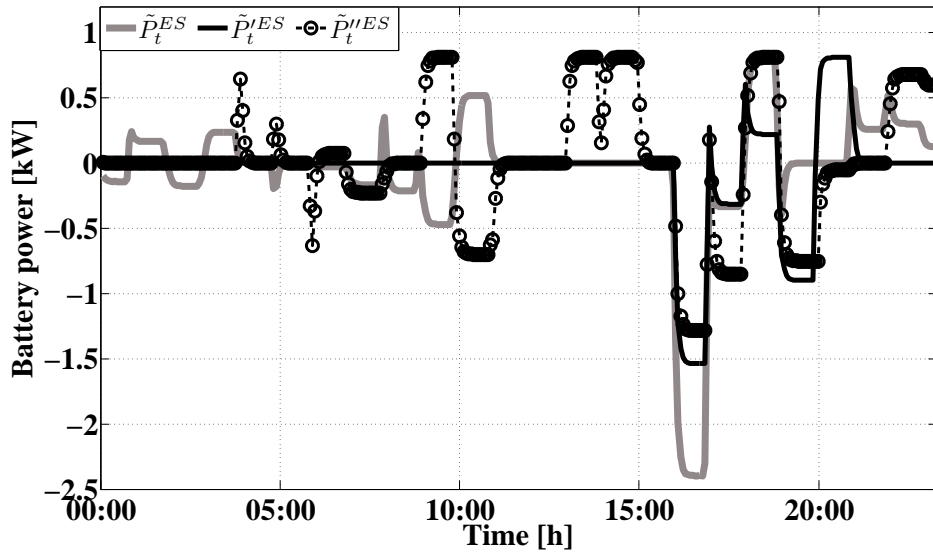
Figure 5.68: ES charge/discharge power during system daily operation
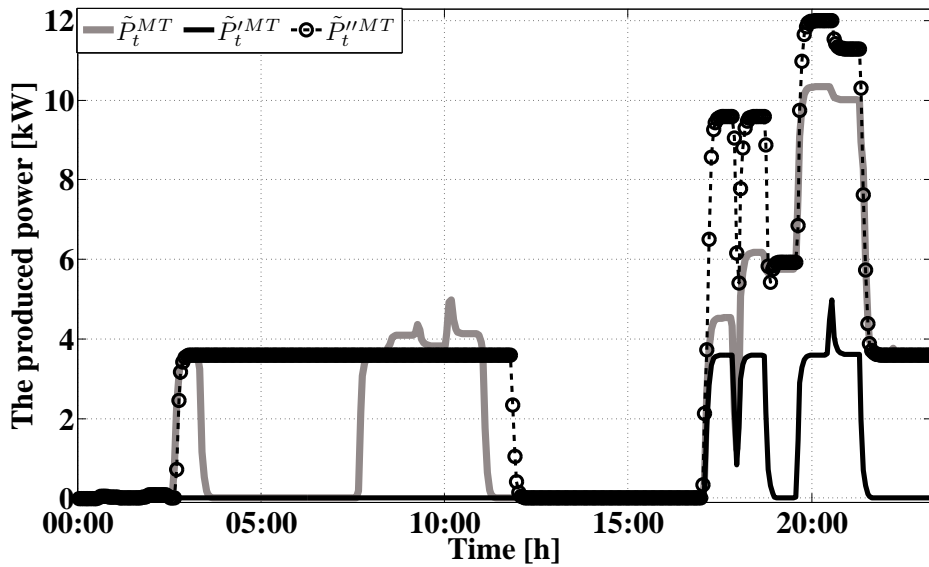
Figure 5.69: ES charge/discharge power during system daily operation

opposite of this case. Also, about 48% of the times the value of $P_t'^{TCP}$ is less than P_t^{TCP} and about 17% of the times is also more. During period 1,

174

the value of P_t^{TCP} is always greater than $P_t'^{TCP}$ and $P_t''^{TCP}$. In this period, noting that λ_t^{MCP} has a higher value relative to the periods 2 and 3, so the algorithm with the increase of the consumed load takes step for increasing more profit for the owner of the MG. While, the heuristic algorithms follow the strategy of reducing the cost of consumed electricity for the consumers.

During the period 20:30 to 21:30 the value of $P_t'^{TCP}$ is more than the value of TCP in the other algorithms. During this time interval the average value of $\lambda_t'^{MCP}$ is equal to 0.82 €/kWh that shows that more amount of consumers with smaller MCP is fed. In this algorithm the excess power generated is spent on feeding ES so that the situation of SOC improves. Noting that the average of the value of λ_t^{MCP} at period 1 is high as a result the algorithm is decided to keep the average of the value of P_t^{TCP} at the lowest level possible. Gradually a average value of the periods 2 and 3 that the average value of $\lambda_t'^{MCP}$ also decreases, also the average value of P_t^{TCP} is increased. At period 4 because of the occurrence of scenario 2 the average value of P_t^{TCP} is increased significantly. Also, at this time interval, the average value of λ_t^{MCP} is reached its maximum value during daily operation. This trend is also repeated for other algorithms. The statement of this point is essential that the minimum of TCP is at period 1 and belongs to the $EOS - MACO$ algorithm. In this time period the $EOS - MACO$ algorithm is consumed respectively the amount of 34% and 31% relative to the algorithms $EOS - MACO$ and $EOS - MGSA$.

This means that by noting the minimumness of MCP in this time interval, more amount of load in the $EOS - MINLP$ algorithm is fed with less cost relative to other value of MCP is obtained for each of the three algorithms at period 4. In this period, the average value of TCP in the $EOS - MACO$ algorithm is about 5.6% more than the other algorithms.

The bargraph related to charge/discharge power of ES, purchasing from the grid or selling to the grid, RLD load, UP and EGP are shown in Figure 5.71. As it is observed from the figure, more P_t^{EGP} power at period 1 for feeding RLD and selling to the national grid is generated. Its reason is that, MT in the $EOS - MINLP$ algorithm during this time interval is always in service and EGP is spent feeding these loads. Although the average value of λ_t^{MCP} at period 1 is more than the periods 2 and 3, however $EOS - MINLP$ algorithm is generated about 55% of its EGP power at this period that 78% of it is spent feeding RLD. Feeding EGP power in period 3 is another way. In this period, about 36% of EGP power is spent on selling to the national grid. As it is observed from Figure 5.71(a), at periods 2 and 4 the algorithm is purchased power from the grid. Noting the lowness of the average value of λ_t^{MCP} in these time intervals, so the operation of the algorithm is adequate.

175
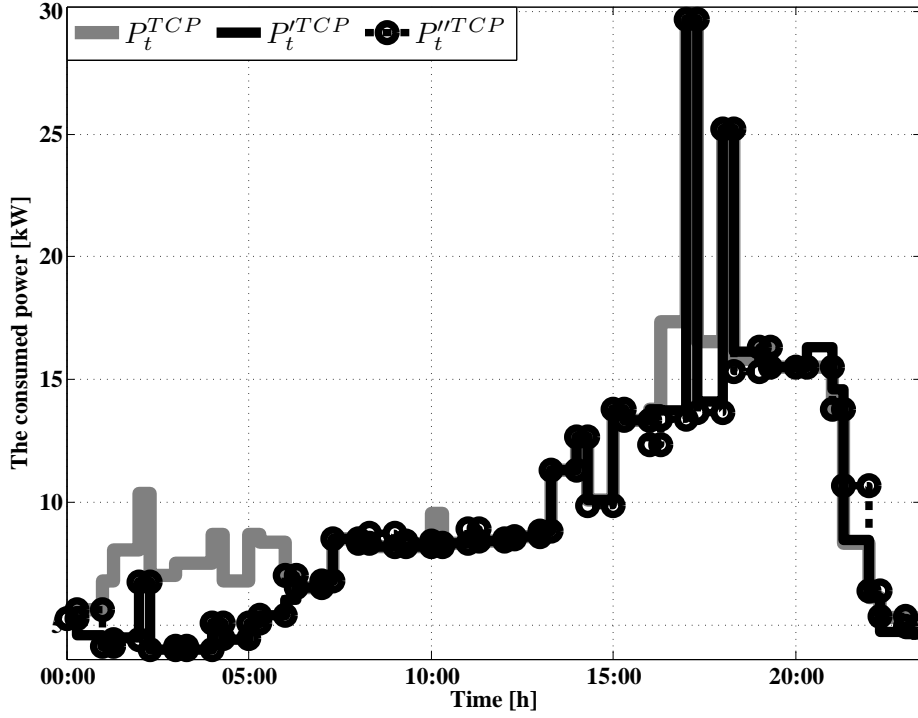
Figure 5.70: Total consumed power during system daily operation

As it is observed from Figure 5.71(b), the EGP power is reduced significantly about 42% relative to the $EOS - MINLP$ algorithm. Meanwhile, about 74% of this power at period 3 which is the average value of $\lambda_t'^{MCP}$ equal to 0.4 €/kWh, is generated that about 77% of this value is spent selling to the national grid. In the $EOS - MACO$ algorithm the purchased power from the network is reduced about 24%, the power generated by MT is reduced about 13% and the discharge ES power is reduced about 57% and finally also the amount of consumed load is reduced 8.5%. As a result in the $EOS - MACO$ algorithm, generation and demand side management is taken place simultaneously in a proper manner. The sold power to the grid is increased about 76% relative to the $EOS - MINLP$ algorithm. As it is observed from Figure 5.71(c) similar to the $EOS - MACO$ algorithm the value of EGP in the $EOS - MGSA$ algorithm is reduced significantly (about 53%, 83%). As it is observed from this figure, only at 16:30 the algorithm is sold a part of the excess power to the grid and at the rest of the times mainly this power is spent feeding RLD. At period 4 in which scenarios 2

176

Table 5.7: The average value of MCP in each 6 hours system operation

Period 1	Period 2	Period 3	Period 4	
0.43	0.41	0.38	0.48	λ_t^{MCP}
0.30	0.41	0.40	0.50	$\lambda_t'^{MCP}$
0.26	0.38	0.43	0.51	$\lambda_t''^{MCP}$

and 3 occur, the $EOS - MGSA$ algorithm is mainly purchased the amount of its power shortage from the main grid. The $EOS - MGSA$ algorithm similar to $EOS - MINLP$ algorithm is supplied about 75% of its power shortage through MT but in the $EOS - MACO$ algorithm this fact is the opposite.

The value of MCP is shown in each interval in Figure 5.72. The average value of MCP is also mentioned for each of the three algorithms in Table 5.7. The value of $\lambda_t'^{MCP}$ in about 71% of time intervals is less than the value of λ_t^{MCP}. Under these conditions, about 16.7% of the times also the value of $P_t'^{TCP}$ is obtained greater than the value of P_t^{TCP}.

This means that, more consumers with lower MCP is fed. The value of $\lambda_t''^{MCP}$ is also obtained about 56% of the times less than the value of λ_t^{MCP}. Under these conditions, the value of $P_t''^{TCP}$ has become about 15% greater than P_t^{TCP}. During the period of occurrence of scenario 2, the value of $\lambda_t''^{MCP}$ is less than the value of MCP of similar time in the other algorithms. During the time interval 17:00-17:30 the value of $\lambda_t'^{MCP}$ is less than the value of λ_t^{MCP} this is while in the time interval 18:00-18:30 these conditions are become the opposite. The value of $\lambda_t'^{MCP}$ during the occurrence of scenario 3 is less than the value of MCP in the two other algorithms. This fact shows that in this algorithm when the renewable resources go out of service the value of electricity generation cost in the $EOS - MINLP$ algorithm has become much more than the other algorithms.

5.2.2 The comparison between $EMS - MINLP$ and $EMS - MPSO$ algorithms

In this section, a CEMS for implementing the algorithms $EMS - MINLP$ and $EMS - MPSO$ has been suggested as shown in figure 5.73. CEMS that is indeed a central control and receives the information related to each micro-
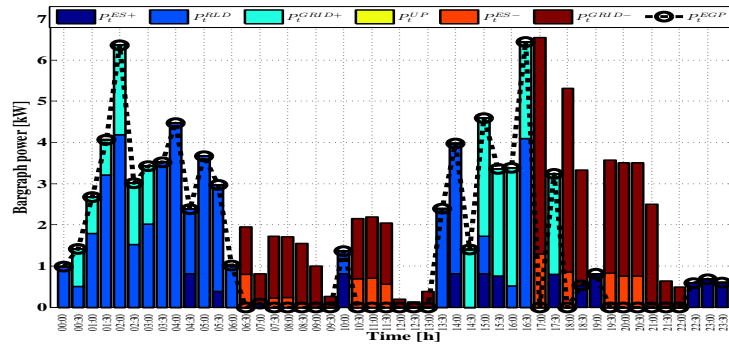
(a) $EOS - MINLP$
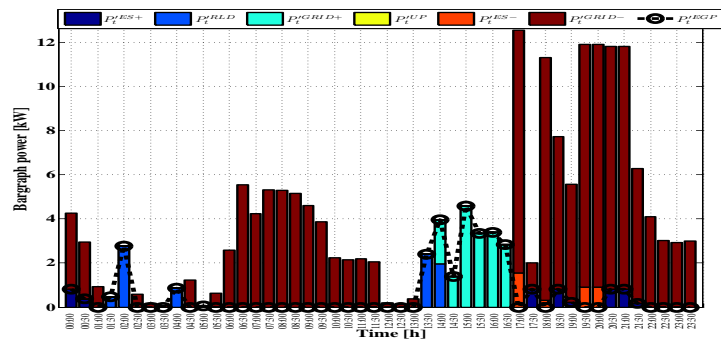
(b) $EOS - MACO$
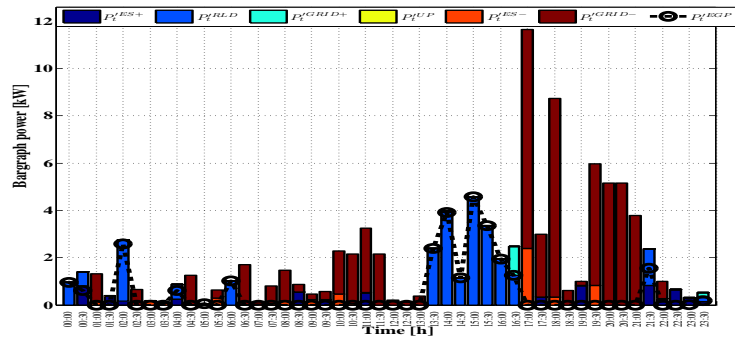
(c) $EOS - MGSA$

Figure 5.71: The baragraph related to RLD, ES (Charging/ discharging), grid (selling/buying) and UP during system performance
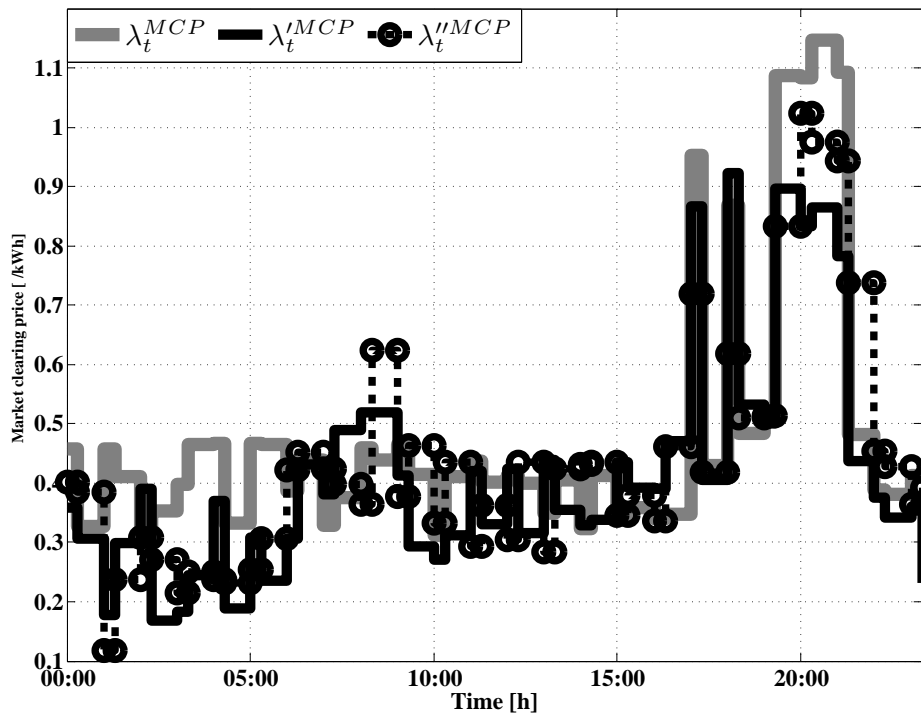
Figure 5.72: MCP in every time interval during system daily operation

source including the generated instantaneous power also the price offer as an information package. Also, it receives the amount of power needed in each instant from the consumers. By noting to the EMS algorithm that has been implemented in the CEMS unit, the optimum values for the micro-sources also consumers in each time interval will be sent. The suggested system must be able to provide the necessary conditions for managing other resources by considering the best optimum performance and the least expense after the occurrence of each incident in the system. In addition to generation side management, the suggested system is able to perform load side management also by using DR management can feed the UP by using the presented mathematical model. In the investigated system, the data of WT, PV and main load from the real networks are measured by the IREC Company.
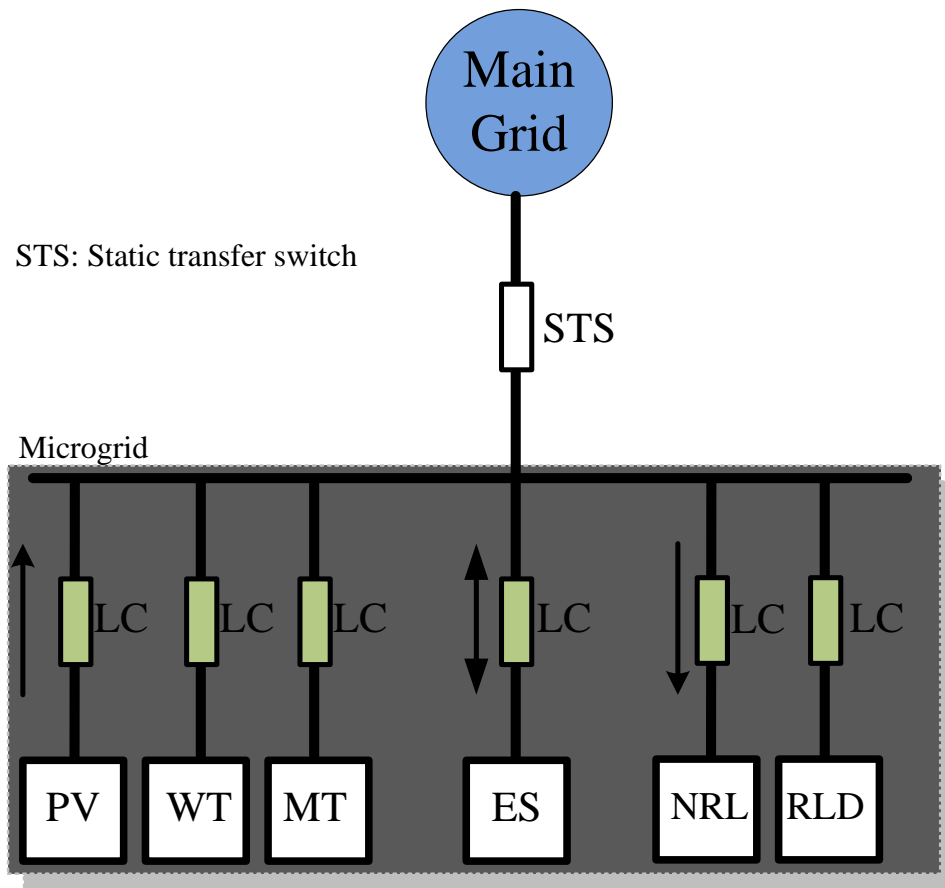
Figure 5.73: The suggested structure for implementing the control system

Results

In this section, the experimental and simulation results are presented resulting from the implementation of the three algorithms. The duration of the 24h system operation is divided to 4 periods called period 1, period 2, period 3 and period 4 that each period is a 6 hours duration.

SOC and ES are shown respectively in Figures 5.74 and 5.75. In both of the algorithms the value of SOC at the end of period 1 is reached its $\overline{SOC}$. in the $EMS - MINLP$ algorithm mainly the value of charge ES is supplied through the generated power MT because MT during the period 1 has always been in service with the power $\underline{P}^{MT}$. ES in the $EMS - MINLP$ algorithm during the period 00:00-04:30 is operated in the ideal mode. A

major part of the generated power by MT (about 74%) is also used during this time interval for feeding RLD and the rest is spent feeding the grid. MT in the $EMS - MPSO$ algorithm is completely out of service. SOC in the $EMS - MPSO$ algorithm is until 17:00 stayed at the value $\overline{SOC}$. At this moment, after the occurrence of scenario 2, ES is started discharging until the required power by customers is supplied.

Using ES in the two algorithms during the time period of the occurrence of scenario 3 (19:30-21:00) is completely different. In the $EMS - MPSO$ algorithm a major part of the required power is supplied by the main grid, then the rest is supplied by MT and ES. In the $EMS - MINLP$ algorithm also by noting that SOC is equal to $\overline{SOC}$ so part of the power is supplied by ES also MT is entered service with the generation capacity $\overline{P}^{MT}$ and only a negligible part of the required power is purchased from the grid. At the end of period 4, the value of SOC_t is a littlie more than SOC_I while in the heuristic algorithm is reached the value $\overline{SOC}$. Therefore, in the $EMS - MINLP$ algorithm the reliability of the system for supporting it by ES for the next day in the isolated mode is much less than $EMS - MPSO$ algorithm.
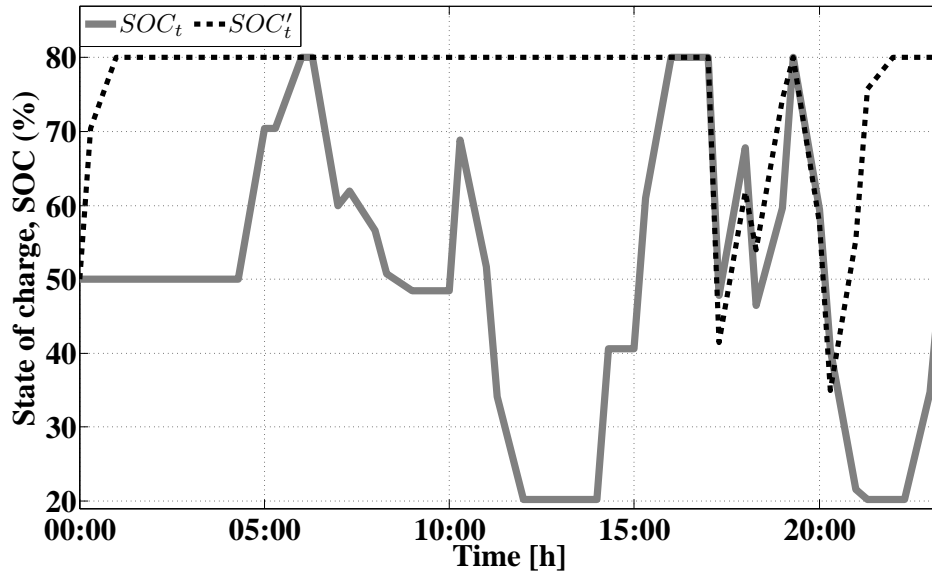
Figure 5.74: SOC during system daily operation

MT power profile is shown in figure 5.76. Using MT is about 12.5% and purchasing the required power from the upstream grid is about 77% in the
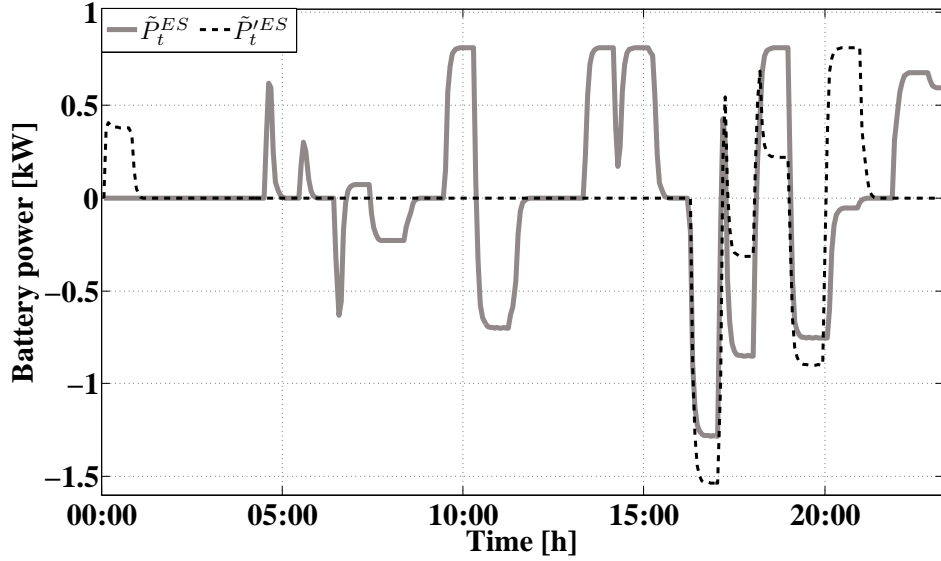
Figure 5.75: ES charge/ discharge power during system daily operation

$EMS - MPSO$ algorithm and this ratio in the $EMS - MINLP$ algorithm is respectively 75 and 46 percent. The percentage of MT participation in the $EMS - MINLP$ algorithm is significantly increased. Its reason is that in this algorithm ES has less participation in supplying the required power by the load. MT in the $EMS - MPSO$ algorithm is mainly entered service with the power $\underline{P}^{MT}$ and purchases most of its required power from the grid. In other algorithms a power much less from the grid is purchased and MT is entered service with more capacity.

TCP profile is shown in Figure 5.77. About 48% of the times also the value of $P_t'^{TCP}$ is less than P_t^{TCP} and about 17% of the times is also greater. At period 1, the value of P_t^{TCP} is always greater than $P_t'^{TCP}$. At this period, noting that λ_t^{MCP} has a higher value relative to the periods 2 and 3, so the algorithm with the increase of consumed load steps for increasing more profile for the Microgrid owner. While the heuristic algorithms follow the strategy of reducing the consumed electricity cost for the consumers. During the period 20:30-21:30 the value of $P_t'^{TCP}$ is more than the value of TCP in the other algorithm. During this time interval the average value of $\lambda_t'^{MCP}$ is equal to 0.82 €/kwh that shows that more amount of consumers are meet with smaller MCP. In this algorithm the excess generated power (EGP) is spent on feeding ES so that the situation of SOC improves. Noting that

182
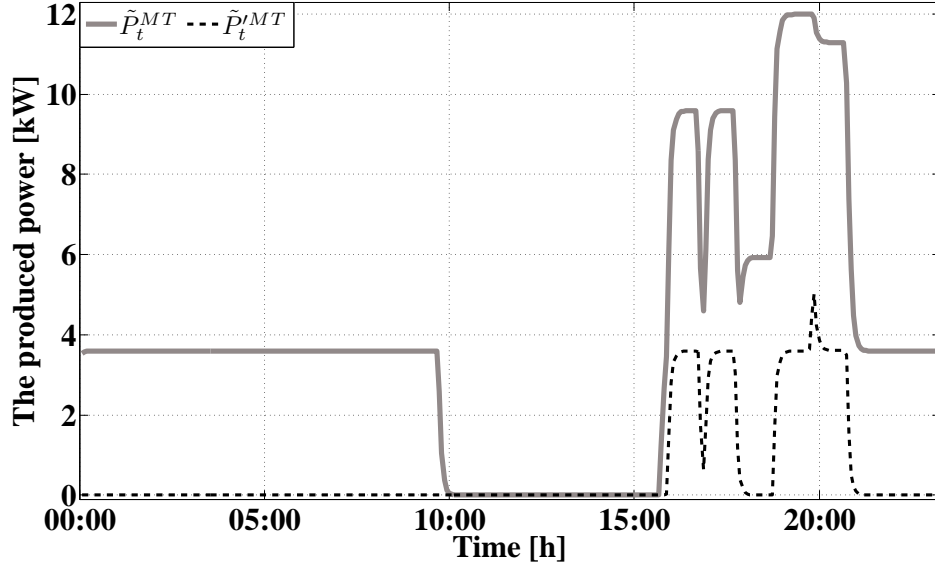
Figure 5.76: The power generated by MT during system daily operation

the average value of λ_t^{MCP} at period 1 is high as a result the algorithm is decided to keep the average of the value of P_t^{TCP} during this period at the lowest possible level. Gradually at the periods 2 and 3 in which the average value of λ_t^{MCP} also reduces, the average value of P_t^{TCP} is also increased. At period 4 because of the occurrence of scenario 2 the average value of P_t^{TCP} is significantly increased. Likewise, in this time interval, the average value of λ_t^{MCP} is reached its maximum value during daily operation. This trend is also repeated for other algorithm. The statement of this point is essential that the minimum TCP is at period 1 and belongs to the $EMS - MPSO$ algorithm. In this time period the $EMS - MINLP$ algorithm is respectively consumed 34% more TCP relative to the $EMS - MPSO$ algorithm. This means that by noting the minimumness of MCP in this time interval, more load in the $EMS - MINLP$ algorithm is supplied relative to other algorithm. The maximum value of the average of MCP is also obtained for each of the three algorithms at period 4. In this period, the average value of TCP in the $EMS - MPSO$ algorithm is about 5.6% more than the other algorithm.

The bargraph related to ES charge/discharge power, purchasing from the grid or selling to the grid, RDL, UP and EGP load are shown in Figure 5.78. As it is observed from the figure, more P_t^{EGP} power is generated at period
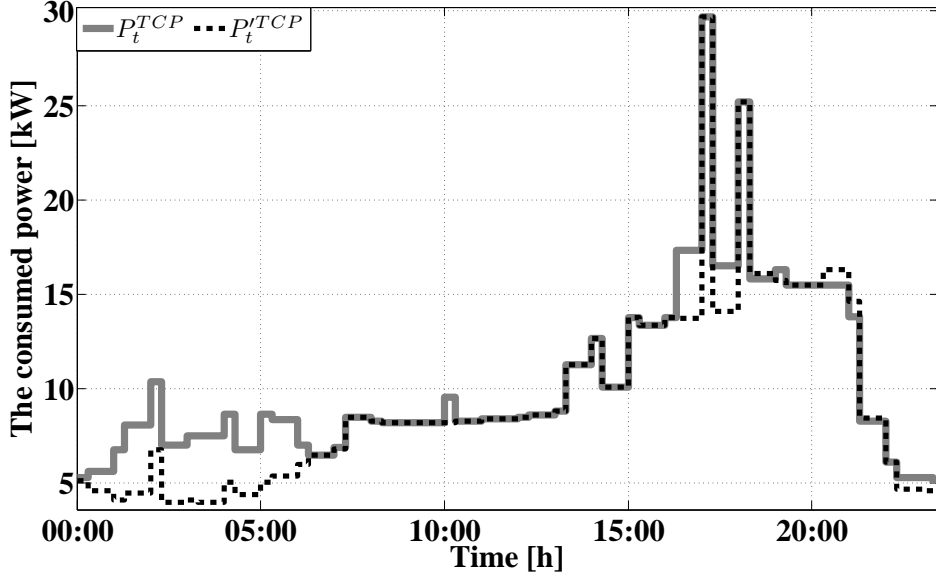
Figure 5.77: TCP during system daily operation

1 for feeding RLD and selling to the main grid. The reason is that, MT in the $EMS-MINLP$ algorithm is always in service during this time interval and EGP is spent feeding these loads. Although the average value of λ_t^{MCP} at period 1 is more than periods 2 and 3, however the $EMS-MINLP$ algorithm is generated about 55% of its EGP power at this period that 78% of it is spent feeding RLD. Feeding the EGP power at period 3 is in another way. In this period, about 36% of EGP power is spent selling to the main grid. As it is observed from Figure 5.78(a), at periods 2 and 4 the algorithm is purchased power from the grid. Noting the lowness of the average value of λ_t^{MCP} in these time intervals, so the performance of the algorithm is adequate. As it is observed from Figure 5.78(b), the EGP power is significantly reduced about 42% relative to the $EMS-MINLP$ algorithm. Meanwhile, about 74% of this power at period 3 that the average value $\lambda_t'^{MCP}$ is equal to 0.4 €/kWh is generated that about 77% of this value is spent selling to the main grid. In the $EMS-MPSO$ algorithm the power purchased from the grid is about 24%, the power generated by MT is about 13% and the power discharge ES is reduced about 57% and also finally the consumed load is also decreased 8.5%. As a result, in the $EMS-MPSO$ algorithm, generation and demand side management is taken

place simultaneously is a proper manner. The power sold to the grid is increased about 76% relative to the $EMS - MINLP$ algorithm.
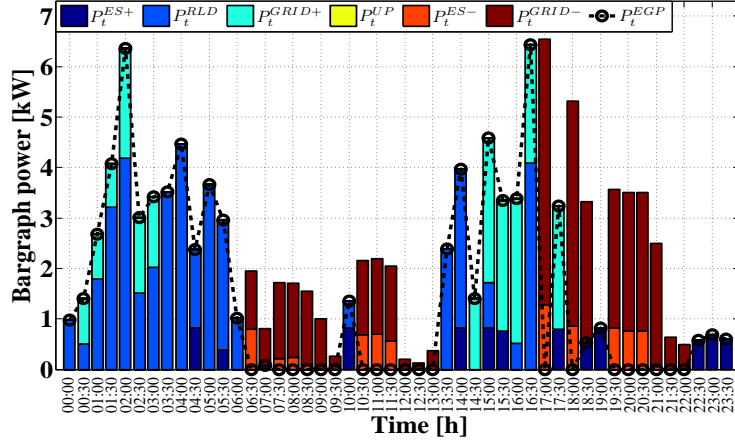
(a) $EMS - MINLP$
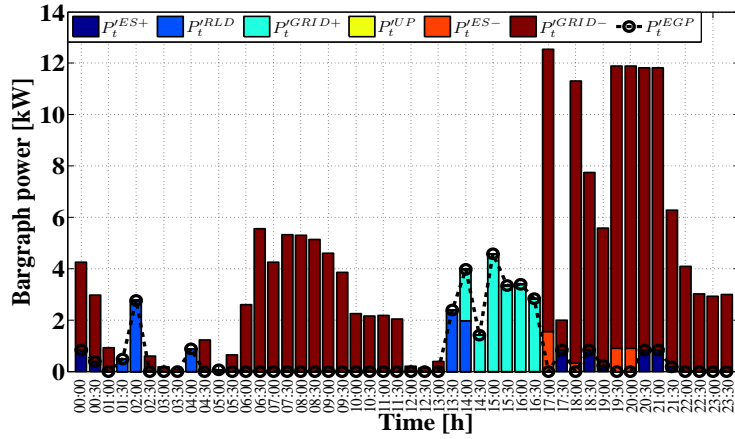
(b) $EMS - MPSO$

Figure 5.78: Bar graph related to power ES during the performance of charging and discharging mode, DR, UP and EGP

The value of MCP is shown in each interval in Figure 5.79. The average value of MCP is also mentioned for each of the three algorithms in Table 5.8. The value of $\lambda_t'^{MCP}$ at about 71% of the time intervals is smaller than the value of λ_t^{MCP}. Under these conditions, at about 16.7% of the times also the value of $P_t'^{TCP}$ is obtained greater than the value of P_t^{TCP}. This means

185

Table 5.8: The average value of MCP in each 6 hours system operation

Period 1	Period 2	Period 3	Period 4	
0.43	0.41	0.38	0.48	λ_t^{MCP}
0.30	0.41	0.40	0.50	$\lambda_t'^{MCP}$

that, more consumers is supplied with lower MCP. During the time interval 17:00-17:30 (occurrence of scenario 2) the value of $\lambda_t'^{MCP}$ is less than the value of λ_t^{MCP}. This is while in the time interval 18:00-18:30 (the occurrence of scenario 2) the conditions have become the opposite. The value of $\lambda_t'^{MCP}$ during the occurrence of scenario 3 is less than the value of MCP in both of the other algorithm. During this time interval, the value of MCP in the $EMS - MINLP$ algorithm is greater than its value in the other algorithms. This fact shows that in this algorithm by putting the renewable sources out of service the value of electricity generation cost in the $EMS - MINLP$ algorithm has become much more than the other algorithm.
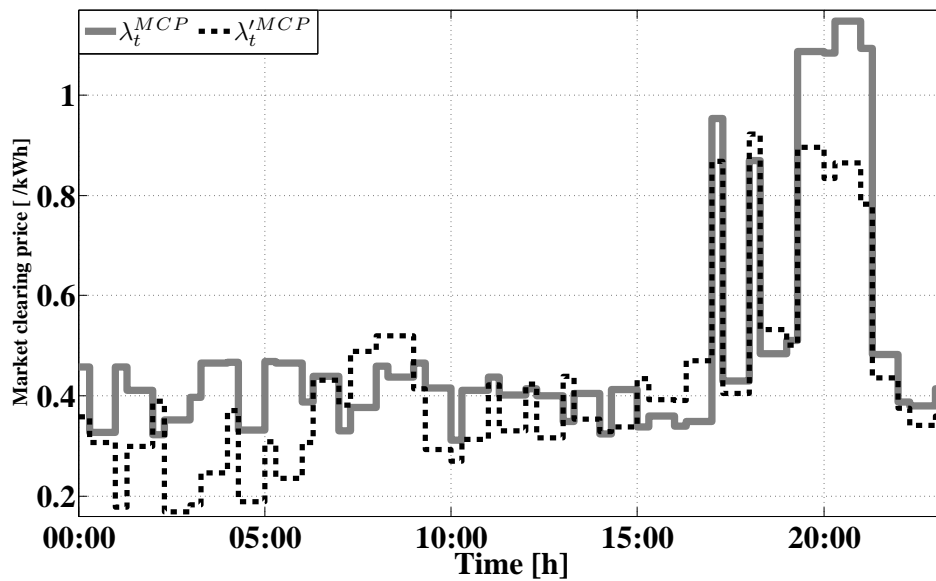
Figure 5.79: MCP in each time interval during system daily operation

5.2.3 The comparison between $EOS - MINLP$ and $EMS - MICA$ algorithms

The single line IREC's MG structure is shown in Fig. 5.80. The power profile related to renewable devices (PV and WT in this study) and also the power consumed by the non-responsive load (NRL) is also obtained from [2] as shown in Figs. 5.81(a) to 5.81(c). the value of the optimum power determined by the algorithm in each time interval is also shown in these figures. The price offer related to the renewable generators, non-renewable generators, non-responsive load and the penalty resulting from unmet power (UP) are mentioned in Table 5.6 [2,3].
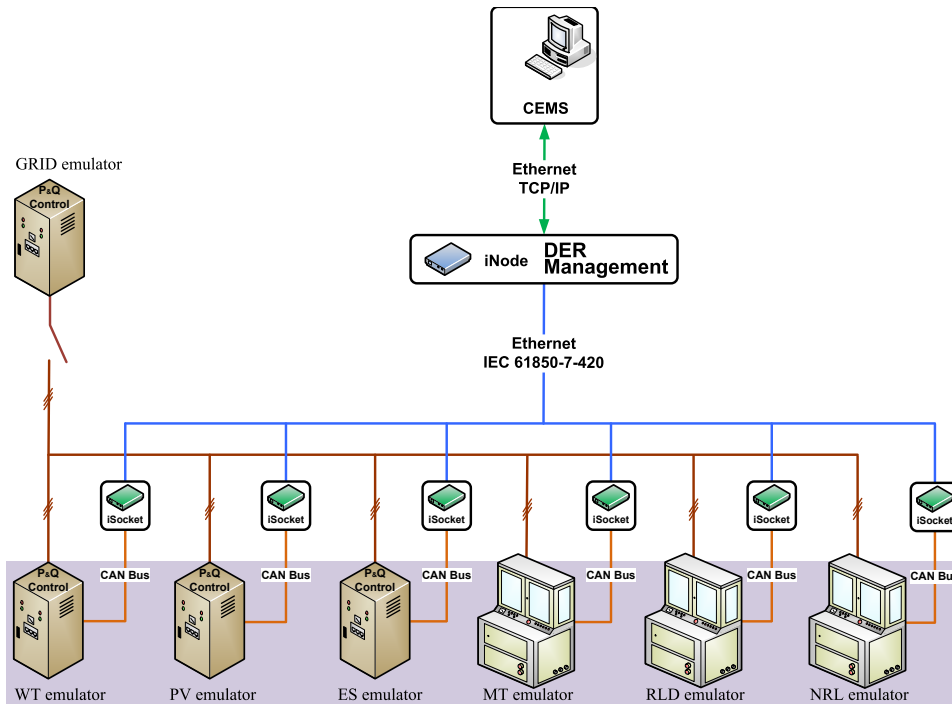
Figure 5.80: Schematic of the MG system under study

Results

SOC and ES have been shown for both algorithms in Figures. 5.82 and 5.83 respectively. During period 1, ES in the EMS-MICA algorithm starts charging and after 04:00 o'clock reaches the $\overline{SOC}$ value and stays in the same value until the end of this period. This is while ES in the EMS-MINLP

187

algorithm has stayed at the SOC_I initial value until 05:00 o′clock. Then, at this moment starts charging and at the end of period 1 has reached the value $\overline{SOC}$. During period 1, MT in the EMS-MINLP algorithm always generated power with the power $\underline{P}^{MT}$ and ES has no participation in supplying the power required by the NRL load. The greater part of the excess power generated by MT has also been spent on feeding RLD and the total RLD load value in this algorithm has been estimated about 86% more than its value in the EMS-MICA algorithm during period 1. Noting the higherness of RLD offer relative to ES, as a result the EMS-MICA algorithm has decided to spend EGP on feeding ES. So that in addition to reducing the consumed cost for the intervals, ES has had more change for the time intervals in itself. During this period, MT is out of service at the rest of the times except at 00:00 o′clock. During period 2, ES in the EMS-MICO algorithm starts discharging only at a stort interval and again returns to the charging mode such that at the end of period 2 its SOC value reaches $\overline{SOC}$. MT is in service in this algorithm until 19:00 o′clock and its power shortage is compensated by it. This is while that ES has operated in the ideal mode until this moment. But after this time, MT has turned off and the power shortage has been supplied by ES. This is while that, MT in the EMS-MINLP algorithm has continued its generation with the power $\underline{P}^{MT}$ and has gone out of service at 10:30. At this instance ES starts discharging and until the end of period 2 operates in this mode until the value of its SOC reaches $\underline{SOC}$. During period 3 SOC'_t stays at its same value (that is $\overline{SOC}$) and the algorithm fulfils its power shortage even during the occurrence of scenario 2 through MT. In the EMS-MINLP algorithm after a period of charging ES, during the occurrence of scenario 2 ES starts charging and its value stops until 46% at the end of this period. During period 3, ES in the EMS-MICA algorithm has no role in supplying the required power and its value stops at this period until 46%.

During period 3, ES in the EMS-MICA algorithm has no role in supplying the required power and power shortage has been supplied by MT and or purchasing from the national grid. while, ES in the EMS-MINLP algorithm has a more colorful role relative to the national grid and only a negligible part of the power shortage has been purchased from the national grid. As it is observed from Figure 5.83, at the end of the 24 hours system operation, SOC'_t has become 28% more than SOC_t. So, ES has more charge for using the next day in case of need. By the analysis done it has been determined that the average value of is about 77% that is about 36% more than the average value during the system daily operation. So, in the EMS-MICA algorithm by the better charging of ES if the system is put in the isolated

mode it tries to increase the system ability in supporting the load.

MT power profile has been shown in Figure 5.84. As it is observed from the figure, MT in the EMS-MINLP algorithm is in service 75% of the times while this value in the EMS-MICA algorithm has reduced to 35%. Noting the lowerness of π^{GRID-} offer relative to π^{MT} the EMS-MICA algorithm has as a result tried to compensate its power shortage through the national grid so the result of this action is the general reduction in generation cost and also the improvement of ES profile by this algorithm. As it is observed from the figure, MT in the EMS-MICA algorithm is mainly out of service during the periods 1 and 2 and has purchased from the national grid. This is while that in the EMS-MINLP algorithm, MT is in service during all of period 1 and part of period 2 is always in service with the power $\underline{P}^{MT}$ and during these time intervals has not purchased power from the national grid. During the occurrence of scenario 2, P_t^{MT} is 36% greater than $P_t'^{MT}$ and the average value of $P_t'^{GRID-}$ power has been obtained about 51% more than the average value of P_t^{GRID-} at this time interval. This fact is also true for scenario 3. During the occurrence of this scenario, the average value of P_t^{MT} has become 21% more than the average value of $P_t'^{MT}$ and as a result the purchased power has also become less than its value in the EMS-MICA algorithm (about 54%). Mentioning this point has special important because noting the highness of the average value of MCP at period 2 and 3 so need for feeding the consumers with sources with lower price offer is felt more than before. For reaching this goal, EMS-MICA algorithm has been pioneer by noting the lowerness of π^{GRID-} offer relative to π^{MT} offer in this field.

National grid power profile has been shown in Figure 5.85. As it is observed from the figure, at period 1, this profile is completely different in both of the algorithms. Although in the EMS-MINLP algorithm it has been tried to sell power to the national grid (about 46% of the time) however 62% of the times EMS-MICA algorithm has purchased electricity from the national grid. Noting that the average value of $\lambda_t'^{MCP}$ has its minimum value during the system daily operation, so purchasing electricity from the national grid is a proper act in this time interval and will cause the profit increase for the owner of the Microgrid. At period 2 no power is sold to the national grid by the two algorithms and the EGP power is mainly spent feeding RLD and or ES. In this time interval, at 85% of the times EMS-MINLP algorithm has supplied its power shortage from the national grid. This value in the EMS-MICA algorithm has reached 92% of the value and the algorithm has tried to reduce the share of MT in supplying the load demand. Because the average value of MCP has increased in this time interval and so the algo-

rithm must be searching for power source with lower price offer for reducing its production cost. At period 3, EMS-MINLP algorithm has tried more to sell more power to the national grid (about 46%) so that spends this excess power on feeding RLD.

During this period this algorithm by noting the increase of MCP and also by considering this fact that the offer of π^{GRID+} is lower than π^{RLD}, so by selling more EGP power to the national grid has tried to consider feeding consumers with lower price. This is while the EMS-MICA algorithm has gone through on opposite trend. At 77% of the times the EGP power has been spent feeding RLD and a negligible part of it has been sold to the national grid.

As a result more profit for the owner of the Microgrid has been considered more in this algorithm. At period 4 noting the highness of MCP, power has been purchased from the national grid in both of the algorithms. In this time interval, MT in the EMS-MICA algorithm has generated about 32% less power relative to the other algorithm this is while the power purchased from the national grid in this algorithm has increased about 64%. Noting the difference between the π^{GRID-} offer and π^{MT} and the profit increase policy for the owner of Microgrid and the cost reduction for the consumers, this trend is the best choice by the EMS-MICA algorithm.

TCP power profile has been shown in Figure 5.86 for both of the algorithms. At period 1 at all the times the value of P_t^{TCP} has become more than the value of $P_t'^{TCP}$. Noting the highness of the average value of λ_t^{MCP} relative to $\lambda_t'^{MCP}$ in this time interval, so the EMS-MINLP algorithm has fed more consumer with higher price. At periods 2 and 3, TCP in both of the algorithms have almost followed similar model. Suddenly at 16:30 to 17:00 the value of P_t^{TCP} has become more than $P_t'^{TCP}$ that this fact is because MT has entered service with the power $\underline{P}^{MT}$ and the feeding of excess power to RLD and national grid. At this time interval, the value of MCP in both of the algorithms is equal so the EMS-MINLP algorithm has fed more consumers with equal price at this time interval. These conditions have also occurred in the time interval 17:30-18:00. In this time interval the value of λ_t^{MCP} is more than $\lambda_t'^{MCP}$ and MT in the EMS-MINLP algorithm has entered service similar to the previous case with the power $\underline{P}^{MT}$ and the EGP power has caused the charging of ES with the power $\overline{P}^{ES+}$ and the rest of EGP power has been sold to the national grid. While the EMS-MICA algorithm has purchased its required power from the national grid and in addition to supplying NRL has also fed NRL a very negligible amount.

Also at period 4 at 31% of the times P_t^{TCP} has become greater than $P_t'^{TCP}$.

Because in this time interval, the value of MCP in both of the algorithms has its maximum value so the EMS-MINLP algorithm despite this fact, has fed more consumers in this time interval. This fact states that the cost of feeding the consumers has increased severely relative to the EMS-MICA algorithm.

The bar Graph related to ES power, RLD, UP, GRID, and EGP has been shown in Figure 5.87 for both of the algorithms. As it is observed from Figure 5.87(a) the EMS-MINLP algorithm has spent most of the EGP power on feeding RLD. Also, GRID has allocated a significant share of EGP power to itself. The reason is that the algorithm has always put MT with the power $\underline{P}^{MT}$ in service and has spent the excess power on feeding RLD. However, 78% and 19% of the EGP power have respectively been used for feeding RLD and selling to the national grid.

Noting the lowness of the average value of λ_t^{MCP} in this time interval, although ES has presented higher offer for charging relative to the GRID and RLD, however most of the excess power has been spent feeding RLD. Because MT in the EMS-MICA algorithm is out of service, so much less EGP has been generated relative to the EMS-MINLP algorithm. Under these conditions, the algorithm is after supplying the power required by NRL by considering the reduction of final generation cost. At period 2, gradually the power consumed by NRL has increased as a result the EMS-MINLP algorithm in addition to supplying part of its required power by using MT, has supplied the other part through the national grid. Such that, PV also enters the circuit and by the increase of the power generated by it, gradually MT has exited service. In the EMS-MICA algorithm also the situation is this way with this difference that the power purchased from the national grid is 51% more than the power supplied by MT. Noting the increase of the average value of $\lambda_t'^{MCP}$ in this time interval to period 1, the EMS-MICA algorithm by noting the lowerness of the offer of π^{GRID-} relative to the offer of π^{MT} has decided to supply a greater part of its required power through the national grid. At period 3 always the average value of MCP has increased in both of the algorithms however the performance of the two algorithms for the optimum use of EGP power is different. Despite the highness of the average value of $\lambda_t'^{MCP}$ relative to the periods 1 and 2, however the EMS-MICA algorithm has allocated 79% of the generated EGP power for feeding RLD and the rest has been sold to the national grid. Because SOC in this time interval is equal to $\overline{SOC}$ as a result no share of the EGP power has been allocated for charging ES. In the EMS-MINLP algorithm the share of EGP power for the consumers is 51% for selling to the national grid, 38% for feeding RLD and finally 12% has been used for charging ES. As

it is observed, the algorithm has not only operated by noting the priority of the offer of each of these consumer but also has considered the technical considerations and the constraints considered such as maximum ES charging power, maximum power exchanged between the national grid and Microgrid and etc. At period 4, the shares of the power generated in the EMS-MICA algorithm by the renewable sources, spinning reserve sources, energy storage sources and the national grid for supplying the power required have become respectively 23%, 43%, 1%, and 33% respectively.

The participated of these sources in supplying the required power in the EMS-MINLP algorithm are respectively 24%, 63%, 1% and 12% respectively. As it is observed, the EMS-MICA algorithm at period 4, noting the highness of the average value of MCP in this period, by considering the lower offer of π^{GRID-} relative to π^{MT} has decided, to buy more share of its required power from the national grid relative to the EMS-MINLP algorithm.

In Figure 5.88 the share of each generation unit has been shown for supplying the required power for both of the algorithms. As it is observed from Figure 5.89(a), after midnight part of the load demand has been supplied by renewable resources (REW) (including PV and WT in this study) and another part has been supplied by spinning reserve (SP) (MT in this study). During the start of the day upon the increase of load demand, noting that the power generated by REW has reduced, so part of the required power has been supplied from the national grid.

Since 09:00 o′clock noting that PV has also entered service, so the power generated by REW has increased significantly and a negligible part of the required power has been supplied by SP. Electricity purchase from the national grid has taken place during the periods 06:00-10:00 and also 18:00-21:00 by the EMS-MINLP algorithm. During sunset in which the power generated by REW has reduced significantly, so the algorithm has fulfilled its load demand through SR. In the EMS-MICA algorithm it has been tried such that the maximum generated power be used by REW. So during the time period after midnight to the morning, the share of REW in supplying the load demand in this algorithm is much more than the other algorithm. In this time interval SR has no role in generation. The other difference between the two algorithms is in the amount of using SR and national grid for supplying the power required by the load. As it is observed from Figure 5.89(b), the amount of the power supplied through SR during the time interval 19:00-00:00 has become much less and instead the share of national grid that has less π^{GRID-} offer, has increased significantly. As a result, the consumers pay much less MCP for purchasing electricity.

The percentage of the usage of generated excess power for feeding each

Table 5.9: Average MCP value during the 6 hours period of system operation

Period 1	Period 2	Period 3	Period 4	
0.41	0.40	0.47	0.68	λ_t^{MCP}
0.28	0.38	0.45	0.60	$\lambda_t'^{MCP}$

of the consumers including RLD, national grid, and ES have been shown in Figure 5.89. As it is observed from Figure 11a, RLD load in the EMS-MINLP algorithm has been mainly fed at period 1 also a negligible part of it has been fed at period 3. This is while that in the EMS-MICA algorithm this fact is exactly opposite of this state. The share of the excess power generated for selling to the national grid in the EMS-MICA algorithm has been considered much less the other algorithm. Because ES in this algorithm has operated in much less time intervals relative to the EMS-MINLP algorithm in the charging mode, so in this amount has allocated less share of the power generated for charging ES relative to the EMS-MINLP algorithm to itself.

Figure 5.90 Shows the value of MCP for both of the algorithm in each time interval. During system daily operation at 71% of the times the value of λ_t^{MCP} has become greater than $\lambda_t'^{MCP}$.

Significant difference between these two quantities does not exist at periods 2 and 3 and mainly the difference has appeared at periods 1 and 4. The minimum and maximum value of λ_t^{MCP} is respectively equal to 0.28 and 1.09 that at 10:30 (minimum value) also 20:00 and 21:00 (maximum value) has been obtained. During the obtaining of the minimum value of MCP in the EMS-MINLP algorithm, no excess power has been generated and part of the power has been purchased from the national grid. Minimum value of $\lambda_t'^{MCP}$ has been obtained at 03:00 in which all of the power consumed has only been supplied by WT. But the maximum value of $\lambda_t'^{MCP}$ has been obtained during the occurrence of scenario 3 (20:30) and the EMS-MICA algorithm has tried by noting the priority inserted in Table. 5.9, brings MT with less power into service and instead has purchased more power from the national grid.

5.2.4 The comparison between $EMS - MINLP$ and $EMS - MABC$ algorithms

The single line structure of IREC′ MG is shown in Figures 5.73. This system has a central energy management system (CEMS) that receives the information related to all the microsources through an iNode and through a communication link Ethernet TCP/IP. Furthermore, iNode has been connected by using the Ethernet IEC 61850 communication protocol with iSockets that operate as local controller for each emulator. Communication protocol between the iSocket and emulators is of the CAN type. The details related to the specifications of this system and the method of configuration of the present emulators has been presented completely in the previous papers [2, 3]. The power profile related to renewable devices (PV and WT in this study) also the power consumed by Non-responsive loads (NRL) has also been derived from [2] and has been shown in Figure 5.91(a) to 5.91(c). the price offer related to renewable generators, non renewable generators, Non-responsive load demand, purchasing/ selling electricity tariff from/ to the man grid and the penalty resulting from unmet power have been mentioned in Table. 5.6 [2].

Results

SOC and ES power have been shown respectively in Figure 5.92 and 5.93. During the period 1, ES in the EMS-MABC algorithm is first discharged completely and its value reaches $\underline{SOC}$. For compensating the discharged energy in ES, this algorithm in the next interval by bringing MT into service and mainly by purchasing power from the main grid starts charging ES. ES in the EMS-MINLP algorithm has operated in another way. ES in this algorithm is in the ideal mode until 05:00 then MT while fulfilling the required power by the load, part of its power generated also is spent charging ES. At the end of period 1 the value of SOC in both of the algorithms has become equal to $\overline{SOC}$. At period 2, ES in the EMS-MABC algorithm has not changed until 09:30 and respectively 42.6% and 23.5% of the power shortage has been supplied by MT and purchasing from the grid. However, in the EMS-MINLP algorithm in addition to discharging ES, has always brought MT with the power $\underline{P}^{MT}$ into service. In addition, in this algorithm part of the power (about 46%) has been supplied by purchasing from the main grid. The operation of ES in each algorithm in period 3 in which scenario 2 occurs is different. ES in both algorithms at 17:00 operate in the ideal mode and power shortage in the EMS-MABC algorithm is mainly compen-

sated by purchasing from the grid. In this instant, EMS-MINLP algorithm has supplied most of its power shortage through putting MT into service. But at 18:00, part of the power shortage in the EMS-MINLP algorithm has also been supplied by ES then has been respectively fulfilled from MT and purchasing the rest of the required power.

This is while in the EMS-MABC algorithm mainly the full feeding of the load has been supplied by the main load then by using MT. At period 4 also scenario 3 has occurred. During the occurrence of scenario 3, MT in the EMS-MINLP algorithm has entered service with the power $\overline{P}^{MT}$ during this time interval and then part of the power has also been supplied by ES. In this algorithm, the main grid has the responsibility of providing a negligible part of supplying the system required power. But in the EMS-MABC algorithm MT and the main grid has been used and ES is always in the ideal mode. SOC in the EMS-MABC algorithm at them that end of the 24hour system operation has a value much more than the other optimization algorithm that this fact shows that the reliability of the grid by this algorithm is for backing up load in the next day.

MT power profile has been shown in Figure 5.94. As it is observed from the figure, during period 1, MT in the EMS-MINLP algorithm is always operating with the power $\underline{P}^{MT}$. This is while in the EMS-MABC algorithm is only in service 7.7% of the times. During period 2, the participation of MT in supplying the required power in the EMS-MINLP algorithms and EMS-MABC algorithms is respectively about 61.54% and 46.15%. In this case the EMS-MABC algorithm has decided to supply most of its required power (about 77%) through purchasing from the grid. At period 3 (occurrence of scenario 2) the value of participation of MT and the main grid in supplying power in the EMS-MABC algorithm is respectively about 15.3% and 30.7%. This is while in the EMS-MINLP algorithm this participation is exactly the opposite. During this period, the average values of MCP in both of the algorithms are equal to each other.

Noting that π^{GRID-} is less than π^{MT}, so the EMS-MABC algorithm has a very proper operation in selecting its load power supply source. Meaning that by noting the lowerness of the proposed offer by the main grid by noting the equalness of the average value of MCP in both of the two algorithms. Therefore, it is better that more power be bought from the main grid so that the system total cost has more reduction. At period 4 participation of MT and the main grid for feeding the load in the EMS-MABC algorithm are equal and about 61.5%. While in the EMS-MINLP algorithm is respectively estimated to be about 38.5% and 84.6%. Noting that in this period

195

the average value of MCP has its maximum value during the day. Also by considering the proposed offer by each of these sources EMS-MINLP algorithm has decided to supply its load demand by using MT which is an incorrect decision. Because π^{MT} is greater than π^{GRID-} and it is proper that for reducing the total cost, more power be purchased from the grid by the algorithm and the power generated by MT be reduced.

The profile of the total power consumed by the consumers has been shown in Figure 5.95 in each time interval. During the period 1, the value of P_t^{TCP} in all the time intervals is greater than the value of $P_t'^{TCP}$. Noting the higherness of the average value of λ_t^{MCP} relative to its value during the periods 2 and 3, as a result it was better that the algorithm have less TCP relative to the periods 2 and 3. During this period, the RLD load is mainly fed and also a significant part of the load has been sold to the national grid. During period 2 almost only at 7.7% of the times the value of P_t^{TCP} has been obtained greater than $P_t'^{TCP}$. In the EMS-MINLP algorithm in addition to supplying part of the power from the national grid, also ES has operated in the discharging mode.

Also at period 3 similar to period 1, more RLD load has been fed by the EMS-MINLP algorithm relative to the other algorithm and also in this algorithm more power has been sold to the grid. Following it the value of its TCP will also be more than EMS-MABC algorithm (about 61.5% of the times). At period 4 the EMS-MINLP algorithm has decided to charge ES in some of its intervals. Noting that the day, so for reducing cost for the consumers it is proper that the optimization algorithm transfers the charging time ES and or feeding RLD to another time with lower MCP value.

The power Bargraph includes the ES charge/ discharge power, power purchased/ sold/ to the national grid, RLD, UP load and EGP have been shown in Figures 5.96(a) and 5.96(b). RLD load in the EMS-MINLP algorithm has fed about 72.8% and 26% of its required power during the day respectively during period 1 and period 3. During period 1 the average value of MCP is high, so better operation is that most of this load be fed during period 3 in which the average value of λ_t^{MCP} is the minimum value of MCP during the day.

RLD load in the EMS-MABC algorithm has also been mainly fed during the first 3 periods that the values of its fed power in these periods are respectively equal to 17%, 15.6% and 65%. Despite this fact, noting that the average value of $\lambda_t'^{MCP}$ during period 3 is much less than the average value of λ_t^{MCP} during the period 1, as a result of it the consumers pay less expense for feeding their loads. However, the value of RLD fed power during the system daily operation in the EMS-MABC algorithm has become

about 55% less than the other optimization algorithms and the EMS-MABC algorithm has mostly tried to improve the situation of charging ES during the day. The value of the power sold to the national grid in the EMS-MABC algorithm has also reduced about 4%. The reason is that in this algorithm, the value of the generated power by MT is about 47% less than the EMS-MINLP optimization algorithm. On the other hand, significant reduction in the cost resulting from starting up MT has taken place in the EMS-MABC algorithm.

UP power in none of the optimization algorithms exists during system daily operation its reason is that despite the occurrence of scenarios 2 and 3 however lack of power is compensated completely by purchasing from the grid. The power purchased from the national grid in the EMS-MABC algorithm has become 61% more than the other optimization algorithm. Noting the significant reduction of MT (about 47%) and the higherness of π^{MT} relative to π^{GRID-} we can obtain significant reduction in the cost of supplying electricity. Also, the total EGP power during daily operation in the EMS-MABC algorithm has shown about 51% reduction relative to the other algorithm. The reason is that the EMS-MABC algorithm has mainly followed the policy of supplying the NRL load feed and has fed less RLD (about 55%) during system daily operation. Also, has sold less power to the national grid. In this algorithm ES has performed about 81.2% of the times during the day in the charging mode. While ES in the EMS-MINLP algorithm has operated only 27% of the times in the charging mode. Hence, SOC is much better than the ES system SOC in the EMS-MINLP algorithm

MCP has been shown in each interval in both of the algorithms in Figure 5.97. Also, the average value of MCP during the periods 1 to 4 has been presented in Table. 5.10. During period 1 in all of the time intervals the value of P_t^{TCP} is more than the value of $P_t'^{TCP}$. Noting that in this time interval the value of λ_t^{MCP} at 85% of the times is more than the value of $\lambda_t'^{MCP}$, so the EMS-MINLP algorithm has fed more load with higher cost. During period 2 with the reduction of λ_t^{MCP}, change has not been created in the total value of TCP power in the EMS-MINLP algorithm this is while in the EMS-MABC algorithm, the sum of $P_t'^{TCP}$ power has increased about 36% in this time interval.

During period 3 always the sum of the values of $P_t'^{TCP}$ have shown increase (about 42%) as a result the EMS-MABC algorithm has tried to keep the value of MCP low during this period. During period 3 the sum of the values of P_t^{TCP} has become 46% more than the sum of its values at period 2. Noting the significant reduction of λ_t^{MCP} during the period 3, so the operation of the EMS-MINLP algorithm in reducing cost by considering the consumption

197

Table 5.10: Average value of MCP during each 6 hours period of system operation

Period 1	Period 2	Period 3	Period 4	
0.41	0.40	0.47	0.68	λ_t^{MCP}
0.25	0.36	0.38	0.50	$\lambda_t'^{MCP}$

increase, has been very adequate. During period 4 in which the value of MCP in both of the algorithms has its maximum value during the day, so its better that less consumers are fed by the optimization algorithms. In this direction the EMS-MABC algorithm has fed about 1.5% less load relative to the EMS-MINLP algorithm.

Conclusion

In this thesis has applied all proposed probabilistic methods for Energy and Operation Schaduling (EOS) in the grid connected MGs. $EOS - MGSA$ and $EOS - MACO$ algorithms have been developed for the optimum planning of energy in the grid connected MGs with Optimal Demand Side Management (ODSM) and the reduction of MCP. The optimization problem comprises a wide range of resources that are mainly found in an MG system. The constraints that reflect the model of each one of these resources have been used in an MG system with small scale. The responses are completely affected by different variables such as the cost of exploitation of each one of the generation resources, the tariffs related to the purchasing and selling electricity from/to the upstream grid and the penalty resulting from the load not being fed completely. In the proposed algorithms, a self-adaptive method was proposed for increasing the effectiveness of these algorithms in solving different problems with different cost functions and different landscapes. Eventually, the proposed probable algorithms have been tested experimentally over IREC's MG Testbed under different scenarios. The obtained results clearly state the proper operation of the proposed algorithms and the determination of the optimum power of generation sources by considering the cost function for each one of them. Furthermore, the results state the capability and the accuracy of the system model presented and the proposed algorithms are for reaching the two goals including reduction of generation cost and complete fulfillment of load demand. The analysis done can be with different loads

Table 5.11: Advantages and disadvantages of the implemented optimization algorithms

Option	MINLP	MICA	MABC	MACO	MPSO	MGSA
Execution time (Sec)	6	196.96	187.8	1.14	27.45	62.74
Objective function	34.91	35.98	35.61	37.43	36.12	35.56
Error(%)	0	3	2	7	3.5	1.86

and also can be easily generalized for periods more than one day. All of the presented optimization algorithms are a good choice for the complete supplying of load demand. The simulation and experimental results show the very proper and suitable effectiveness of proposed algorithms for the optimum use of generation sources and also the reduction of consumed electricity price by the consumers relative to MCEMS algorithm. Furthermore, the results have demonstrated that the proposed optimization algorithm can provide robust, optimistic, reliable and high quality solutions at a satisfactory simulation time for the problems related to EOS.

The obtained results can be summarized in Table 5.11. As seen in this table, MACO has the minimum execution time among heuristic methods however the objective function in this algorithm shows a much higher value compared to other methods. As shown in this table, the nearest value of objective function compared to realistic method (MINLP) is related to MGSA algorithm.
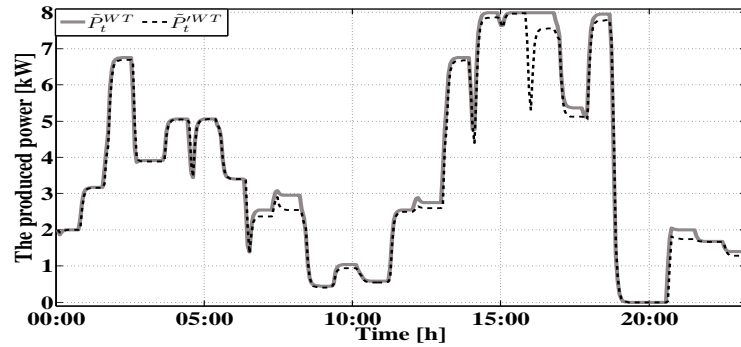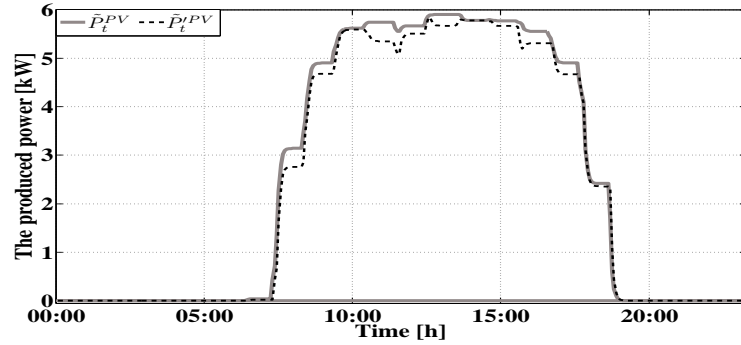
(a) WT emulator
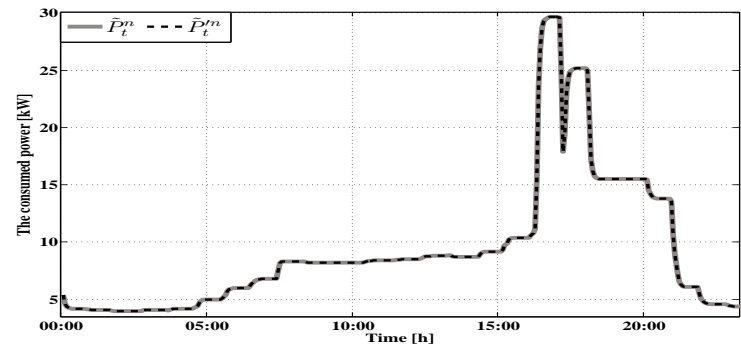
(b) PV emulator

(c) NRL emulator

Figure 5.81: WT, PV and NRL power from the emulators (Solid light-gray line indicates $MCEMS$ algorithm and dash black lines represent output of $EMS - MICA$ algorithm)
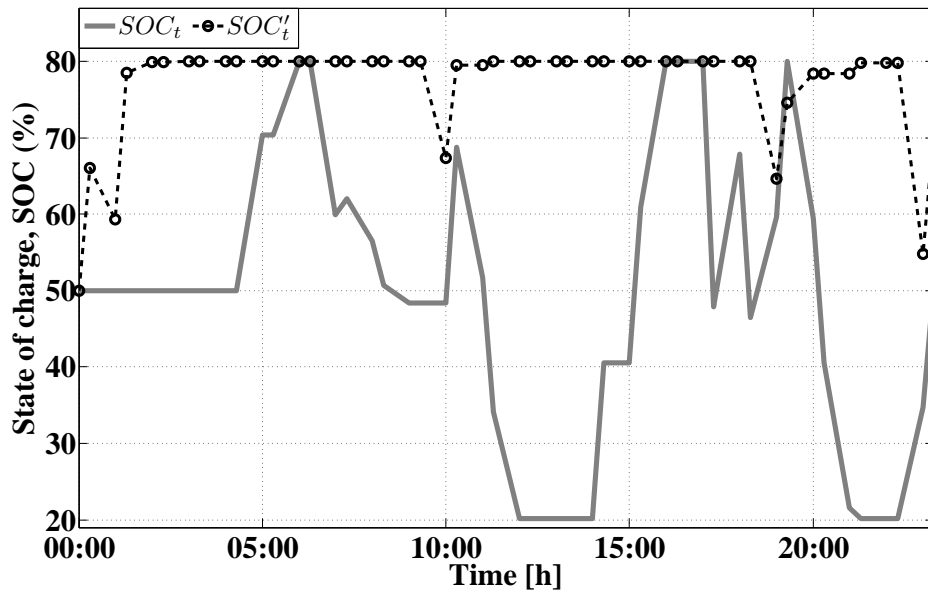
Figure 5.82: SOC during the system daily operation
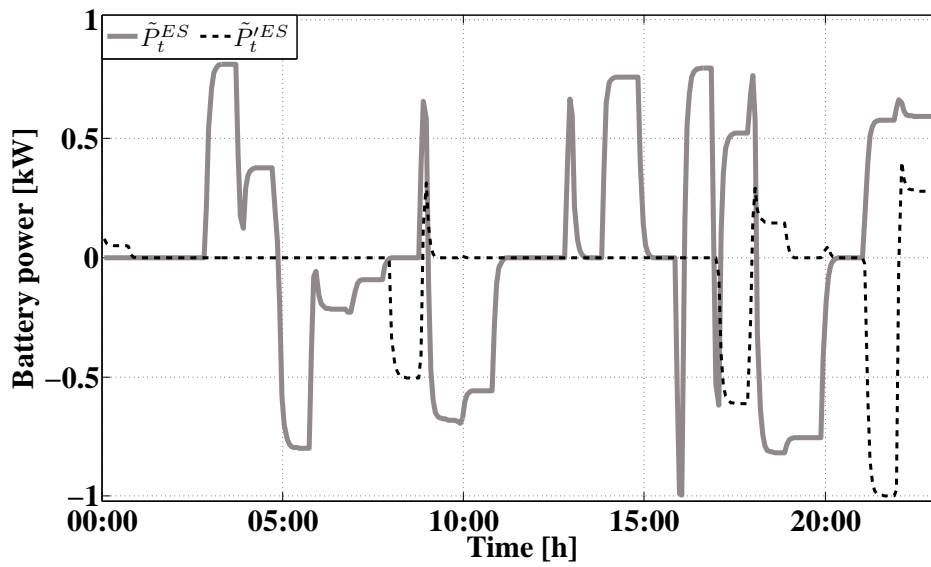
Figure 5.83: ES charge/ discharge power during the system daily operation
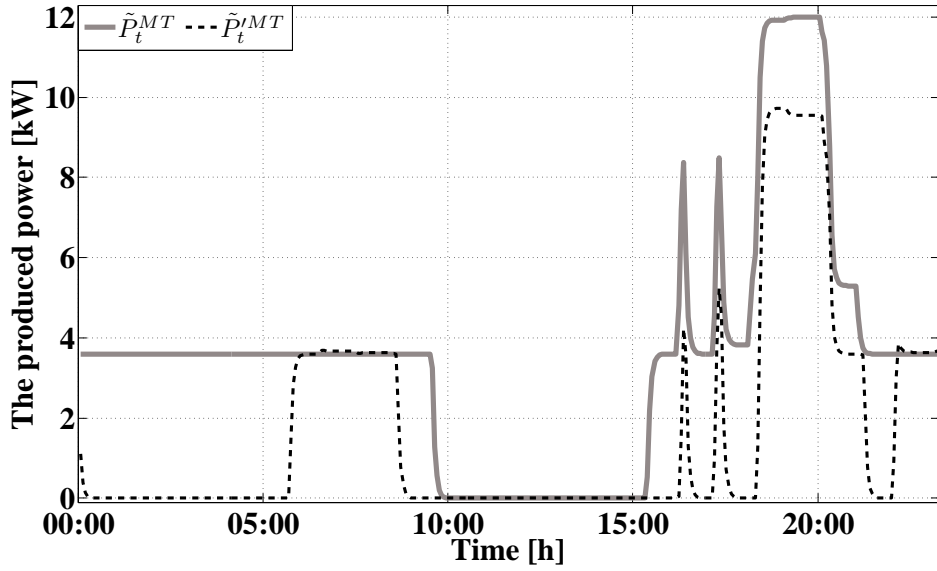
Figure 5.84: ES charge/ discharge power during the system daily operation
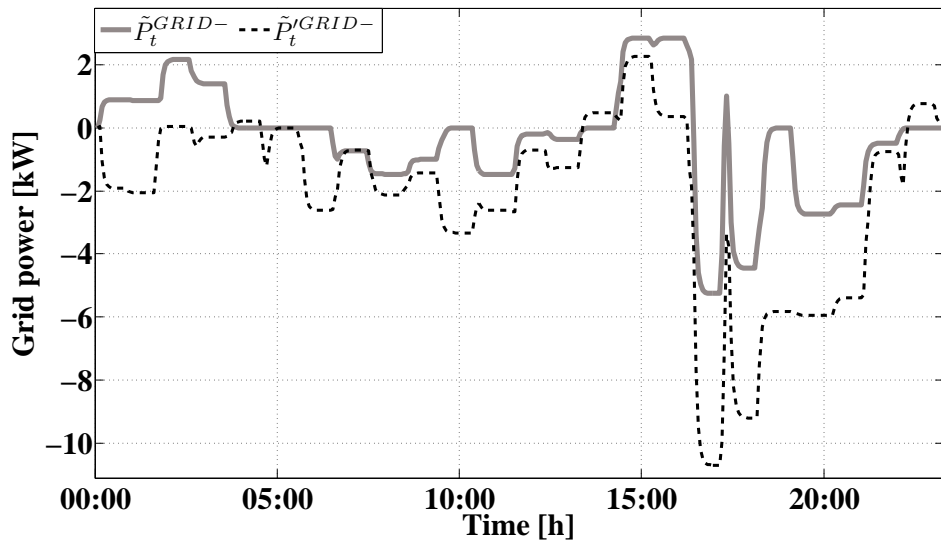
Figure 5.85: Power purchased/ sold from/ to the main grid
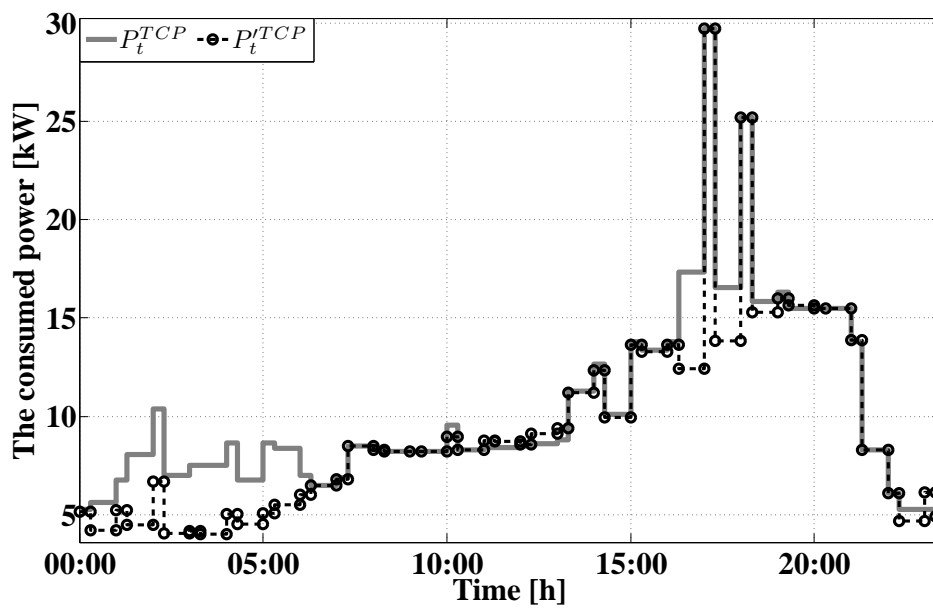
Figure 5.86: Total power consumed during system daily operation
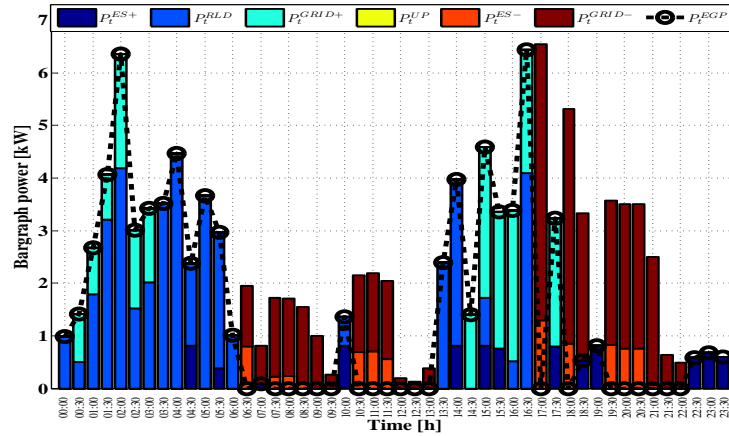
(a) EMS-MINLP
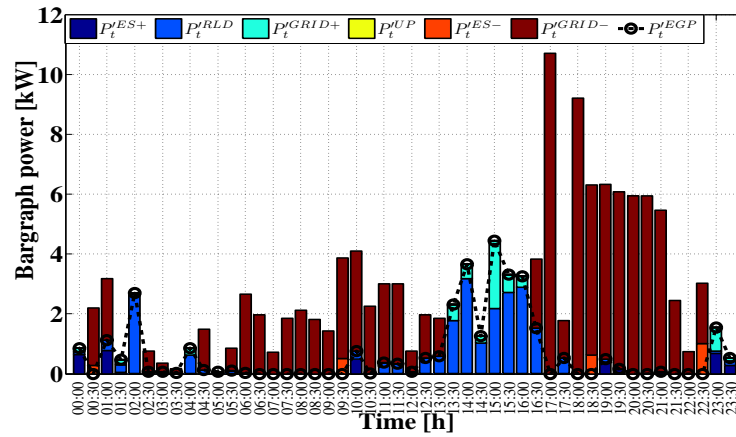
(b) EMS-MICA

Figure 5.87: Bargraph of the ES charging/ discharging power, purchased/ sold power from/ to the national grid, UP, RLD, and EGP

204

(a) EMS-MINLP
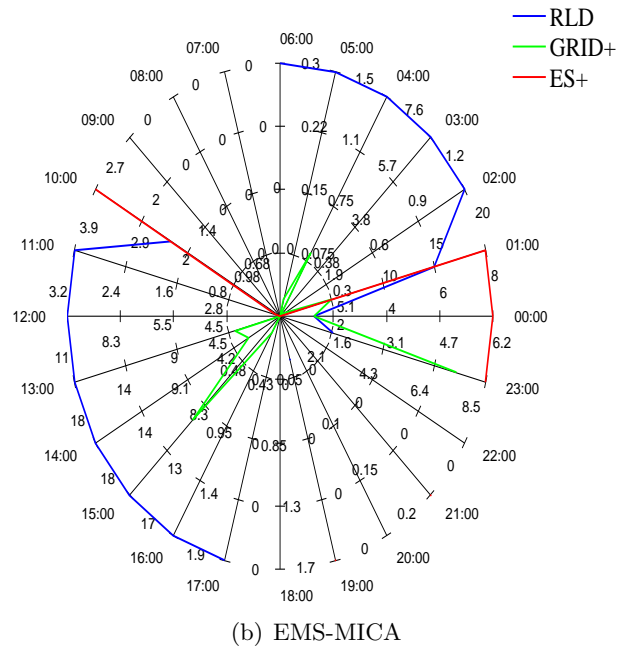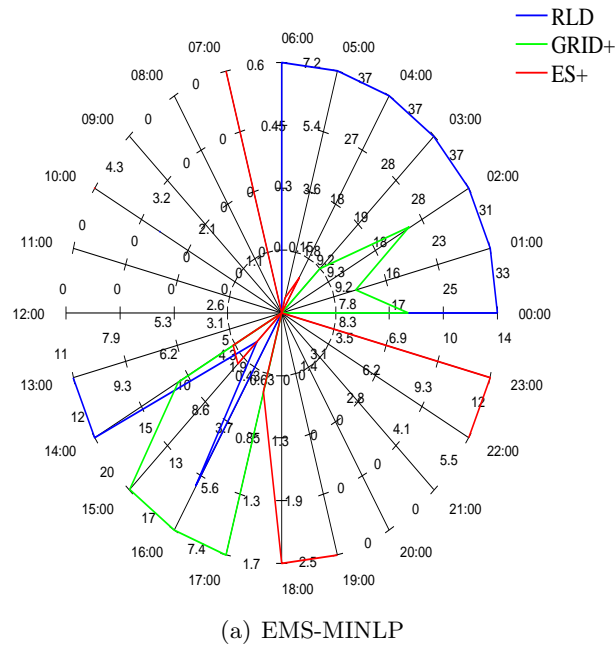
(b) EMS-MICA

Figure 5.88: Daily dispatch share of generation units for feeding the consumer demands
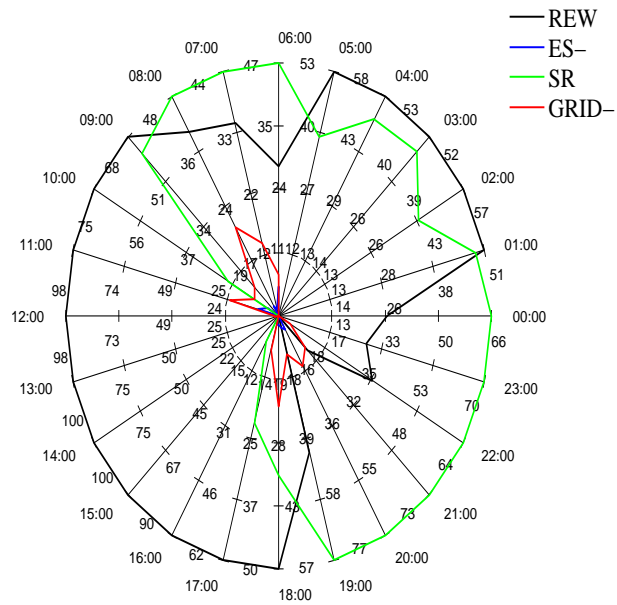
(a) EMS-MINLP
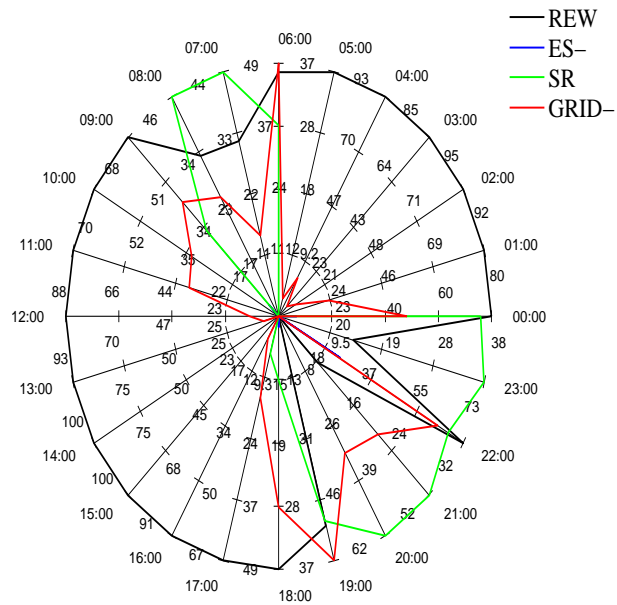
(b) EMS-MICA

Figure 5.89: Daily supplied power shares of consumption units

206
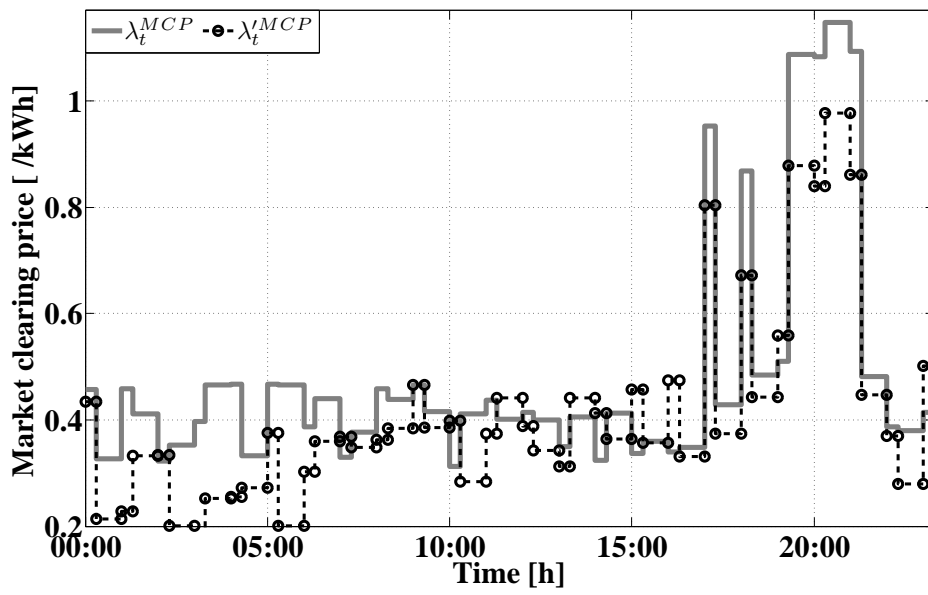
Figure 5.90: MCP in each time interval during system daily operation
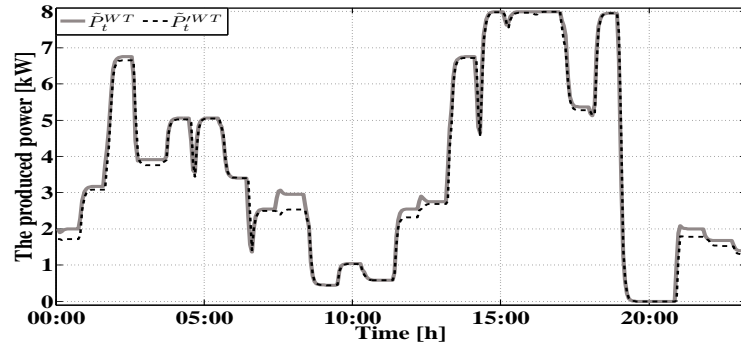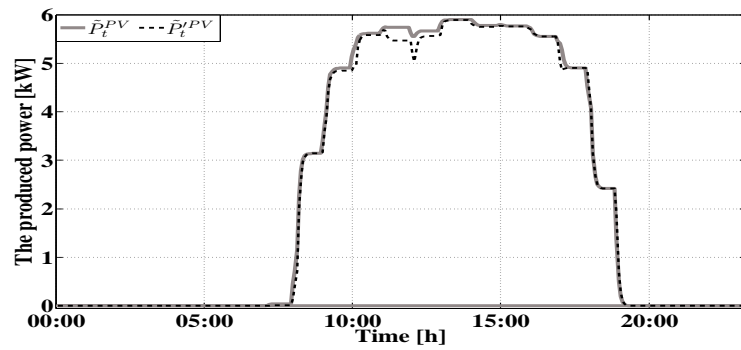
(a) WT emulator
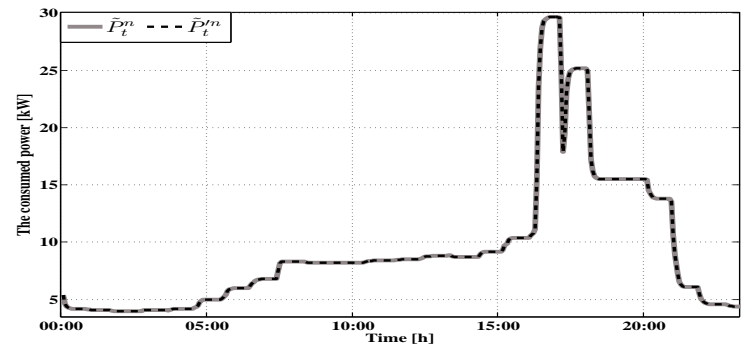
(b) PV emulator

(c) NRL emulator

Figure 5.91: The power generated and consumed by each of the WT, PV and NRL emulators in each time interval
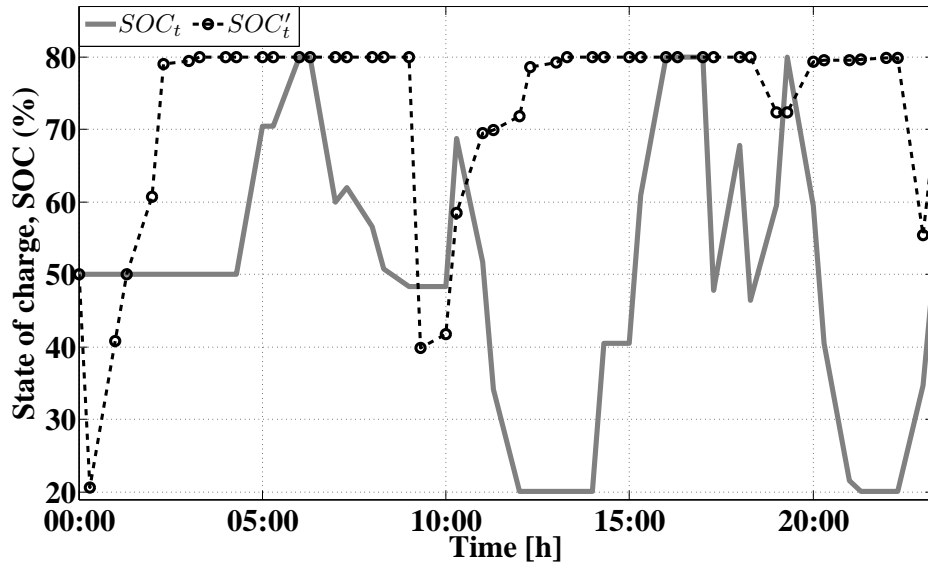
Figure 5.92: SOC during system daily operation
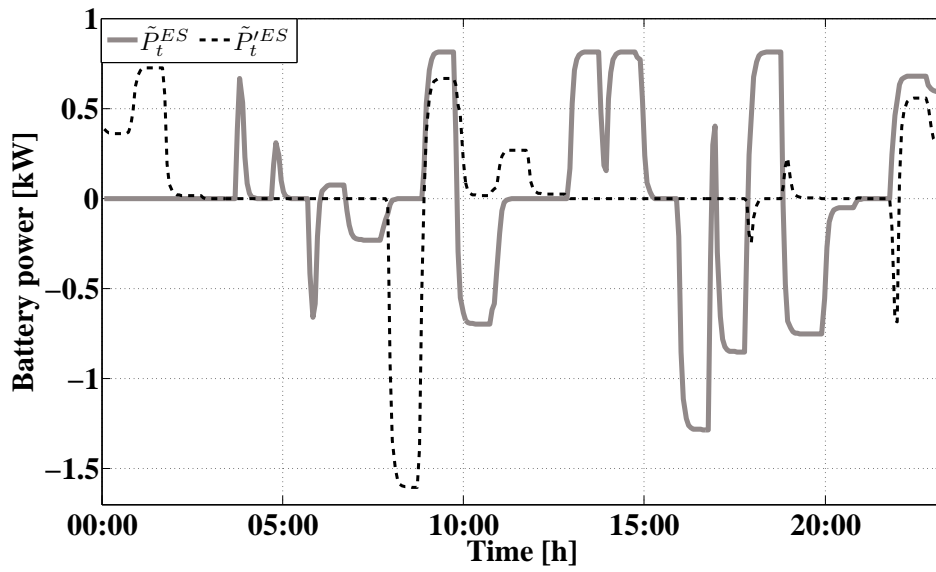
Figure 5.93: ES charge/ discharge power during the system daily operation
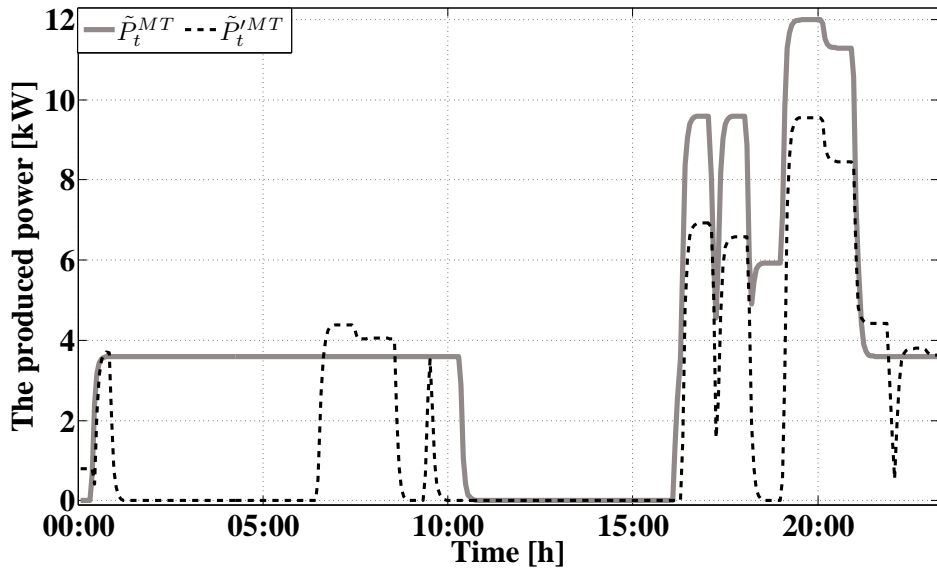
Figure 5.94: Power generated by MT during system daily operation
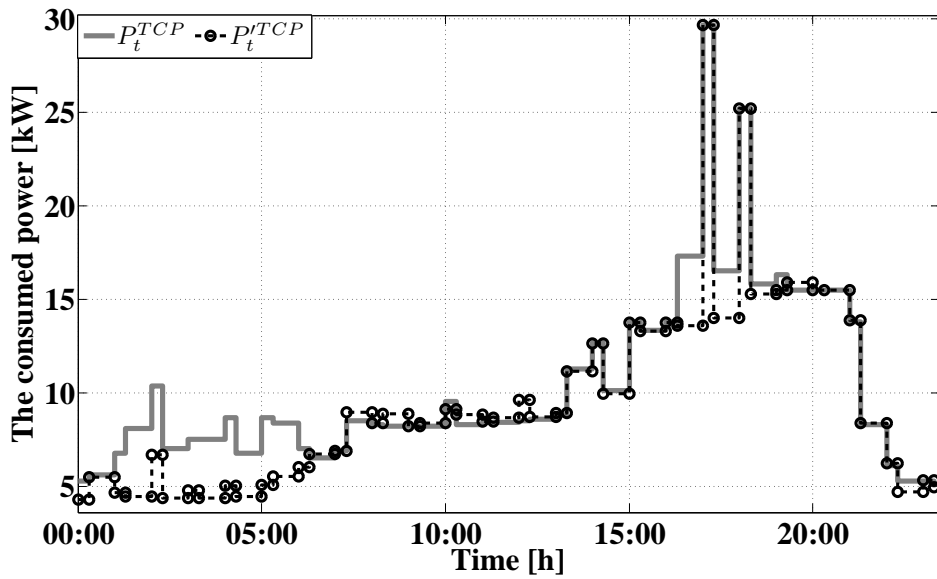
Figure 5.95: Total power consumed during the system daily operation
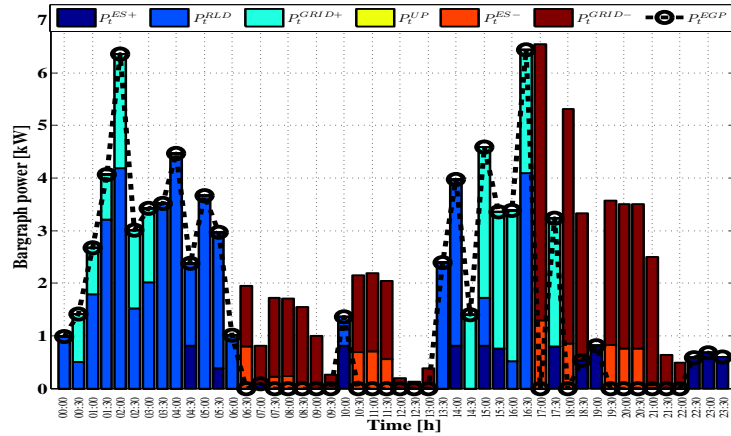
(a) EMS-MINLP
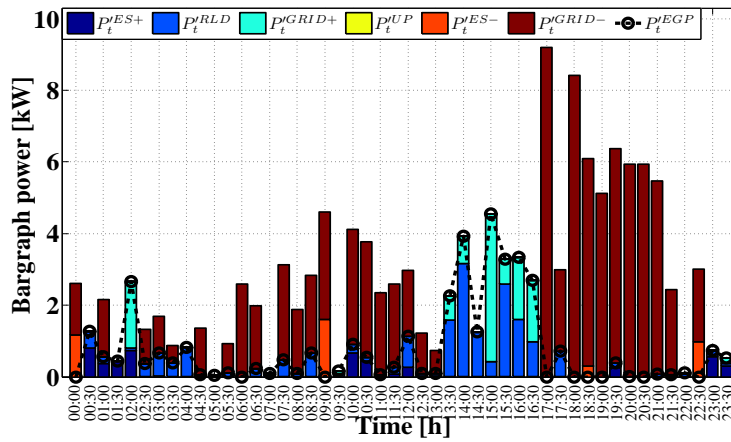
(b) EMS-MICA

Figure 5.96: ES charging/ discharging power bargraph, power purchased/ sold from/to the national grid UP, RLD, and EG

211
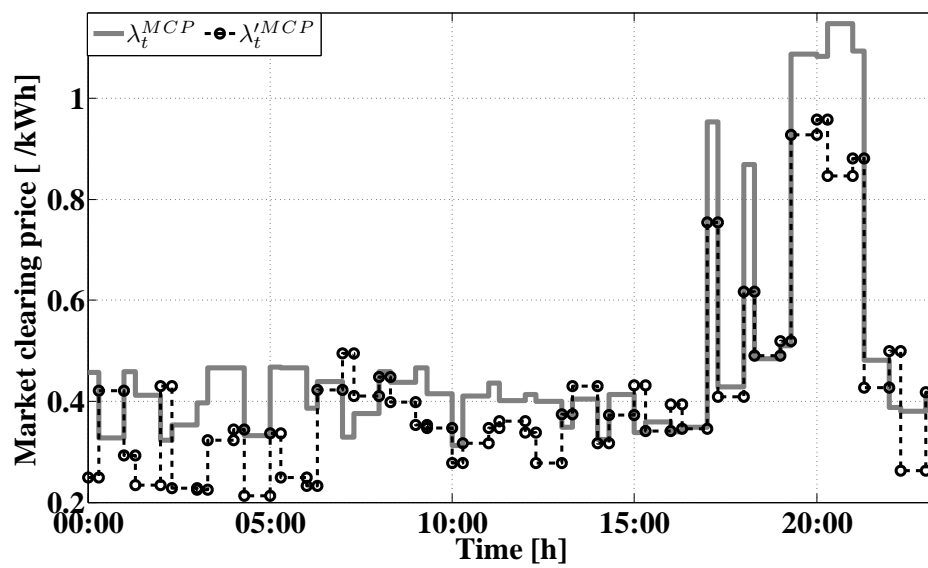
Figure 5.97: MCP in each time interval during the system daily operation

6

Conclusions

6.1 Conclusions

In this research, several intelligent EMS based on LEM have been presented to guarantee optimal operation of islanded and grid connected MG consisting of different DGs through optimal scheduling. The optimization algorithms used in this study includes MINLP, PSB, MICA, MABC, MACO, MPSO and MGSA which have been implemented on an experimental MG testbed, i.e., IREC's MG. The DG's priority and responsive load management have also been considered in the proposed objective function and technical and economic constraints. Simulation and experimental results reveals a significant reduction in total operation cost of the MG using the aforementioned optimization algorithms. In addition, simulation results prove that the proposed algorithms have shown an adequate behavior in encountering unwanted incidents and demand side management. The proposed experimental setup and the results obtained also reveal applicability and practical capabilities of the proposed algorithms in energy management of an islanded MG. Furthermore, the execution time and objective function for all of the proposed algorithms have been compared with each other. It is clear that deterministic algorithms based on MILP/MINLP have presented the best optimal solution but other optimization algorithms should also be investigated to optimize in the large-scale grids. Hence, it has found and proved competitive ratios for the optimal real-time heuristic algorithms for these problems. It has concluded that it is necessary to develop randomized or adaptive algorithms to improve upon the performance of the optimal deterministic algorithms. According to the results of the analysis, it has proposed some

adaptive heuristics methods that are based on an analysis of historical data on the resource usage for energy and performance efficient. As illustrated in the thesis, MACO is fastest method to find the optimum solution compared to other heuristic methods. Likewise, the minimum objective function can be calculated by MGSA in comparison to other heuristic algorithms.

The MG operated by using the optimization algorithms have been able to perform optimum, robust, safe and stable by considering the following cases:

1. These algorithms increases the system income playing the DG bids and by considering that the total consumed power by loads and also the total generated power by renewable sources are used as well;

2. These algorithms maximizes the satisfaction load rate by minimizing the operation cost in the both operating modes (islanded and grid connected mode);

3. Managing renewable units in long-term period by using real time schedule layer for the intelligent optimization of MG and the better using of resources with intermittent power based on real time forecasting data;

4. Exact adjustment of the setpoint related to production units in real time schedule layer for the optimization of power distribution and sending these data by using dispatch layer based on real time data;

5. Proper and fast algorithm reaction to the occurrence of unwanted incidents resulting from the exit/entrance and or increase/reduction of the capacity of non-dispatchable sources and the increase of demand related to NRL and finally making the proper decision by considering all the real time forecast data.

6.2 Future work

From this thesis, future research lines have arisen, which appear listed in the following:

- To implement an energy management in the integrated Microgrid (MG) laboratory system with a flexible and reliable multimicrogrid structure in order to consider stability and reliability under different conditions, including transition mode and fault events;

- To propose a multi agent based management among multiple MG participating in the market considering economically and profitably concepts;

  In this project, a multi agent system (MAS) for energy resource scheduling of power system with distributed resources, which has several MGs and lumped loads interconnected each other. The algorithm behind the proposed MAS has the following three stages:

  1. To schedule each MG in the network individually to satisfy its internal demand.
     This step helps to find out possible bids of MGs.

  2. To find out the possible bids of each MG for exporting power to the network and compete in a wholesale market to provide power for lumped loads.
     The market outcomes for each scheduling hour are known.

  3. To reschedule each MG individually to satisfy its total demand. The total demand of a MG is the addition of internal demand and the external demand, which is from the outcome of wholesale energy market.

- To implement a multi ownership MG system in the market structure;

- To construct an electricity market within MG based on dynamic pricing rates;

- Multi-objective operation management for a multiple MG.

215

Bibliography

[1] X. Liao, J. Zhou, S. Ouyang, R. Zhang, and Y. Zhang. "an adaptive chaotic artificial bee colony algorithm for short-term hydrothermal generation scheduling". *Electrical Power and Energy Systems*, 53(1):34–42, 2013. XVIII, 67, 239, 241

[2] M. Marzband, A. Sumper, A. Ruiz-Álvarez, J. Luis Domínguez-García, and B. Tomoiagă. Experimental evaluation of a real time energy management system for stand-alone microgrids in day-ahead markets. *Applied Energy*, 106(0):365–76, 2013. 1, 3, 4, 5, 6, 9, 25, 26, 28, 29, 35, 49, 104, 105, 107, 187, 194

[3] M. Marzband, A. Sumper, J. L. Domínguez-García, and R Gumara-Ferret. "experimental validation of a real time energy management system for microgrids in islanded mode using a local day-ahead electricity market and MINLP". *Energy Conversion and Management*. In press. 1, 3, 4, 6, 9, 22, 25, 26, 28, 29, 35, 80, 187, 194

[4] R. H. Lasseter. Microgrids and distributed generation. *Energy Eng.,*, 133:144–52, 2007. 1

[5] R. Palma-Behnke, C. Benavides, F. Lanas, B. Severino, L. Reyes, J. Llanos, and D. Saez. "a microgrid energy management system based on the rolling horizon strategy". *IEEE Transactions on Smart Grid*, 4(2):996–1006, 2013. 3, 7

Bibliography

[6] S. J. Ahn, S. R. Nam, J. H. Choi, and S. I. Moon. "power scheduling of distributed generators for economic and stable operation of a microgrid". *IEEE Transactions on Smart Grid*, 4(1):398–405, 2013. 3

[7] Y. Zhang, N. Gatsis, and G.B. Giannakis. "robust energy management for microgrids with high-penetration renewables". *IEEE Transactions on Sustainable Energy*, PP(99):1–10, 2013. 3

[8] B. Belvedere, M. Bianchi, A. Borghetti, C.A. Nucci, M. Paolone, and A. Peretto. "a microcontroller-based power management system for standalone microgrids with hybrid power supply". *IEEE Transactions on Sustainable Energy*, 3(3):422–31, 2012. 3, 4

[9] P. Siano, C. Cecati, Yu Hao, and J. Kolbusz. "real time operation of smart grids via FCN networks and optimal power flow". *IEEE Transactions on Industrial Informatics*, 8(4):944–52, 2012. 3, 7

[10] J. Mitra and M.R. Vallem. "determination of storage required to meet reliability guarantees on island-capable microgrids with intermittent sources". *IEEE Transactions on Power Systems*, 27(4):398–405, 2012. 3, 5

[11] M. A. Hassan and M. A. Abido. "optimal design of microgrids in autonomous and grid-connected modes using particle swarm optimization". *IEEE Transactions on Power Electronics*, 26(3):755–69, 2011. 3

[12] C. M. Colson, M. H. Nehrir, R.K. Sharma, and B. Asghari. "improving sustainability of hybrid energy systems part ii: Managing multiple objectives with a multiagent system", 2013. 3

[13] E. Rokrok and M. E. H. Golshan. "adaptive voltage droop scheme for voltage source converters in an islanded multibus microgrid". *IET Transmission Distribution Generation*, 4(5):562–78, 2010. 3

[14] M. Mohammadi, S.H. Hosseinian, and G.B. Gharehpetian. "GA-based optimal sizing of microgrid and DG units under pool and hybrid electricity markets". *International Journal of Electrical Power & Energy Systems*, 35(1):83–92, 2012. 3

[15] M. Tasdighi, H. Ghasemi, and A. Rahimi-Kian. "residential microgrid scheduling based on smart meters data and temperature dependent thermal load modeling". *IEEE Transactions on Smart Grid*, PP(99):1–9, 2013. 3

218

[16] N. Bottrell, M. Prodanovic, and T.C. Green. "dynamic stability of a microgrid with an active load". *IEEE Transactions on Power Electronics*, 28(11):5107–19, 2013. 3

[17] S. A. Pourmousavi and M. H. Nehrir. "real-time central demand response for primary frequency regulation in microgrids". *IEEE Transactions on Smart Grid*, PP(99):1, 2012. 3

[18] A. Ghazanfari, M. Hamzeh, H. Mokhtari, and H. Karimi. "active power management of multihybrid fuel cell/supercapacitor power conversion system in a medium voltage microgrid". *IEEE Transactions on Smart Grid*, 3(4):1903–10, 2012. 3

[19] M. Prodanovic and T.C. Green. "high-quality power generation through distributed control of a power park microgrid". *IEEE Transactions on Industrial Electronics*, 53(5):1471–82, 2006. 3

[20] Y. H. Chen, S. Y. Lu, Y. R. Chang, T. T. Lee, and M. C. Hu. "economic analysis and optimal energy management models for microgridsystems: A case study in taiwan". *Applied Energy*, 103(0):145–54, 2013. 3

[21] C. Chen, S. Duan, T. Cai, B. Liu, and G. Hu. "smart energy management system for optimal microgrid economic operation". *IET Renewable Power Generation*, 5(3):258–67, 2011. 3, 5

[22] X. Guan, Z. Xu, and Q. S. Jia. "energy-efficient buildings facilitated by microgrid". *IEEE Transactions on Smart Grid*, 1(3):243–52, 2010. 3

[23] C. Marnay, G. Venkataramanan, M. Stadler, A.S. Siddiqui, R. Firestone, and B. Chandran. "optimal technology selection and operation of commercial-building microgrids". *IEEE Transactions on Power Systems*, 23(3):975–82, 2008. 3, 5

[24] L. Valverde, F. Rosa, and C. Bordons. "design, planning and management of a hydrogen-based microgrid". *IEEE Transactions on Industrial Informatics*, 9(3):1398–404, 2013. 4

[25] A.G. Tsikalakis and N.D. Hatziargyriou. "centralized control for optimizing microgrids operation". *IEEE Transactions on Energy Conversion*, 23(1):241–48, 2008. 4

Bibliography

[26] T. Logenthiran, D. Srinivasan, A.M. Khambadkone, and Htay Nwe Aung. "multiagent system for real-time operation of a microgrid in real-time digital simulator". *IEEE Transactions on Smart Grid*, 3(2):925–33, 2012. 4, 7

[27] A. Chaouachi, R.M. Kamel, R. Andoulsi, and K. Nagasaka. "multiobjective intelligent energy management for a microgrid". *IEEE Transactions on Industrial Electronics*, 60(4):1688–99, 2013. 4, 5

[28] Q. Jiang, M. Xue, and G. Geng. "energy management of microgrid in grid-connected and stand-alone modes". *IEEE Transactions on Power Systems*, 28(3):3380–89, 2013. 4

[29] Y. Sugaya, S. Omachi, A. Takeuchi, and Y. Nozaki. "a statistical analysis on operation scheduling for an energy network project". *IEEE Transactions on Parallel and Distributed Systems*, 23(9):1583–92, 2012. 4

[30] J.A. Peas Lopes, C.L. Moreira, and A.G. Madureira. "defining control strategies for microgrids islanded operation". *IEEE Transactions on Power Systems*, 21(2):916–24, 2006. 4

[31] F. A. Mohamed and H. N. Koivo. "online management genetic algorithms of microgrid for residential application". *Energy Conversion and Management*, 64(0):562 – 568, 2012. 4

[32] M. Silva, H. Morais, and Z. Vale. "an integrated approach for distributed energy resource short-term scheduling in smart grids considering realistic power system simulation". *Energy Conversion and Management*, 64(0):273–88, 2012. 4

[33] S. A. Pourmousavi, M. H. Nehrir, C. M. Colson, and C. Wang. "real-time energy management of a stand-alone hybrid wind-microturbine energy system using particle swarm optimization". *IEEE Transactions on Sustainable Energy*, 1(3):193–201, oct. 2010. 5, 6

[34] S. Conti, R. Nicolosi, S. A. Rizzo, and H. H. Zeineldin. "optimal dispatching of distributed generators and storage systems for MV islanded microgrids". *IEEE Transactions on Power Delivery*, 27(3):1243–51, 2012. 5

[35] B. Zhao, X. Zhang, J. Chen, C. Wang, and L. Guo. "operation optimization of standalone microgrids considering lifetime characteristics

of battery energy storage system". *IEEE Transactions on Sustainable Energy*, PP(99):1–10, 2013. 5

[36] M. E. Khodayar, M. Barati, and M. Shahidehpour. Integration of high reliability distribution system in microgrid operation. *IEEE Transactions on Smart Grid*, 3:1997–2006, 2012. 5

[37] B. Falahati, Fu. Yong, and Wu. Lei. Reliability assessment of smart grid considering direct cyber-power interdependencies. *IEEE Transactions on Smart Grid*, 3:1515–24, 2012. 5

[38] A. Khodaei and M. Shahidehpour. Microgrid-based co-optimization of generation and transmission planning in power systems. *IEEE Transactions on Power Systems*, 28:1582–90, 2013. 5

[39] S. Wang, Z. Li, L. Wu, M. Shahidehpour, and Z. Li. New metrics for assessing the reliability and economics of microgrids in distribution system. *IEEE Transactions on Power Systems*, pages 1–10, 2013. 5

[40] H. Nikkhajoei and R. H. Lasseter. "distributed generation interface to the CERTS microgrid". *IEEE Transactions on Power Delivery*, 24(3):1598–608, 2009. 5

[41] I. Bae and J. Kim. Reliability evaluation of customers in a microgrid. *IEEE Transactions on Power Systems*, 23:1416–22, 2008. 5

[42] M. Erol-Kantarci, B. Kantarci, and H. T. Mouftah. Reliable overlay topology design for the smart microgrid network. *IEEE Network*, 25:38–43, 2011. 5

[43] S. Anand and B. G. Fernandes. Reduced-order model and stability analysis of low-voltage DC microgrid. *IEEE Transactions on Industrial Electronics*, 60:5040–49, 2013. 5

[44] D. Salomonsson, L. Soder, and A. Sannino. An adaptive control system for a DC microgrid for data centers. *IEEE Transactions on Industry Applications*, 44:1910–17, 2008. 5

[45] T. Ghanbari and E. Farjah. Unidirectional fault current limiter: An efficient interface between the microgrid and main network. *IEEE Transactions on Power Systems*, 28:1591–98, 2013. 5

[46] K. T. Tan, P. L. So, Y. C. Chu, and M. Z. Q. Chen. A flexible AC distribution system device for a microgrid. *IEEE Transactions on Energy Conversion*, pages 1–10, 2013. 5

221

Bibliography

[47] R. S. Balog, W. W. Weaver, and P. T. Krein. The load as an energy asset in a distributed dc smartgrid architecture,. *IEEE Transactions on Smart Grid*, 3:253–60, 2012. 5

[48] C. Lee, R. Jiang, and P. Cheng. A grid synchronization method for droop-controlled distributed energy resource converters. *IEEE Transactions on Industry Applications*, 49:954–62, 2013. 5

[49] T. L. Vandoorn, B. Meersman, J. D. M. De Kooning, and L. Vandevelde. Transition from islanded to grid-connected mode of microgrids with voltage-based droop control. *IEEE Transactions on Power Systems*, pages 1–10, 2013. 5

[50] H. E. Farag, M. M. A. Abdelaziz, and E. F. El-Saadany. Voltage and reactive power impacts on successful operation of islanded microgrids. *IEEE Transactions on Power Systems*, 28:1716–27, 2013. 5

[51] M. Datta, T. Senjyu, A. Yona, T. Funabashi, and Kim Chul-Hwan. A coordinated control method for leveling pv output power fluctuations of pv-diesel hybrid systems connected to isolated power utility. *IEEE Transactions on Energy Conversion*, 24:153–62, 2009. 5

[52] A. K. Abdelsalam, A. M. Massoud, S. Ahmed, and P. Enjeti. High-performance adaptive perturb and observe MPPT technique for photovoltaic-based microgrids. *IEEE Transactions on Power Electronics*, 26:1010–21, 2011. 5

[53] W. A. Najy, H. H. Zeineldin, and W. L. Woon. "optimal protection coordination for microgrids with grid-connected and islanded capability". *IEEE Transactions on Industrial Electronics*, 60(4):1668–77, 2013. 5

[54] D.E. Olivares, C.A. Canizares, and M. Kazerani. "a centralized optimal energy management system for microgrids". In *IEEE Power and Energy Society General Meeting*, pages 1 –6, july 2011. 5

[55] S. Obara, M. Kawai, O. Kawae, and Y. Morizane. "operational planning of an independent microgrid containing tidal power generators, SOFCs, and photovoltaics". *Applied Energy*, (0):1–15, 2012. 5

[56] H. Ren and W. Gao. "a MILP model for integrated plan and evaluation of distributed energy systems". *Applied Energy*, 87(3):1001 – 1014, 2010. 5

[57] S. Nikolova, A. Causevski, and A. Al-Salaymeh. Optimal operation of conventional power plants in power system with integrated renewable energy sources. *Energy Conversion and Management,*, 65(0):697–03, 2013. 5

[58] H. Dagdougui, R. Minciardi, A. Ouammi, M. Robba, and R. Sacile. "modeling and optimization of a hybrid system for the energy supply of a "green" building". *Energy Conversion and Management,*, 64(0):351–63, 2012. 5

[59] R. M. Kamel, A. Chaouachi, and K. Nagasaka. Enhancement of micro-grid performance during islanding mode using storage batteries and new fuzzy logic pitch angle controller. *Energy Conversion and Management,*, 52(5):2204 –16, 2011. 5

[60] M. Basu. "artificial bee colony optimization for multi-area economic dispatch". *Electrical Power and Energy Systems*, 49(1):181–87, 2013. 5

[61] E. Alvarez, A. M. Campos, P. Arboleya, and A. J. Gutiérrez. "microgrid management with a quick response optimization algorithm for active power dispatch". *International Journal of Electrical Power & Energy Systems*, 43(1):465–73, 2012. 5

[62] F. A. Mohamed and H. N. Koivo. "multiobjective optimization using mesh adaptive direct search for power dispatch problem of microgrid". *International Journal of Electrical Power & Energy Systems*, 42(1):728–35, 2012. 5

[63] F. A. Mohamed and H. N. Koivo. "system modelling and online optimal management of microgrid using mesh adaptive direct search". *International Journal of Electrical Power & Energy Systems*, 32(5):398–407, 2010. 5

[64] A. Hajizadeh and M. A. Golkar. "intelligent power management strategy of hybrid distributed generation system". *International Journal of Electrical Power & Energy Systems*, 29(10):783 – 795, 2007. 5

[65] G. C. Liao. "solve environmental economic dispatch of smart microgrid containing distributed generation system- using chaotic quantum genetic algorithm". *International Journal of Electrical Power & Energy Systems*, 43(1):779 – 787, 2012. 5

Bibliography

[66] M. E. Jahromi, M. Ehsan, and A. Fattahi Meyabadi. "a dynamic fuzzy interactive approach for DG expansion planning". *International Journal of Electrical Power & Energy Systems*, 43(1):1094–105, 2012. 5

[67] N. Amjady and V. Vahidinasab. Security-constrained self-scheduling of generation companies in day-ahead electricity markets considering financial risk. *Energy Conversion and Management*, 65(0):164–72, 2013. 5

[68] P. Kanakasabapathy and K. Shanti Swarup. Bidding strategy for pumped-storage plant in pool-based electricity market. *Energy Conversion and Management,*, 51(3):572 – 579, 2010. 5

[69] H.Y. Yamin, Q. El-Dwairi, and S.M. Shahidehpour. "a new approach for gencos profit based unit commitment in day-ahead competitive electricity markets considering reserve uncertainty". *International Journal of Electrical Power & Energy Systems*, 29(8):609–16, 2007. 5

[70] G. Mokryani and P. Siano. "evaluating the integration of wind power into distribution networks by using monte carlo simulation". *International Journal of Electrical Power & Energy Systems*, 53:244–255, 2013. 5, 6

[71] G. Mokryani and P. Siano. "combined monte carlo simulation and opf for wind turbines integration into distribution networks". *Electric Power Systems Research*, 103:37–48, 2013. 5, 6

[72] G. Mokryani and P. Siano. "optimal wind turbines placement within a distribution market environment". *Applied Soft Computing*. In press. 5, 6

[73] P. Siano and G. Mokryani. "probabilistic assessment of the impact of wind energy integration into distribution networks". *IEEE Transactions on Power Systems*. In Press. 5, 6

[74] V. Miranda and Pun Sio Hang. Economic dispatch model with fuzzy wind constraints and attitudes of dispatchers. *IEEE Transactions on Power Systems,*, 20(4):2143 – 2145, nov. 2005. 6

[75] J. Hetzer, D.C. Yu, and K. Bhattarai. An economic dispatch model incorporating wind power. *IEEE Transactions on Energy Conversion,*, 23(2):603 –611, june 2008. 6

[76] C.A. Hernandez-Aramburo, T.C. Green, and N. Mugniot. Fuel consumption minimization of a microgrid. *IEEE Transactions on Industry Applications,*, 41(3):673 – 681, may-june 2005. 6

[77] W. Caisheng, C.M. Colson, M.H. Nehrir, and L. Jian. Power management of a stand-alone hybrid wind-microturbine distributed generation system. In *Power Electronics and Machines in Wind Applications (PEMWA)*, pages 1–7, june 2009. 6

[78] T. Logenthiran, D. Srinivasan, A.M. Khambadkone, and H. Aung. Multiagent system for real-time operation of a microgrid in real-time digital simulator. *IEEE Transactions on Smart Grid,*, 3(2):925–33, 2012. 6

[79] J. Soares, M. Silva, T. Sousa, Z. Vale, and H. Morais. "distributed energy resource short-term scheduling using signaled particle swarm optimization". *Energy*, 42(1):466 – 476, 2012. 6, 7

[80] M. Welsch, M. Howells, M. Bazilian, J.F. DeCarolis, S. Hermann, and H.H. Rogner. "modelling elements of smart grids- enhancing the oseMOSYS (open source energy modelling system) code". *Energy*, 46(1):337 – 350, 2012. 7

[81] T. Niknam, F. Golestaneh, and A. Malekpour. "probabilistic energy and operation management of a Microgrid containing Wind-Photovoltaic-Fuel cell generation and energy storage devices based on point estimate method and self-adaptive gravitational search algorithm". *Energy*, 43(1):427–37, 2012. 7

[82] P. O. Kriett and M. Salani. "optimal control of a residential microgrid". *Energy*, 42(1):321–30, 2012. 7

[83] D. Quiggin, S. Cornell, M. Tierney, and R. Buswell. "a simulation and optimisation study: Towards a decentralised microgrid, using real world fluctuation data". *Energy*, 41(1):549–59, 2012. 7

[84] A. A. Moghaddam, A. Seifi, T. Niknam, and M. R. Alizadeh Pahlavani. "multi-objective operation management of a renewable MG (micro-grid) with back-up micro-turbine/fuel cell/battery hybrid power source". *Energy*, 36(11):6490–507, 2011. 7

[85] T. Niknam, H.Z. Meymand, and H.D. Mojarrad. "an efficient algorithm for multi-objective optimal operation management of distribu-

Bibliography

tion network considering fuel cell power plants". *Energy*, 36(1):119 – 132, 2011. 7

[86] S. Obara, S. Watanabe, and B. Rengarajan. "operation method study based on the energy balance of an independent microgrid using solar-powered water electrolyzer and an electric heat pump". *Energy*, 36(8):5200–13, 2011. 7

[87] P. K. Naraharisetti, I. A. Karimi, A. Anand, and D. Y. Lee. "a linear diversity constraint- application to scheduling in microgrids". *Energy*, 36(7):4235 –43, 2011. 7

[88] V. Vahidinasab and S. Jadid. "joint economic and emission dispatch in energy markets: A multiobjective mathematical programming approach". *Energy*, 35(3):1497 – 1504, 2010. 7

[89] X. Yuan, A. Su, Y. Yuan, H. Nie, and L. Wang. "an improved PSO for dynamic load dispatch of generators with valve-point effects". *Energy*, 34(1):67–74, 2009. 7

[90] E. R. Sanseverino, M. L. Silvestrea, M. G. Ippolitoa, A. Paolab, and G. Reb. "an execution, monitoring and replanning approach for optimal energy management in microgrids". *Energy*, 36:3429–36, 2011. 7

[91] W. Saad, Zhu Han, H. V. Poor, and T. Basar. "game-theoretic methods for the smart grid: An overview of microgrid systems, demand-side management, and smart grid communications". *IEEE Signal Processing Magazine*, 29(5):86–105, 2012. 7

[92] R. Majumder, A. Ghosh, G. Ledwich, and F. Zare. "power management and power flow control with back-to-back converters in a utility connected microgrid". *IEEE Transactions on Power Systems*, 25(2):821–34, 2010. 7

[93] B. Wang, M. Sechilariu, and F. Locment. "intelligent DC microgrid with smart grid communications: Control strategy consideration and design". *IEEE Transactions on Smart Grid*, 3(4):2148–56, 2012. 7

[94] H. Zhou, T. Bhattacharya, D. Tran, S. T. Siew, and A. M. Khambadkone. "composite energy storage system involving battery and ultracapacitor with dynamic energy management in microgrid applications". *IEEE Transactions on Power Electronics*, 26(3):923–30, 2011. 7

226

[95] A. drud, CONOPT. Available at: `http://www.gams.com/dd/docs/solvers/conopt.pdf`. [accessed July 31 2012]. 24, 25, 50

[96] C. A. Floudas. "nonlinear and mixed-integer optimization. fundamentals and applications". *Journal of Global Optimization*, 12:108–10, 1998. 25, 50

[97] M. Marzband, A. Sumper, M. Chindriş, and B. Tomoiagă. "energy management system of hybrid microgrid with energy storage". Suceava, Romania, June 2012. *The International Word Energy System Conference (WESC)*. 48, 92, 95

[98] F. Christodoulos and X. Lin. "mixed integer linear programming in process scheduling: Modeling, algorithms, and applications". *Annals of Operations Research*, 139:131–62, 2005. 50

[99] J.W. Chinneck. *Practical Optimization: A Gentle Introduction*. Carleton University, 2004. 50

[100] R.E. Bellman. *Dynamic Programming*. Princeton University Press, Princeton, NJ, 1957 (Republished 2003). 53

[101] E. Atashpaz Gargari and C. Lucas. "imperialist competitive algorithm: An algorithm for optimization inspired by imperialistic competition". In *IEEE Congress on Evolutionary Computation (CEC-2007)*, volume 7, pages 4661–67, 2007. 55, 238

[102] M. A. Ahmadi, M. Ebadi, A. Shokrollahi, and S. M. Javad Majidi. "evolving artificial neural network and imperialist competitive algorithm for prediction oil flow rate of the reservoir". *Applied Soft Computing*, 13(1):1085–98, 2013. 55, 239

[103] S. M. Mousavi, R. Tavakkoli Moghaddam, B. Vahdani, H. Hashemi, and M. J. Sanjari. "a new support vector model-based imperialist competitive algorithm for time estimation in new product development projects". *Robotics and Computer-Integrated Manufacturing*, 29(1):157–68, 2013. 55, 58

[104] L. Dos, S. Coelho, L. D. Afonso, and P. Alotto. "a new support vector model-based imperialist competitive algorithm for time estimation in new product development projects". *IEEE Transactions on Magnetics*, 48(2):579–82, 2012. 55, 60

Bibliography

[105] S. Nazari Shirkouhi, H. Eivazy, R. Ghodsi, K. Rezaie, and E. Atashpaz Gargari. "solving the integrated product mix-outsourcing problem using the imperialist competitive algorithm". *Expert Systems with Applications*, 37(1):7615–26, 2010. 55, 56, 57, 58, 60, 61, 62, 63

[106] L. D. Afonso, V. C. Mariani, and L. dos Santos Coelho. "modified imperialist competitive algorithm based on attraction and repulsion concepts for reliability-redundancy optimization". *Expert Systems with Applications*, 40(1):3794–802, 2013. 56

[107] V. Rashtchi, E. Rahimpour, and H. Shahrouzi. "model reduction of transformer detailed R-C-L-M model using the imperialist competitive algorithm". *Expert Systems with Applications*, 6(4):233–42, 2012. 56, 60

[108] M. Yousefi, A.N. Darus, and H. Mohammadi. An imperialist competitive algorithm for optimal design of plate-fin heat exchangers. *International Journal of Heat and Mass Transfer*, 55:3178–85, 2012. 62

[109] A. Ghasemi. "a fuzzified multi objective interactive honey bee mating optimization for environmental/economic power dispatch with valve point effect". *Electrical Power and Energy Systems*, 49(1):308–21, 2013. 67

[110] M. Rezaei-Adaryani and A. Karami. "an adaptive chaotic artificial bee colony algorithm for short-term hydrothermal generation scheduling". *Electrical Power and Energy Systems*, 53(1):219–30, 2013. 67, 239

[111] D. Merkle, M. Middendorf, and H. Schmeck. "ant colony optimization for resource-constrained project scheduling". *IEEE Transactions on Evolutionary Computation*, 6(4):333–346, 2002. 69

[112] A. Ahuja, S. Das, and A. Pahwa. "an AIS-ACO hybrid approach for multi-objective distribution system reconfiguration". *IEEE Transactions on Power Systems*, 22(3):1101–11, 2007. 69

[113] M. Lopez-Ibanez and T. Stutzle. "the automatic design of multiobjective ant colony optimization algorithms". *IEEE Transactions on Evolutionary Computation*, 16(6):861–875, 2012. 69

[114] J. G. Vlachogiannis, N. D. Hatziargyriou, and K. Y. Lee. "ant colony system-based algorithm for constrained load flow problem". *IEEE Transactions on Power Systems*, 20(3):1241–49, 2005. 69

228

[115] J. Kennedy and R. Eberhart. Particle swarm optimization,. 4:1942–48, 1995. 71, 242

[116] A. Ruiz-Alvarez, A. Colet-Subirachs, F. F. Alvarez-Cuevas, O. Gomis-Bellmunt, and A. Sudria-Andreu. "operation of a utility connected microgrid using an IEC 61850-based multi-level management system". *IEEE Transactions on smart grid*, 3(2):858–65, 2012. 92, 104, 267, 270

[117] A. Colet-Subirachs, A. Ruiz-Álvarez, O. Gomis-Bellmunt, F. Álvarez-Cuevas-Figuerola, and A. Sudriá-Andreu. "centralized and distributed active and reactive power control of a utility connected microgrid using IEC 61850". *IEEE Systems Journal*, 6(1):58 –67, March 2012. 92, 104, 267, 270

[118] Lithium-ion (li-ion) battery system. Available at: `http://www.saftbatteries.com/Technologies/ Lithium/Liion/`. [accessed July 31, 2012]. 93

[119] Renewable energy concepts. Available at: `http://www.renewable-energy-concepts.com/wind -energy/wind-basics/wind-power.html`. [accessed July 31 2012]. 93

[120] Estacions automátiques (XEMA). Available at: `http://www.meteo.cat/xema/AppJava/SeleccioPerComarc a.do`. 93

[121] European photovoltaic solar energy conference and exhibition. Available at: `http://www.eupvsec-proceedings.com/`. [accessed July 31 2012]. 93

[122] Day-ahead energy market. Available at: `http://www.pjm.com/markets-and-operations/energy/ day-ahead.aspx`. [accessed July 31 2012]. 93

[123] Binod Shaw, V. Mukherjee, and S.P. Ghoshal. A novel opposition-based gravitational search algorithm for combined economic and emission dispatch problems of power systems. *International Journal of Electrical Power & Energy Systems*, 35(1):21–33, 2012. 237

[124] Soumitra Mondal, Aniruddha Bhattacharya, and Sunita Halder nee Dey. Multi-objective economic emission load dispatch solution using

Bibliography

gravitational search algorithm and considering wind power penetration. *International Journal of Electrical Power & Energy Systems*, 44(1):282–92, 2013. 237

[125] T. Niknam, M. Bornapour, and A. Gheisari. "combined heat, power and hydrogen production optimal planning of fuel cell power plants in distribution networks". *Energy Conversion and Management*, 66(0):11–25, 2013. 237

[126] R. Enayatifar, M. Yousefi, A. Hanan Abdullah, and A. Nordin Darus. "MOICA: A novel multi-objective approach based on imperialist competitive algorithm". *Applied Mathematics and Computation*, 219(1):8829–41, 2013. 239

[127] U. Kiliç and K. Ayan. "optimizing power flow of AC-DC power systems using artificial bee colony algorithm". *International Journal of Electrical Power & Energy Systems*, 53(0):592–602, 2013. 239

[128] P. Faria and Z. Vale. "demand response in electrical energy supply: An optimal real time pricing approach". *Energy*, 36(8):5374 – 5384, 2011. 241

[129] P. Faria, Z. Vale, J. Soares, and J. Ferreira. Demand response management in power systems using a particle swarm ptimization approach. *IEEE Intelligent Systems,*, PP(99):1–1, 2011. 241

[130] M. R. AlRashidi and M.E. El-Hawary. A survey of particle swarm optimization applications in electric power systems. *IEEE Transactions on Evolutionary Computation*, 13(4):913–918, 2009. 241

[131] Y Del Valle, G K Venayagamoorthy, S Mohagheghi, J C Hernandez, and R G Harley. Particle swarm optimization: Basic concepts, variants and applications in power systems. *IEEE Transactions on Evolutionary Computation,*, 12(2):171–195, 2008. 241, 242

[132] K Y Lee and M A Elsharkawi. *Modern Heuristic Optimization Techniques: Theory and Applications to Power Systems*. Wiley-Interscience, 2008. 241, 242

[133] V Miranda and N Fonseca. EPSO-evolutionary particle swarm optimization, a new algorithm with applications in power systems. In *IEEE/PES Transmission and Distribution Conference and Exhibition*, volume 2, pages 745–750 vol.2, 2002. 242

[134] A I Selvakumar and K Thanushkodi. A new particle swarm optimization solution to nonconvex economic dispatch problems. *IEEE Transactions on Power Systems,*, 22(1):42–51, 2007. 242

[135] F. Díaz-González, A. Sumper, O. Gomis-Bellmunt, and R.V. Robles. A review of energy storage technologies for wind power applications. *Renewable and Sustainable Energy Reviews,*, 16(4):2154 – 2171, 2012. 270

[136] IEC 61850 communication networks and systems for power utility automationpart 7-420: Basic communication structure-distributed energy resoruces logical nodes, 2009-03. 270

[137] A. Ruiz-Álvarez, A. Colet-Subirachs, O. Gomis-Bellmunt, and A. Sudriá-Andreu. Design, management and comissioning of a utility connected microgrid based on IEC 61850. In *Innovative Smart Grid Technologies Conference Europe (ISGT Europe)*, pages 1 –7, Gothenburg, Sweden, oct. 2010. 270

[138] A. Colet-Subirachs, A. Ruiz-Álvarez, O. Gomis-Bellmunt, F. Álvarez-Cuevas-Figuerola, and A. Sudriá-Andreu. Control of a utility connected microgrid. In *Innovative Smart Grid Technologies Conference Europe (ISGT Europe)*, pages 1 –7, Gothenburg, Sweden, oct. 2010. 270

[139] M. Roman-Barri, I. Cairo-Molins, A. Sumper, and A. Sudriá-Andreu. Experience on the implementation of a microgrid project in barcelona. In *Innovative Smart Grid Technologies Conference Europe (ISGT Europe)*, pages 1 –7, Gothenburg, Sweden, oct. 2010. 270

232

A
List of Publications

In this chapter, the list of publications both journals and conferences papers, derived from the development of the thesis are presented.

A.1 Journal articles

A.1.1 Published papers

[**J1**] **Marzband M**, Sumper A, Ruiz-Álvarez A, Domínguez-García J.L, Tomoiagă, B. Experimental Evaluation of a Real Time Energy Management System for Stand-Alone Microgrids in Day-Ahead Markets, Elsevier Applied Energy, 106(0) (2013), 365-376.

[**J2**] **Marzband M**, Sumper A, Domínguez-García J. L., Gumara-Ferret R., Experimental Validation of a Real Time Energy Managment System for Microgrids in Islanded Mode Using a Local Day-Ahead Electricity Market and MINLP. Elsevier Energy Conversion and Management, 76(0) (2013), 314-322.

[**J3**] **Marzband M**, Khaneh Zarrin R, Sumper A, Baghramian A, Economic Cost Analysis of Stand-Alone Hybrid Microgrids with Minimum COE Using Homer, Majlesi Journal of Electrical Engineering, 2(1) (2013), 1-7.

[**J4**] Tomoiagă B, Chindriç M, Sumper A, **Marzband M**, The Optimization of Microgrids Operation through a Heuristic Energy Management Algorithm, Advanced Engineering Forum, 8(185) (2013), 185-94.

A.1.2 Under review

[**J5**] **Marzband M**, Sumper A, Real time experimental implementation of optimum energy management system in standalone Microgrid by using Multi-layer Ant Colony Optimization, IEEE Transaction on Power Systems, FIRST REVIEW.

[**J6**] **Marzband M**, Sumper A, Domínguez-García J.L, An Experimental Study on Multi-dimension Gravitational Search Algorithm Based Optimization Approach for Energy Management in Islanded Microgrids, Elsevier Energy Conversion and Management.

[**J7**] **Marzband M**, Sumper A, Experimental evaluation of a Real-Time Energy Management System for Microgrids in Islanding Mode, IEEE Transaction on Smart Grid.

A.1.3 Under preparation

[**J8**] **Marzband M**, Tomoiagă B, Sumper A, Domínguez-García J.L, A pivot source based heuristic method for optimum real time energy management system for Microgrids in islanded mode.

[**J9**] **Marzband M**, Sumper A, The optimal programming of generation unit and demand response in an isolated Microgrid considering production cost reduction and MCP using multi-dimension artificial bee colony.

[**J10**] **Marzband M**, Sumper A, Demand side optimal management in an isolated Microgrid including renewable resources using multi-dimension imperialist competition.

A.2 Conference articles

[**C1**] **Marzband M**, Sumper A, Implementation of an Optimal Energy Management within Islanded Microgrid, ICREPQ′14, Cordoba, Spain.

[**C2**] **Marzband M**, Sumper A, Chindriç M, Tomoiagă B. Energy management system of hybrid microgrid with energy storage, EPE2012, WESC, Romania.

[**C3**] Tomoiagă B, Chindriç M, Sumper A, Sudria-Andreu A, **Marzband M**. Fuzzy Numbers Based Algorithm for Interruptions Frequency Estimation on Distribution Smart Grids, EPE2012, IASI, Romania.

[**C4**] **Marzband M**, Sumper A, Gomis-Bellmunt O, Sudria-Andreu A, Chindriç M. Modeling and simulation of the fixed speed wind power generation system for grid studies, EPQU2011, Lisbon, Portugal.

[**C5**] **Marzband M**, Sumper A, Gomis-Bellmunt O, Pezzini P, Chindriç M. Frequency control of isolated wind and diesel hybrid MicroGrid power system by using fuzzy logic controllers and PID controllers, EPQU2011, Lisbon, Portugal.

B

A review of selected optimization methods

A quick overview presented in this chapter will give enough information for some of the proposed optimization algorithm to compare their advantages and drawbacks.

B.1 Gravitational search algorithm (GSA)

Noting to the advantages of GSA method relative to other algorithms, optimization algorithm based on it has been developed in this thesis [123–125]. GSA is based on the Newton dynamics laws. According to these laws, there exists gravitational attractive force that this forces between the bodies in the world space. These forces have direct ratio with the product of their masses and inverse ratio with the square of the distance. The characteristics of GSA relative to the PSO and CFO population algorithms can be compared as follows:

1. GSA and PSO:

   a) GSA is an algorithm that includes a number of searching members that all of them can be given a value in different points of space and follow exploration in parallel in several working points. Whereas in the PSO algorithm exploration operation starts only from two points;

   b) GSA is without memory and the evaluation of the masses in each operation is updated after the moment that they are put in the

new position. As a result, it is possible that at the beginning, a mass has been the best but after t iterations its mass becomes zero and is eliminated from the space;

c) In PSO, the best position for any agent will be calculated only by using two parameters: pbest and gbest. But in GSA, the best position of each agent will be calculated by noting the total force obtained by the other agents;

d) In PSO, updating is done without considering the quality of solving the problem and the values of the fitnesses have no significance in the updating process; but, in GSA the force is proportional to the value of fitness. So, the agents see the search space around themselves effected by the force;

e) In PSO, updating is done without considering the distance between the solutions while in GSA the force has inverse ratio with the distance of the solutions;

2. GSA and CFO:

a) The main difference between these two methods is that CFO is inherently deterministic and no random parameter has been used in its formulas while GSA method is a stochastic search method and the values of the parameter changes randomly;

b) The relations related to the calculation of displacement, acceleration and calculation of the masses in GSA is different from the CFO method;

c) In CFO, the initial distribution of the probe (agent) is systematic (according to the deterministic nature of this method) and it doesnot have an important effect over the convergence of the algorithm while the initial distribution in GSA is random;

d) The G parameter in CFO is constant while in GSA, there is a controllable parameter.

B.2 Imperialist competition algorithm (ICA)

ICA has been introduced by Atachpaz and Lucas in 2007 based on the population and based on political and social evolution of the human society [101]. Similar to the other evolutionary algorithms, this algorithm also begins with an initial population that each part of this population is defined as a country

with attention to the assigned constraints for the considered problem. The countries are divided into two groups including colony and imperialist. One imperialist and their colonies make an empire. The basic concept of ICA is based on imperialist competition between the empires.

The struggle of the imperialists to obtain more colonies is called the imperialist completive process. Noting this process, the power of the more powerful and weaker empires gradually increases and reduce, respectively. If the empire looses all of its colonies, this empire will collapse. With the passing of time, the most powerful imperialist will remain in the world and all the countries will become the colony of this unique empire. Under such condition, the situation of the imperialist and the colonies will become the same [102, 126].

B.3 Artificial bee colony (ABC)

Artificial bee colony (ABC) is an evolutionary computational technique that has been first introduced by Caraboga 2005 [1]. This algorithm is based on the food finding behavior of the honey bees. Caraboga and Acay at 2009 have also evaluated the effectiveness of ABC over different test methods compared with other optimization algorithms including genetic algorithm particle swarm optimization (PSO), Differential Evaluation (DE) and evolution strategy. The results obtained from this evaluation states that although the ABC algorithm has less control parameters relative to other algorithms under study, its effectiveness and performance in finding near optimum points is much better than other algorithms [110]. Also, this algorithm is used in multi-modal optimum findings and multi-dimensional optimum finding, effectively [1, 110, 127]. The collective intelligence of honey bee is made up three main parts including food sources, worker searchers and idol searchers. The value of a food source depends on many factors such as its proximity to the nest, concentration and its richness of energy and facility of its extraction. For simplicity, the effect of these factors can be shown with one variable by the name of the profitability of food sources. Each one of the bees that have been considered as working searchers, belong to a specific source that are using them. These bees have with themselves information including distance and their position relative to the nest and the amount of profitability of food sources. This information are put in common use with other bees with special probability. Idol searchers are bees that are consistently searching a food source for using it. This class of bees are divided into two types: pioneers and spectators. Pioneer bees search new food sources

around the nest while spectators wait in the nest for receiving information about the food source from the working searching bees. The number of pioneer bees is on the average about 5 to 10 percent of spectators.

Exchanging information between the bees is the most important part of forming the knowledge of the collective intelligence of honey bee. Therefore, the most important part of beehive in which exchange of information regarding the quality and place of food source is taken place, is the beehive dancing salon. In this salon, the spectators can choose the food source with high profitability variable then can act for using it. Worker searching bees share the information related to food source in proportion to profitability of the source by dancing with spectators such that the duration of dancing is in proportion with the profitability of the source.

Figure B.1 has been presented graphically for the honey bee. As it is observed in the figure, two food sources called A and B have been found by working searchers. At the beginning, an idol searcher is considered. This searcher has no knowledge about the food sources around the nest and can get this information by using the following methods:

1. It can be a pioneer bee and can start finding food source around its nest by noting some internal motives and or external clue (route S);

2. It can be a spectator bee and can be sent toward food source after observing dance by worker ants (route R).

After finding the food source, idol searcher transforms into a worker searcher and by using its ability has kept its place and starts using the found food source. Then, transforms some of the nectar to the beehive and after discharging it chooses one of the following choices:

1. After cracking of the source, it transforms to a nonnumerous follower (UF route);

2. It puts the information at the disposal of spectators by dancing and convinces them to use the found food sources (EF1 route);

3. It continues its food searching without informing the other bees (EF2 route)

The significant point is that all the bees donot start searching simultaneously. New bees start searching at a rate proportional with the difference between the total number of the bees and the number of present searching bees.
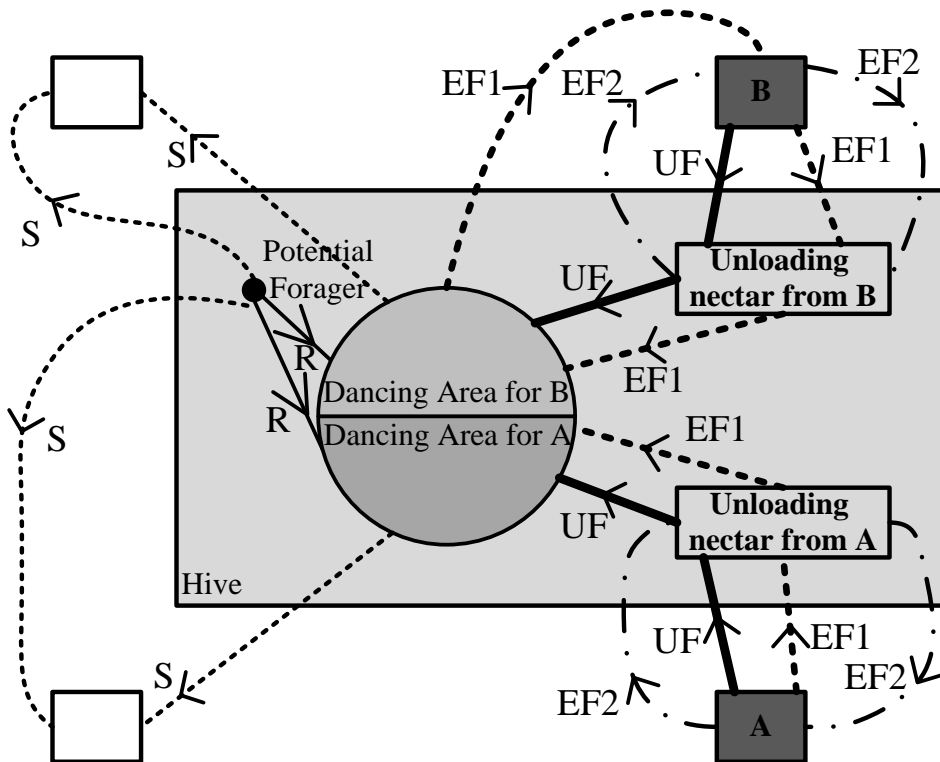
Figure B.1: The behavior of honey bee during searching nectar [1]

B.4 Particle swarm optimization (PSO)

PSO intelligent optimization methods have been used for solving some of the optimization problems in power systems with similar properties [128–132]. This method is a random search algorithm which is modeled from the social behavior of the flock of birds. Firstly, this optimization method was applied for discovering the governing models over the simultaneous flight of the birds, the sudden changes of their path as well as optimum deformation of the flock of birds. Then, this method was discussed for optimizing non-linear continuous functions and it was indicated that the PSO method is a super-innovative method based on the population that is used for finding the minimum of the object function. In this algorithm, each member of the society that is called particle, moves in the search space. The displacement of the particles in the search space is affected by their experience and knowledge and their neighbor′s knowledge. So, the position of the other particles

241

of a group affects the manner of a particle searching. Members in the group learn from each other and based on the knowledge obtained, they move toward their best neighbor. The PSO operation is based on this principle that in each moment, each member adjusts its location in the search space noting to the best place that is located in it up to now and the best place that exists in all of the neighbors of that member. In this method, an iteration process for improving the answer is executed and during this process the members of group repeatedly investigated the fitness of different cases of the candidate and gradually move toward best-position points. The best answer found by all the members of the group in each iteration is identified as the best position. Each of the group members put the found information at the disposal of their neighbor. So the members of the group are able to identify the positions that the other members have been successful in it. In fact, movement strategy in the search space is based on the global awareness and stand point of the positions of other neighbors and move toward a better region from the point of view of response. Some methodologies have been proposed in literature in order to implement PSO.

The classic PSO relies upon constant value of the particle velocity, inertia, memory and weights in whole of the search process of the birds flock (PSO iterations) [115, 132].

In order to prevail this limitation, some prescriptions of the PSO method have been suggested in the references [131, 133, 134]. Some of the prescriptions of PSO are mostly related to the solving of completely specified problems such as solving optimization problems with multi objective functions [29-31]. In this regard, the leap of the main parameters (including inertia, memory and cooperation) and selection by using disturbance theory has been suggested. This method has been named EPSO and its efficiency has been proven in the solving of several optimization problems. In this thesis, the repetition of particles for increasing the probability of finding more solutions that also can widen the diversity of the search space, has been evaluated.

In [134] a modification over the velocity equation has been suggested in order to involve the components related to the particle′s bad experience next to the best position.

Including the component of bad experience for remembering the best position that had obtained before the at present moment will help notiably. The method suggested in this thesis has been named NePSO. The author of the thesis has claimed the superirity of this method over the PSO classic method in properties such as convergence and robustness.

The execution time of this method is a little more compared to PSO

because of the need for more calculations in the search process related to the bad experience component of the particle.

No mutation process like EPSO has been considered in this method. Although, the possibility of the variation of the weights through the search process exists in EPSO by adding more diversity in it, the subject of particle velocity limitation during the iteration process still remains in its place. Sometimes, particle velocity variation can become better based on an intelligent mechanism, however the implemented mutation in EPSO is still done by using a disturbance process.

Previously presented works over PSO method can be summarized as follows:

- Making the algorithm compatible with the problem brought up.

- Presenting different topologies [16,10]

- With enhanced diversity.

- Presenting methods for changing the particle velocity at each time interval [11, 8].

- Presenting algorithms for solving discrete problems [7, 18].

243

Optimization Algorithms

C.1 MCEMS unit

Algorithm 4 CALCULATING OF SOC_t AND P_t^{ES} DURING CHARGING AND DISCHARGING PROCESS

Require: Generation units and load demand active power profiles, SOC_t, MG charactristic

1: **if** $(P_t^n \leq (P_t^{WT} + P_t^{PV})$ & $(SOC_t \leq \overline{SOC}))$ **then**

$$SOC_{t+1} = SOC_t \cdot (1 - \delta_t) + (I_t^{ES,c} \cdot \eta_c \cdot \Delta t)/C^{ES} \tag{C.1}$$

$$P_t^{Req} = (P_t^{WT} + P_t^{PV}) - P_t^n \tag{C.2}$$

$$I_t^{ES,c} = P_t^{Req}/V_t^{ES} \tag{C.3}$$

2:     subjected to:

$$P_t^{Req} \leq \bar{P}^{ES,c} \tag{C.4}$$

$$SOC_{t+1} \leq \overline{SOC} \tag{C.5}$$

$$V_t^{ES} \leq \overline{V}^{ES} \tag{C.6}$$

3: **end if**

Algorithm 4 (continued)

4: **if** $I_t^{ES,c} \leq \tilde{I}_t^{ES}$ **then**$I_t^{ES,c} = \tilde{I}_t^{ES}$
5:     Where:

$$\tilde{I}_t^{ES} = \max\{0, \min(\overline{I}^{ES,c}, \frac{\overline{SOC} - SOC_t}{\Delta(t)})\} \tag{C.7}$$

6: **else if** $P_t^n \geq (P_t^{WT} + P_t^{PV}) \ \& \ (SOC_t \geq \underline{SOC})$ **then**

$$SOC_{t+1} = SOC_t \cdot (1 - \delta_t) - (I_t^{ES,d} \cdot \Delta t)/C^{ES} \tag{C.8}$$

$$P_t^{Req} = P_t^n - (P_t^{WT} + P_t^{PV}) \tag{C.9}$$

$$I_t^{ES,d} = P_t^{Req}/V_t^{ES} \tag{C.10}$$

7:     subjected to:

$$P_t^{Req} \leq \bar{P}^{ES,d} \tag{C.11}$$

$$SOC_{t+1} \geq \underline{SOC} \tag{C.12}$$

$$V_t^{ES} \geq \underline{V}^{ES} \tag{C.13}$$

8:     **if** $I_t^{ES,d} \geq \tilde{\tilde{I}}_t^{ES}$ **then**$I_t^{ES,d} = \tilde{\tilde{I}}_t^{ES}$
9:         Where:

$$\tilde{\tilde{I}}_t^{ES} = \max\{0, \min(\overline{I}^{ES,d}, \frac{C^{ES} \cdot (SOC_t - \underline{SOC})}{\Delta(t)})\} \tag{C.14}$$

10:     **end if**
11: **end if**
12: **return** SOC_t and P_t^{ES}

Algorithm 5 MCEMS UNIT

Require: PV, WT and load demand profile of the MG, the initial SOC of ES and the characteristic of system as contained in Table 5.1.
1: *Initialization*
2: **for** $i \leftarrow 0 : 24$ **do**

$$P_t^{Req} = ((P_t^{WT} + P_t^{PV}) - P_t^n); \tag{C.15}$$

3:     **if** $P_t^{Req} \geq 0$ **then**
4:         **if** $SOC_t \geq \overline{SOC}$ **then**
5:             Go to **Fully Charged Mode**
6:             Exit the **for** loop
7:         **else if** $P_t^{Req} \geq \overline{P}^{ES,c}$ **then**

$$P_t^{ES} = \overline{P}^{ES,c}; \tag{C.16}$$

$$P_t^{EWH} = (P_t^{Req} - P_t^{ES}); \tag{C.17}$$

Algorithm 5 (continued)

8:          if $V_t^{ES} \geq \overline{V}^{ES}$ then

9:   Go to **Over charging protection mode**
     Exit the **for** loop

10:             **else**
11:                 Go to **Charging Mode**
12:                 Exit the **for** loop
13:             **end if**
14:         **end if**
15:     **else if** $SOC_t \leq \underline{SOC}$ **then**
16:         Go to **Fully Discharged Mode**
17:         Exit the **for** loop
18:     **else**

$$P_t^{Req} = \mid P_t^{Req} \mid;$$ (C.18)

19:         **if** $P_t^{Req} \geq \overline{P}^{ES,d}$ **then**

$$P_t^{ES} = \overline{P}^{ES,d};$$ (C.19)

$$P_t^{MT} = (P_t^{Req} - P_t^{ES});$$ (C.20)

20:         **end if**
21:         **if** $V_t^{ES} \leq \underline{V}^{ES}$ **then**

22:   Go to **Over Discharging Protection Mode**
     Exit the **for** loop

23:             **else**
24:                 Go to **Discharging Mode**
25:                 Exit the **for** loop
26:             **end if**
27:         **end if**
28: **end for**
29: **return** P_t^{ES}, P_t^{MT} and P_t^{EWH}

C.1.1 The mathematical implementation of DR unit

Algorithm 6 DR ᴜɴɪᴛ

Require: $P_t^{UP}, P_t^n, P_t^{EGP}, P_t^{EWH}$ *and DR*

$$DR = \sum_t P_t^{UP} + 20\% \ \times \ \sum_t P_t^n \tag{C.21}$$

$$t \in \{00:00, \cdots, 24:00\}$$

1: **if** $P_t^{UP} > 0$ **then**

$$P_t^{TCP} = P_t^n - P_t^{UP}; \tag{C.22}$$

$$P_t^{DR} = 0; \tag{C.23}$$

$$P_t^{EWH} = 0; \tag{C.24}$$

2: **else if** $P_t^{EGP} > 0$ **then**
3:     **if** $DR = 0$ **then**

Algorithm 6 (continued)

4:     **if** $(P_t^{EGP} - P_t^{ES,c}) \geq \overline{P}_t^{EWH}$ **then**

$$P_t^{EWH} = \overline{P}_t^{EWH}; \tag{C.25}$$

$$P_t^{DR} = P_t^{EGP} - P_t^{ES,c} - P_t^{EWH}; \tag{C.26}$$

$$P_t^{TCP} = P_t^n + P_t^{ES,c} + P_t^{DR} + P_t^{EWH}; \tag{C.27}$$

5:     **else**

$$P_t^{EWH} = P_t^{EGP} - P_t^{ES,c}; \tag{C.28}$$

$$P_t^{TCP} = P_t^n + P_t^{ES,c} + P_t^{EWH}; \tag{C.29}$$

6:     **end if**
7:   **else if** $(P_t^{EGP} - P_t^{ES,c}) \geq DR$ **then**

$$P_t^{DR} = DR; \tag{C.30}$$

$$P_t^{EWH} = P_t^{EGP} - P_t^{ES,c} - P_t^{DR}; \tag{C.31}$$

$$P_t^{TCP} = P_t^n + P_t^{ES,c} + P_t^{DR} + P_t^{EWH}; \tag{C.32}$$

$$DR = 0; \tag{C.33}$$

8:     **else**

$$P_t^{DR} = P_t^{EGP} - P_t^{ES,c}; \tag{C.34}$$

$$P_t^{EWH} = 0; \tag{C.35}$$

$$P_t^{TCP} = P_t^n + P_t^{ES,c} + P_t^{DR}; \tag{C.36}$$

$$DR = DR - (P_t^{EGP} - P_t^{ES,c}); \tag{C.37}$$

9:     **end if**
10: **end if**
11: **return** P_t^{DR}, P_t^{TCP} *and* P_t^{EWH}

C.2 PSB unit

Algorithm 7 PSB UNIT

Require: PV, WT and load demand profile of the MG, the initial SOC of ES and the characteristic of system.

Initialization

for $t = 0 : 24$ **do**

- **sort** *ascendant the sources list by the criterion of energy price*
- **find** the **PivotSource**
- **if PivotSource** *is* **renewable***: use the entire potential*
    1. **if** $E_t^{ES} \leq \overline{E}^{ES}$ (Eq. (4.10)): *charge the ES*
    2. **if** *power balance (Eq. (4.11)) is not satisfied:*
        - *Start to increase/decrease the consumed power of RLD*
- **if PivotSource** *is not* **renewable***: try to do not use this source*
    1. **if** $E_t^{ES} \geq \underline{E}^{ES}$ (Eq. (4.10)): **and** *the load demand is covered: discharge the ES*
    2. **else** *: use this PivotSource*
        a) **if** $E_t^{ES} \leq \overline{E}^{ES}$ *(Eq. (4.10)): charge the ES*
        b) **if** *power balance (Eq. (4.11)) is not satisfied:*
            - *Start to increase/decrease the consumed power of RLD*

end for

C.3 MICA unit

Algorithm 8 MICA UNIT

Require: PV, WT and load demand profile of the MG, the initial SOC of ES and the characteristic of system.

Initialization

for $t = 0 : 24$ **do**   ▷ cycle 1

    1. k = 1;

                                                        ▷ cycle 2

        a) *creating a random value for the problem independent variables by noting their minimum and maximum value;*

        b) *creating a random value for the problem dependent variables with attention to independent variables information and the problem constraints;*

        c) *creation of a country using the variable values in a $1 \times N_{var}$ matrix (Eq. 4.13);*

        d) *the calculation of the created country cost (Eq. 2.10);*

        e) k + 1

    2. *until $k < N_{pop}$ is held cycle 2 shall be done;*

    3. *the ascending grouping of the countries based on their expense;*

    4. *selecting N_{imp} so the best member of the population that have the least expense are used as imperialist and allocating the rest of the created population as colony;*

    5. *dividing the colonies between the imperialist (Eq. 4.16- 4.18);*

    6. *decade = 1;*

                           ▷ cycle 3   ▷ cycle 4

        a) *selecting the ith empire;*   ▷ cycle 5

            i. *selecting the jth colony from the ith empire;*

            ii. *the movement of the jth colony toward its imperialist and reaching the new position;*

            iii. *if the balance constraint was not held;*

            iv. *reestablishing balance;*

            v. *the end of the condition;*

            vi. *calculating the cost of the new position of the jth colony (Eq. 2.10);*

        b) *as long as all the colonies of empire i^{th} are chosen cycle 5 shall be done;*

    7. *as long as all the empires are chosen cycle 4 shall be done;*   ▷ cycle 6

    8. *choosing the ith empire;*   ▷ cycle 7

        a) *selecting the jth colony from the ith empire;*

        b) *creating a random number;*

        c) *if revolution rate was less than $P_{revolution}$;*

            i. *creating a random value for the problem independent variables by noting their minimum and maximum value;*

            ii. *creating a random value for the problem dependent variables with attention to independent variables information and the problem constraints;*

            iii. *creation of a country putting the created values for the problem variables in a matrix $1 \times N_{var}$ (Eq. 4.13);*

            iv. *calculating the cost of the new position of the jth colony (Eq. 2.10);*

    9. *until when all the colonies of the ith empire are chosen cycle 7 shall be done;*

        a) *until when all the empires are chosen cycle 6 shall be done;*   ▷ cycle 8

        b) *choosing the ith empire;*

        c) *if a colony in the ith empire exists that has less expense than its imperialist;*

            i. *the position of colony and the imperialist changes;*

            ii. *end of condition;*

        d) *until when all the empires are chosen cycle 8 must be done;*

        e) *calculating the total power of all the empires;*

        f) *choosing the weakest empire;*

        g)   **if** *the weakest empire has a colony* **then**

            i. *choosing the weakest colony of this empire;*

            ii. *choosing an empire by the roulette cycle;*

            iii. *allocating the weakest colony to the chosen empire;*

        h)   **else**

            i. *choosing an empire by the roulette cycle;*

            ii. *allocating the weak empire to the chosen empire;*

            iii. *end of the condition;*

        i)   **end if**

        j) *decade = Decade + 1;*

    10. *until when $D < maxdecade$, cycle 3 must be done;*

    11. *imperialist with the least expense must be considered as the best response then send to memory;*

    12. *t = t +1;*   251

end for

C.4 MABC unit

Algorithm 9 $MABC$ UNIT

Require: PV, WT and load demand profile of the MG, the initial SOC of ES and the characteristic of system.
Initialization (control parameters and the problem parameters)
for $t = 0 : 24$ **do**

    1. *generating the initial population (Eq.(4.24))*

    2. *evaluating the fitness of the population (Eq.(2.10))*

    3. $Cycle = 1$

    4.   **while** $Cycle < MCN$ **do**

    5.   ▷ for each employed bee

        a) generating a new response (Eq.(4.25)) and checking the constraints
        b) calculating fitness (Eq.(2.10))
        c) applying greedy process

    6. *calculating the probability value P_t^i for the responses (Eq.(4.26))*

    7.   ▷ for each onlooker

        a) choosing a response by noting P_t^i
        b) generating new response (Eq.(4.25)) and checking the constraints
        c) calculating the fitness (Eq.(2.10))
        d) applying greedy process

    8. *leaving exhausted sources by the bees according to Limit*

    9.   ▷ pioneer bee (if left out source existed)

        a) generating a new random response (Eq.(4.27))
        b) replacing the left out response with new response
        c) calculating the fitness (Eq.(2.10))

   10. *remembering the best response that is found up to now*

   11. $Cycle = Cycle + 1$

   12.   **end while**

end for

C.5 MACO unit

Algorithm 10 EMS-MACO UNIT

Require: PV, WT and load demand profile of the MG, the initial SOC of ES and the characteristic of system as contained in Table 5.1.
1: *Initialization*
2: **for** $t \leftarrow 0 : 24$ **do**
3:     **if** $P_t^{PV} \leq (P_t^{WT} + P_t^{PV})$ **then**

$$P_t^{Req} = (P_t^{WT} + P_t^{PV}) - P_t^n; \tag{C.38}$$

4:         **if** $SOC_t \leq \overline{SOC}$ **then**
5:             **if** $P_t^{Req} \leq \overline{P}^{ES,c}$ **then**
6:                 **if** $(E_t^{ES} + P_t^{Req} \times \Delta t) \leq \overline{E}^{ES}$ **then**

$$P_t^{ES,c} = P_t^{Req}; \tag{C.39}$$

$$P_t^{ES,d} = P_t^{MT} = P_t^{EWH} = 0; \tag{C.40}$$

7:                 **else**

$$P_t^{ES,c} = \frac{[\overline{E}^{ES} - E_t^{ES}]}{\Delta t}; \tag{C.41}$$

$$P_t^{ES,d} = P_t^{MT} = 0; \tag{C.42}$$

$$P_t^{EWH} = P_t^{Req} - P_t^{ES,c}; \tag{C.43}$$

8:                 **end if**
9:             **else if** $((E_t^{ES} + \overline{P}^{ES,c}) \times \Delta t) \leq \overline{E}^{ES}$ **then**

$$P_t^{ES,c} = \overline{P}^{ES,c}; \tag{C.44}$$

$$P_t^{ES,d} = P_t^{MT} = 0; \tag{C.45}$$

$$P_t^{EWH} = P_t^{Req} - \overline{P}^{ES,c}; \tag{C.46}$$

10:             **else**

$$P_t^{ES,c} = \frac{[\overline{E}^{ES} - E_t^{ES}]}{\Delta t}; \tag{C.47}$$

$$P_t^{ES,d} = P_t^{MT} = 0; \tag{C.48}$$

$$P_t^{EWH} = P_t^{Req} - P_t^{ES,c}; \tag{C.49}$$

11:             **end if**
12:         **else**

$$P_t^{ES,d} = P_t^{ES,c} = P_t^{MT} = 0; \tag{C.50}$$

$$P_t^{EWH} = P_t^{Req}; \tag{C.51}$$

13:         **end if**

$$P_t^{Req} = P_t^n - (P_t^{WT} + P_t^{PV}); \tag{C.52}$$

253

Algorithm 10 (continued)

14:   **else if** $SOC_t \leq \underline{SOC}$ **then**
15:     **if** $P_t^{Req} \leq \underline{P}^{MT}$ **then**
16:       **if** $(\underline{P}^{MT} - P_t^{Req}) \leq \overline{P}^{ES,c}$ **then**

$$P_t^{ES,c} = \overline{P}^{ES,c};\tag{C.53}$$

$$P_t^{ES,d} = 0;\tag{C.54}$$

$$P_t^{MT} = \underline{P}^{MT};\tag{C.55}$$

$$P_t^{EWH} = \underline{P}^{MT} - \overline{P}^{ES,c} - P_t^{Req};\tag{C.56}$$

17:       **else**
$$P_t^{ES,c} = \underline{P}^{MT} - P_t^{Req};\tag{C.57}$$

$$P_t^{ES,d} = P_t^{EWH} = 0;\tag{C.58}$$

$$P_t^{MT} = \underline{P}^{MT};\tag{C.59}$$

18:       **end if**
19:     **else if** $P_t^{Req} + \overline{P}^{ES,c} \leq 1$ **then**

$$P_t^{ES,c} = \overline{P}^{ES,c};\tag{C.60}$$

$$P_t^{ES,d} = P_t^{EWH} = 0;\tag{C.61}$$

$$P_t^{MT} = P_t^{Req} + \overline{P}^{ES,c};\tag{C.62}$$

20:     **else if** $P_t^{Req} \leq \overline{P}^{MT}$ **then**
$$P_t^{ES,c} = \overline{P}^{MT} - P_t^{Req};\tag{C.63}$$

$$P_t^{ES,d} = P_t^{EWH} = 0;\tag{C.64}$$

$$P_t^{MT} = \overline{P}^{MT};\tag{C.65}$$

21:     **else**
$$P_t^{ES,c} = P_t^{ES,d} = P_t^{EWH} = 0;\tag{C.66}$$

$$P_t^{MT} = \overline{P}^{MT};\tag{C.67}$$

22:     **end if**
23:   **else if** $P_t^{Req} \leq \overline{P}^{ES,d}$ **then**
24:     **if** $(E_t^{ES} - P_t^{Req} \times \Delta t) \geq \underline{E}^{ES}$ **then**

$$P_t^{ES,c} = P_t^{MT} = P_t^{EWH} = 0;\tag{C.68}$$

$$P_t^{ES,d} = P_t^{Req};\tag{C.69}$$

Algorithm 10 (continued)

25:        **else if** $(E_t^{ES} + \overline{P}^{ES,c} \times \Delta t) \leq 1$ **then**
26:            **if** $(\frac{E_t^{ES}}{\Delta t} + \overline{P}^{ES,c}) \leq \underline{P}^{MT}$ **then**

$$P_t^{ES,c} = \overline{P}^{ES,c}; \tag{C.70}$$

$$P_t^{ES,d} = 0; \tag{C.71}$$

$$P_t^{MT} = \underline{P}^{MT}; \tag{C.72}$$

$$P_t^{EWH} = \underline{P}^{MT} - P_t^{Req} - P_t^{ES,c}; \tag{C.73}$$

27:            **else if** $(P_t^{Req} + \overline{P}^{ES,c}) \leq \overline{P}^{MT}$ **then**

$$P_t^{ES,c} = \overline{P}^{ES,c}; \tag{C.74}$$

$$P_t^{ES,d} = P_t^{EWH} = 0; \tag{C.75}$$

$$P_t^{MT} = P_t^{Req} + P_t^{ES,c}; \tag{C.76}$$

28:            **else if** $P_t^{Req} \leq \overline{P}^{MT}$ **then**

$$P_t^{ES,c} = \overline{P}^{MT} - P_t^{Req}; \tag{C.77}$$

$$P_t^{ES,d} = P_t^{MT} = P_t^{EWH} = 0; \tag{C.78}$$

29:            **else if** $(P_t^{Req} - \overline{P}^{MT}) \leq (E_t^{ES} + \underline{E}^{ES}) \times \Delta t$ **then**

$$P_t^{ES,d} = P_t^{Req} - \overline{P}^{MT}; \tag{C.79}$$

$$P_t^{ES,c} = P_t^{EWH} = 0; \tag{C.80}$$

$$P_t^{MT} = \overline{P}^{MT}; \tag{C.81}$$

30:            **else**

$$P_t^{ES,d} = \frac{E_t^{ES} - \underline{E}^{ES}}{\Delta t}; \tag{C.82}$$

$$P_t^{ES,c} = P_t^{EWH} = 0; \tag{C.83}$$

$$P_t^{MT} = \overline{P}^{MT}; \tag{C.84}$$

31:            **end if**
32:        **else if** $(P_t^{Req} + \frac{(\overline{E}^{ES} - E_t^{ES})}{\Delta t}) \leq \underline{P}^{MT}$ **then**

$$P_t^{ES,c} = \frac{\overline{E}^{ES} - E_t^{ES}}{\Delta t}; \tag{C.85}$$

$$P_t^{ES,d} = 0; \tag{C.86}$$

$$P_t^{MT} = \underline{P}^{MT}; \tag{C.87}$$

$$P_t^{EWH} = \underline{P}^{MT} - P_t^{Req} - P_t^{ES,c}; \tag{C.88}$$

Algorithm 10 (continued)

33:      **else if** $(P_t^{Req} + \frac{(\overline{E}^{ES} - E_t^{ES})}{\Delta t}) \leq \overline{P}^{MT}$ **then**

$$P_t^{ES,c} = \frac{\overline{E}^{ES} - E_t^{ES}}{\Delta t}; \qquad \qquad \text{(C.89)}$$

$$P_t^{ES,d} = P_t^{EWH} = 0; \qquad \qquad \text{(C.90)}$$

$$P_t^{MT} = P_t^{Req} + P_t^{ES,c}; \qquad \qquad \text{(C.91)}$$

34:      **else if** $P_t^{Req} \leq \overline{P}^{MT}$ **then**

$$P_t^{ES,c} = \overline{P}^{MT} - P_t^{Req}; \qquad \qquad \text{(C.92)}$$

$$P_t^{ES,d} = P_t^{EWH} = 0; \qquad \qquad \text{(C.93)}$$

$$P_t^{MT} = \overline{P}^{MT}; \qquad \qquad \text{(C.94)}$$

35:      **else if** $(P_t^{Req} - \overline{P}^{MT}) \leq \frac{E_t^{ES} - \underline{E}^{ES}}{\Delta t}$ **then**

$$P_t^{ES,d} = P_t^{Req} - \overline{P}^{MT}; \qquad \qquad \text{(C.95)}$$

$$P_t^{ES,c} = P_t^{EWH} = 0; \qquad \qquad \text{(C.96)}$$

$$P_t^{MT} = \overline{P}^{MT}; \qquad \qquad \text{(C.97)}$$

36:      **else**

$$P_t^{ES,d} = \frac{E_t^{ES} - \underline{E}^{ES}}{\Delta t} \qquad \qquad \text{(C.98)}$$

$$P_t^{ES,c} = P_t^{EWH} = 0; \qquad \qquad \text{(C.99)}$$

$$P_t^{MT} = \overline{P}^{MT}; \qquad \qquad \text{(C.100)}$$

37:      **end if**
38:   **else if** $(P_t^{Req} - \underline{P}^{MT}) \leq \overline{P}^{ES,d}$ **then**
39:      **if** $E_t^{ES} - \frac{(P_t^{Req} - \underline{P}^{MT})}{\Delta t} \geq \underline{E}^{ES}$ **then**

$$P_t^{ES,d} = P_t^{Req} - \underline{P}^{MT}; \qquad \qquad \text{(C.101)}$$

$$P_t^{ES,c} = P_t^{EWH} = 0; \qquad \qquad \text{(C.102)}$$

$$P_t^{MT} = \underline{P}^{MT}; \qquad \qquad \text{(C.103)}$$

40:      **else if** $E_t^{ES} + \overline{P}^{ES,c} \times \Delta t \leq \overline{E}^{ES}$ **then**
41:         **if** $(P_t^{Req} - \overline{P}^{ES,c}) \leq \underline{P}^{MT}$ **then**

$$P_t^{ES,c} = \overline{P}^{ES,c}; \qquad \qquad \text{(C.104)}$$

$$P_t^{ES,d} = 0; \qquad \qquad \text{(C.105)}$$

$$P_t^{MT} = \underline{P}^{MT}; \qquad \qquad \text{(C.106)}$$

$$P_t^{EWH} = \underline{P}^{MT} - P_t^{Req} - P_t^{ES,c}; \qquad \qquad \text{(C.107)}$$

Algorithm 10 (continued)

42:      **else if** $P_t^{Req} + \overline{P}^{ES,c} \leq \overline{P}^{MT}$ **then**

$$P_t^{ES,c} = \overline{P}^{ES,c}; \tag{C.108}$$

$$P_t^{ES,d} = P_t^{EWH} = 0; \tag{C.109}$$

$$P_t^{MT} = P_t^{Req} + \overline{P}^{ES,c}; \tag{C.110}$$

43:      **else if** $P_t^{Req} \leq \overline{P}^{MT}$ **then**

$$P_t^{ES,c} = \overline{P}^{MT} - P_t^{Req}; \tag{C.111}$$

$$P_t^{ES,d} = P_t^{EWH} = 0; \tag{C.112}$$

$$P_t^{MT} = \overline{P}^{MT}; \tag{C.113}$$

44:      **else if** $(P_t^{Req} - \overline{P}^{MT}) \leq \frac{E_t^{ES} - \underline{E}^{ES}}{\Delta t}$ **then**

$$P_t^{ES,d} = P_t^{Req} - \overline{P}^{MT}; \tag{C.114}$$

$$P_t^{ES,c} = P_t^{EWH} = 0; \tag{C.115}$$

$$P_t^{MT} = \overline{P}^{MT}; \tag{C.116}$$

45:      **else**

$$P_t^{ES,d} = \frac{E_t^{ES} - \underline{E}^{ES}}{\Delta t}; \tag{C.117}$$

$$P_t^{ES,c} = P_t^{EWH} = 0; \tag{C.118}$$

$$P_t^{MT} = \overline{P}^{MT}; \tag{C.119}$$

46:      **end if**

47:    **else if** $P_t^{Req} + \frac{\overline{E}^{ES} - E_t^{ES}}{\Delta t} \leq \underline{P}^{MT}$ **then**

$$P_t^{ES,c} = \frac{\overline{E}^{ES} - E_t^{ES}}{\Delta t}; \tag{C.120}$$

$$P_t^{ES,d} = 0; \tag{C.121}$$

$$P_t^{MT} = \underline{P}^{MT}; \tag{C.122}$$

$$P_t^{EWH} = \underline{P}^{MT} - P_t^{Req} - \overline{P}^{ES,c}; \tag{C.123}$$

48:    **else if** $P_t^{Req} + \frac{\overline{E}^{ES}}{\Delta t} \leq \overline{P}^{MT}$ **then**

$$P_t^{ES,c} = \frac{\overline{E}^{ES} - E_t^{ES}}{\Delta t}; \tag{C.124}$$

$$P_t^{ES,d} = P_t^{EWH} = 0; \tag{C.125}$$

$$P_t^{MT} = P_t^{Req} + \overline{P}^{ES,c}; \tag{C.126}$$

49:    **else if** $P_t^{Req} \leq \overline{P}^{MT}$ **then**

$$P_t^{ES,c} = \overline{P}^{MT} - P_t^{Req}; \tag{C.127}$$

$$P_t^{ES,d} = P_t^{EWH} = 0; \tag{C.128}$$

$$P_t^{MT} = \overline{P}^{MT}; \tag{C.129}$$

Algorithm 10 (continued)

50:     **else if** $(P_t^{Req} - \overline{P}^{MT}) \leq \frac{E_t^{ES} - \underline{E}^{ES}}{\Delta t}$ **then**

$$P_t^{ES,d} = P_t^{Req} - \overline{P}^{MT};$$

(C.130)

$$P_t^{ES,c} = P_t^{EWH} = 0;$$

(C.131)

$$P_t^{MT} = \overline{P}^{MT};$$

(C.132)

51:     **else**

$$P_t^{ES,d} = \frac{E_t^{ES} - \underline{E}^{ES}}{\Delta t};$$

(C.133)

$$P_t^{ES,c} = P_t^{EWH} = 0;$$

(C.134)

$$P_t^{MT} = \overline{P}^{MT};$$

(C.135)

52:     **end if**
53: **else if** $(E_t^{ES} + \overline{P}^{ES,c} \times \Delta t) \leq \overline{E}^{ES}$ **then**
54:     **if** $(P_t^{Req} - \overline{P}^{ES,c}) \leq \overline{P}^{MT}$ **then**

$$P_t^{ES,c} = \overline{P}^{ES,c};$$

(C.136)

$$P_t^{ES,d} = P_t^{EWH} = 0;$$

(C.137)

$$P_t^{MT} = P_t^{Req} + P_t^{ES,c};$$

(C.138)

55:     **else if** $P_t^{Req} \leq \overline{P}^{MT}$ **then**

$$P_t^{ES,c} = \overline{P}^{MT} - P_t^{Req};$$

(C.139)

$$P_t^{ES,d} = P_t^{EWH} = 0;$$

(C.140)

$$P_t^{MT} = \overline{P}^{MT};$$

(C.141)

56:     **else if** $(P_t^{Req} - \overline{P}^{MT}) \leq \frac{E_t^{ES} - \underline{E}^{ES}}{\Delta t}$ **then**

$$P_t^{ES,d} = P_t^{Req} - \overline{P}^{MT};$$

(C.142)

$$P_t^{ES,c} = P_t^{EWH} = 0;$$

(C.143)

$$P_t^{MT} = \overline{P}^{MT};$$

(C.144)

57:     **else**

$$P_t^{ES,d} = \frac{E_t^{ES} - \underline{E}^{ES}}{\Delta t};$$

(C.145)

$$P_t^{ES,c} = P_t^{EWH} = 0;$$

(C.146)

$$P_t^{MT} = \overline{P}^{MT};$$

(C.147)

58:     **end if**
59: **else if** $(P_t^{Req} + P_t^{ES,c}) \leq \overline{P}^{MT}$ **then**

$$P_t^{ES,c} = \frac{\overline{E}^{ES} - E_t^{ES}}{\Delta t};$$

(C.148)

$$P_t^{ES,d} = P_t^{EWH} = 0;$$

(C.149)

$$P_t^{MT} = P_t^{Req} + P_t^{ES,c};$$

(C.150)

Algorithm 10 (continued)

60:    **else if** $P_t^{Req} \leq \overline{P}^{MT}$ **then**

$$P_t^{ES,c} = \overline{P}^{MT} - P_t^{Req}; \qquad\qquad\qquad\text{(C.151)}$$

$$P_t^{ES,d} = P_t^{EWH} = 0; \qquad\qquad\qquad\text{(C.152)}$$

$$P_t^{MT} = \overline{P}^{MT}; \qquad\qquad\qquad\text{(C.153)}$$

61:    **else if** $(P_t^{Req} - \overline{P}^{MT}) \leq \frac{E_t^{ES} - \underline{E}^{ES}}{\Delta t}$ **then**

$$P_t^{ES,d} = P_t^{Req} - \overline{P}^{MT}; \qquad\qquad\qquad\text{(C.154)}$$

$$P_t^{ES,c} = P_t^{EWH} = 0; \qquad\qquad\qquad\text{(C.155)}$$

$$P_t^{MT} = \overline{P}^{MT}; \qquad\qquad\qquad\text{(C.156)}$$

62:    **else**

$$P_t^{ES,d} = \frac{E_t^{ES} - \underline{E}^{ES}}{\Delta t}; \qquad\qquad\qquad\text{(C.157)}$$

$$P_t^{ES,c} = P_t^{EWH} = 0; \qquad\qquad\qquad\text{(C.158)}$$

$$P_t^{MT} = \overline{P}^{MT}; \qquad\qquad\qquad\text{(C.159)}$$

63:    **end if**

$$E_{t+1}^{ES} = E_t^{ES} + (P_t^{ES,c} - P_t^{ES,d}) \times \Delta t); \qquad\qquad\qquad\text{(C.160)}$$

$$SOC_{t+1} = \frac{E_{t+1}^{ES}}{E_{Tot}^{ES}}; \qquad\qquad\qquad\text{(C.161)}$$

64: **end for**
65:

Algorithm 11 DR UNIT

1: **for** $t \leftarrow 0 : 24$ **do**

$$P_t^{UP} = (P_t^n + P_t^{EWH} + P_t^{ES,c}) - (P_t^{WT} + P_t^{PV} + P_t^{MT} + P_t^{ES,d}); \qquad (\text{C.162})$$

2: **end for**

$$DR = \sum_t P_t^{UP}; \qquad (\text{C.163})$$

3: **for** $t \leftarrow 0 : 24$ **do**
4:     **if** $P_t^{Req} \leq (P_t^{WT} + P_t^{PV})$ **then**

$$P_t^{Req} = P_t^{PV} + P_t^{WT} - P_t^n; \qquad (\text{C.164})$$

5:       **if** $SOC_t \leq \overline{SOC}$ **then**
6:         **if** $P_t^{Req} \leq \overline{P}^{ES,c}$ **then**
7:           **if** $(E_t^{ES} + P_t^{Req} \times \Delta(t)) \leq \overline{E}^{ES}$ **then**

$$E_t^{ES,c} = P_t^{Req}; \qquad (\text{C.165})$$

$$P_t^{ES,d} = P_t^{MT} = P_t^{EWH} = 0; \qquad (\text{C.166})$$

8:           **else if** $DR \geq (P_t^{Req} - P_t^{ES,c}$ **then**

$$E_t^{ES,c} = \frac{\overline{E}^{ES} - E_t^{ES}}{\Delta(t)}; \qquad (\text{C.167})$$

$$P_t^{ES,d} = P_t^{MT} = P_t^{EWH} = 0; \qquad (\text{C.168})$$

$$P_t^{DR} = P_t^{Req} - P_t^{ES,c}; \qquad (\text{C.169})$$

$$DR = DR - (P_t^{Req} - P_t^{ES,c}); \qquad (\text{C.170})$$

9:           **else**

$$E_t^{ES,c} = \frac{\overline{E}^{ES} - E_t^{ES}}{\Delta(t)}; \qquad (\text{C.171})$$

$$P_t^{EWH} = P_t^{Req} - P_t^{ES,c} - DR; \qquad (\text{C.172})$$

$$P_t^{DR} = DR; \qquad (\text{C.173})$$

$$P_t^{ES,d} = P_t^{MT} = DR = 0; \qquad (\text{C.174})$$

10:           **end if**
11:         **else if** $(E_t^{ES} + \overline{P}^{ES,c} \times \Delta(t)) \leq \overline{E}^{ES}$ **then**
12:           **if** $DR \geq (P_t^{Req} - P_t^{ES,c})$ **then**

$$E_t^{ES,c} = \overline{P}^{ES,c}; \qquad (\text{C.175})$$

$$P_t^{ES,d} = P_t^{MT} = P_t^{EWH} = 0; \qquad (\text{C.176})$$

$$P_t^{DR} = P_t^{Req} - P_t^{ES,c}; \qquad (\text{C.177})$$

$$DR = P_t^{DR} - (P_t^{Req} - P_t^{ES,c}); \qquad (\text{C.178})$$

Algorithm 11 (continued)

13:                else
$$E_t^{ES,c} = \overline{P}^{ES,c}; \qquad (C.179)$$

$$P_t^{EWH} = P_t^{Req} - P_t^{ES,c} - DR; \qquad (C.180)$$

$$P_t^{ES,d} = P_t^{MT} = P_t^{EWH} = 0; \qquad (C.181)$$

$$P_t^{DR} = DR; \qquad (C.182)$$

$$P_t^{ES,d} = P_t^{MT} = DR = 0; \qquad (C.183)$$

14:            **end if**
15:            **else if** $DR \geq (P_t^{Req} - P_t^{ES,c})$ **then**

$$P_t^{ES,c} = \frac{(\overline{E}^{ES} - E_t^{ES})}{\Delta(t)}; \qquad (C.184)$$

$$P_t^{ES,d} = P_t^{MT} = P_t^{EWH} = 0; \qquad (C.185)$$

$$P_t^{DR} = P_t^{Req} - P_t^{ES,c}; \qquad (C.186)$$

$$DR = DR - (P_t^{Req} + P_t^{ES,c}); \qquad (C.187)$$

16:                else
$$P_t^{ES,c} = \overline{P}^{ES,c}; \qquad (C.188)$$

$$P_t^{EWH} = P_t^{Req} - P_t^{ES,c} - DR; \qquad (C.189)$$

$$P_t^{DR} = DR; \qquad (C.190)$$

$$P_t^{ES,d} = P_t^{MT} = DR = 0; \qquad (C.191)$$

17:            **end if**
18:            **else if** $DR \geq (P_t^{Req} - P_t^{ES,c})$ **then**

$$P_t^{ES,c} = P_t^{ES,d} = P_t^{MT} = P_t^{EWH} = 0; \qquad (C.192)$$

$$P_t^{DR} = P_t^{Req}; \qquad (C.193)$$

$$DR = P_t^{DR} - P_t^{Req}; \qquad (C.194)$$

19:        else
$$P_t^{EWH} = P_t^{Req} - DR; \qquad (C.195)$$

$$P_t^{DR} = DR; \qquad (C.196)$$

$$P_t^{ES,c} = P_t^{ES,d} = P_t^{MT} = P_t^{EWH} = 0; \qquad (C.197)$$

20:            **end if**
21:    **else**
22:        Exit the **for** loop
23:    **end if**

$$E_{t+1}^{ES} = E_t^{ES} + (P_t^{ES,c} - P_t^{ES,d}) \times \Delta(t); \qquad (C.198)$$

$$SOC_{t+1} = \frac{E_{t+1}^{ES}}{E_{Tot}^{ES}}; \qquad (C.199)$$

$$OF = OF + Eq. \ (2.10) \qquad (C.200)$$

24: **end for**
25: **return** P_t^{ES}, P_t^{MT}, P_t^{DR} and P_t^{EWH}

Algorithm 12 MACO UNIT

Require: $P_t^{WT}, P_t^{PV}, P_t^{ES}, P_t^{MT}, P_t^{EWH}, P_t^n, P_t^{DR}$

1: *Initialization*   ▷ Definition of pheromone, ρ, λ, $\Sigma\rho$ matrixes
2: Nant = 1000;   ▷ Nant: Number of Ants
3: Maxit = 50;   ▷ Maxit: Maximum iteration limit

$$\Sigma pheromone = \sum pheromone; \tag{C.201}$$

4: **for** $It = 1 : Maxit$ **do**   ▷ It: Number of iteration
5:   **for** $t = 1 : \frac{24}{\Delta(t)}$ **do**   ▷ $\Delta(t)$: depend on pre-defined index intervals
6:    **for** $i = 1 : 11$ **do**   ▷ i: is a counter for allowable values

$$\rho_t^i = pheromone_t^i./\Sigma pheromone_t; \tag{C.202}$$

         ▷ ρ: Probability selection on the allowable values

7:    **end for**

$$\Sigma\rho_t^1 = \rho_t^1; \tag{C.203}$$

8:    **for** $i = 1 : 11$ **do**

$$\Sigma\rho_t^i = \rho_t^i + \Sigma\rho_t^{i-1}; \tag{C.204}$$

9:    **end for**
10:   **for** $k = 1 : Nant$ **do**

$$\lambda(k) = Rand; \tag{C.205}$$

   ▷ Rand is an uniformly distributed pseudorandom numbers on the open interval (0,1)
11:          ▷ λ: position of ant at each iteration
12:    **if** $\lambda(k) \leq \rho_t^{i-1} \& \lambda(k) \leq \rho_t^i$ **then**

$$X_t^k = MPESc_t^i; \tag{C.206}$$

▷ MPESc: A matrix for ES during charging operation mode with i^{th} allowable value at time t

$$Y_t^k = MPEWH_t^i; \tag{C.207}$$

$$Z_t^k = MPMT_t^i; \tag{C.208}$$

$$W_t^k = MPESd_t^i; \tag{C.209}$$

$$V_t^k = MPDR_t^i; \tag{C.210}$$

$$Index_t^k = i; \tag{C.211}$$

13:     **end if**
14:    **end for**
15:   **end for**
16:   **for** $t = 1 : \frac{24}{\Delta(t)}$ **do**
17:    **if** $index_t^a == i$ **then**

$$pheromone_t^i = pheromone_t^i + \Delta pheromone; \tag{C.212}$$

   ▷ Δpheromone: the value of a pheromone that in the case of the shortestness is added to the route pheromone so the chance of choosing this path in the next iteration become more
18:    **else**

$$pheromone_t^{i+1} = \zeta \times pheromone_t^{i+1}; \tag{C.213}$$

   ▷ ζ: a coefficient that is deducted from other pathes so their chances for being selected in the other iteration becomes less
19:    **end if**
20:   **end for**   ▷ Exit the time interval loop
21: **end for**   ▷ Exit the iteration loop
22: **return** $P_t^{WT}, P_t^{PV}, P_t^{MT}, P_t^{ES}, P_t^{DR}$ and P_t^{EWH}

C.6 MPSO unit

Algorithm 13 $MPSO$ UNIT

Require: PV, WT and load demand profile of the MG, the initial SOC of ES and the characteristic of system.
  Initialization (pBestsL, pBestsF, gBestL, gBestF, L, V)

                         ▷ Particles-num = 40, time-points = 48, max-it = 500

  for $I = 1 : \overline{I}$ **do**
    [pBestsL pBestsF gBestL gBestF meanF(iteration) SOC PWT PPV PESc PESd PEWH PMT PDR]= evaluate-fitness-GC(L,pBestsL,pBestsF,gBestL,gBestF,PWT,PPV,Pn,Particles-num);
    for $I = 1 : 1 : Particles - num$ **do**

$$
\begin{aligned}
V(i,:) \quad &= \quad w \times V(i,:) \\
&+ \quad c1 \times rand(1, time-points). \times (pBestsL(i,:) - L(i,:)) \\
&+ \quad c2 \times rand(1, time-points). \times (gBestL - L(i,:))
\end{aligned} \tag{C.214}
$$

$$
V(i,:) = fit - bound(V(i,:), Vmin, Vmax); \tag{C.215}
$$

$$
L(i,:) = round(L(i,:) + V(i,:)); \tag{C.216}
$$

$$
L(i,:) = fit - bound(L(i,:), Lmin, Lmax); \tag{C.217}
$$

    end for
  end for
  if $L(j) > i - 1$ & $L(j) <= i$ **then**

$$
\begin{aligned}
P(j) \quad &= \quad MPWT(i,j) \\
Q(j) \quad &= \quad MPPV(i,j) \\
X(j) \quad &= \quad MPESc(i,j) \\
Y(j) \quad &= \quad MPRLD(i,j) \\
Z(j) \quad &= \quad MPMT(i,j) \\
W(j) \quad &= \quad MPESd(i,j) \\
B(j) \quad &= \quad MPBUY(i,j) \\
S(j) \quad &= \quad MPSELL(i,j)
\end{aligned} \tag{C.218}
$$

  end if

Algorithm 13 (continued)

---

for $i = 1 : 48$ **do**

$$
\begin{aligned}
f \quad = \quad & f + (P(i) \times PIWT + Q(i) \times PIPV + Z(i) \times PIMT - X(i) \times PIESc \\
- \quad & S(i) \times PISELL + B(i) \times PIBUY + W(i) \times PIESd - Y(i) \times PIRLD \\
+ \quad & (Pn(i) - P(i) - Q(i) - Z(i) + X(i) - W(i) + Y(i) + S(i) \\
- \quad & B(i)) \times PIUP) \times 0.5
\end{aligned}
\tag{C.219}
$$

end for

function[pBestsL pBestsF gBestL gBestF meanF SOC EES PWT PPV PESc PESd PMT PRLD PBUY PSELL t PUP]= evaluate-fitness-GC(L,pBestsL,pBestsF,gBestL,gBestF,PWT,PPV,Pn,Particles-num)

for $i = 1 : N$ **do**   ▷ For each particle

    [fit(i) SOC EES PWT PPV PESc PESd PRLD PMT PBUY PSELL t PUP]= DACALC-GC(L(i,:),PWT,PPV,Pn,Particles-num)

    if isBetter(fit(i),pBestsF(i),goal) **then**

        pBestsF(i)=fit(i)

        pBestsL(i,:)=L(i,:)

    end if

end for

function tf = isBetter(a,b, goal)

tf=false

if a **then** ¡ b

    tf=true

end if

function X = fit-bound(X,low,up)

[dim,time-points] = size(X)

for $i = 1 : time - points$ **do**

    [fit(i) SOC E_t^{ES} P_t^{WT} P_t^{PV} P_t^{ES+} P_t^{ES-} P_t^{RLD} P_t^{MT} P_t^{GRID-} P_t^{GRID-} t P_t^{UP}]=

    Tp = X(1,i)¿ up

    Tm = X(1,i)¡ low

    X(1,i) = (X(1,i) × ((Tp+Tm)))+ up × Tp + low × Tm

end for

return $P_t^{WT}, P_t^{PV}, P_t^{MT}, P_t^{ES}, P_t^{RLD}, P_t^{GRID+}, P_t^{GRID-}$

C.7 MGSA unit

Algorithm 14 $EMS - MGSA$ UNIT

Require: Definition (Fitness function, constants, conditions, rules, limitation, variables, boundaries and number of agents)
1: *Initialization*
2: Evaluation and update (G, M, best and worst of the agents) (Eqs. (4.47) -(4.50));
3: Calculation of F (Eqs. (4.38) and (4.41)), a (Eq. (4.42)), velocity (Eq. (4.45)) and new agents′ position (Eq. (4.46))
4: Checking agents′ position in space-boundaries and return or reinitialize those agents being out of space
5: End of criterion is met?

    1. No. go to Step 3

    2. Yes. return the best solution

Algorithm 15 $EMS - MGSA$

Require: Input data   ▷ Number of agents, max iteration, Limits,···
  Space definition ▷ Number of spaces, dimension and boundaries. For example: 12 spaces, DIM = 4 (2 hours), D = 5 Independent variables
  for $k = 1 : 12$ **do**   ▷ 12: Number of spaces
  Initialization (Algorithm 16)
    for $I = 1 : \overline{I}$ **do**   ▷ $\overline{I}$: Max number of iteration
      for $J = 1 : N$ **do**   ▷ N: Number of agents
  calculating of Objective function for each agent (Equation 2.10)
      end for   ▷ Return fitness for all agents
  Finding of the best fitness (Value: Best and Index: best_X) [Best, best_X] = minimum value of (fitness)
            ▷ $best\_$X: Index of the best Object function in each iteration
    if $I == 1$ **then** Fbest = Best, Lbest = [XM,EM,YM]
    end if   ▷ Fbest: the final best value of Object function in each space
              ▷ Lbest: The location of the best agent in each space
  Mass calculation (Equation 4.48-4.50)
  Update gravitational constant (Equation 4.47)
  Calculation of the force and acceleration (Equation 4.41, 4.42 and 4.52)
  Calculation of the velocity and movement of agents (Equation 4.45 and 4.46)
  Check agents′ location in space boundaries
    end for
  Saving the final best objective function and the location of the best agent in space (K)
  Updating SOC and DR
  end for
  return the total best value of objective function and total best location in the whole universe

---

Algorithm 16 INITIALIZATION

Require: Update max WT, PV and load demand vectors in space K

    for $J = 1 : N$ **do** *random value for WT and PV between (0, max available power) also for MT between* $(\overline{P}^{MT}, \underline{P}^{MT})$

        for $I = 1 : DIM$ **do** X_I^{ES} = *randome value [0,1]*

            if $X_I^{ES} == 1$ **then** *Charging mode*

$P_{I,J}^{ES+}$ = *randome value* $[0, P_{limit}^{ES+}]$

$P_{I,J}^{ES-} = 0$

            end if

            if $I == 1$ **then** $SOC_{1,J} = SOC_I + P_{I,J}^{ES+}.\Delta t$

            else $SOC_{I,J} = SOC_{I-1,J} + P_{I,J}^{ES+} \times \Delta t$

            end if

            if $SOC_{I,J} > \overline{SOC}$ **then** $SOC_{I,J} = \overline{SOC}$

                if $I == 1$ **then** $P_{1,J}^{ES+} = \frac{SOC_{1,J} - SOC_I}{\Delta t}$

                else $P_{I,J}^{ES+} = \frac{SOC_{I,J} - SOC_{I-1,J}}{\Delta t}$

                end if

            else   ▷ discharging mode

$P_{I,J}^{ES-}$ = *random value between* $[0, P_{limit}^{ES-}]$

$P_{I,J}^{ES+} = 0$

                if $I == 1$ **then** $SOC_{1,J} = SOC_I - P_{1,J}^{ES-}.\Delta t$

                else $SOC_{I,J} = SOC_{I-1,J} - P_{I,J}^{ES-}.\Delta t$

                end if

                if $SOC_{I,J} < \underline{SOC}$ **then** $SOC_{I,J} = \underline{SOC}$

                    if $I == 1$ **then** $P_{1,J}^{ES-} = \frac{SOC_I - SOC_{1,J}}{\Delta t}$

                    else $P_{I,J}^{ES-} = \frac{SOC_{I-1,J} - SOC_{I,J}}{\Delta t}$

                    end if

                end if

            end if

        end for

    return $P_J^{ES-}, P_J^{ES+}, SOC_J and X_J^{ES}$

    Calculation of $\overline{P}_J^{GRID}$ *(Equation 4.65)*

    random value for P_J^{GRID} *between* $[-\overline{P}_J^{GRID}, \overline{P}_J^{GRID}]$

        if $P_J^{GRID} > 0$ **then** $P_J^{GRID-} = P_J^{GRID}$

        else $P_J^{GRID+} = -P_J^{GRID}$

        end if *Calculation of power balance*

$\Delta P_J = P_J^{WT} + P_J^{PV} + P_J^{MT} + P_J^{ES-} + P_J^{GRID-} - P_J^{ES+} - P_J^n - P_J^{GRID+}$

        for $I = 1 : DIM$ **do**

            if $\Delta P_J < 0$ **then** $P_{I,J}^{RLD} = 0$

$P_{I,J}^{UP} = | \Delta P_{I,J} |$

            else $P_{I,J}^{UP} = 0$

                if $\Delta P_{I,J} > P_{I,J}^{GRID}$ **then**

                    if $(\Delta P_I - P_{I,J}^{GRID-}) <= \overline{P}^{RLD}$ **then** $P_{I,J}^{GRID-} = 0$

$\overline{P}^{RLD} = \overline{P}^{RLD} - P_{I,J}^{RLD}$

                    else $P_{I,J}^{RLD} = \overline{P}^{RLD}$

$P_{I,J}^{GRID+} = P_{I,J}^{GRID+} + \Delta P_{I,J} - P_{I,J}^{GRID-} - \overline{P}^{RLD}$

$P_{I,J}^{GRID-} = 0$

$\overline{P}^{RLD} = 0$

                  end if

                else $P_{I,J}^{GRID-} = P_{I,J}^{GRID-} - \Delta P_{I,J}$

$P_{I,J}^{GRID+} = 0$

$P_{I,J}^{RLD} = 0$

                end if

            end if

        end for *Save* $XM_J, EM_J and YM_J$

$XM_J = [P_J^{WT}, P_J^{PV}, P_J^{MT}, SOC_J, P_J^{GRID}]$

$EM_J = [P_J^{ES+}, P_J^{ES-}, X_J^{ES}]$

$YM_J = [P_J^{UP}, P_J^{GRID+}, P_J^{RLD}, P_J^{GRID-}]$

    end for

    return matrix $[XM, EM, YM]$

D

Experimental setup

IREC has developed a utility-connected low voltage MG based on peer-to-peer and plug-and-play concepts [116, 117]. This MG includes generation and consumption units. Some of these units are commercial equipments and some others are emulators which can be programmed to behave as power devices.

In this study, six emulators have been used to validate the algorithm presented in Section C. An emulator is a power electronic device that is capable to emulate the behavior of different power system elements (e.g. generators and loads) by injecting and observing power. Emulators make possible to test different scenarios without having to wait for appropriate weather conditions. Figures D.1 and D.2 show the experimental setup.

The experimental platform is composed of three main systems:

- Control system;

- Power system.

- Communication system;

D.1 Control system

Some operations of the MG control system are time-critical (e.g. a unit emergency disconnection). For this reason, it is preferrable to split the control sytem in a layered architecture, and to decentralize and reorganize control tasks among these layers. This study proposes a two interconnected layer architecture (Figure D.3):
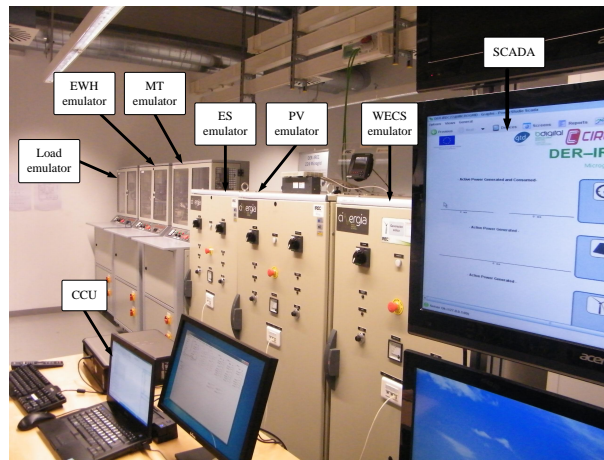
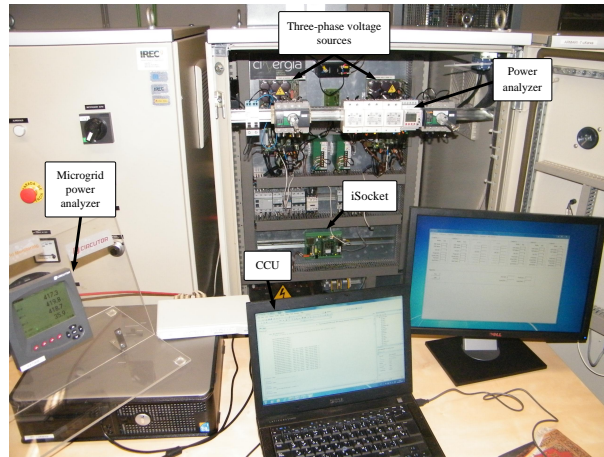Figure D.1: System configuration of IREC′s MG

Figure D.2: Experimental setup

- The CCU layer;

- The iSocket layer.

Each emulator has a dedicated iSocket. iSockets are intelligent electronic devices performing tasks that precise a very fast time response and that imply a high information exchange with power equipment, such as:

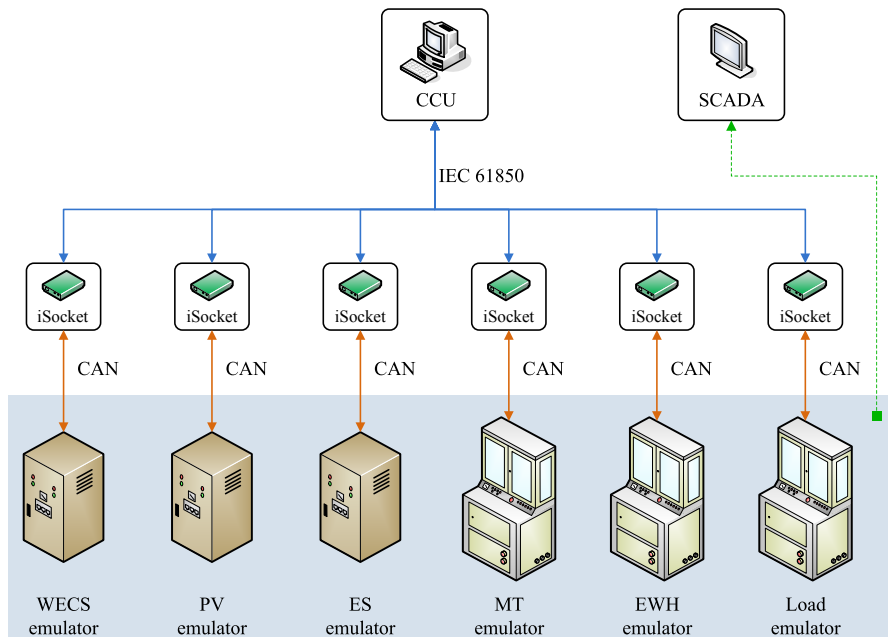- To command active power setpoints to emulators;

Figure D.3: The schematic diagram of control system in IREC′s MG

- To deal with alarms and events in order to guarantee electrical security;

- To aggregate relevant information from the emulator and make it visible to CCU.

On the other hand, the CCU layer is just responsible for load flow. At this layer, one single computer executes the $MCEMS_{-LEM}$ algorithm previously presented.

Moreover, a commercial SCADA has been used to validate results from the CCU. This SCADA neither is part of the CCU nor has any decision power. It just retrieves measurements from commercial meters installed in the emulators.

D.2 Power system

The six emulators have been programmed to behave as:

- Generation units

269

The different types of generation including WT, PV, ES and MT have been emulated using the real experimental profile.

- Consumption units
  The real behavior of different types of consumption such as controllable (for instance EWH) and non-controllable load demand using the experimental profile measured in a real grid.

- Energy storage unit
  A storage system has been emulated which can be acted as a battery or other storage devices [135].

Each emulator is composed of two identical three-phase voltage sources in back-to-back configuration, allowing bidirectional power flow. When emulating a generation unit or a storage unit in Discharging Mode, power flows from the lower voltage source to the upper one (Figure D.4). When emulating a consumption unit or a storage device in Charging Mode, power flows from the upper voltage source to the lower one (Figure D.4).

D.3 Communication system

Communications among the CCU and iSockets are according to IEC 61850 [136]. iSockets communicate with emulators via CAN as shown in Figure D.3. The procedures to implement communication system has been explained in details in our previous study [116, 117, 137–139], hence, they are not repeated in the present work.
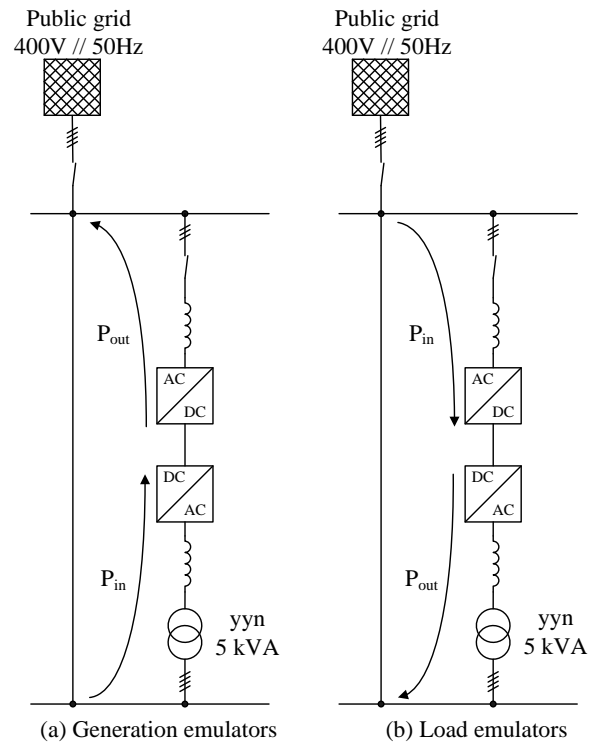
(a) Generation emulators   (b) Load emulators

Figure D.4: Single line diagram of the MG′s testbed in IREC